Substrate targeting and recognition in the flagellar type III secretion pathway

Owain James Bryant

Queens' college

University of Cambridge

This dissertation is submitted for the degree of Doctor of Philosophy

September 2019

Declaration of Originality

This thesis is the result of my own work and includes nothing which is the outcome of work done in collaboration except as declared in the Preface and specified in the text. It is not substantially the same as any that I have submitted, or, is being concurrently submitted for a degree or diploma or other qualification at the University of Cambridge or any other University or similar institution except as declared in the Preface and specified in the text. I further state that no substantial part of my dissertation has already been submitted, or, is being concurrently submitted for any such degree, diploma or other qualification at the University of Cambridge or any other University or similar institution except as declared in the Preface and specified in the text. It does not exceed the prescribed word limit for the relevant Degree Committee

Owain J Bryant

September 2019

Substrate targeting and recognition in the flagellar type III secretion pathway
Owain James Bryant

Summary

The bacterial flagellum is a complex molecular machine that enables bacteria to move as well as having additional roles in biofilm formation, adhesion and host cell invasion. The sequential assembly of the flagellar rod, hook and filament requires the export of thousands of structural subunits across the bacterial cell membrane by a specialised flagellar type III secretion system (fT3SS) located at the base of each flagellum. These subunits are unfolded and exported into a narrow 20Å wide channel in the centre of each flagellum energised by the proton motive force (PMF) and facilitated by a cytoplasmic ATPase complex comprising FliH, FliI and FliJ, which are evolutionarily related to components of the F1 ATPase. Unfolded subunits transit the length of the channel to the flagellum tip where they fold into the nascent structure. The order of subunit export is determined by the stage of flagellum assembly. Early subunits are exported to assemble the rod and hook substructures after which a substrate specificity switch in the fT3SS allows late subunit export.

The first aim of this study was to determine how the export signals that reside within early flagellar subunits contribute to export. In this thesis it was found that early flagellar subunits dock at the cytoplasmic domain of FlhB to correctly position an export signal at the subunit extreme N-terminus. The distance between the extreme N-terminal signal and the FlhB gate recognition motif (GRM) was found to be critical for subunit export. Evidence is presented to show that the extreme N-terminal signal of early flagellar subunits converts the FliPQR components of the export gate from a closed to open conformation, allowing subunits to enter the central channel within the flagellum. Further evidence was presented to show that the FlhA component of the flagellar export machinery is involved in export gate opening. Increasing the proton-motive force (PMF) improved subunit export by a strain encoding a FlhA variant defective in export gate opening, indicating that the PMF energises opening of the export gate. The data are compatible with the view that early subunits dock at the cytoplasmic

domain of FlhB to correctly position the extreme N-terminal export signal to trigger PMF-driven opening of the export gate.

The late filament structural subunits are delivered from their site of synthesis in the cytoplasm to the flagellar export machinery at the membrane by their cognate chaperones. Using motility and export assays, and *in vitro* and *in vivo* affinity chromatography pull down assays, data are provided that build on what is currently known about the sequence of binding events between chaperoned subunits and the flagellar export machinery. Specifically, evidence is presented to show that the FlgN chaperone binds the FliJ component of the ATPase complex after FlgN has docked and been released from the cytoplasmic domain of FlhA.

The final aim of this study was to determine whether the flagellar export chaperones regulate activation of the PMF-driven fT3SS export machinery. The FliJ stalk component of the ATPase binds the export gate protein FlhA, allowing it to utilise $\Delta\Psi$ to drive highly efficient subunit export. This thesis showed that the flagellar export chaperones regulate FliJ activation of FlhA. The data showed that chaperones and FlhA compete for a common binding site on FliJ, and that unladen chaperones, which would be present in the cell when subunit levels are low, disrupt the FliJ-FlhA interaction, preventing activation of the export gate. This provides a mechanism whereby the export gate is only activated when subunits are available.

Acknowledgements

I thank my supervisor, Dr Gillian Fraser, for her support, guidance and constructive criticism during my PhD. I thank Dr Betty Chung for her unyielding encouragement, and great discussions. Thank you to Dr Nicholas Greene, Dr Maryia Karpiyevich and Dr Anthony Davidson for their discussions, technical support and helpful advice throughout my PhD. I would also like to thank Dr Paul Bergen for his invaluable assistance, help and advice during his time in the Fraser lab. Outside the lab, many thanks to my family and friends for their support but especially Eric. Finally, I would like to thank the department of Pathology for funding my studentship throughout my four years of study.

Table of contents

List of Abbreviations

Å	Angstrom
A600	absorbance at 600 nm
$FlhA_N$	N-terminal portion of FlhA, residues 1-327
$FlhA_C$	C-terminal domain of FlhA, residues 328-692
amp	ampicillin
ATP	adenosine triphosphate
ATPase	adenosine triphosphatase
bp	base pair
°C	degrees Celsius
CBD	chaperone binding domain
CCW	counterclockwise
Cm	chloramphenicol
C-ring	cytoplasmic ring
cryo-EM	cryo-electron microscopy
cryo-ET	cryo-electron tomography
C-terminus	carboxyl-terminus
CW	clockwise
DNA	deoxyribonucleic acid
dNTP	deoxyrbonucleotide
DSN	duplex-specific nuclease
DTT	dithiothreitol
EDTA	ethylene diaminetetracetic acid
FlhBN	N-terminal portion of FlhB, residues 1-210
FlhBc	FlhB cytoplasmic domain, residues 211-383
FlhBcc	FlhB cytoplasmic C-terminal domain, residues 270-383
fT3SS	flagellar type III secretion system
GRM	gate recognition motif
GST	glutathione S-transferase
HBB	hook-basal body
IPTG	isoproyl β-D-thiogalactopyranoside
Kan	kanamycin
kDa	kilodalton
MCP	methyl-accepting chemotaxis protein
MDa	megadalton
mRNA	messenger ribonucleic acid
MS	membrane-supramembrane
MW	molecular weight
NEB	new england biolabs
N-terminus	amino-terminus
ONC	overnight cultures
PCR	polymerase chain reaction
PBS	phosphate-buffered saline

PBST	phosphate-buffered saline containing 0.05% Triton X-100
pI	isolectric point
PMF	proton motive force
RNA	ribonucleic acid
RNAse	ribonuclease
RPM	revolutions per minute
SDS-PAGE	sodium doodecyl sulphate polyacrylamide gel electrophoresis
SMF	sodium motive force
SOC	super optimal broth with catabolite reepression
TAT	twine-arginine translocation
T3SS	Type III secretion system
TCA	trichloroacetic acid
(v/v)	volume/volume
(w/v)	weight/volume

List of Figures

List of Tables

Chapter 1

Introduction

1.1 Bacterial motility

Many organisms are motile, allowing them to move to more favourable environments or away from less favourable environments, giving them a selective advantage over their non-motile competitors[1]. Bacteria can move in response to a range of external stimuli including oxygen levels, osmolarity, toxins, intensity and wavelength of light, and concentration of chemicals (in a process known as chemotaxis)[2,3,4]. This directed motility enables bacteria to avoid harmful chemicals or move away from potential predators, allowing them to adapt to a constantly changing and competitive environment to promote their survival. Motility also plays a significant role in bacterial pathogenesis, facilitating biofilm formation, cell adhesion, host cell invasion and in some cases flagella-mediated secretion of cytotoxins[2,5,6].

Bacteria display several types of motility, the most common and extensively studied being swimming motility[2,3,4]. Many bacteria swim by propelling themselves using rotary motors that drive rotation of helical propellers, called flagella, which extend from the bacterial surface. The flagellum is a large macromolecular complex and its assembly requires strict regulation to ensure a functional structure is assembled[7,8,9]. Each flagellum comprises at least 25 different proteins with copy numbers ranging from one to several thousand[8,9]. Furthermore, effective regulation of flagellum biogenesis is critical as the energetic cost of assembly, regulation and maintenance is significant, with the highly expressed flagellar genes representing 1% of the chromosome in *Salmonella enterica* serovar Typhimurium (hereafter *Salmonella*)[10].

1.2 Bacterial flagellar motility

Bacteria employ two types of flagellar motility – swimming and swarming[1]. Swimming motility involves the movement through liquids, whereas swarming motility is a population based movement over a solid surface and typically

involves higher levels of flagellar gene expression than required for swimming motility[1]. The number of flagella and their position on the cell surface differs greatly between species with some species such as *Bdellovibrio bacteriovorus* and *Legionella pneumophila* building a single polar flagellum (monotrichous) whilst others such as *Proteus mirabilis*, *Escherichia coli* and *Salmonella* assemble multiple flagella distributed across the cell surface in an arrangement termed peritrichous[11,12,13].

Salmonella typically have 6-10 flagella per cell that come together to form a bundle when they rotate in a counterclockwise (CCW) direction. The rotation of the flagellar bundle produces a force that propels the cell forward. Switching the rotational direction of the flagellar motors to clockwise (CW) disrupts the bundle of flagella causing cells to tumble[14]. CCW rotation restores the bundle of flagella and the cell swims in a new direction[14]. Positive or negative chemotactic signals can alter the frequency of cell tumbling such that cells are less likely to tumble if they are swimming towards a positive chemotactic signal[15]. This biasing of swimming motility towards a beneficial positive stimulus or towards regions with a lower concentration of a toxic, negative stimulus in a process termed chemotaxis relies on a CheA-CheY histidine-aspartate phosphorelay system that responds to the chemotactic signals by regulating the rotary activity of the flagellar motors[16,17,18]. Methyl-accepting chemotaxis proteins (MCPs) sense attractants or repellents and modulate the autophosphorylation activity of the sensor kinase CheA[16,17]. Binding of a repellent to a MCP results in CheA autophosphorylation and the transfer of the phosphate group to CheY[16]. Phosphorylated CheY (CheY-P) can interact with the FliM component of the flagellar switch complex composed of FliM, FliN and FliG[19]. The CheY-P/FliM interaction signals to the stator subunit MotA to switch motor rotation from CCW to CW causing the cell tumble[20]. Binding of an attractant signal to a MCP represses CheA autophosphorylation, preventing CheY phosphorylation and the switch in motor direction such that cells continue to swim towards the attractant. Rotation of flagella is driven by motor complexes embedded in the cell envelope. In *Salmonella*, MotA-MotB stator complexes are anchored in the peptidoglycan

layer and utilise the proton-motive force (PMF) to drive flagellar rotation[21]. Alternatively, some bacterial species utilise the sodium motive force (SMF) using an alternative PomA/PomB stator complexes[22]. Both the Mot and Pom stator complexes share a common mechanism as demonstrated by the engineering of functional Mot/Pom chimeric complexes[23,24]. These stator complexes interact with the flagellar rotor to allow the movement of proton or sodium ions down their electrochemical potential across the inner membrane, which energises motor rotation[23]. Harnessing of the PMF/SMF in this way enables flagella to rotate at speeds of over 60 Hz in *E.coli* and for the sodium driven polar flagella of *Vibrio alginolyticus*, rotations of 600 Hz have been observed in 50 mM NaCl at room temperature with rotation increasing to 1700 Hz in 300 mM NaCl at 35ºC[25]. Bacterial swimming speeds have been observed at over 70 $\mu m\ s^{-1}$ in *Salmonella* and speeds of over 140 $\mu m\ s^{-1}$ in *Vibrio alginolyticus*, equating to swimming speeds of over 10 times the length of the cell per second[26,27].

1.3 Motility and pathogenesis

In many bacterial pathogens, flagella are involved at almost every stage of infection, enabling bacteria to reach preferred sites within the host, promoting colonisation and invasion or dispersal to new infection sites or hosts[28,29]. Bacteria are very small compared to many of their hosts meaning directed swimming to reach target sites is more favourable than relying on diffusion[30,2]. Many pathogens use chemotaxis to reach their preferred site of infection, for example, the human pathogen *Helicobacter pylori* uses chemotaxis to preferentially colonise sites of gastric injury[5]. *Vibrio cholerae* relies on chemotaxis to preferentially infect the lower half of the small intestine[3], whilst *Campylobacter jejuni* detects chemoattractants such as mucins and glycoproteins present in the mucus to promote its colonisation of the mucus-filled crypts, its primary site of infection within the intestine[4]. Enterrohemorrhagenic *Escherichia coli* (EHEC) actually increases flagellar gene expression in response to some short chain fatty acids commonly found in the intestine, promoting penetration of the surface mucus layer[31]. In addition to swimming towards infection sites, bacteria can also engage in near surface swimming, increasing the local pathogen density at

surfaces to aid identification of target sites on the host cell surface[32,33]. Similarly, some plant pathogens rely on chemotaxis and flagellar motility to reach sites of infection such as the bacterial wilt pathogen *Ralstonia solanacearum* that is attracted towards root exudates, with wild type strains able to outcompete non-tactic mutants by 100-fold in tomato plant coinfections [2].

Once, pathogens have reached their target site, many need to adhere before they can invade[34,35,36]. The main component of the flagellar filament, FliC, has been shown to promote adherence to the host cell surface, with the exoprotein adhesin EtpA produced by enterotoxigenic *Escherichia coli* (ETEC) mediating an interaction between FliC and host cells[34]. Similarly, the flagellar filament cap protein, FliD, has been shown to promote adherence of atypical enteropathogenic *Escherichia coli* (aEPEC) to human enterocytes[35]. Flagella are also important for the transition from free living cells to biofilms, which are multicellular aggregates held together by a physical meshwork of polysaccharides, DNA and proteins, with flagella performing a structural role in biofilms[37]. Some studies have found that non-motile mutant strains are less able to form biofilms relative to wild type bacteria, meaning non-motile cells are more susceptible to antimicrobials and the immune system[37,36,38].

Many pathogens require flagella for the secretion of virulence factors or effector proteins[39,6,40,41,42]. Hemolysins, phospholipases, cytotoxins and other effectors that modulate host cell signalling pathways have been identified that require a functional flagellum for secretion[39,6,40]. *Campylobacter* invasion (cia) proteins are secreted *via* the flagellar export pathway to promote *C. jejuni* internalization into host cells[41,42].

Flagellin (FliC) is a major antigen on the bacterial cell surface and is recognised by the host innate and adaptive immune responses[43,44]. Extracellular FliC is recognised by the host encoded Toll-like receptor 5 (TLR5), a receptor dedicated to the detection of highly conserved Pathogen Associated Molecular Patterns (PAMPS) in flagellin [43]. Flagellin is also recognised by the host cytosolic Nod-

like receptor, Ipaf, and both TLR5 and Ipaf receptors induce downstream signalling pathways to induce an immune response[43,44,45,46]. Bacteria employ many strategies to circumvent the immunogenicity of flagellin, including switching off flagellar gene expression upon invasion, glycosylation of FliC or producing different flagellins (FliC and FljB) that are antigenically distinct in a process known as phase variation[47,48,49,50].

The majority of the exported proteins are unfolded and exported *via* a specialised type III secretion system enclosed in the base of the flagellum into a narrow 20 Å wide channel in the centre of each flagellum energised by the proton motive force and ATP hydrolysis[51,52]. These unfolded subunits must transit the length of the channel to the flagellum tip up to 15-20 μm away, equivalent to about 10 cell lengths, where they fold and assemble into the nascent structure[8,9]. How do all these thousands of subunits reach the export machinery? Furthermore, how does the energy derived from the proton motive force contribute to subunit export?

1.4 Biogenesis and structure of the bacterial flagellum

Flagella biogenesis has predominantly been studied in *Salmonella* and *Escherichia coli*. The flagellum extends from the cytoplasm to the cell exterior and consists of three distinct substructures: the basal body, the hook and the filament. The basal body anchors the flagellum in the cell envelope and is connected to the long helical filament *via* the curved hook substructure (Figure 1.1 and Figure 1.2).

1.4.1 The basal body

The flagellar basal body is a large (8 MDa) protein complex consisting of the export machinery a set of rings, and central rod structure that traverses the periplasmic space and outer membrane[53,54]. Basal body assembly begins with the oligomerisation of a single protein (FliF) into a ring complex termed the MS (membrane-supramembrane) ring[10]. The MS-ring serves as a platform for the assembly of the other basal body components. Attached to the MS-ring, the

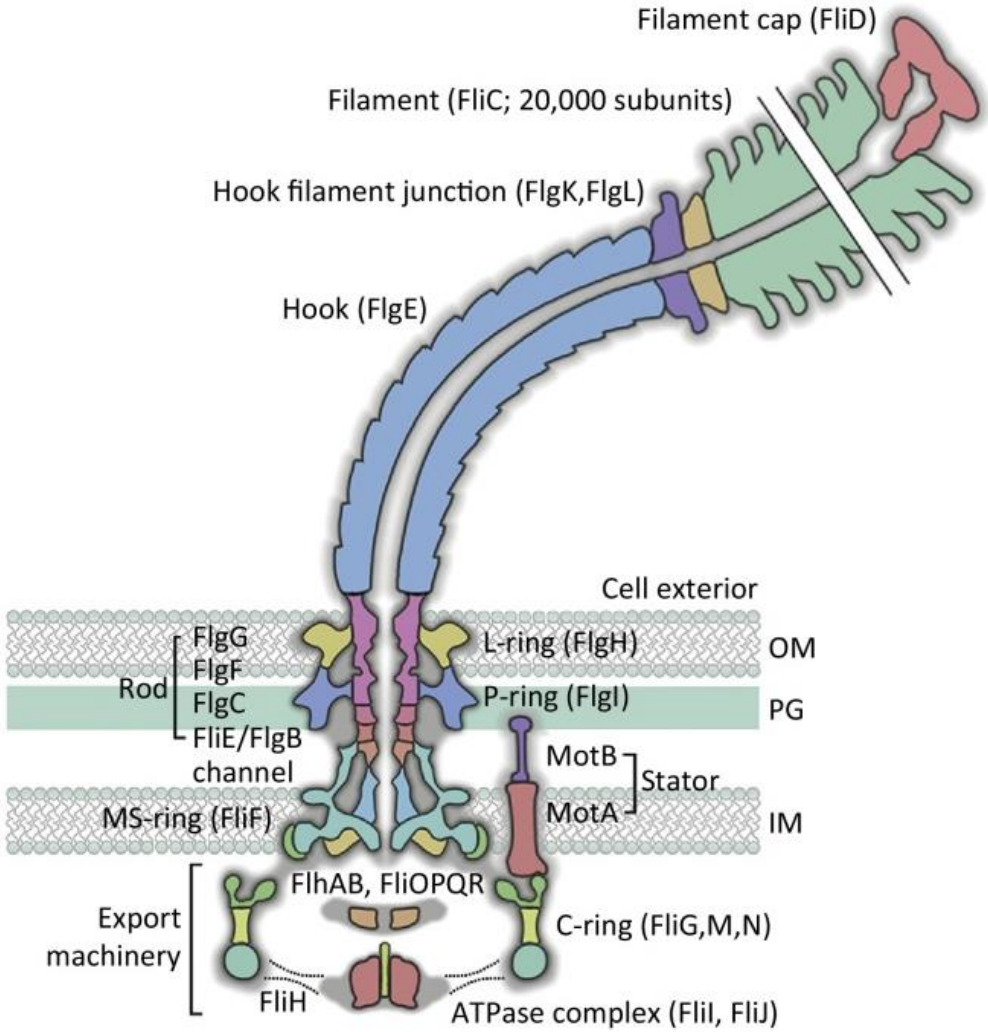

Figure 1.1. The structure of the *Salmonella* flagellum
The bacterial flagellum spans the inner and outer membrane and extends into the extracellular environment reaching a length of 15 - 20 µm. Subunits are produced in the cytoplasm, interact with components of the export machinery before being unfolded and translocated into the channel within the centre of the flagellar filament. These unfolded subunits transit to the flagellar tip where they refold and assemble into the structure. Figure adapted from Evans *et al*. 2013.

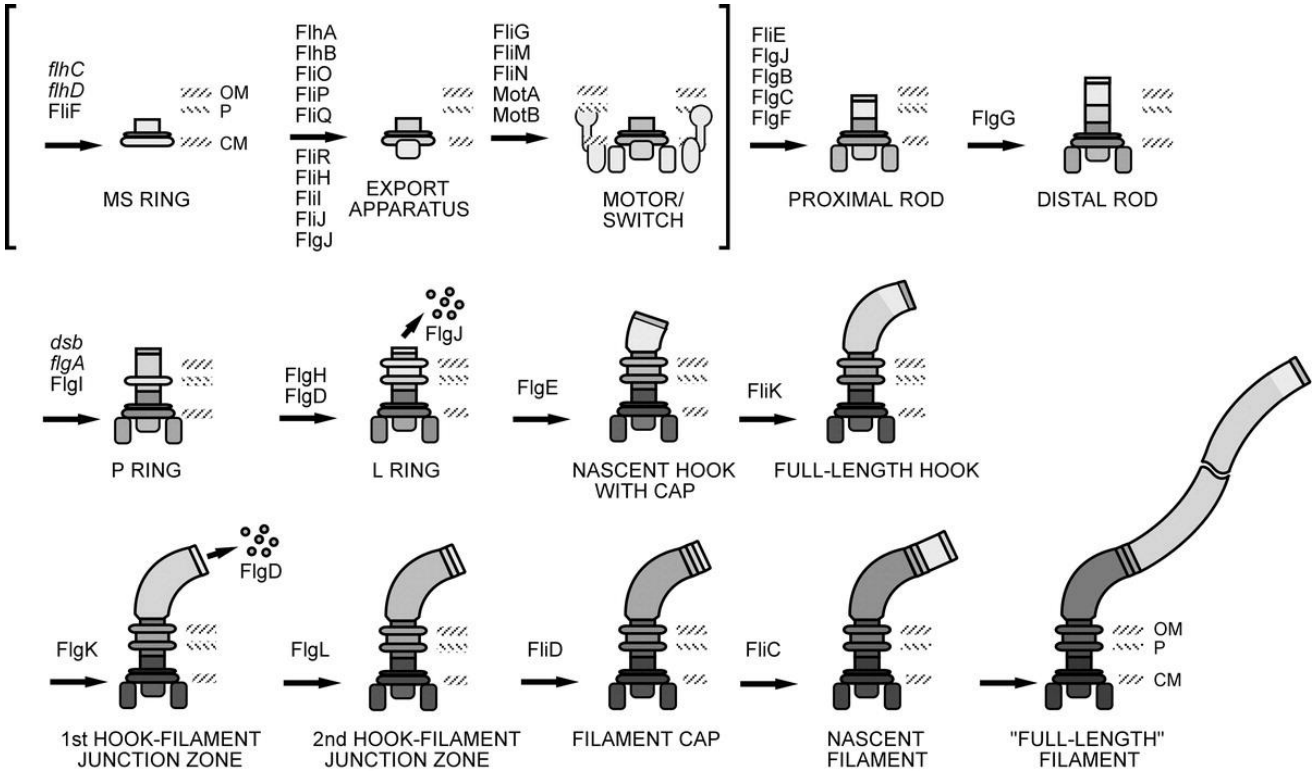

Figure 1.2. Flagellar morphogenesis in gram-negative bacteria
Early substructures assemble to form a functional type III secretion system that can recognise and export certain flagellar substrates depending on their location in the sequential rod/hook or filament. Substructures are labelled dark grey (early substructures) to light grey (late substructures). Figure adapted from Macnab 2003.

cytoplasmic C-ring is a bell-like structure containing the switch proteins FliM, FliN and FliG. Together, the MS- and C-rings house the specialised export machinery - the flagellar Type III secretion system (fT3SS) - that is required for export of protein subunits that assemble to form the rod, hook and filament.

Upon completion of assembly of the type III secretion machinery, the rod subunits (FliE, FlgB, FlgC, FlgF, FlgG) can be exported across the inner membrane and polymerise to form the helical rod structure which effectively functions as a 'drive shaft'[10]. In addition to the rod subunits, a hook cap subunit (FlgJ) containing muramidase activity, the hook subunit (FlgE), hook cap subunit (FlgD) and hook length control protein (FliK) can be exported by the export machinery[55]. These rod components assemble to form a hollow rigid structure with the stoichiometries of FliE, FlgB, FlgC, FlgF and FlgG being estimated at 9, 6, 6, 6 and 26 respectively[53,56,57]. In Gram-negative bacteria, an additional set of rings - the P (peptidoglycan) and L (lipopolysaccharide) rings - polymerise around the distal rod to form a pore that allows the rod to penetrate the cell envelope and protects the cell envelope against lateral shearing forces generated by flagellar rotation[58,53]. The length of the FlgG distal rod is determined by the distance between the inner and outer membrane which in turn is determined by Braun's lipoprotein[59]. As the distal rod assembles and reaches the L-ring in the outer membrane, the structure ceases to assemble FlgG subunits and begins to assemble the hook subunit, FlgE[60].

1.4.2 The hook

The flagellar hook is a short, tubular, helical, curved structure that functions as a universal joint, transmitting the torque from the motor and drive shaft rod to the filament[10]. The hook is assembled from approximately 120 copies of a single subunit, FlgE, and is regulated to a length of approximately 55 nM, which is thought to be an optimal length for efficient flagellar bundle formation in peritrichous flagellated bacteria[61,54,53]. The hook length control protein, FliK, detects when the hook has reached its mature length and terminates rod and

hook subunit export by inducing a substrate specificity switch within the export machinery[62,63,64,65].

The *Salmonella* FlgE protein has three domains: D0, D1 and D2. Domain 0 forms the inner core of the hook and is composed of two bundled alpha helices comprising the extreme N-terminal and C-terminal regions of FlgE that are essential for hook assembly[66]. The D1 and D2 domains are positioned radially from the inside to the outside of the hook[66]. The inner D0 domains are packed more tightly than the outer domains providing mechanical stability, the D1 domain is packed more loosely allowing the hook to adopt curved conformations, whilst the outer D2 domain is thought to provide twisting rigidity[67,66,68]. Hook flexibility is also important for flagellar bundle formation[69]. However, why this curved flexible structure is also found in monotrichous flagellated bacteria, where flagella bundle formation doesn't occur, is unknown.

1.4.3 The hook-filament junction proteins

The hook is connected to the filament *via* the hook-filament junction proteins, FlgK and FlgL. These proteins form two split-ring like structures comprising 11 copies each of FlgK, which is connected to and assembles on the hook, followed by FlgL, which assembles on FlgK and is connected to the filament[70]. These hook-filament junction proteins provide a nucleation site for the assembly of the filament, with deletion of either FlgK and FlgL resulting in the release of unassembled flagellin to the extracellular environment[71]. It has been proposed that the hook-filament junction proteins in *C. jejuni* accommodate the symmetry mismatch between the 7 versus 11 protofilament organisation of the flagellar filament and hook, respectively[68]. However, in *Salmonella* there is no symmetry mismatch between the filament and hook, suggesting that the hook-filament junction also plays another role, possibly in maintaining the flexibility of the hook whilst allowing assembly of the more rigid filament[72].

1.4.4 The filament

The filament is composed of 20,000 – 30,000 copies of a single protein, FliC, which assembles to form a helical structure, comprising 11 protofilaments, that grows up to 15-20 μm in length[73]. FliC has four domains: D0, D1, D2 and D3. Similar to the FlgE hook subunit structure, the FliC D0 domain forms the inner core of the filament and comprises the N- and C-terminal regions of FliC, and the D1, D2 and D3 domains are positioned radially from inside to outside[73]. Filaments can exist in two distinct helical forms: left-handed or right-handed, whereby protofilaments can adopt two distinct protofilament conformations: L- and R-type[74,75,76]. During reversal of the motor rotary direction to clockwise rotation, a twisting force results in the transition of the filament from the left-handed to the right-handed helical form, causing the flagellar bundle to fall apart, resulting in cell tumbling[77]. These conformational changes in the bacterial flagellum are known as polymorphic transitions[77,78]. A cap structure at the distal end of the growing filament promotes the assembly of FliC into the nascent structure, minimising the loss of monomeric FliC into the extracellular environment[79,80]. This filament cap is composed of the FliD subunit, which in *Salmonella* adopts a pentameric structure, although other oligomeric forms have been observed in other species[81,82]. It has been proposed that the five C-terminal domains of *Salmonella* FliD adjust their conformations such that they always maintain a single flagellin binding site available for flagellin insertion into the nascent structure[80].

1.5 Hierarchical flagellar gene expression

Assembly of the bacterial flagellum is an energetically expensive process with over 70 genes in the flagellar assembly and chemosensory regulons[83]. Flagellar export and assembly are ordered processes, with components of the basal body and hook being exported and assembled during the early export phase, both the flagellar hook and injectisome needle grow to a strict length upon which the export machinery changes export specificity such that the late export subunits (exported after hook/basal-body assembly) are synthesised, recognised by the export machinery and exported during the late assembly phase. Early and late

export subunits need to be efficiently discriminated by the export machinery so that the correct subunits can be exported according the stage of assembly. This discrimination is especially important for peritrichous flagellated bacteria such as *Salmonella* which have multiple flagella at different stages of assembly and therefore have both early and late export subunits in the cytoplasm at any given time. There are two main ways in which this ordered export and assembly is achieved. The first is by controlling the production of subunits at the level of transcription and the second is by the export machinery, regulating a substrate specificity switch so that early subunits are only exported during the early phase of assembly and the late subunits during the late phase[83,84,55].

The flagellar genes are organised into a transcriptional hierarchy controlled by three promoter classes: class I, class II and class IIIa/b[85,83]. At the top of the hierarchy are the *flhD* and *flhC* genes which are under the control of the class I promoter and encode the FlhD and FlhC proteins which form a complex ($FlhD_4C_2$)[85]. In *Salmonella* and *E.coli, flhDC* expression is regulated by several regulatory circuits that respond to a range of environmental and physiological signals that determine class I promoter activity and therefore *flhDC* expression[86,87,88]. $FlhD_4C_2$ binds class II promoters and in combination with σ^{70} activates their transcription, resulting in the expression of the genes that encode components required for the early stages of assembly as well as a few additional regulatory genes[89] (Figure 1.3). Two of these regulatory genes include the sigma factor σ^{28} (FliA) required for the transcription of genes from class III promoters and an anti-σ^{28} factor (FlgM) that binds and sequesters σ^{28} and prevents expression of class III genes[90,91]. Once assembly of the hook and basal body is complete the export machinery becomes competent to export late export substrates, including FlgM which is exported, freeing σ^{28} to activate the transcription of genes under the control of class III promoters, many of which encode for the subunits required after completion of the hook and basal body[91,92].

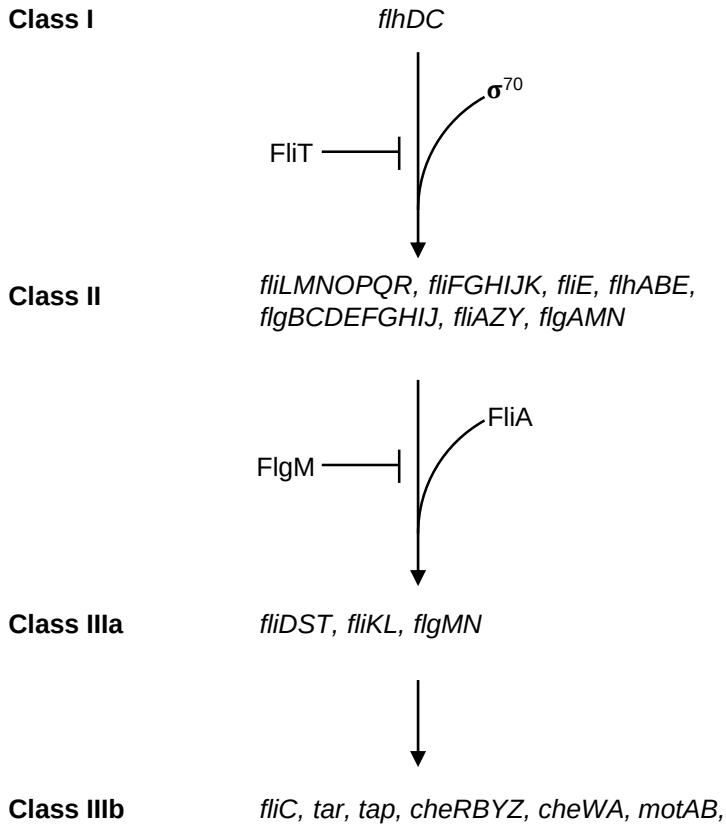

Figure 1.3. Flagellar gene regulation in *Salmonella*
Flagellar genes are separated into three classes (I, II and III). The class I genes are the *flhD* and *flhC* (*flhDC*) genes which encode for the 'master regulator' $FlhD_2C_4$. $FlhD_2C_4$ recruits σ^{70} to promote class II gene expression. Class III genes are expressed by FliA recruitment of RNA polymerase. FlgM (anti sigma/FliA factor) binds to FliA and prevents FliA from recruiting RNA polymerase. Once the hook has reached its mature length and the switch in the export machinery from early to late subunit export has occurred, FlgM is exported and FliA can recruit RNA polymerase and promote class III gene expression. Class IIIa genes are under the control of both class II and class III promoters. Figure modified from Chevance FF and Hughes KT 2014.

1.6 Bacterial export systems

The movement of proteins, small molecules and DNA from the cytoplasm across the inner membrane, into the environment or into other bacterial or eukaryotic cells is an essential process for a range of biological processes such as nutrient acquisition, adaption and survival to stressors, or for pathogenicity[93]. Bacteria have evolved a range of specialised secretion systems to transport substrates, with bacteria producing a different number and complement of these secretion systems depending on the environment they inhabit or their lifestyle[93]. More than ten classes of protein secretion systems have been identified in Gram-negative bacteria[94]. Furthermore, some environmental bacteria appear to lack all known bacterial secretion systems, suggesting novel secretion systems may still be discovered[94]. In Gram-negative bacteria, these secretion systems can be divided into two categories: those that span both the inner and outer membranes and those that are span either the inner or outer membrane[93].

Secretion of proteins across the inner membrane is often carried out by the Sec pathway, which translocates proteins in an unfolded state or *via* the twin-arginine translocation (TAT) system that transports folded proteins[95,96]. Some of these secreted proteins are subsequently transported across the outer membrane *via* the type II or type V secretion systems whilst other proteins remain in the periplasm or incorporate into the inner membrane. The type I, III, IV and VI systems span both the inner and outer membrane and substrates are typically transported *via* a 'one-step mechanism', directly from the cytoplasm into the environment or target cell[93].

These secretion systems use various energy sources to power transport. Some utilise the proton- or sodium-motive force, whilst other systems use ATP hydrolysis or a combination of both[93]. Some systems such as the type V autotransporters transport proteins across the outer membrane without the assistance of an ion gradient or ATP hydrolysis but instead folding of the protein substrate is the driving force for outer membrane translocation[97,98]. One of the challenges is forming a protein or small molecule conduit in the membrane whilst

maintaining a permeability barrier. The mechanisms used to regulate channel opening are not fully understood but in many cases, substrate binding to components of the export machinery induces conformational changes that promotes channel opening and export activity[99,100,101,102,103,104,96]. The flagellar type III secretion system (fT3SS) has been shown to utilise both the PMF and SMF to energise subunit export whilst a flagellar ATPase facilitates the use of the PMF. The permeability barrier of the inner membrane is maintained in the fT3SS by the FliP, FliQ, FliR components of the export gate complex[105]. However, the mechanisms used to regulate channel opening are unclear.

1.7 The flagellar export machinery

To assemble the bacterial flagellum, thousands of subunits must be exported by a dedicated export machinery which translocates subunits across the inner membrane into the flagellar central channel[8,9] (Figure 1.4). The export machinery is highly conserved between the flagellar and virulence type III secretion systems[105,106,107,108,109]. Within and below the plane of the inner membrane resides a nonameric ring of FlhA which is thought to function as a proton-protein antiporter, using the energy from the proton-motive force to translocate proteins across the inner membrane[110,52,51,111]. The transmembrane region of FlhA is predicted to contain 8 transmembrane helices with helices 4 and 5 connected *via* a large conserved loop named FHIPEP which contains multiple conserved residues that has been proposed to function as a gate, regulating substrate entry into the export channel[112,113]. The transmembrane region of the FlhA nonamer is connected to a cytoplasmic domain, which forms a nonameric ring that engages with export cargo during subunit export[108,114,115,116]. Positioned above FlhA is a protein complex composed of FliP FliQ FliR and the N-terminal portion of FlhB ($FlhB_N$). The structure of the FliPQR complex showed that the complex forms a helical assembly, with the centre of the complex forming a pore for subunit translocation[105]. Furthermore, the structure shows that multiple points of contact within the centre of the pore maintain a closed conformation[105]. How the open conformation is stabilised to allow subunit export is currently unknown.

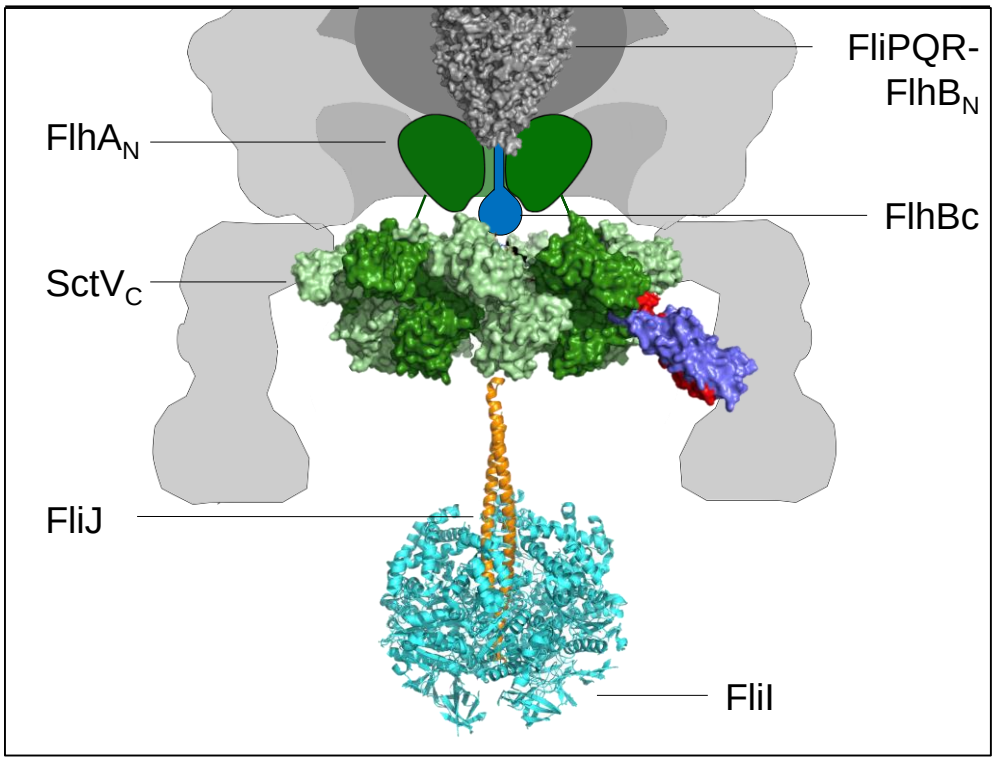

Figure 1.4. The export machinery
Connected to the cytoplasmic sorting platform via FliH/SctL is the ATPase (FliI hexamer, blue, PDB:2DPY) whereby chaperone-subunit complexes can dock. Chaperone-subunit complexes are thought to then interact with the export gate component FlhA/SctV (green, PDB:3A5I). Following subunit unfolding and release from their cognate chaperone, empty chaperones are then thought to interact with the FliJ/SctO escort protein (FliJ, orange, PDB:3AJW) component of the ATPase complex, which is proposed to function as a chaperone escort protein, recycling chaperones and transferring them to new cognate subunit.

$FlhB_N$ is predicted to contain four helices. Crosslinking analysis showed that $FlhB_N$ does not reside within the membrane but actually forms part of the FliPQR complex[105], which would place the FlhB cytoplasmic domain of (FlhBc) within or just below the plane of the membrane. Furthermore, a *fliR-flhB* fusion exists in *Clostridium*, and in *Salmonella* a *fliR-flhB* fusion can complement a *fliR-flhB* null strain suggesting that these two components are located proximal to each other in the export machinery[117]. Associated with the cytoplasmic face of the export apparatus is a highly conserved ATPase complex composed of three subunits – FliH, FliI and FliJ. The ATPase complex shares significant sequence and structural similarity with components of the F_1F_0 ATP synthase[118,119,120,121]. The FliI ATPase component oligomerises into a hexamer and shares structural similarity with the alpha and beta subunit of the F_1F_0 ATP synthase[122,106,120], FliJ folds into a two stranded alpha helical coiled coil and binds the centre of the FliI hexamer ring resembling the γ subunit of the F_1F_0 ATP synthase[107], FliH anchors the ATPase to the C-ring, analogous to the stator subunit of the F_1F_0 ATP synthase: the N- and C-terminal regions of FliH share sequence similarity with b and δ subunits of the F_1F_0 –ATP synthase[123]. ATP hydrolysis by FliI is thought to drive rotation of the central stalk subunit FliJ, allowing FliJ to contact all nine binding sites on FlhA, turning the export machinery into a highly efficient $\Delta\psi$ driven export machine[111,124].

1.8 Targeting of substrates to the T3SS export machinery

Following assembly of a competent type III export apparatus, the flagellar T3SS begins exporting early type substrates that assemble to form the rod and hook substructure or in the case of the virulence T3SSs the rod and needle substructures[10,8,9]. Once the hook or needle reaches its mature length, the export apparatus switches substrate specificity and can begin to export late export substrates which are the filament type subunits in the fT3SS or the translocator and effector proteins for the vT3SS[125,126]. The type III export apparatus must recognize and distinguish different types of type III secretion substrates and one way they achieve this is by recognising different export signals on the substrates.

1.8.1 Nucleic acid signals

Several effector proteins for the vT3SS have been shown to contain RNA signals that play a role in secretion[127,128,129,130]. Frameshift mutations that alter the peptide sequence as well as point mutations in the N-terminus of the *Yersinia* effector proteins YopE, YopN and YopQ failed to abolish secretion[127,128]. Furthermore, synonymous mutations in the secretion signal of YopQ that altered the RNA but retained the amino acid sequence caused secretion defects[129]. This led to the suggestion that the signal for the secretion of Yops is not proteinaceous but resides in the mRNA.

Studies in other species have demonstrated similar results. The addition of the first 28 residues of the *Xanthomonas* plant effector protein AvrBs2 to a reporter gene retained the ability to secrete protein following +1 or +2 frameshift mutations[131]. Furthermore, frameshift mutagenesis in the *Salmonella* length control protein InvJ showed that the InvJ secretion signal could tolerate significant changes in its protein sequence[132].

More recent studies have provided evidence indicating that the secretion signal in YopE is encoded by the protein rather than the mRNA. Frameshifts in the initial codons of YopE abolished secretion in a strain lacking the YopE cognate chaperone[133]. This is further supported by the observation that the replacement of residues 2-8 of YopE with combinations of serine and isoleucine that form amphipathic sequences can restore secretion[134]. Furthermore, *in silico* frameshift mutations showed that some T3SS effectors can retain their original amino acid composition, which may explain why some T3SS substrates can tolerate frame shifts[135,136].

It has since been shown that the untranslated (UTR) regions of the flagellar gene *fliC* are important for FliC secretion *via* the flagellum. Fusions of the 5'-UTR and 3'-UTRs of the flagellar *fliC* gene to the non-flagellar proteins Peb1, an enolase (Eno), GFP and to a fibronectin binding protein were sufficient to direct their export into the growth medium[130]. A more recent study in 2013 screened the 5'-

UTR from 42 *Salmonella* type III secretion effectors and found that five were sufficient to direct the translocation of an adenylate cyclase reporter into macrophage[137].

1.8.2 Protein signals

The export signals that direct substrates to the export machinery are not fully understood. It has been shown that the N-terminus of T3SS substrates contain a peptide secretion signal important for subunit export[138,139,140,141,142]. Unlike classical N-terminal secretion signals, they often do not share a common signal sequence, furthermore this signal is not cleaved off during secretion[143].

Studies analysing the N-terminal type III secretion signals have not led to the identification of a conserved amino acid sequence motif, except in a group of *Salmonella* effector proteins[144] and more recently a subset of flagellar and virulence T3SS substrates[141] (discussed later). The secretion signal is believed to be in the first 50-100 residues whereas early studies in *Yersinia* have showed that the first 15 residues of the effector proteins YopE, and first 17 of YopH are sufficient to allow secretion, whereas the first 50 residues of YopE and first 71 residues are required for translocation into host cells[145]. The importance and degenerate nature of the N-terminal signal are highlighted by studies from the *Yersinia* effector protein YopE using synthetic secretion signals[134]. Replacing residues 2-8 of YopE with all possible combinations of serine/isoleucines showed that combinations producing amphipathic sequences were secreted more efficiently than hydrophobic or hydrophilic sequences[134]. This led authors to propose that the amphipathic sequence itself may be the signal for export. *In silico* studies from a range of pathogenic animal and plant T3SS effectors support the idea that the N-terminal secretion signal is highly variable with a tendency towards polar residues, particularly serine[146,147,135]. Analysis of the amino acid composition of the export signals in *P. syringae* effector proteins showed that the N-termini have a bias towards serine residues and have a low tendency towards aspartate, leucine and lysine residues[148]. The same study also showed that the N-termini of *Salmonella* effector proteins have a tendency

towards serine and aspartate[148]. These studies suggest that there isn't a classical signal but rather the N-termini have a significant residue tendency that appears to be important for subunit export.

Another shared feature of Type III substrates is that the first 30-50 residues are frequently unstructured and flexible[149,150,151,152,153,154]. An *in silico* study showed that T3SS effectors are more likely to have an N-terminus that is unstructured or form an N-terminal coiled sequence compared to non-T3SS substrates[136]. Furthermore, structures of T3SS substrates have shown that many substrates have N-terminal sequences that lack significant structure[149,150,151]. The solution NMR structures of the type III needle proteins PrgI, BsaL and MxiH show that the first 20 residues have partial alpha helical character and regions of random coil[155]. Furthermore the termini of flagellar proteins that assemble to form the rod, hook and filament structures are disordered in solution and only assume structure upon assembly into the nascent structure or upon interacting with certain binding partners[152,153,154]. Whether this feature may form part of the signal remains unknown but is unlikely to act alone as the signal for subunit export.

1.8.3 Early subunit interactions with the export machinery

The early flagellar subunits that assemble to form the flagellar rod, hook and hook cap do not bind cognate chaperones for their delivery to the export machinery but instead bind directly to the cytoplasmic domain of FlhB[141,156] (Figure 1.5). This is achieved by a small hydrophobic N-terminal five-residue motif on the subunit termed the gate recognition motif (GRM) with the consensus sequence Fxxxϕ (where ϕ is typically any hydrophobic residue)[141]. This motif is conserved among early flagellar subunits and the rod, needle and length control proteins in the virulence systems, with deletion of the GRM considerably reducing subunit export[156,157,141]. The GRM of early subunits recognises a surface exposed hydrophobic pocket on the C-terminal domain of FlhB[141]. These subunit interactions with the FlhBc export gate are weak with micromolar dissociation constants, as might be expected for subunits that need to interact

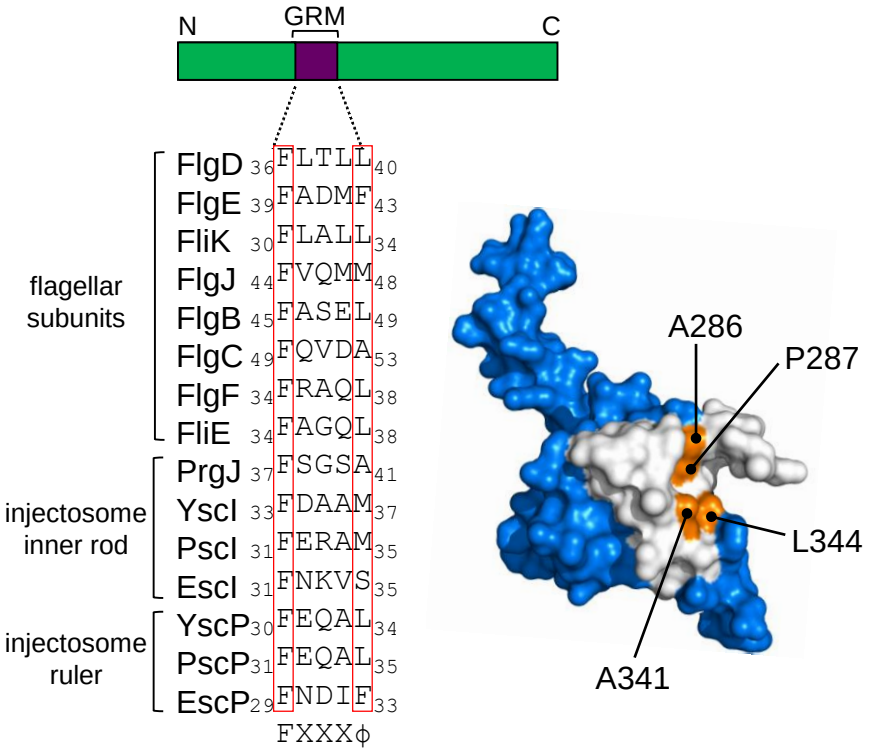

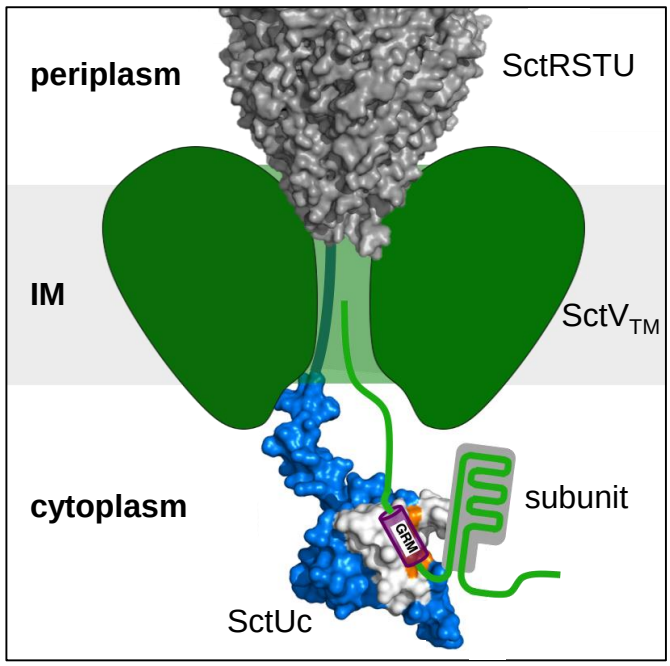

Figure 1.5. Early subunit interactions with the FlhBc/SctUc export gate
Amino acid sequence alignment of the gate recognition motif (GRM) of early flagellar subunits and early subunits of the injectisome T3SS (top, left).
Mapping the hydrophobic subunit binding pocket on the FlhBc export gate structure (PDB 3B0Z). Residues that abolish subunit binding (orange) are surrounded by a subunit docking surface (grey) (top, right).
A model depicting how subunits may dock at the FlhBc export gate (bottom).

transiently with the export machinery prior to being exported[141,8,9]. It has been proposed that the C-terminus of early subunits already present within the export channel can interact with the N-terminus of the preceding subunit docked at FlhBc and this subunit-subunit interaction can pull the subunit from FlhBc and into the channel, freeing the hydrophobic binding pocket on FlhBc for docking of a subsequent subunit[141]. More recently a similar binding pocket has been identified in the *Yersinia* virulence T3SS FlhB homologue (YscU), with early virulence T3SS subunits also binding transiently to the export gate, indicating that the mode of early subunit docking at FlhBc/SctU gate is conserved in both the flagellar and virulence systems[158].

Once the flagellar hook or the virulence needle has reached its mature length the export machinery switches subunit export specificity such that it no longer exports early subunits and can begin exporting the late export subunits[62,64,159,160,161]. This is in part achieved by a secreted molecular ruler protein, FliK/SctP that like other early subunit contains a GRM but doesn't assemble into the structure and is instead secreted directly into the extracellular environment. FliK/SctP is secreted intermittently during rod and hook/needle assembly, when the hook/needle has reached its mature length, the C-terminal domain of FliK/SctP interacts with the FlhBc/SctU export gate, causing an export specificity switch such that the export machinery can no longer recognise early subunits[162]. The precise mechanism of how FliK/SctP achieves this substrate specificity switch is currently unclear[161,65].

1.9 Export chaperones

A number of ancillary proteins have been identified that support efficient protein export *via* type III secretion systems. These ancillary proteins are often encoded by genes adjacent to the gene encoding the secreted virulence factor[163]. Early interaction studies revealed that these ancillary proteins can often associate with the secreted protein after their synthesis in the cytoplasm, forming a specific complex with their cognate secreted protein hence the term chaperone-like protein[164,165]. Unlike the traditional molecular chaperones such as GroEL and

Hsp protein families, T3SS chaperones lack nucleotide binding or nucleotide-hydrolysing activity and don't exhibit protein folding activity but instead protect their cognate subunits from degradation and aid their delivery to the export machinery[165,163]. Furthermore, T3SS chaperones have also been implicated in a number of other roles such as regulating gene expression and substrate secretion by the export machinery[166,167,168] (Figure 1.3). Chaperones have been identified for both the flagellar and virulence type III secretion systems, although structurally diverse and often lacking primary sequence identity they share many common features such as low molecular weight (10-20 kDa), acidic pI (4-5) and their deletion typically reduces the secretion of their cognate subunit(s) often with no affect on the export of other non-cognate subunits[163] (Figure 1.6). Their Importance is highlighted by the fact that deletion or mutant chaperones often result in significant virulence defects in animal and plant models of infection, or in the case of the flagellar T3SS cause motility and export defects[169,170,171,172,173]. The chaperones for the vT3SS have been separated into three classes depending on the substrate(s) they interact with: class I chaperones bind effector proteins, class II bind the translocon proteins, and class III chaperones bind the needle subunits.

1.9.1 The flagellar chaperones

The biogenesis of the bacterial flagellum requires the ordered export of thousands of structural subunits across the inner membrane and their transit through a narrow channel to their assembly site at the tip of the flagellum[9,8]. The rate of flagellar protein export is approximately 1700 amino acids per second during the initial stages of assembly, far greater than the rate of translation by the ribosome, indicating multiple ribosomes are actively synthesizing flagellar proteins at any one time[174,175]. To sustain this rate of protein export, flagellar-specific chaperones aid efficient delivery of subunits from their site of synthesis at the ribosome to the flagellar export machinery[176,177,116].

The late flagellar structural subunits that form the long helical filament (FliC), the cap (FliD) and the junction that connects the filament to the hook (FlgK and FlgL)

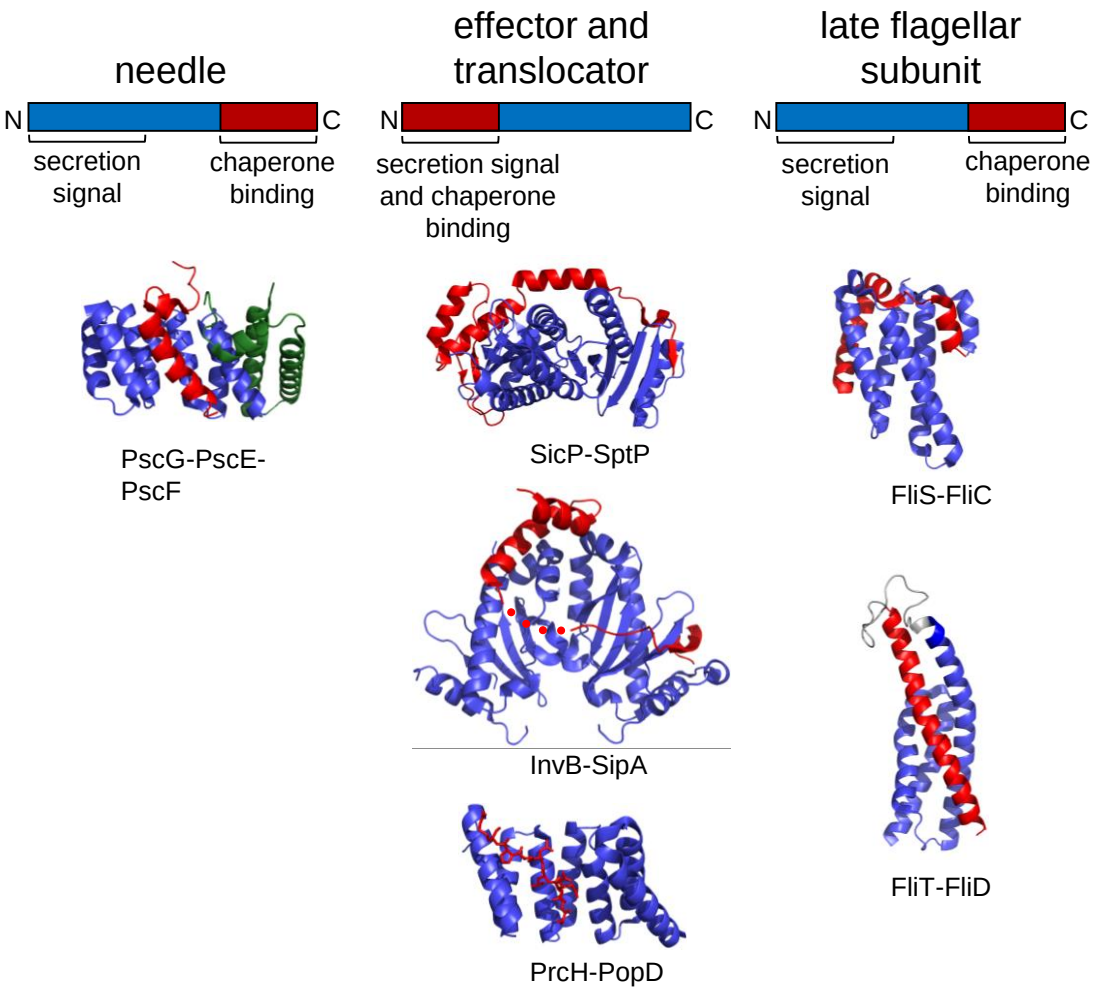

Figure 1.6. Structures of chaperones in complex with cognate substrate
Structure of a needle chaperone PscG-PscE (blue and green) in complex with a fragment of PscF (red) (PDB:2UWJ) (left). Structure of an effector chaperone, SicP (blue) in complex with a fragment of SptP (red) (PDB:1JYO) (centre, top). Structure of an effector chaperone, InvB (blue) in complex with a fragment of SipA (red) (PDB:2FM8) (centre, middle). Structure of a translocator chaperone, PcrH (blue) in complex with a fragment of PopD (red) (PDB:2XCB) (centre, bottom). Structure of the flagellar chaperones, FliS (blue) in complex with a fragment of FliC (red) (PDB:1ORY) (right, top) and FliT (blue) connected by a linker (grey) to a fragment of FliD (red) (PDB:5KRW) (right, bottom) .

are delivered to the export machinery by subunit specific chaperones (FliS, FliT or FlgN). The chaperones interact with the C-terminal ~40 residues of the subunit, a region that forms an amphipathic helix involved in quaternary interactions between adjacent subunits in the assembled structure[178,153]. The crystal structure of FliS in complex with a C-terminal fragment of FliC revealed that FliS binds an extensive region of FliC, analogous to substrate binding by vT3SS chaperones, suggesting a common mode of recognition between virulence and flagellar T3SS chaperones and their substrates (Figure 1.6)[179,149,151]. The flagellar chaperones are structurally distinct from the virulence T3SS chaperones in that they adopt an antiparallel alpha helical bundle fold[179,180,181]. Deletion of the chaperone FlgN for the hook-filament junction proteins results in attenuated hook-filament junction assembly accompanied by increased levels of unpolymerised FliC release into the extracellular medium[173]. Deletion of the flagellin specific chaperone (FliS) results in short filaments consistent with a defect in FliC export. Furthermore, FliS prevents *in vitro* polymeristion of FliC into filaments consistent with FliS acting as FliC specific chaperone, preventing premature polymerization of FliC in the cytoplasm[182,183].

1.9.2 The virulence T3SS chaperones

1.9.2.1 Needle chaperones

The vT3SS needle substructure is assembled from a single secreted protein termed SctF. In some bacterial species these subunits are bound in the cytoplasm by needle chaperones, also known as Class III chaperones, that are characterised by having three tetratricopeptide repeat (TPR) motifs[184]. Unlike the other chaperone classes, class III chaperones are active as a ternary complex with the needle subunit, SctF[184,185,186]. Structures of the *Pseudomonas* PscF-PscG-PscE heterotrimeric complex revealed that the needle protein PscF contains an amphipathic helix which interacts with the concave hydrophobic surface of the PscG component of the complex[184]. Structures from *Yersinia* (YscF/YscE/YscG) and *Aeromonas* (AscE/AscG) have also been solved[185,186].

The second co-chaperone PscE/YscE/AscE does not interact with the needle protein but appears to be essential for the stability of PscG/YscG/AscG which, when deleted, reduces needle subunit export and cytotoxicity[171]. Interestingly, no chaperones have been identified for the flagellar FlgE subunit that assembles to form the equivalent flagellar hook structure, possibly because of the greater propensity of SctF to polymerise *in vitro*.

1.9.2.2. Tip complex and translocon chaperones

The vT3SS in most species contain a pentameric tip complex at the distal end of the needle, composed of the hydrophilic protein SctA. These tip proteins can be separated into two families based on their structural differences but also differ in the way they are targeted to the export machinery[187,188]. The *Shigella*/*Salmonella* family of tip proteins contain an alpha helical N-terminal domain that functions as an intramolecular chaperone, preventing premature oligomerisation within the cytoplasm[187]. The v-tip family of tip proteins, including LcrV (*Yersinia* spp) and PcrV (*Pseudomonas aeruginosa*) are bound by a specific chaperone, preventing self-aggregation but also have an additional role in regulating effector secretion[188,189,190,191].

Effector delivery across the host cell membrane and into the target cell requires the assembly of a protein translocon complex in the target eukaryotic host cell membrane[192,193]. This translocon complex is composed of multiple copies of two hydrophobic translocator proteins, SctB and SctE, which form a protein channel through which effectors can transit[194,192]. Efficient secretion of both translocator proteins depends on a shared chaperone, termed a class II chaperone[195]. The crystal structures of *Yersinia*, *Shigella* and *Pseudomonas* translocator chaperones revealed that, as for the early subunit chaperones, the translocator chaperones display a tetratricopeptide repeat fold and contain a mainly hydrophobic concave binding region that recognizes a conserved chaperone binding motif on the translocator subunits which consists of a hexapeptide containing 3 hydrophobic residues at positions 1, 3 and 6[196,197,198,199,200].

1.9.2.3. Effector chaperones

The class I effector chaperones are the most extensively studied and are further divided into two subclasses: class IA and IB. Class IA chaperones interact with a single substrate, usually encoded by a gene adjacent to the effector gene and include the SycE and SycH chaperones from *Yersinia*, SicP from *Salmonella* and SpcU from *Pseudomonas*. Class IB chaperones bind to multiple effector proteins and are typically encoded by a gene located in an operon containing genes that encode for structural components of the secretion apparatus[201] and includes the chaperones InvB from *Salmonella*, Spa15 from *Shigella* and CesT from enteropathogenic *E.coli* (EPEC). The Class I group of chaperones although sharing little sequence similarity, share a common structure consisting of an αβα sandwich fold and form highly stable dimers in solution (figure 1.6)[195,151.]

Crystal structures of these chaperones in complex with cognate subunit show that these chaperones maintain an extensive region of the substrate in an unfolded state[149,202]. The first structure of a Class I secretion chaperone in complex with substrate came from the crystal structure of the *Salmonella* chaperone SicP in complex with the chaperone binding domain of the effector protein SptP[149]. This revealed that approximately 100 amino acids at the N-terminus of SptP interacts with SicP by a combination of hydrophobic, polar and salt bridge interactions maintaining the chaperone binding domain of SptP in a non-globular state[149] . The crystal structure of the chaperone-binding domain of the *Yersinia* effector protein YopE in complex with its cognate chaperone, SycE showed that as seen in the SicP-SptP complex, that YopE wraps around a SycE chaperone homodimer and is maintained in a non-globular state[202]. Further structures of chaperone-effector complexes from *Yersinia* (SycH-YopH) and *Pseudomonas* (SpcU-ExoU) confirmed this, indicating that this is a common feature for all class I chaperones and may play a critical role in function[203,204]. Lilic et al. 2006 identified a conserved chaperone binding motif $[(LMIF)_1XXX(IV)_5XX(IV)_8XN_{10}]$ on type III effector proteins termed the beta motif which forms an intermolecular beta sheet with the hydrophobic pocket on class I chaperones[150]. This maintenance of the N-termini of effector proteins in a

largely unfolded state may aid substrate entry into the export channel where proteins must be unfolded for transit. As well as maintaining substrates in a non-globular state, many of the chaperones binding domains on effectors serve as membrane localization signals or transmembrane regions within the host cell membrane. These hydrophobic regions on the effector are buried by extensive contacts with the chaperone. In fact, chaperones have been shown to prevent erroneous targeting of effector proteins that contain membrane localization signals to the bacterial inner membrane by binding and occluding the localization signal[205,206].

1.10. Chaperone and substrate interactions with the T3SS export machinery

Unlike the early flagellar substrates, targeting of the late substrates to the export machinery is aided by export chaperones. Once subunits have engaged with their cognate export chaperones, these chaperone-subunit complexes are competent to interact with various components of the export machinery, although the sequence in which these interactions takes place are not fully understood. There is evidence that chaperone-subunit complexes can dock at the ATPase complex, the FlhA membrane export gate, and in the case of the vT3SS export chaperones, the C-ring[207,208,115,177,114,209,210]. Interactions at each of these components play distinct roles in preparing subunits for export as well regulating export activity and maintaining a secretion hierarchy.

1.10.1 The C-ring (C-pod)

The SpaO/FliM-N family of proteins forms a cytoplasmic ring (C-ring) structure at the cytoplasmic face of the inner membrane. The flagellar C-ring has been visualized by electron micrographs of purified flagellar basal bodies and more recently the C-ring of the *Shigella flexneri* virulence T3SS has been visualized by *in situ* cryoelectron tomography where the C-ring appears as a series of pod-like structures at the cytoplasmic face of the injectisome[211,212]. As well as localizing the ATPase to the inner membrane *via* the OrgB/FliH family of proteins, the injectisome SpaO family of proteins also function as a docking platform for

T3SS substrates[213,214]. HrcQ (the *Xanthomonas* SpaO homologue) interacts with both early and late T3SS substrates, suggesting the injectisome C-ring can recruit both early and late substrates[215]. The injectisome C-ring has been proposed to function as a 'sorting platform' that determines the order of protein secretion[210]. Immunoprecipitation of the C-ring protein SpaO from *Salmonella* showed that SpaO forms part of a higher molecular weight complex composed of SpaO (C-ring), InvC (the ATPase), OrgB (ATPase stator), OrgA (the ATPase cofactor), the T3SS needle tip, SipD and the translocases SipB and SipC. In the absence of the SipB, SpiC and SipD (which need to be export before the effectors) higher levels of the effectors SipA and SptP appear in the SpaO complex, suggesting the C-ring plays a role in substrate binding and controlling secretion hierarchy.

1.10.2 The ATPase complex

Chaperone-subunit complexes can dock at the FliI component of the ATPase complex, likely representing the first chaperone-subunit interaction at the export machinery[207]. Subunits must dissociate from their chaperones prior to secretion and be unfolded to transit through the narrow export channel[75,66]. The vT3SS ATPase was shown to achieve both dissociation of chaperone from their cognate subunit and subunit unfolding *in vitro*, a process dependent on ATP hydrolysis[208]. Authors proposed that T3SS ATPases may function in a similar manner to AAA+ ATPase disassembly machines *i.e.* disassemble protein complexes as well as recognize and unfold T3SS substrates[208,216]. However, chaperone-subunit complexes can dock at the FlhAc/SctVc component of the export machinery - an interaction thought to take place post-ATPase docking[115,217]. Furthermore, mutations in the export machinery that modulate energy transduction suppress export defects caused by deletion or inactivation of the ATPase, suggesting that unfolding and chaperone release may occur by an alternative mechanism[51,111,218]. The main role of the flagellar ATPase complex appears to be to localize FliJ at the export apparatus where it can bind to the export gate component, FlhA, allowing the export apparatus to efficiently use the proton motive force for subunit export[110,111]. These results suggest that chaperone-

subunit interactions with the flagellar ATPase may serve to enhance chaperone-subunit delivery to other components of the export machinery. In fact, It is proposed that the ATPase complex and associated C-ring components are in dynamic exchange between the cytoplasm and membrane export machinery[219,220,58]. This dynamic exchange has been suggested to aid subunit delivery to the export machinery[219]. The rate of subunit export is far greater than the rate of exchange, suggesting this exchange may enhance efficiency rather than being central for subunit delivery.

The ATP bound form of FliI/SctN enhances docking of chaperone-subunit complexes at FliI/SctN[221]. This Indicates that chaperone-subunit complexes preferentially bind the ATP-bound conformation of FliI/SctN. It is conceivable that ATP hydrolysis and FliJ-dependent activation of the export machinery is coupled to release of chaperone-subunit complexes from FliI/SctN for subsequent binding to the membrane export gate, SctVc. A number of studies have identified interactions between the injectisome chaperones and the T3SS ATPase, SctN[106,222,223]. For the EPEC chaperone CesAB, NMR revealed that a combination of acidic, basic and polar residues and a conserved tyrosine residue in CesAB are involved in mediating its interaction with the EPEC T3SS ATPase, EscN[222]. Modelling based on mutations that abrogate an SctN-chaperone interaction indicated that chaperones bind the membrane proximal face of SctN[223], which would be favourable for handover of chaperone-subunit complexes to the membrane export gate, FlhAc/SctVc.

The FliJ/SctO stalk component of the ATPase complex interacts with the membrane export gate, FlhA/SctV, activating the export machinery to promote efficient $\Delta\psi$ driven protein export[224,111]. The injectisome SctO stalk also binds the chaperones for the translocator proteins and in the case of the flagellar T3SS, the chaperones for the filament cap and hook-filament junction proteins[225,226]. This FliJ/SctO-chaperone interaction can only occur when chaperones are not bound to subunit[226]. The flagellar subunits have been shown to capture FliJ-bound chaperones from FliJ/SctO, this capture of chaperones by subunits was

proposed to serve as a mechanism to recruit the chaperones for the hook-filament junction and cap subunits and retain them at the export machinery to promote the export of the hook-filament junction and filament cap proteins to ensure that the hook-filament junction complex and filament cap assembles prior to filament assembly[226].

1.10.3 The FlhA export gate

Chaperone-subunit complexes can also interact with the cytoplasmic domain of SctV/FlhA[177,116,115,227]. The first interaction between a member of the SctV/FlhA family and export chaperone was identified in a yeast-two hybrid screen [228]. The multi-effector chaperone HpaB from *Xanthomonas axonopodis* pv. Citri was found to interact with the C-terminal domain of SctV (HrcV)[228,229]. More recently, interactions between the flagellar homologue, FlhA and flagellar chaperone-substrate complexes have been identified for all three flagellar chaperones: FlgN, FliT and FlgN[177,116,115]. Indicating that chaperone binding to FlhA is a conserved mechanism in type III secretion. The flagellar chaperone-FlhAc interaction occurs *via* a conserved tyrosine residue found on all three flagellar chaperones and a highly conserved hydrophobic pocket in FlhAc[116,115,227]. The binding affinities of FlhAc for the FlgN-FlgK and FliT/FliD complexes were found to be 37 nM and 43 nM respectively[115]. In contrast**,** the binding affinity of the FliS-FliC complex to FlhAc was found to be 14-fold weaker than for FlgN-FlgK and FliT-FliD, at 500 nM[115]. These different binding affinities may promote efficient assembly of the hook-filament junction and filament cap prior to filament assembly or alternatively may reflect differences in the expression levels of flagellin and the hook-filament junction and filament cap proteins. The exact role of chaperone-subunit binding at FlhAc is unclear although it is feasible that the position of FlhAc directly below the $FlhA_N$ proton channel may allow energy derived from PMF to aid subunit unfolding[108,227]. In fact, a study by Minamino and colleagues identified bypass mutants of a *Salmonella ΔfliS* mutant that were all located in the *fliC* gene[230]. These bypass mutants decreased the thermal stability of FliC and increased the rate of FliC export in the absence of its cognate chaperone, FliS. This led authors to propose that the binding of the FliS-FliC

chaperone-subunit complex to FlhAc may serve to anchor FliC to the FlhAc platform for efficient FliC unfolding[230].

Molecular dynamic simulations of FlhAc supported by biochemical and genetic analysis of FlhAc mutants suggest that FlhAc fluctuates between an open and closed state and that this dynamic motion of FlhAc is essential for protein export[109,231]. More recently, the structures of the open and closed forms of *Salmonella* FlhAc show that the chaperone-binding site is occluded in the closed form and reduces the binding affinity of FlhAc for flagellar chaperones[232]. It is feasible that the closed FlhAc conformation is stabilized during early subunit export and that the export specificity switch stabilises the open FlhAc conformation, allowing chaperone-subunit complexes to bind FlhAc and therefore promote the export of late substrates[231,232].

Once the chaperoned subunits have been delivered to FlhAc, they are thought to be released from their cognate chaperone, unfolded and translocated across the inner membrane, where they transit sequentially through the FlhAB-FliPQR export gate, the rod, the hook or needle and, in the case of the injectosome, into the host cell or, in the case of the flagellum, through the filament to the flagellar tip where they fold into the nascent structure[8,9,105].

1.11 Energising subunit transit through the export channel

Once subunits have been unfolded and translocated into the export channel at the core of the flagellum, they must transit to the tip where they refold into the nascent structure[141,8,9]. It is assumed that the proton motive force is the primary energy source for energising the movement of subunit across the inner membrane into the export channel, however, how subunits subsequently transit the long distance to the flagellum tip is much debated in the field, with several models having been proposed to explain how subunit transit is energised through the central channel in the needle or filament[233,141,174]. Each model is described in detail in the following sections.

1.11.1 Electrostatic repulsion

The electrostatic repulsion model proposed that charged residues on the transiting subunit and on the interior wall of the channel would propel subunits through the channel[233]. This model was based on the incorrect model of the vT3SS needle, which predicted a strong negative charge in the channel[233]. The solid-state NMR structures of the needle shows that the channel is in fact mostly lined with polar residues and contains a single C-terminal arginine residue (also present in the flagellar hook and filament) which introduces a positive charge in the channel[234,235,236,73]. Furthermore, subunits and recombinant proteins that can be efficiently exported *via* T3SSs contain a combination of both positive and negative charges that, by this model, would result in both repulsive and attractive forces, meaning that some regions of transiting polypeptides could interact with the wall of the channel slowing down export[233,237,238].

1.11.2 Chain mechanism

Evans and colleagues proposed that subunits transit through the channel by forming interactions between their N- and C-termini, effectively forming a multi-subunit chain from the export machinery to the filament tip[141]. The chain mechanism predicts that the N-terminus of a subunit exported into the channel interacts with C-terminus of the preceding subunit already inserted into the channel. As subunits reach the distal tip, subunits fold into the nascent structure, which anchors the chain and provides it directionality for chain movement. Subunit folding tightens the chain and this is proposed to provide enough force to pull the next subunit that is docked at the export machinery into the export channel, repeating the process. Experimental evidence for this model was provided by three observations. The first was that *in vitro*, early subunits docked at FlhBc could be captured by the C-terminus of free subunits in a concentration dependent manner. These capture assays were all performed with FlgD (hook cap) subunit docked at FlhBc and challenged with FlgE, FlgD or FliK subunits. One criticism may be that all of these challenge subunit are known to interact with FlgD either in the assembled structure or during export[239,240]. Therefore, capture of FlgD from FlhBc could be due to other weak interactions taking place

between subunits rather than head-to-tail capture between subunit termini. The second piece of evidence comes from *in vitro* and *in vivo* cysteine crosslinking experiments, whereby early or late subunits could form intermolecular disulphide bonds when cysteine residues were placed between residues 14 and 32 of the N-terminus and residue 400 (FlgE) or residue 488 (FliC) of the C-terminus. These termini regions were predicted to form head-to-tail parallel coiled-coils that hold the chain together until the subunits are released from the channel. The recent structure of the rod and hook revealed that the central channel is narrower (13 Å) than the filament (20 Å), whether such a head-to-tail coiled coil structure can be accommodated in the export channel is uncertain, the diameter of canonical coiled-coil structures such as leucine zippers have a diameter that exceeds the width of the export channel[241,242], suggesting that if subunits do interact at their termini within the channel then they must form an alternative structure. The third interesting observation was that deletion of the C-terminus of FlgE attenuated its export, which authors proposed was caused by the inability of subunits to form a subunit chain[141].

1.11.3 Diffusion

The diffusion model proposes that subunits transit through the channel by single file diffusion and that a pump in the membrane powered by the PMF supplies subunits into the export channel[243,174]. Two publications used fluorescence real time imaging to show that the filament growth rate decreases with filament length[244,174]. Initial filament growth rate in *Salmonella* was found to be 100 nM/min which decreased to 20 nM/min for longer filaments[174]. This led Renault and colleagues to propose a model whereby subunits are injected into the export channel and that subunits subsequently diffuse to the filament tip, as the filament lengthens and the distance a subunit needs to travel increases the rate of subunit export decreases. Authors also showed that cells producing flagellin variants that do not contain the C-terminal D0 domain of flagellin that would be expected to disrupt the formation of head-to-tail linkages had no affect on filament growth rate, providing evidence against the chain mechanism. Of course, it is possible that any sequence at the termini is sufficient to form a head-to-tail interaction in

the narrow confines of the export channel and that specifically deleting the D0 domain does not break a chain. There are many unanswered questions such as whether subunits interact with the channel wall, what structure if any do subunits form during subunit transit, and if/how subunits interact at their termini during subunit transit?

1.12 Aims of this thesis

The aim of this study is to gain an understanding of how the export signals that reside within early flagellar subunits contribute to subunit export, how the proton motive force (PMF) contributes to the export mechanism and how this is regulated. Many of the core export components that recognise export substrates and energise subunit export are conserved between the flagellar and virulence type III secretion systems, meaning that the mechanism of export and subunit interactions with the export machinery may be conserved accross these two systems. A combination of genetic, biochemical and microbiological techniques was used to gain insight into some of the outstanding questions in type III secretion:

1) How does early subunit docking at the FlhBc export gate contribute to subunit export?
2) What triggers opening of the export gate?
3) What energises opening of the export gate?
4) How is FliJ-dependent activation of the export machinery regulated?
5) Do flagellar export chaperones interact sequentially with components of the export machinery?

It is hoped that my findings will contribute to the understanding of how the type III export machinery achieves highly efficient subunit export. In understanding how the export machinery operates, it may allow scientists to develop new therapeutics against a range of pathogenic bacteria. Furthermore, understanding how the export machinery is regulated may allow engineering of strains optimised for maximal secretion of recombinant proteins for biotechnological purposes.

Chapter 2

Materials and Methods

2.1 Reagents, buffers and media

Chemicals were purchased from established commercial suppliers namely: New England Biolabs, ThermoFisher Scientific, Sigma-Aldrich, Cambridge Bioscience, Illumina and GE Healthcare. Details of buffers and media composition can be found in Table A1.1.

2.2 Enzymes

All enzymes were purchased from New England Biolabs, ThermoFisher Scientific or Sigma-Aldrich and used according to the manufacturer's instructions.

2.3 Oligonucleotides

All oligonucleotides were purchased from Sigma-Aldrich at desalt purification. Primers were stored in deionised water at -20°C.

2.4 Antibiotics

Antibiotics were purchased from Sigma-Aldrich and used at the following concentrations: ampicillin 50 μg/ml, carbenicillin 50 μg/ml, kanamycin 50 μg/ml, chloramphenicol 20 μg/ml and spectinomycin 100 μg/ml. Stock solutions of 50 mg/ml ampicillin and carbenicillin were prepared using 50% ethanol and were sterilised by filtration through a 0.22 μm syringe filter (Sartorius). 20 mg/ml chloramphenicol was prepared in 100% ethanol, whilst 50 mg/ml kanamycin and 50 mg/ml spectinomycin stocks were prepared with deionised water. All antibiotic stocks were stored at -20°C.

2.5 Plasmids

All plasmids were stored in deionised water at -20°C. A list of plasmids used in this study can be found in table A1.2.

2.6 Isolation, manipulation and analysis of DNA

2.6.1. Isolation of plasmid DNA

Plasmid DNA was isolated from 5 ml of overnight liquid culture using PureLink Quick Plasmid Miniprep Kit (ThermoFisher Scientific). Plasmid DNA was eluted from the column with 30 μl deionized water.

2.6.2 Agarose gel electrophoresis and DNA extraction from agarose gels

DNA was analysed by agarose gel electrophoresis with 1% agarose in 1x TAE buffer containing 1x SYBR-safe. DNA was visualized with Blue light using an Azure Biosystems c500 gel imaging system. Fragment sizes were estimated by comparing with a 2-log DNA ladder (NEB). Gel bands were excised and DNA extracted using a GeneJET gel extraction kit (ThermoFisher Scientific). DNA was eluted from the columns with 30 μl deionized water.

2.7 Polymerase Chain Reaction (PCR)

2.7.1 Amplification of DNA by PCR

DNA was amplified using Q5 hot start high-fidelity polymerase (NEB) according to manufacturer's instructions. Extension time was adjusted depending on the PCR fragment length, and primer annealing temperatures were adjusted depending on the estimated primer melting temperature. Reactions were set up as follows:

Reaction mix

5X Q5 polymerase buffer	10 μl
10 mM dNTPs	1 μl
10 μM Forward primer	2.5 μl
10 μM Reverse primer	2.5 μl
Template DNA	variable
Q5 High-Fidelity DNA polymerase	0.5 μl
5X Q5 High GC Enhancer	10 μl
Nuclease-free water	to 50 μl

Thermocycling conditions

Initial denaturation	98°C, 30 seconds
30 cycles	98°C (denaturation), 10 seconds
	50-72°C (annealing), 30 seconds
	72°C (extension), 30 seconds/kb
Final extension	72°C, 2 minutes
Hold	10°C

2.7.2 Overlap extension PCR

Overlap extension PCR was used to introduce mutations, insertions or deletions at a specific location in a target DNA molecule (Figure 2.1). Overlap extension PCR reactions were performed using the same reagents and conditions as for standard PCR. Two primers reverse complementary to each other were designed such that they introduced a mutation in the middle of each primer. Another two outer primers were designed to amplify the full-length DNA sequence of interest. Two rounds of PCR were used. The first round generated two PCR fragments containing the mutation of interest. These two fragments were excised from the agarose gel, purified and were then used as template in a second round of PCR using the two outer primers to generate the DNA fragment containing the desired mutation(s). This product was then used in the construction of bacterial strains or to generate recombinant plasmids.

2.8 Construction of recombinant plasmids

2.8.1 Preparation of vector and insert

Insert and vector DNA were digested with restriction enzymes (NEB or ThermoFisher Scientific) at 37°C for 3 hours. 10 U of calf intestinal alkaline phosphatase (NEB) was included in the vector digest reaction to dephosphorylate the cut vector 5' end and prevent self-ligation. Digested vector was run on a 1% agarose gel, excised and purified using a GeneJET gel extraction kit (ThermoFisher Scientific) according to the manufacturer's

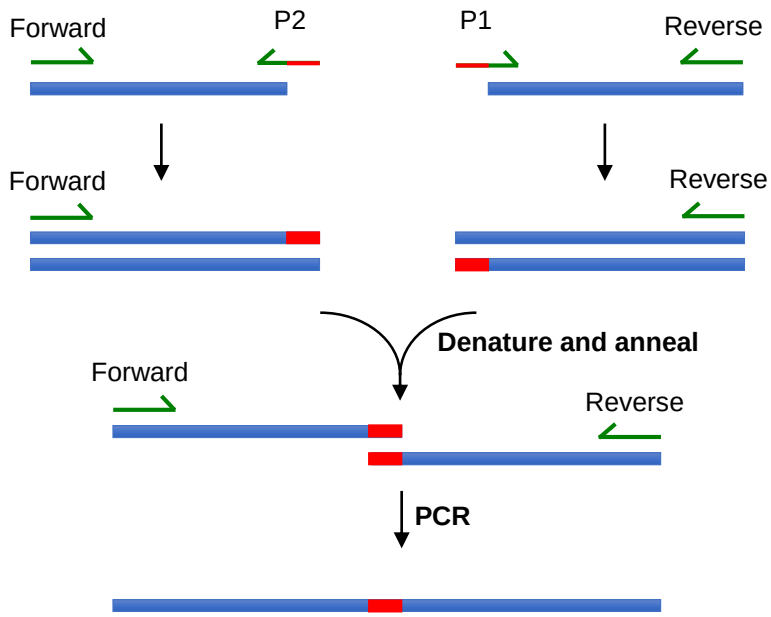

Figure 2.1. Overlap extension PCR
Overview of the overlap extension PCR protocol. Two internal primers (P1 and P2) contain complementary regions (red) which introduce mutations, deletions or a fusion to the desired region of interest. The first round of PCR produces two PCR products that contain the complementary region (red) and contains the mutations, deletion or fusion of interest. The final PCR is carried out by mixing, denaturing and annealing the two PCR products from the first round and carrying out a final PCR reaction using the forward and reverse primers.

instructions. Digested inserts were purified directly using a GeneJet gel extraction kit (ThermoFisher Scientific).

2.8.2 DNA ligation

Insert and vector DNA were mixed at a 3:1 molar ratio with 1x T4 DNA ligase buffer and 5 U T4 DNA ligase (ThermoFisher Scientific) and incubated at 22°C for 1 hour. The T4 DNA ligase was inactivated by heating the reaction mixture at 70°C for 5 minutes. The ligation mixture (4 μl) was transformed by electroporation into 50 μl of electrocompetent TOP10 or DH10β cells and recovered in SOC media at 37°C with shaking (200 rpm) for 1 hour before being plated onto LB-agar plates containing appropriate antibiotics. Following overnight incubation of plates, colonies were tested to check if they contained the vector and the desired insert using colony PCR.

2.8.3 Verification of recombinant plasmids

To check that the vector contained the desired insert, transformants were screened for by colony PCR using vector-specific and insert-specific primers using Reddymix PCR 2X Master Mix (ThermoFisher Scientific). Overnight cultures and plasmids were purified and sent to the Department of Biochemistry sequencing facility for Sanger sequencing.

2.9 Preparation and transformation of electrocompetent cells

2.9.1 Escherichia coli and Salmonella enterica serovar Typhimurium strains

A single colony was used to inoculate LB broth and cultures were grown overnight at 37°C with shaking (200 rpm). Overnight cultures were diluted 1:100 in LB broth and grown with shaking (200 rpm) at 37°C to A_{600} 0.4-0.6. Cultures were cooled by placing the culture flask on ice for 10 minutes and cells were collected by centrifugation (5000 g, 3 min, 4°C). Cells were resuspended twice in deionized water pre-cooled to 4°C and collected by centrifugation (5000 g, 3 min, 4°C). Cells to be used immediately for transformation were resuspended in a small volume of cooled deionized water and stored on ice. Cells to be stored

for later use were resuspended in 10% glycerol and 100 μl aliquots were snap frozen in liquid nitrogen and stored at -80°C. Prior to transformation, electrocompetent cells were thawed on ice. Thawed cells (50 μl) were mixed with DNA in a 1 mm cuvette (Bio-Rad). Cells were transformed by electroporation with the Gene Pulser II system (Bio-Rad) with the following settings: 200 Ω, 1.25 kV, 25 μF. Transformed cells were resuspended in SOC media and recovered at 37°C for 1 hour with shaking at 200 rpm before being plated onto LB agar plates containing appropriate antibiotics.

2.10 Construction of bacterial strains

Escherichia coli and *Salmonella enterica* serovar Typhimurium strains were constructed using a method modified from Hoffman *et al.*, 2017 (Figure 2.2)[245]. Oligonucleotides were designed to replace the desired gene with either a kanamycin (containing an internal I-*Sce*I endonuclease site) or spectinomycin resistance cassette. To replace a target gene with the I-*Sce*I containing kanamycin resistance cassette, oligonucleotides were designed to amplify the resistance cassette encoded on plasmid pWR717. Oligonucleotides were designed such that the amplified resistance cassette was flanked at its 5' and 3' ends by 45 nucleotides homologous to the regions flanking the target gene. A lambda red recombinase controlled by a heat-inducible promoter encoded on plasmid pWRG730 was used to integrate the desired resistance cassette into the chromosome.

Salmonella or *E.coli* strains were transformed with the pWRG730 vector and spread onto LB agar plates containing 20 μg/ml chloramphenicol and incubated overnight at 30°C. LB broth containing chloramphenicol (20 μg/ml) was inoculated with a single transformant colony and grown overnight at 30°C with shaking (200 RPM). The overnight culture was diluted 1:300 into 50 ml LB broth containing 20 μg/ml chloramphenicol and grown at 30°C with shaking (200 RPM) to A_{600} 0.5. Cultures were then incubated in a 42°C water bath with shaking (100 RPM) for 12 minutes to induce expression of the lambda red recombinase. Cultures were cooled on ice for 10 minutes before being washed twice in cooled

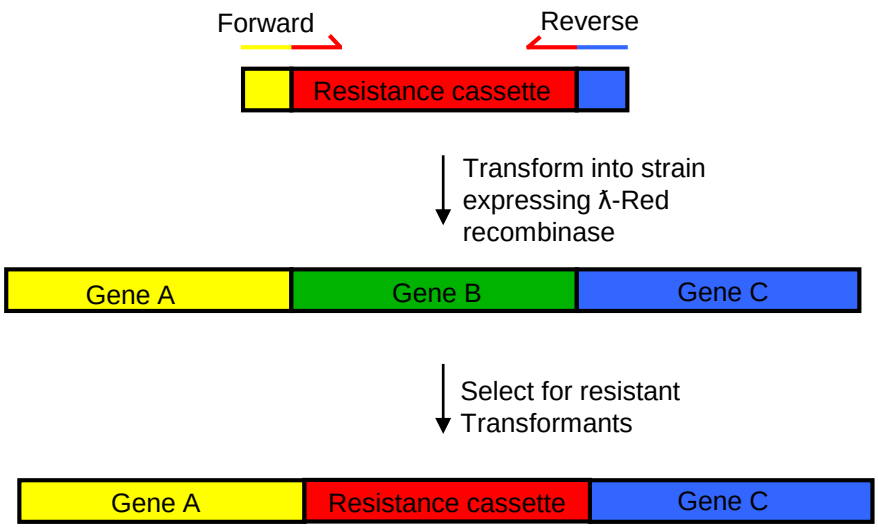

Figure 2.2. Generating gene deletions within *Salmonella*
A resistance cassette is amplified by PCR using forward and reverse primers that contain at least 40 bp homology extensions (blue or yellow) to the flanking regions of the desired disruption site. A strain expressing ƛ-Red recombinase is transformed with the PCR product and antibiotic resistant transformants are selected.

deionised water. Cells were resuspended in 200 μl cooled deionized water before being transformed with 50-100 ng of PCR product and recovered for 1 hour at 30°C in 500 μl SOC. Transformants were selected on LB agar plates containing 50 μg/ml kanamycin and 20 μg/ml chloramphenicol at 30°C. Cells containing the resistance cassettes were confirmed by sequencing. Kanamycin was replaced with 100 μg/ml spectinomycin for recombineering with the spectinomycin resistance cassette.

To remove the kanamycin resistance cassette to introduce in-frame chromosomal deletions, point mutations or insertions, strains encoding the I-*Sce*I restriction site containing kanamycin cassette and carrying the lambda red recombinase and tetracycline-inducible I-*Sce*I endonuclease on pWRG730 were made electrocompetent as described above, except cells were resuspended in 10 ml cooled deionized water following the wash steps. Overlap extension PCR was used to generate a PCR product containing the desired in-frame deletion, point mutation or insertion flanked at the 5' and 3' end by 150 nucleotides homologous to the region flanking the chromosomally-encoded kanamycin resistance cassette. The cells were transformed with the PCR product and recovered for 1 hour at 30°C in 500 μl SOC. Cells were plated on LB agar containing 20 μg/ml chloramphenicol and 500 ng/ml anhydrotetracycline to induce expression of the I-*Sce*I endonuclease. The endonuclease recognises the 18-bp I-*Sce*I restriction site within the kanamycin resistance cassette causing a double strand break and killing any cells still containing the kanamycin resistance cassette, leaving only cells that have removed the cassette. Colonies in which the resistance cassette was replaced with the desired sequence were confirmed by sequencing. Cells were plated onto LB agar plates and incubated overnight at 42°C to remove pWRG730. To confirm the loss of pWRG730 vector, colonies were streaked onto LB agar and onto LB agar containing 20 μg/ml chloramphenicol and incubated overnight at 37°C. Strains that grow on LB agar but not on the chloramphenicol containing LB agar have successfully lost the pWRG730 vector.

2.11 Expression of recombinant proteins for purification

E.coli C41 (DE3) cells were transformed with recombinant expression plasmid carrying the desired gene(s) and plated onto LB agar containing the appropriate antibiotics. LB broth containing the appropriate antibiotic(s) was inoculated with a single colony and incubated overnight at 37°C with shaking (200 RPM). The overnight culture was diluted 1:100 into 2X Yeast Tryptone (2XYT) broth with appropriate antibiotic(s) and incubated at 37°C with shaking (200 RPM) until cultures reached A_{600} 0.6. Cultures were cooled to 18°C and protein expression induced by the addition of isopropylthiogalactoside (IPTG) to a final concentration of 0.5 mM. Cells were incubated at 18°C with shaking (200 RPM) for a further 12-16 hours. Cells were harvested by centrifugation (6,000 g, 10 min, 4°C) and cell pellets frozen (-20°C) for later use.

2.12 Protein purification

2.12.1 Purification of His-tagged proteins

Cells were resuspended in buffer A (table A1.1) supplemented with one tablet of EDTA-free cOmplete protease inhibitor cocktail (ROCHE) and 2 U DNAse I (ThermoFisher Scientific) per cell pellet (corresponding to cells collected from a 1 litre culture). Cells were lysed by mechanical disruption at 30 kpsi (Constant Systems LTD). Supernatants were clarified by centrifugation (40000 g, 60 min, 4°C) and loaded onto a 1 ml HITRAP excel Nickel column (GE healthcare). The column was washed with 40 ml of buffer A. Proteins were eluted with buffer B and dialysed overnight in Buffer C (table A1.1).

2.12.2 Purification of glutathione-S-transferase (GST)-tagged proteins

Cells containing GST-tagged proteins were resuspended in buffer D (table A1.1) supplemented with one tablet of EDTA-free cOmplete protease inhibitor cocktail (ROCHE) and 2 U DNAse I (ThermoFisher Scientific) per litre cell pellet. Cells were lysed by mechanical disruption at 30 kpsi (Constant Systems LTD). Supernatants were clarified by centrifugation (40,000 g, 60 min, 4°C). Supernatants were mixed with 400 μl washed Glutathione Sepharose 4B resin (GE Healthcare) and washed with 20 column volumes of buffer E (table A1.1).

2.13 Electrophoresis of proteins

Proteins were separated according to size by sodium dodecyl sulphate polyacrylamide gel electrophoresis (SDS-PAGE). Samples were resuspended in 2x SDS loading buffer containing 100 mM β-mercaptoethanol and boiled at 95°C for 10 minutes to denature the proteins. Samples were run on 10%, 12.5% or 20% SDS-PAGE depending on the molecular weight of the protein of interest. Gels were run at 150 volts for 60 minutes and proteins were visualized by staining with InstantBlue (Expedeon).

2.14 Immunoblotting of proteins

Proteins were separated by SDS-PAGE and were transferred onto nitrocellulose membrane with a pore size 0.45 μm (GE Healthcare). Transfer was carried out at 400 mA, 100V for 1.5 hours in Transfer buffer (10 mM CAPS pH 11.0, 10% (v/v) methanol) in a TE22 wet transfer tank (Hoefer). Following transfer, membranes were blocked in phosphate buffered saline containing 0.05% (v/v) Triton X-100 (VWR) (PBST) and 5% (w/v) skimmed milk (Marvel) for one hour.

Membranes were transferred to fresh blocking solution (5 ml) containing diluted primary antibody and 250 μl of SJW1103 Δ*flhDC* soluble lysate to aid removal of non-specific background signal and were incubated for between 1 hour to overnight. Membranes were washed three times, 5 minutes each in PBST. Membranes were placed in fresh blocking solution (5 ml) containing IRDye 680RD donkey anti-mouse of IRDye 800CW donkey anti-rabbit secondary antibodies (LI-COR Biosciences) at a dilution of 1:5000 and incubated in the dark for one hour. Membranes were subsequently washed once in PBST and once in PBS. Blots were analysed with an Azure Biosystems c500 imaging system.

2.15 Subunit export assay

For complementation and dominance studies, *Salmonella* SJW1103 and derived strains carrying pTrc99a encoding wild type or variant proteins were grown in LB broth containing antibiotic and inducing agent (as appropriate) to A_{600} 1.0. Cells were centrifuged (6000*g*, 5 min) and resuspended in fresh media and grown for

a further 60 min at 37°C. Cells were pelleted by centrifugation (16,000*g*, 5 min) and the supernatant passed through a 0.22 µm nitrocellulose filter (Sartorius). Proteins were precipitated with 10% trichloroacetic acid (TCA) and 1% Triton-X100 on ice for 1 hour, pelleted by centrifugation (16,000*g*, 10 min, 4°C), washed with ice-cold acetone and resuspended in SDS-PAGE loading buffer (volumes calibrated according to cell densities). Fractions were analysed by immunoblotting. Subunit export assays of strains not carrying pTrc99a were performed essentially as described above except antibiotic and inducing agents were not included in the LB broth.

2.16 Swimming motility assay

For complementation and dominance studies, *Salmonella* SJW1103 and derived strains carrying pTrc99a encoding wild type or variant proteins were grown in LB broth containing antibiotic and inducing agent (as appropriate) to A_{600} 1.0. Two microlitres of culture was inoculated into soft tryptone agar plates (0.3% agar, 1% w/v tryptone and 0.5% w/v sodium chloride) containing IPTG (0 – 1 mM) to induce recombinant protein expression. Plates were incubated at 37°C for between 3 and 6 hours.

2.17 Swarming motility assay

For swarming motility, one microliter of overnight culture grown in LB broth was inoculated onto tryptone agar plates (0.6% agar, 1% w/v tryptone, 0.5% w/v sodium chloride) containing appropriate antibiotics and inducing agents and supplemented with 0.3% glucose and incubated at 30 °C for 12-16 hours.

2.18 In vitro and in vivo affinity chromatography purification assays

In vitro pull-down assays were carried out using GST-tagged or His-tagged proteins as bait. Cleared cell lysates containing overexpressed prey proteins were incubated for one hour with glutathione sepharose 4B resin (GE healthcare; for GST-tagged proteins) or with cobalt resin or nickel resin (ThermoFisher scientific, Qiagen; for His-tagged proteins) at 4°C. Samples were washed extensively with wash buffer E (GST-tagged proteins) or buffer D (His-tagged proteins; table A1.1). Cell lysates containing over expressed untagged prey

proteins were then incubated with the resin pre-bound by GST/His-bait. Resins were washed extensively with wash buffer and proteins were eluted in SDS loading buffer. The *in vivo* pull-down of His-tagged FliJ was carried out using cobalt-NTA resin (Qiagen). Cleared cell lysates were incubated with Co-NTA resin for 1 hour at 4°C. The resin was washed with 10 column volumes of wash buffer D (table A1.1). Proteins were eluted from the resin by boiling in SDS loading buffer, separated by 15% SDS-PAGE and analysed by staining with InstantBlue (Expedeon).

2.19 In vitro binding competition assay

Recombinant proteins were expressed in *E.coli* C41 and mechanically lysed as described for the co-purification assays. Cleared lysates containing His-tagged FliJ were incubated with cobalt affinity resin for 1 hour. After extensive washing, cell lysates containing overexpressed untagged $FlhA_C$ were added to each resin fraction and an equal volume of lysates containing wild type FliT94, FliT94 L72A, wild type FlgN or FlgN W78A were added. Proteins were incubated for 1 hour, the resin was washed extensively with buffer D (table A1.1) and proteins were eluted by boiling in SDS-PAGE loading buffer. Proteins were separated by SDS-PAGE and analysed by immunoblotting.

2.20 Choline sensitivity assay

The choline sensitivity assay was performed essentially as described in Ward *et al.*[246]. Cells were grown overnight at 32°C in terrific broth (TB) medium with shaking (200 PRM). The overnight cultures were diluted 1:50 in TB and grown at 32°C with shaking (200 RPM) to an A_{600} 1.0. These cultures were diluted 1:50 in TB containing choline at concentrations as indicated in Figure 4.3. The cultures were grown for 4.5 hours at 32°C with shaking (200 RPM) and the A_{600} measured. The Miles and Misra method[247] was used to determine the colony forming units for strains grown in 300 mM choline. 10-fold dilutions of the cultures (as indicated in Figure 4.3) were spotted (10 μl) onto LB agar plates and grown overnight at 37°C.

2.21 Ribosome profiling and RNA-sequencing

2.21.1 Growing and harvesting cells for ribosome profiling

Bacteria were streaked onto a LB agar plate and incubated overnight at 37°C. A single colony was used to inoculate LB (10 ml) and incubated overnight at 37°C with shaking (180 RPM). The overnight culture was diluted 1:100 in LB (50 ml) and grown in a 250 ml flask at 37°C with shaking (180 RPM) in a water bath (to avoid any large perturbations in temperature). Once the culture reached A_{600} 1.0, 500 μl of chloramphenicol (150 mg/ml in 100% ethanol) was added to the culture, which was incubated in the water bath with shaking for 1 minute. The culture was immediately poured over frozen LB containing chloramphenicol (1500 μg/ml) into a new 250 ml flask and cells were immediately pelleted by centrifugation (6000 g, 2 min, 4°C). Cells were resuspended in profiling buffer (1 ml; table A1.1), frozen by plunging in liquid nitrogen and stored at -80°C for later use.

2.21.2 Preparation of cell extracts

Frozen cells were ground to a fine powder in liquid nitrogen using a pestle and mortar. The ground cells were allowed to thaw and were immediately transferred to a 2 ml tube and clarified by centrifugation (13,000 g, 2 min, 4°C). The supernatant was transferred to a new tube and the A_{254} was adjusted to 10 with profiling buffer. Aliquots (100 μl) of lysate were snap frozen in liquid nitrogen and stored at -80°C.

2.21.3 Nuclease footprinting and ribosome recovery

Cell extracts (100 μl) were thawed on ice and 7.5 μl RNase I (Ambion, 100 U/μl) was added and incubated in a thermoblock for 30 minutes at 28°C with shaking (400 RPM). To stop the nuclease digestion, 10 μl SUPERase•In RNase inhibitor (ThermoFisher Scientiific) was added before placing the sample on ice. To purify monosomes, digested extracts were spun through pre-equilibrated S400 columns by centrifugation (600 g, 2 min, 20°C). To extract the RNA, TRIzol (1 ml) was added and incubated at room temperature for 2 minutes. Chloroform (200 μl) was added to the TRIzol solution and vortexed for 10 seconds. The organic and aqueous phases were separated by centrifugation (13,000 g, 10

min, 4°C). The upper clear aqueous phase was placed in a new 1.5 ml tube and glycoblue (2 μl), 3 M sodium acetate pH 5.2 (70 μl) and ice-cold isopropanol (700 μl) was added and the sample stored at -80°C for 12 hours to precipitate the RNA. The precipitated RNA was collected by centrifugation (13,000 g, 10 min, 4°C), washed twice in ice-cold 80% ethanol and resuspended in 10mM Tris-HCl pH 7.5 (10 μl). A Ribo-Zero rRNA Removal Kit (Bacteria) Magnetic Kit (Illumina) was used to deplete ribosomal RNA and enrich for nuclease protected fragments (following the manufacturer's instructions).

2.21.4 RNA extraction for RNA sequencing (RNA-seq)

To extract total RNA, an aliquot (100 μl) of cell extract was thawed on ice. TRIzol (1 ml) was added and incubated at room temperature for 2 minutes. Chloroform (200 μl) was added to the TRIzol solution and vortexed for 10 seconds. The organic and aqueous phases were separated by centrifugation (13,000 g, 10 min, 4°C). The upper clear aqueous phase was placed in a new 1.5 ml tube and glycoblue (2 μl), 3 M sodium acetate pH 5.2 (70 μl) and ice-cold isopropanol (700 μl) was added. The sample was stored at -80°C for 15 hours to precipitate the RNA. The precipitated RNA was collected by centrifugation (13,000 g, 10 min, 4°C) and washed twice in ice-cold 80% ethanol. Ribosomal RNA was depleted using a Ribo-Zero rRNA Removal Kit (Bacteria) Magnetic Kit (Illumina) (following the manufacturer's instructions).

2.21.5 RNA fragmentation for RNA-seq

RNA was fragmented by alkaline hydrolysis. Total RNA (10 μl) was added to 2x fragmentation buffer (10 μl) (table A1.1) and incubated at 95°C for 15 minutes. The reaction was stopped by adding 280 μl alkaline hydrolysis stop solution (table A1.1) followed by 750 μl ice-cold ethanol and was incubated overnight at -80°C to precipitate RNA. The RNA was washed twice in ice-cold 80% ethanol and resuspended in 5 μl 10mM Tris-HCl pH 7.5.

2.21.6 Generation of libraries for next generation sequencing

Libraries were generated in the same way for both RNA extracted from nuclease footprinting and from RNA fragmentation. RNA was treated with T4 polynucleotide kinase (PNK; Sigma) in PNK buffer without ATP to remove the 3' phosphoryl group from the RNA. The reaction was set up as follows:

3' phosphatase reaction mix:

RNA	5 μl
10X PNK buffer A (No ATP)	1 μl
SUPERase•In RNase inhibitor	0.5 μl
T4 PNK (10 U/μl)	2 μl
Water	1.5 μl

Conditions:

Phosphatase reaction	37°C, 2 hours
Heat Inactivation	75°C, 10 minutes

PNK treated RNA was separated by electrophoresis on a 15% TBE-UREA polyacrylamide gel at 120V for 50 minutes and stained with SYBR Gold (ThermoFisher Scientific) and visualized under blue light. To select for RNA corresponding to the size of ribosome protected fragments gel fragments excised from the region just below a 28 nucleotide marker up to a 34 nucleotide marker. The same region was collected for the alkaline hydrolysis treated RNA samples. The RNA was extracted by overnight incubation in 600 μl RNA gel extraction buffer (table A1.1). The gel fragments were removed from the RNA extraction buffer by filtering through a 0.22 μm pore size acetate filter. The RNA was precipitated with 2 μl glycoblue, 20 μl 3M sodium acetate pH 5.2 and 600 μl ice-cold isopropanol. The RNA was washed twice in ice-cold 80% ethanol and resuspended in 5 μl 10mM Tris-HCl pH 7.5.

A ligation reaction was carried out to ligate a pre-adenylated DNA adapter (5' TGGAATTCTCGGGTGCCAAGG 3') to the dephosphorylated RNA using T4 RNA ligase 2 truncated K227Q (NEB) which specifically ligates the 5' end of pre-adenylated DNA or RNA to the 3' hydroxyl end of RNA. The ligation reaction mix was incubated at 16°C for 16 hours and was set up as follows:

3' ligation reaction mix

RNA	5 μl
5' pre-adenylated DNA adapter (1 μM)	1 μl
10x RNA ligase 2 buffer	1.5 μl
50% PEG8000	3.75 μl
Water	2 μl
SUPERase•In RNase inhibitor	0.75 μl
T4 RNA ligase 2 truncated K227Q (200 U/μl)	1 μl

The RNA in the ligation reactions were separated by electrophoresis on a 10% TBE-UREA polyacrylamide gel at 120V for 50 minutes. The gel was stained with SYBR-Gold and gel fragments collected between 40 and 70 nucleotides to remove excess RNA adapter from the ligated product. RNA was extracted using RNA extraction buffer, filtered through a 0.22 μm pore size acetate filter and RNA precipitated overnight with 2 μl glycoblue, 20 μl 3M sodium acetate pH 5.2 and 600 μl ice-cold isopropanol. The RNA was washed twice in ice-cold 80% ethanol and resuspended in 5 μl 10mM Tris-HCl pH 7.5. The 3' adaptor-ligated RNA was treated with phosphonucleotide kinase (PNK) to ensure the RNA contains a phosphate group at the 5' end. The reaction mix was set up as follows:

5' PNK reaction mix

RNA	5 μl
10X PNK buffer A	1 μl
ATP (10 mM)	1 μl
SUPERase•In RNase inhibitor	0.5 μl
T4 PNK (10 U/μl)	1 μl
Water	1.5 μl

5' PNK reaction conditions

Phosphatase reaction	37°C, 2 hours
Heat Inactivation	75°C, 10 minutes

The PNK treated RNA was precipitated with 2 μl glycoblue, 5 μl sodium acetate pH 5.2 and 150 μl ice-cold ethanol and incubated overnight at -80°C. The RNA was washed twice in ice-cold 80% ethanol and resuspended in 4 μl 10 mM Tris-HCl pH 7.5. A second ligation reaction was carried out to ligate an RNA adapter (5' GUUCAGAGUUCUACAGUCCGACGAUC 3') to the 5' end of the PNK treated RNA using T4 RNA ligase M105A. The reaction was carried out as follows:

5' ligation reaction mix

RNA	5 μl
RNA adapter (0.5 pmole/μl)	1 μl
10x RNA ligase 2 buffer (200 U/μl)	1.5 μl
ATP (10 mM)	1 μl
SUPERase•In RNase inhibitor	1 μl
T4 RNA ligase M105A (10 U/μl)	1 μl
Water	2 μl

The reaction mix was incubated at 16°C for 16 hours and the RNA precipitated with 2 μl glycoblue, 5 μl sodium acetate pH 5.2 and 150 μl ice-cold ethanol and incubated overnight at -80°C. The RNA was washed twice in ice-cold 80% ethanol and resuspended in 3.5 μl 10mM Tris-HCl pH 7.5.

The 5' and 3' ligated RNA was converted to cDNA by reverse transcription using a SuperScript III reverse transcriptase (Invitrogen) a reverse transcription primer (5' GCCTTGGCACCCGAGAATTCCA 3') that recognizes the DNA adaptor ligated to the 3' end of the RNA. The reaction was carried out as follows:

Annealing of RNA and reverse transcription primer

5' and 3' ligated RNA	3.5 μl
Reverse transcription primer (25 μM)	1 μl
dNTP's (25 mM)	0.5 μl

The above mix was incubated at 65°C for 5 minutes and then immediately transferred to 55°C. While the mix was incubating at 55°C, the following reaction mix was prepared:

10x Reverse transcription buffer	1 μl
Magnesium chloride (25 mM)	2 μl
DTT (0.1 M)	1 μl
SUPERase•In RNase inhibitor	0.5 μl
SuperScript III (200 U/μl)	1 μl

The above reaction mix was added to the RNA-reverse transcription primer mix and incubated at 55°C for 50 minutes. The cDNA was amplified by PCR using a forward primer (RP1) that recognizes the cDNA sequence corresponding to the 5' ligated adapter and a second primer that has one region containing an unique sequence to allow multiple libraries to be mixed and sequenced together and a second region that recognizes the cDNA sequence corresponding to the 3' ligated adapter. The PCR was carried out using the following conditions:

Reaction mix

NEBNext High-Fidelity 2x PCR master mix	25 μl
RP1 forward primer (25 μM)	2.5 μl
barcoded reverse primer (25 μM)	2.5 μl
cDNA	10 μl
water	10 μl

Reaction conditions

Initial denaturation	98°C, 3 minutes
13 cycles	98°C (denaturation), 1 minute
	65°C (annealing), 30 seconds
	72°C (extension), 30 seconds
Final extension	72°C, 5 minutes
Hold	10°C

The PCR reaction mixture was separated by electrophoresis on a 10% TBE polyacrylamide gel at 150V for 60 minutes. The PCR product migrated at a molecular weight of 150 nucleotides and the gel fragment was excised and extracted overnight in DNA extraction buffer (table A1.1). Gel fragments were removed by filtering through a 0.22 μm pore size acetate filter and the RNA was precipitated overnight with 2 μl glycoblue, 20 μl 3M sodium acetate pH 5.2 and 600 μl ice-cold isopropanol. The DNA was washed twice in ice-cold 80% ethanol and resuspended in 10 μl 10mM Tris-HCl pH 8.5.

2.21.7 Ribosomal RNA depletion by duplex-specific nuclease treatment

To reduce the amount of barcoded PCR fragments that correspond to ribosomal RNA in the library, duplex-specific nuclease (DSN), which cleaves double stranded DNA with increased activity on perfectly matched duplexes, was used. The initial 98°C step denatures the double stranded cDNA library and the most abundant sequences (corresponding to ribosomal RNA sequences) anneal first during the 68°C incubation period. DSN then specifically degrades the double stranded DNA, enriching for less abundant sequences. The DNA library samples (20 ng in 12 μl 10 mM Tris-Cl pH 8.5) were mixed with 4 μl 4x hybridisation buffer (200 mM HEPES pH 7.5, 2 M NaCl) and incubated at 98°C for 2 minutes, followed by 68°C for 5 hours. Pre-warmed 10x DSN master mix (2 μl) was added and incubated for 10 minutes at 68°C, followed by 4 U DSN. The reaction mix was incubated at 68°C for a further 60 minutes and the reaction stopped by the addition of 20 μl pre-warmed 10 mM EDTA and incubation at 68°C for 5 minutes.

The DNA was extracted with phenol:chloroform:isoamyl alcohol (25:24:1) and the DNA library re-amplified by PCR using the appropriate barcoded primers.

2.22. Bioinformatics

2.22.1 Hydrophobicity plots

Protein sequences were obtained from UniProt. Hydrophobicity plots were generated using the Kyte-Doolittle method using ExPasy tools. A window span of 5 was used for each plot. The vertical axis shows the hydrophobicity values whilst the horizontal axis shows the position of amino acids.

2.22.2 Multiple sequence alignments

Protein sequences were aligned using the Clustal Omega multiple sequence alignment tool hosted by EMBL-EBI. Default parameters were applied.

Chapter 3

An N-terminal export signal required for export gate opening by 'early' flagellar subunits of the rod and hook

3.1 Introduction

Flagellar structural subunits need to be targeted efficiently to the flagellar type III secretion system (fT3SS) export machinery for rapid export (2-3 subunits/second)[174]. The subunits of the flagellar rod, hook and filament are then unfolded and translocated across the inner membrane into the flagellar export channel by the fT3SS, energised by the proton motive force (PMF) and ATP hydrolysis[51,52]. In the flagellum, the fT3SS switches substrate specificity from early rod/hook subunits to late filament subunits when the rod/hook structure reaches its mature length[64,248,65]. These early and late substrates must be exported at the correct stage of flagellum biogenesis. This is achieved by targeting substrates to the export machinery at the right time using a combination of export signals in the substrate mRNA and/or polypeptide. All T3SS substrates contain N-terminal signals for targeting to the export machinery, however they do not share a common peptide sequence[138,139,140,141,142]. Furthermore, targeting of some substrates is aided by specific chaperones that deliver substrates to the T3SS machinery[172,183,249,227,207].

Other protein export systems also utilise export signals that often carry out multiple roles in addition to targeting subunits to the export machinery. Substrates secreted *via* the Sec system contain an N-terminal signal sequence with a tripartite structure: a positively charged N-terminal region, a hydrophobic central region and a polar C-terminal region, each of which has distinct functions in protein targeting and translocation[103]. The number of positively charged residues modulates binding to the export motor protein SecA, and the hydrophobicity of the signal determines binding to the signal recognition particle (SRP)[103].

Substrates of the Twin-arginine translocation (TAT) protein export pathway also contain N-terminal signal sequences with hydrophobic and positively charged regions, and possess a highly conserved twin-arginine motif located between these two regions[96]. Binding of the TAT signal to the TatBC export complex in the inner membrane promotes PMF-dependent TatA polymerisation, which allows the substrate to cross the membrane[96]. In this case, the export signal functions both as a targeting signal and also promotes the assembly of an active export channel to allow its own export[104]. Substrates for Type I secretion systems also appear to contain multiple distinct export signals that are sequentially exposed during substrate unfolding to promote their export, whilst a C-terminal signal recognised during the late stages of export promotes ATPase activity and disassembly of the export system[250].

Despite the identification of export signals in the N-termini of substrates of the flagellar and virulence T3SS, it is unclear what these signals do and how they promote subunit export[138,139,140,141,142]. The late subunits that assemble to form the flagellar filament substructures contain export signals and are also targeted to the export machinery by dedicated export chaperones that are thought to sequentially interact with different components of the export machinery[172,183,249,227,207]. However, the early flagellar subunits that assemble to form the rod and hook substructures are not chaperoned. Instead, all the information for targeting and export of early subunits is determined by export signals that reside within the subunits themselves[141,8].

Whilst we have known for some time that the N-termini of early flagellar subunits contain export signals, little is known about the precise identity of these signals and what role they play in promoting subunit export. Previous work in our laboratory has identified one of these N-terminal signals within the early rod/hook subunits as a small hydrophobic sequence termed the gate recognition motif (GRM), which is essential for efficient subunit export[141]. This GRM binds a surface exposed hydrophobic pocket on the cytosolic domain of the export gate component FlhB, allowing early subunits to dock at the export machinery[141].

However, nothing is known about the fate of early export subunits post-docking at FlhBc, except that these unfolded subunits must pass through an export gate comprising the N-terminal domain of FlhA ($FlhA_N$), the N-terminal domain of FlhB ($FlhB_N$) and FliPQR (hereafter, the ABPQR export gate) before entering the narrow central export channel, through which subunits transit to the flagellum tip where they fold into the nascent structure[105,251].

For subunits, reaching the export machinery is just the first step in export. Once a subunit has docked at the export machinery, *e.g* at FlhB for rod/hook subunits, there are still multiple obstacles to pass before the subunit reaches its final destination. The narrow width of the fT3SS export channel means that subunits must be unfolded[73]. In the case of the chaperoned subunits, this unfolding is thought to be carried out while the subunit is in complex with its cognate chaperone and docked at the cytosolic domain of FlhA (FlhAc)[230]. Subunits also need to be transported actively across the cell membrane into the narrow export channel – this represents a high entropic barrier where the unfolded subunit is placed under considerable configurational constraint whilst transiting into and through the channel[141,174]. Before subunits enter the export channel at core of flagellum, they must pass through the ABPQR gate. The recent structure of the FliPQR components of the export gate has shown that this complex adopts a closed conformation, presumably to maintain the membrane permeability barrier, as supported by data from ion conductance experiments[105,251,246]. This suggests that when a subunit for export docks at the fT3SS, something must signal to the export machinery to open the export gate. Such a signal for T3SS gate opening has not been identified. For early rod/hook subunits, one possibility is that conformational changes associated with subunit docking at FlhBc is the signal that is transmitted to the export gate complex, especially as the N-terminal portion of FlhB ($FlhB_N$) constitutes part of the ABPQR gate.

Previous work in our laboratory identified a new export signal at the extreme N-terminus of FlgD – an early subunit that functions as a cap to promote polymerisation of the FlgE subunit to form the hook substructure[240,252]. A FlgD

variant lacking the extreme N-terminal signal (FlgDΔ2-5) failed to be exported into culture supernatants. Furthermore, the export defect was more severe than a FlgD variant that lacked the gate-recognition motif (GRM), which is required for docking at the FlhBc export gate[141]. The precise role of these export signals in recruiting early rod/hook subunits to the export machinery and promoting their export remain poorly understood. The work described in this chapter aims to further characterise early subunit N-terminal export signals and understand their function in subunit export.

3.2.1 A screen for suppressors of the FlgDΔ2-5 non-motile phenotype

Suppressor screens are a powerful genetic approach that can be used to identify second site mutations that suppress mutant phenotypes, providing more information on a gene or mutation of interest. To gain a better understanding of the function of the early subunit N-terminal signal, a screen to identify genetic suppressors of the phenotype associated with the FlgDΔ2-5 variant was performed. FlgDΔ2-5 is not exported and so cannot assemble into a FlgD cap structure, preventing flagellar hook assembly. A *flgD* null strain producing FlgDΔ2-5 is therefore non-motile on soft-tryptone agar plates. Previous work in the laboratory identified two classes of intragenic suppressor mutations of the non-motile phenotype associated with FlgDΔ2-5[252]. The first class of suppressor strains carried missense mutations in *flgDΔ2-5* that introduced small non-polar residues at the FlgDΔ2-5 extreme N-terminus, indicating that hydrophobicity is an essential feature of the FlgD N-terminal signal. The second class of suppressor mutation was a duplication event that caused an adjacent repeat of FlgD residues 16-21 (GSGSMT). I screened for further suppressors of the FlgDΔ2-5 non-motile phenotype with the aim of identifying new classes of suppressors, including extragenic suppressor mutations. A *Salmonella* Δ*flgD* strain was transformed with pTrc99a encoding FlgDΔ2-5 and single colonies were selected and grown to A_{600} 1.0 before being inoculated into 0.3% soft-tryptone agar. Plates were incubated at 30ºC for 1-2 days until 'spurs' of motile cell populations began to swim away from the site of inoculation. Motile bacteria were taken from the 'spurs' and streaked onto LB agar plates to isolate single

colonies, which were used to inoculate overnight cultures for plasmid preparation and sequencing. This screen identified 32 suppressor mutations, all of which were intragenic (Figure 3.1). Many of these suppressor mutations in *flgD* were novel, but all could be separated into the same two suppressor classes previously identified (Figure 3.2)[252]. The first class of suppressors carried missense mutations in *flgDΔ2-5* that introduced small non-polar residues in the FlgDΔ2-5 N-terminus adjacent to the 2-5 signal deletion, restoring the hydrophobicity of the N-terminus (Figure 3.2). Analysis of the amino acid sequences and the predicted hydrophobicities of the N-termini of all early flagellar subunits demonstrated that all contain small hydrophobic residues upstream of the GRM (Figure 3.3). The deletion of FlgD residues 2-5 deletion removes all small hydrophobic amino acids from its extreme N-terminus (upstream of FlgD residue 15), effectively generating an N-terminus containing only polar residues. A hydrophobicity plot, generated using the Kyte and Doolittle method, of the first 60 residues of FlgD shows that the first 5 residues of FlgD have a hydrophobicity score above 0 (higher hydrophobicity; Figure 3.3). The hydrophobicity score then falls below 0 between FlgD residues 6 and 31, confirming that deletion of residues 2-5 would remove all hydrophobicity from the extreme N-terminus. This indicates that small non-polar residues at the extreme N-terminus of FlgD are required for its efficient export. The second class of suppressor mutations isolated caused duplication or insertion of residues in FlgD, such that additional residues are inserted in the region between the N-terminal 2-5 signal and the GRM, which is located at residues 36-40 (Figure 3.2).

3.2.2 Suppressor mutations that cause duplications or insertions in FlgD reposition Valine-15 relative to the Gate-Recognition-Motif

The second class of mutations that suppress the non-motile phenotype associated with the FlgDΔ2-5 variant duplicate or insert sequences close to the N-terminus of FlgDΔ2-5, suggesting that the distance between the 2-5 and GRM signals might be critical (Figure 3.2). It is also possible that these suppressor mutations duplicate/insert a specific sequence in the N-terminus of FlgDΔ2-5 that

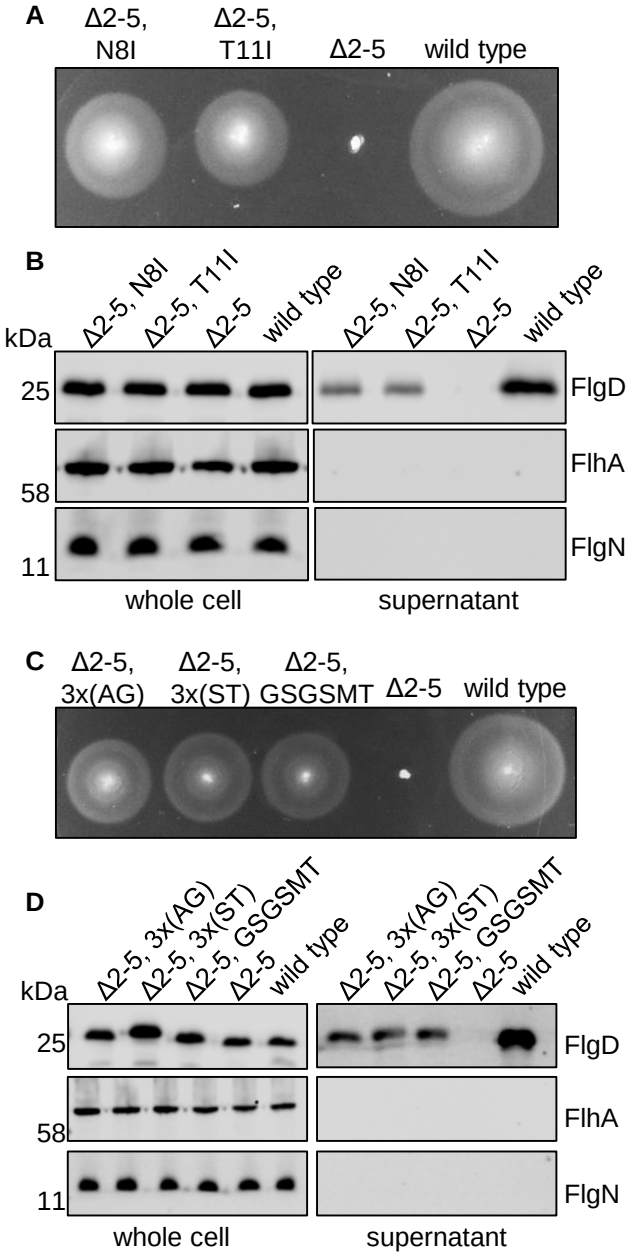

Figure 3.1. Isolation of motile suppressors from the FlgD Δ2-5 variant

(**A**) Swimming motility assays of a *flgD* null strain expressing two gain-of-function mutants isolated from the FlgDΔ2-5 variant: gain-of-function mutants (FlgDΔ2-5, N8I and FlgDΔ2-5, T11I), FlgDΔ2-5 variant (labelled as Δ2-5) and FlgD wild type (labelled as wild type). Cells were inoculated into 0.3% soft-tryptone agar containing 100 µg/ml ampicillin and incubated for 3-6 hours at 37°C.

(**B**) Secretion analysis of two FlgD gain-of-function mutants. Immunoblotting using polyclonal anti-FlgD, anti-FlhA and anti-FlgN sera of whole cell (whole cell) and culture supernatant (supernatant) fractions prepared from the above cells.

(**C**) Effect of insertions between amino acids 19 and 20 in FlgDΔ2-5 on cell motility. Swimming motility of a *flgD* null strain expressing FlgDΔ2-5 variants containing polar (STSTST), non-polar (AGAGAG) amino acids or the isolated gain-of-function insertion (GSGSMT) placed between amino acids 19 and 20. FlgDΔ2-5, ^{19}(AGAGAG)^{20} (labelled as Δ2-5, 3x(AG)), FlgDΔ2-5, ^{19}(STSTST)^{20} (labelled as Δ2-5, 3x(ST)), FlgDΔ2-5, ^{19}(GSGSMT)^{20} (labelled as Δ2-5, GSGSMT), FlgDΔ2-5 (labelled as Δ2-5) and FlgD wild type (labelled as wild type) were expressed in a *Salmonella flgD* null strain, inoculated into 0.3% soft-tryptone agar containing 100 µg/ml ampicillin and incubated for 3-6 hours at 37°C.

(**D**) Secretion analysis of FlgD by immunoblotting using anti-FlgD, anti-FlhA and anti-FlgN sera of whole cell (whole cell) and culture supernatant (supernatant) fractions prepared from the above cells.

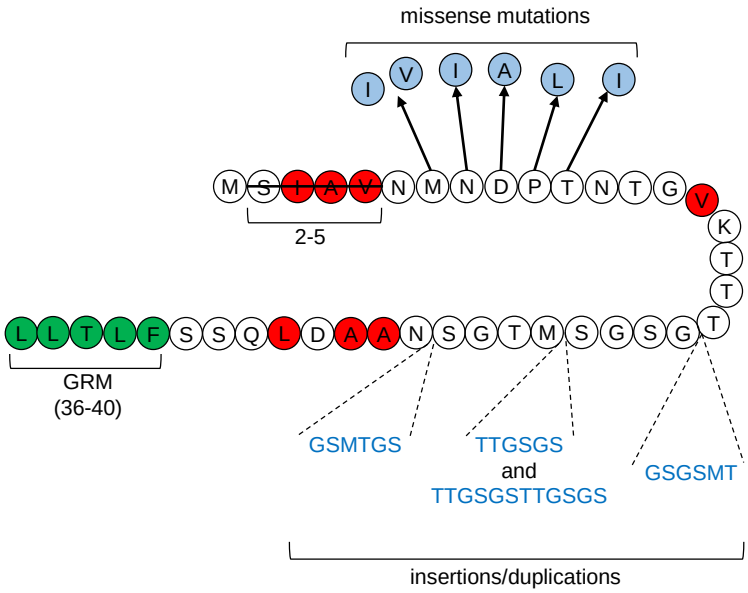

Figure 3.2. A schematic displaying intragenic suppressors isolated from FlgDΔ2-5

A schematic displaying the intragenic suppressors within amino acids 1-40 of FlgD isolated from the FlgDΔ2-5 variant. All suppressors (blue) were located between the gate recognition signal (GRM, green) and the N-terminus, and can be separated into two classes: insertions or duplications positioned downstream from the small hydrophobic amino acid (red) valine-15, or missense mutations that re-introduce small hydrophobic amino acids at the N-terminus.

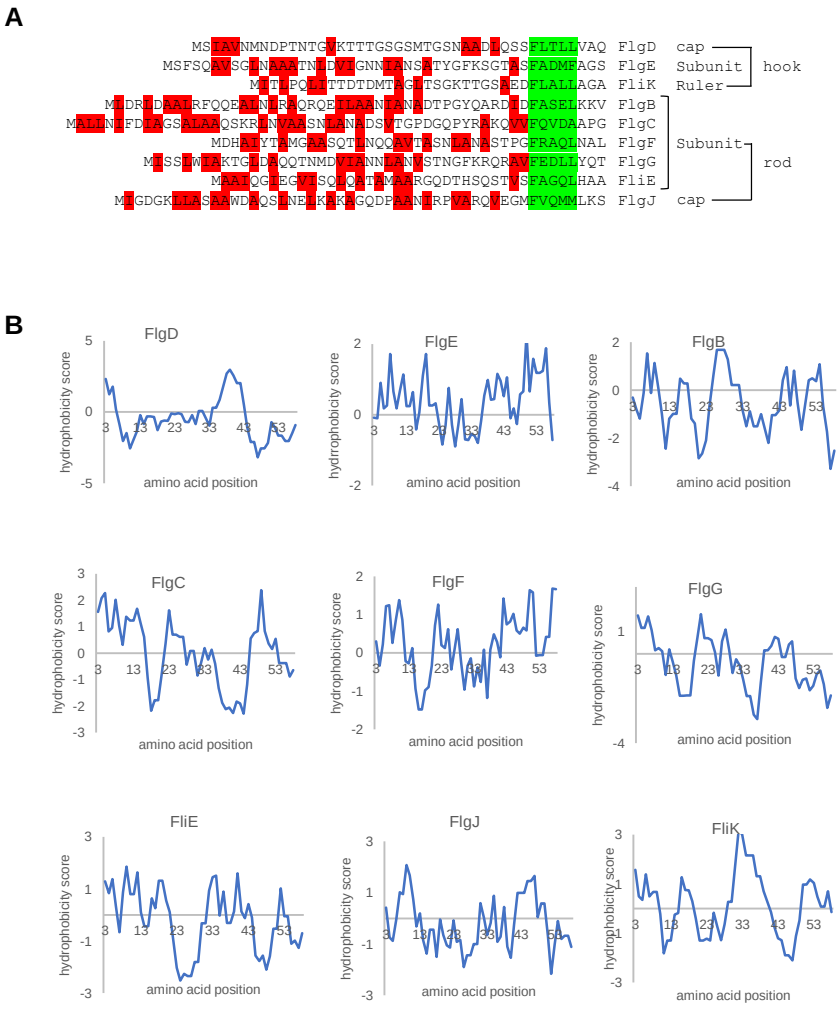

Figure 3.3. Small non-polar residues and hydrophobicity plots of the N-termini of early flagellar subunits

(**A**) The N-termini of early flagellar subunits aligned to their gate-recognition motif (GRM, Green). Small non-polar amino acids (excluding glycine) upstream from the GRM are highlighted in red.

(**B**) Kyte and Doolittle hydrophobicty plots for the N-terminal 60 amino acids for each early flagellar subunit were generated by Expasy tools. Hydrophobicty values are shown on the vertical axis, the amino acid number are shown on the horizontal axis.

compensates for the loss of the 2-5 signal. To test this, I engineered FlgD variants that lacked the 2-5 signal and also contained an insertion of either six non-polar resides (AGAGAG) or six polar residues (STSTST) between residues 19 and 20 and compared the export efficiencies of these variants and a variant (FlgDΔ2-5-^{19}GSGSMT^{20}) isolated from the suppressor screen. A *flgD* null strain was transformed with recombinant pTrc99a expression vectors encoding these FlgD variants and single colonies were isolated and used to inoculate an overnight cultures (ONCs). ONCs were then used to inoculate LB broth cultures containing ampicillin, which were grown to A_{600} 1.0 and centrifuged. Cell pellets were washed, resuspended in fresh media and incubated at 37ºC with shaking (200 RPM). After 60 minutes, whole cells and culture supernatants were collected by centrifugation, exported proteins in culture supernatants were TCA precipitated, and whole cells and exported proteins were separated by SDS-PAGE. Samples were analysed by immunoblotting with anti-FlgD sera, as well as anti-FlhA and anti-FlgN sera as flagellar gene expression and cell lysis controls. The amount of FlgD detected in the culture supernatants was similar for the engineered FlgD variants (AGAGAG or STSTST insertions) and the FlgD variant isolated from the suppressor screen (FlgDΔ2-5-^{19}GSGSMT^{20}; Figure 3.1). Consistent with the export phenotypes, all of these FlgD variants restored swimming motility to the *flgD* null strain (Figure 3.1). The data indicate that the duplication events in FlgDΔ2-5 do not insert a specific sequence that acts as an export signal, but may instead improve export by increasing the distance between the FlgDΔ2-5 extreme N-terminus and the GRM. It is interesting to note that the duplication and insertion suppressor mutations always occurred upstream of the sequence encoding the gate recognition signal (GRM). Indeed, all of the duplications/insertions were observed to increase the distance between the FlgD GRM and valine-15 (the nearest small non-polar residue to the 2-5 deletion), repositioning this valine to take the place of the small non-polar residues usually located at residues 2-5 of the FlgD polypeptide.

To test whether valine-15 is required to enable export of the FlgDΔ2-5 variants containing duplications/insertions, a FlgD variant lacking the 2-5 signal and

containing the six amino acid duplication ^{19}(GSGSMT)^{20} with a valine-15 to alanine substitution (FlgDΔ2-5-^{19}(GSGSMT)^{20}-V_{15}A) was constructed. Substitution of valine-15 to alanine reduced export of the FlgDΔ2-5-^{19}(GSGSMT)^{20}-V_{15}A variant to a level similar to the FlgDΔ2-5 variant (Figure 3.4), indicating that the class of FlgDΔ2-5 intragenic suppressors that encode duplications or insertions result in a repositioning of valine-15 relative to the GRM that compensates for the loss of the small non-polar amino acids removed by deletion of FlgD residues 2-5. In agreement with the export phenotypes, Δ*flgD* cells containing pTrc99a encoding FlgDΔ2-5-19(GSGSMT)-V_{15}A were non-motile in 0.3% soft-tryptone agar (Figure 3.4).

3.2.3 Screening for suppressors of the FlgDΔ2-5-^{19}(GSGSMT)^{20}-V_{15}A non-motile phenotype

The accruing data suggests that small non-polar residues located at the extreme N-terminus of FlgD, upstream of the GRM, are required for efficient FlgD export. As the FlgDΔ2-5-^{19}(GSGSMT)^{20}-V_{15}A variant is non-motile and lacks any small non-polar residues upstream of the GRM, it is probable that intragenic suppressors isolated from this FlgD variant would re-introduce small non-polar residues at the N-terminus of FlgD. Such a suppressor screen was carried out by transforming the Δ*flgD* strain with pTrc99a encoding the FlgDΔ2-5-^{19}(GSGSMT)^{20}-V_{15}A and single colonies were selected and grown to A_{600} 1.0 before being inoculated into 0.3% soft-tryptone agar. Plates were incubated at 30ºC for 1-2 days until spurs of motile cell populations began to swim away from the site of inoculation. Motile bacteria were taken from the spurs and streaked onto LB agar plates to isolate single colonies, which were used to inoculate overnight cultures for plasmid preparation and sequencing. Ten suppressors of the motility defect associated with the FlgDΔ2-5-^{19}(GSGSMT)^{20}-V_{15}A variant were isolated from this screen, all of which resulted in reintroduction of a small non-polar residues at the FlgD N-terminus, indicating that hydrophobicity of the extreme N-terminus is critical for promoting subunit export (Figure 3.4).

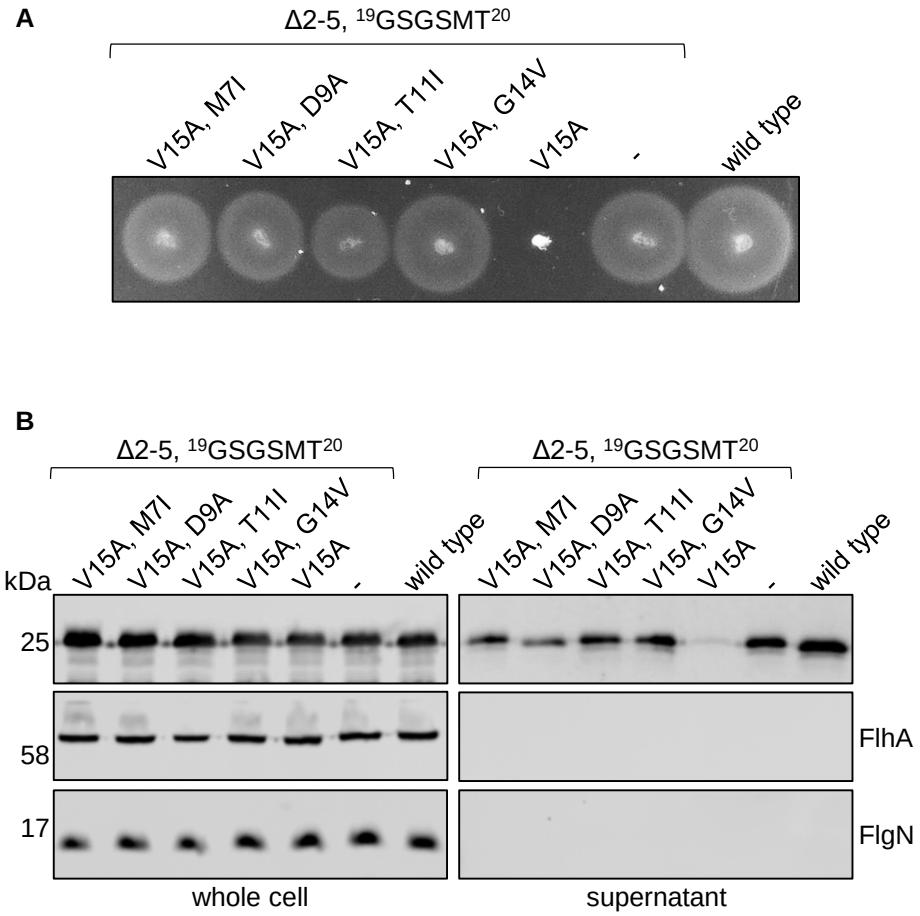

Figure 3.4. Insertions or duplications within the N-terminus of FlgD reposition valine-15

(**A**) Swimming motility assays of a *flgD* null strain expressing gain-of-function mutants isolated from the FlgDΔ2-5, ^{19}(GSGSMT)^{20}, V15A variant (M7I, D9A, T11I, G14V), their parent FlgD variant FlgDΔ2-5, ^{19}(GSGSMT)^{20}, V15A (labelled as V15A), FlgDΔ2-5, ^{19}(GSGSMT)^{20} (labelled with a dash(-)) and FlgD wild type (labelled as wild type). Cells were inoculated into 0.3% soft-tryptone agar containing 100 µg/ml ampicillin and incubated for 3-6 hours at 37°C.

(**B**) Secretion analysis of FlgD by immunoblotting with anti-FlgD, anti-FlhA and anti-FlgN sera of whole cell (whole cell) and culture supernatant (supernatant) fractions prepared from the above cells.

3.3 The FlgDΔ2-5 variant has a dominant-negative effect on motility and export

Export defective flagellar subunits or export components can sometimes give rise to dominant-negative phenotypes when they are expressed in wild type cells. This can be caused by export defective subunits 'stalling' at a specific point along the export pathway, where they sequester export components into non-functional complexes and/or prevent other subunits from docking at the export machinery. Previous preliminary work in our laboratory showed that in a *Salmonella* Δ*recA* strain that was wild type for flagellar biogenesis and motility, expression of FlgDΔ2-5 had a dominant negative effect on the export of flagellar subunits, and that this effect could be suppressed by deletion of the GRM export signal in FlgDΔ2-5^{252}. These data suggest that FlgDΔ2-5 might stall at the export machinery, blocking the binding of other early subunits and attenuating export.

To confirm our preliminary observations, wild type FlgD, FlgDΔ2-5, FlgDΔGRM or FlgDΔ2-5ΔGRM were expressed *in trans* in *Salmonella* and the effect on subunit export and cell motility were assessed (Figure 3.5). Recombinant pTrc99a plasmid encoding the FlgD variants were transformed into a *Salmonella* Δ*recA* strain and expression was induced with 100 μM IPTG. Subunit export and swimming motility assays were performed as described in sections 2.15 and 2.16. Proteins in whole cells and supernatants were separated by SDS-PAGE and analysed by immunoblotting with antisera against representative early (FlgD and FliK) and late (FlgK and FlgL) subunits, as well FlhA and FlgN as loading, expression and lysis controls (Figure 3.5). It should be noted that cells were expressing both chromosomally-encoded FlgD and plasmid-encoded FlgD variants, and it was not possible to distinguish these by immunoblotting. In the *Salmonella recA* null strain, *in trans* expression of FlgDΔ2-5 attenuated export of non-cognate subunits into culture supernatant compared to cells expressing wild type FlgD, FlgDΔGRM or FlgDΔ2-5ΔGRM (Figure 3.5). Consistent with the export phenotypes, cells expressing FlgDΔ2-5 were less motile than cells

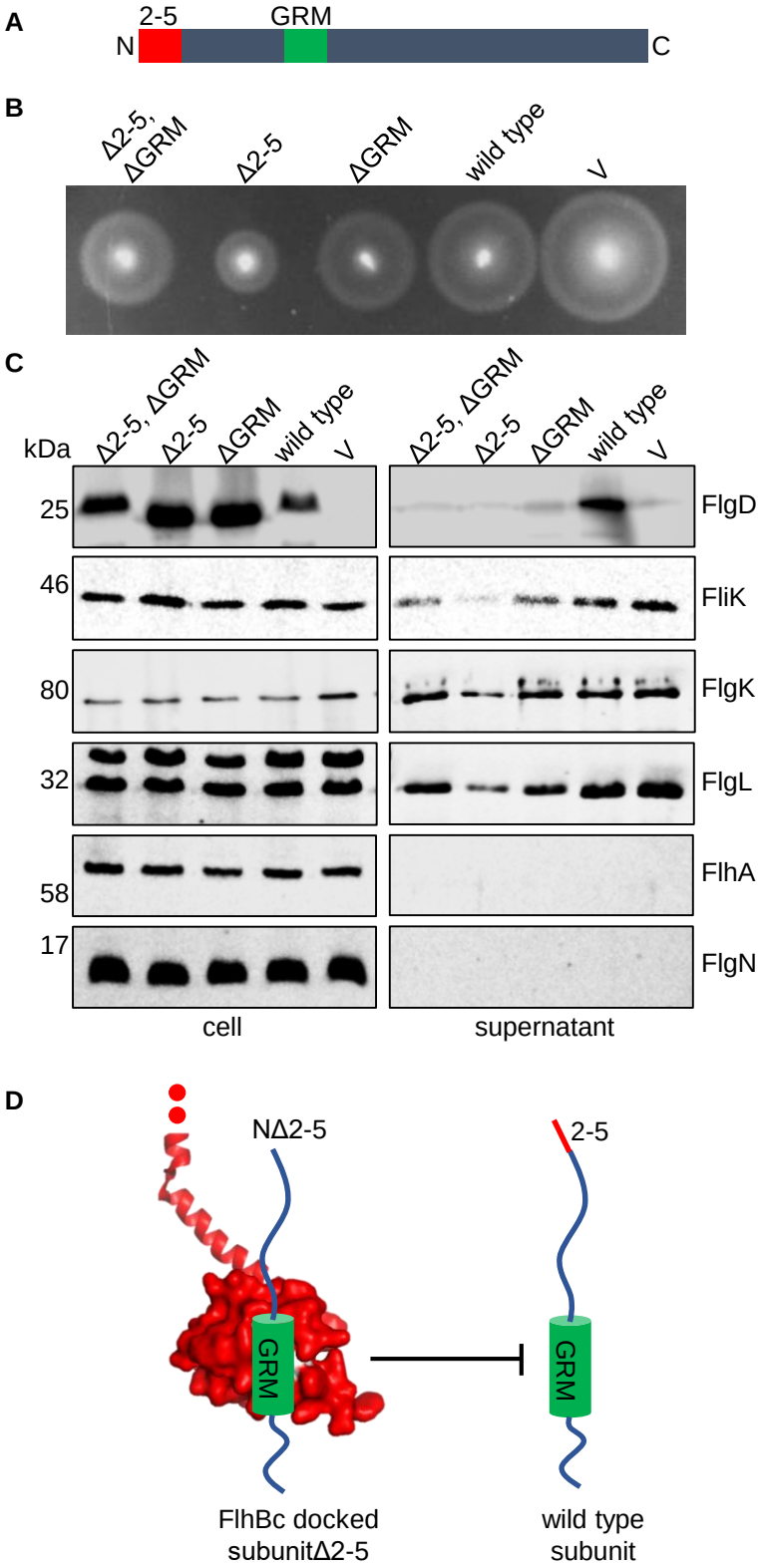

Figure 3.5. Overexpression phenotypes of FlgDΔ2-5 and its variants

(**A**) A Schematic illustrating the N-terminal location of the 2-5 signal (red) relative to the FlhBc gate recognition signal (GRM, green).

(**B**) Swimming motility assays of a *Salmonella* Δ*recA* strain transformed with recombinant pTrc99a plasmids carrying wild type FlgD or its variants (Δ2-5ΔGRM, Δ2-5 or ΔGRM) or empty pTrc99a vector (V). Cells were inoculated into 0.3% soft-tryptone agar containing 100 µg/ml ampicillin and 100 µM IPTG and incubated for 3-6 hours at 37°C and incubated for 3-6 hours at 37°C.

(**C**) Secretion analysis of the above cells by immunoblotting using anti-FlgD, anti-FliK, anti-FlgK, anti-FlgL, anti-FlhA and anti-FlgN sera of whole cell (whole cell) and culture supernatant (supernatant) fractions.

(**D**) FlgDΔ2-5 subunit docked at the FlhBc export gate component (left) prevents other subunits (right) from docking at FlhBc, attenuating subunit export.

expressing wild type FlgD, FlgDΔGRM or FlgDΔ2-5ΔGRM (Figure 3.5). The data support the view that FlgDΔ2-5 stalls at the export machinery and attenuates export of other early flagellar subunits. Suppression of FlgDΔ2-5 negative dominance by deletion of the GRM export signal, which is required for early subunit docking at the FlhBc export gate, suggests that FlgDΔ2-5 might stall at FlhBc, failing to progress to the next step of the export pathway. The data suggest that the early subunit GRM export signal and the N-terminal hydrophobic 2-5 signal are used sequentially, with GRM-mediated docking at FlhBc occuring prior to use of the 2-5 signal.

3.4.1 Export of the FlgD early flagellar subunit is affected by the relative positioning of the N-terminal hydrophobic export signal and the GRM

Sequential deployment of the early subunit GRM export signal and the N-terminal hydrophobic 2-5 signal appear critical for FlgD export. Data on suppressor mutations that introduce duplications or insertions upstream of the FlgDΔ2-5 GRM prompt an additional question: is the distance between the N-terminal hydrophobic 2-5 signal and the GRM important for subunit export? If docking of early subunits at $FlhB_C$, mediated by the subunit GRM, is required before the 2-5 export signal is used, then there may be a minimum distance requirement between the GRM and the N-terminal hydrophobic 2-5 export signal to allow it to engage with the export machinery. If this distance is too short, then the N-terminal hydrophobic 2-5 signal might not be able to carry out its function. To test this hypothesis and to determine the minimum number of residues between the N-terminal hydrophobic 2-5 signal and the GRM required to support subunit export, a suite of FlgD variants was constructed in which the distance between these two export signals was incrementally decreased. An export competent FlgD variant (FlgDΔ9-32-4x[GSTNAS]) was constructed in which the region between the two signals (amino acids 9-32) was deleted and replaced with four repeats of Gly-Ser-Thr-Asn-Ala-Ser (GSTNAS) to restore the wild type distance between the two signals. This FlgD variant was exported and could support cell motility (Figure 3.6). To determine the minimum number of (GSTNAS) repeats that could support efficient FlgD export, FlgD variants with

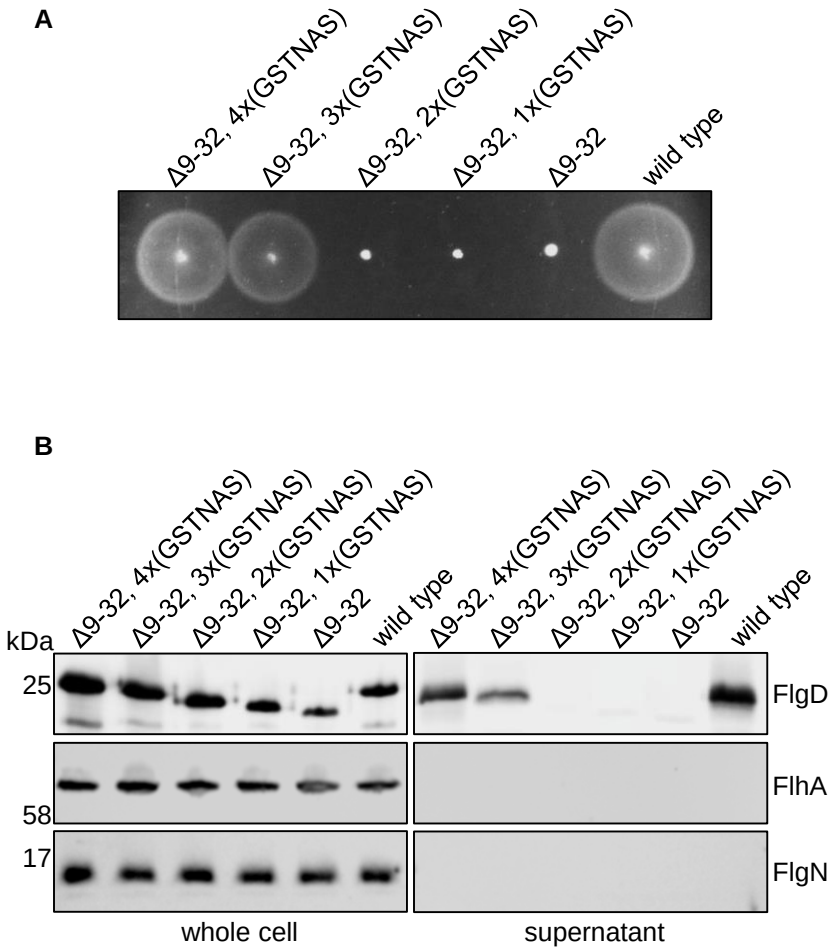

Figure 3.6. Effect of number of GSTNAS repeats between the 2-5 and GRM signals on FlgD subunit export

(**A**) Swimming motility assays of a *flgD* null strain expressing wild type FlgD and FlgD variants whereby residues 9-32 are replaced by repeats of Gly-Ser-Thr-Asn-Ala-Ser (GSTNAS): (Δ9-32 3x(GSTNAS), Δ9-32 2x(GSTNAS), Δ9-32 1x(GSTNAS), Δ9-32). Cells were inoculated into 0.3% soft-tryptone agar containing 100 µg/ml ampicillin and incubated for 3-6 hours at 37°C.

(**B**) Secretion analysis of FlgD by the *flgD* null strain expressing wild type FlgD and the FlgD variants from (a). Whole cell (cell) and culture supernatant (sup) fractions were prepared from the above cells and immunoblotted with anti-FlgD, anti-FlhA and anti-FlgN sera.

progressively fewer copies of the repeat were constructed (Figure 3.6). A Δ*flgD* strain was transformed with pTrc99a encoding these recombinant FlgD variants and export assays were performed as previously described (section 2.15 and 2.16). The minimum number of repeats that could support export was found to be three, and below this threshold export and motility were strongly attenuated (Figure 3.6). This experimental approach was further refined by using the export-deficient FlgDΔ9-32-2x[GSTNAS] (hereon termed $FlgD_{short}$) to construct a set of FlgD variants in which the distance between the N-terminal hydrophobic 2-5 signal and the GRM was increased incrementally one residue at a time to determine the effect on subunit export and cell motility (Figure 3.7). Data from these experiments indicate that the minimum number of residues that FlgD can tolerate between the N-terminal hydrophobic 2-5 signal and the GRM is between 20 and 24 amino acids. The data suggest that the N-terminal hydrophobic 2-5 signal perhaps binds a site on an export machinery component that is positioned at a maximum distance from the GRM binding site on FlhBc equivalent to the contour length of a 20-24 residue polypeptide.

3.4.2 Screening for suppressors of the $FlgD_{short}$ export and motility defects

Further evidence to support the view that the distance between the N-terminal hydrophobic 2-5 signal and the GRM was critical for subunit export was gained by using the Δ*flgD* strain carrying pTrc99a encoding $FlgD_{short}$ to perform a suppressor screen, as previously described (Sections 3.2.1). Twelve motile strains were isolated and all suppressor mutations were found to be intragenic, causing insertions or duplications that introduced additional residues between the N-terminal hydrophobic 2-5 signal and the GRM (Figure 3.8). Three of the isolated suppressors were further characterised using motility and export assays (Figure 3.8). Compared to parental $FlgD_{short}$, swimming motility and FlgD export was significantly improved in strains expressing the $FlgD_{short}$ suppressor variants (rev1-3; Figure 3.8). One of the isolated suppressors (rev 3) was unusual in that a large region including the GRM (amino acids 33-63) was duplicated such that a second, presumably functional, GRM was positioned 56 residues away from the N-terminus (Figure 3.8, rev 3). Cells expressing this suppressor exported

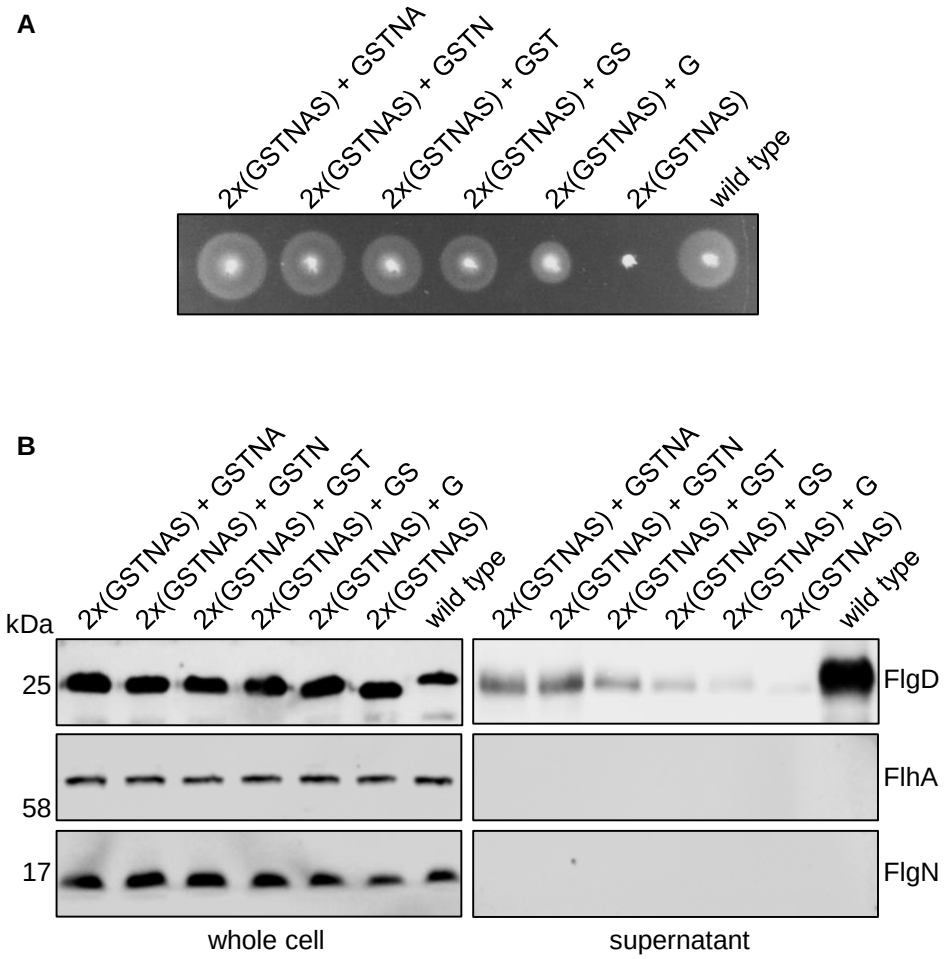

Figure 3.7. Effect of number of amino acids between the 2-5 and GRM signals on FlgD subunit export

(**A**) Swimming motility assays of a *flgD* null strain expressing wild type FlgD, FlgDΔ9-32 2x(GSTNAS) and its variants (FlgDΔ9-32 2x(GSTNAS)+G, FlgDΔ9-32 2x(GSTNAS)+GS, FlgDΔ9-32 2x(GSTNAS)+GST, FlgDΔ9-32 2x(GSTNAS)+GSTN, FlgDΔ9-32 2x(GSTNAS)+GSTNA and FlgDΔ9-32 3x(GSTNAS). Cells were inoculated into 0.3% soft-tryptone agar containing 100 μg/ml ampicillin and incubated for 3-6 hours at 37°C.

(**B**) Secretion analysis of FlgD by the *flgD* null strain expressing wild type FlgD and the FlgD variants from (a). Whole cell (whole cell) and culture supernatant (supernatant) fractions were prepared from the above cells and immunoblotted for FlgD using anti-FlgD, anti-FlhA and anti-FlgN sera.

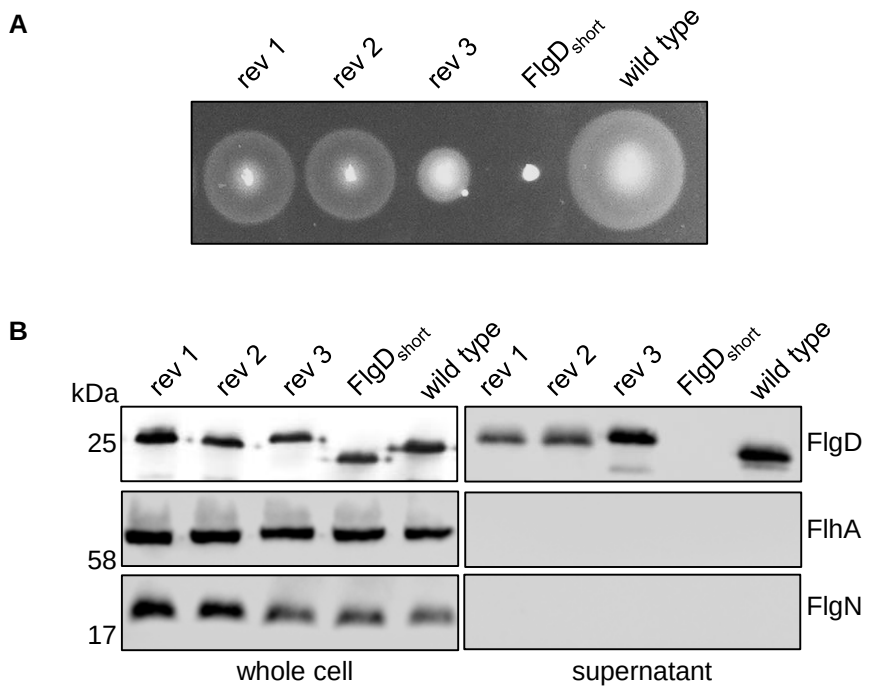

Figure 3.8. Isolation of motile suppressors from the FlgD$_{short}$ variant
(**A**) Swimming motility assays of a *flgD* null strain expressing three gain-of-function mutants isolated from the FlgDΔ2-5 variant: gain-of-function mutants (rev 1, rev 2 and rev 3), FlgD$_{short}$ variant and FlgD wild type (labelled as wild type). Cells were inoculated into 0.3% soft-tryptone agar containing 100 µg/ml ampicillin and incubated for 3-6 hours at 37°C.
(**B**) Secretion analysis of the three FlgD gain-of-function mutants. Immunoblotting using polyclonal anti-FlgD, anti-FlhA and anti-FlgN sera of whole cell (whole cell) and culture supernatant (supernatant) fractions prepared from the above cells.
(**C**) The N-termini of wild type FlgD, FlgD$_{short}$ and its suppressors (rev 1-7) aligned to their gate-recognition motif (GRM, green). Suppressor insertions are highlighted in blue, Gly-Ser-Thr-Asn-Ala-Ser repeats are underlined and the 2-5 signal is highlighted in red.

more $FlgD_{short}$ but were less motile than cells expressing the other $FlgD_{short}$ suppressor variants, suggesting that $FlgD_{short}$ rev3 hook cap assembly is slightly impaired (Figure 3.8). The data from this suppressor screen further supports the view that the function of the N-terminal hydrophobic 2-5 export signal is modulated by its distance from the GRM signal.

3.5 The distance requirement between the N-terminal hydrophobic export signal and the GRM is common to rod, hook and hook cap subunits.

All early flagellar subunits contain a GRM (Figure 3.3), therefore it is possible that the path taken through the export machinery by these subunits is similar. To investigate whether the distance between the N-terminal hydrophobic export signal and the GRM of the rod subunit FlgG and the hook subunit FlgE is important for their export, FlgG residues 11-35 and FlgE residues 9-32 were replaced with four repeats of Gly-Ser-Thr-Asn-Ala-Ser (GSTNAS). Export assays performed using a Δ*flgD* strain transformed with pTrc99a encoding these subunit variants showed that they were exported into culture supernatants at levels similar to wild type (Figure 3.9). Deletion of two GSTNAS repeats strongly attenuated FlgG and FlgE export, indicating that there is a minimum distance requirement between the N-terminal hydrophobic export signal and the GRM in these rod and hook subunits that dock at FlhBc. A Δ*flgE* strain transformed with pTrc99a encoding wild type FlgD, $FlgD_{short}$ or a FlgD variant in which residues 9-32 are replaced by four GSTNAS repeats were used as a control and displayed the same phenotypes as cells producing FlgG and FlgE (Figure 3.9).

3.6.1 Overexpression of $FlgD_{short}$ has a dominant negative effect on motility and export

The accruing data indicate that the GRM and N-terminal hydrophobic export signals are used sequentially, with subunits first docking *via* the GRM at $FlhB_C$ to subsequently allow the N-terminal hydrophobic signal to reach its binding site on the export machinery and carry out its function. I reasoned that early subunit variants containing deletions that decreased the distance between the N-terminal hydrophobic export signal and the GRM, like the FlgDΔ2-5 variant, might

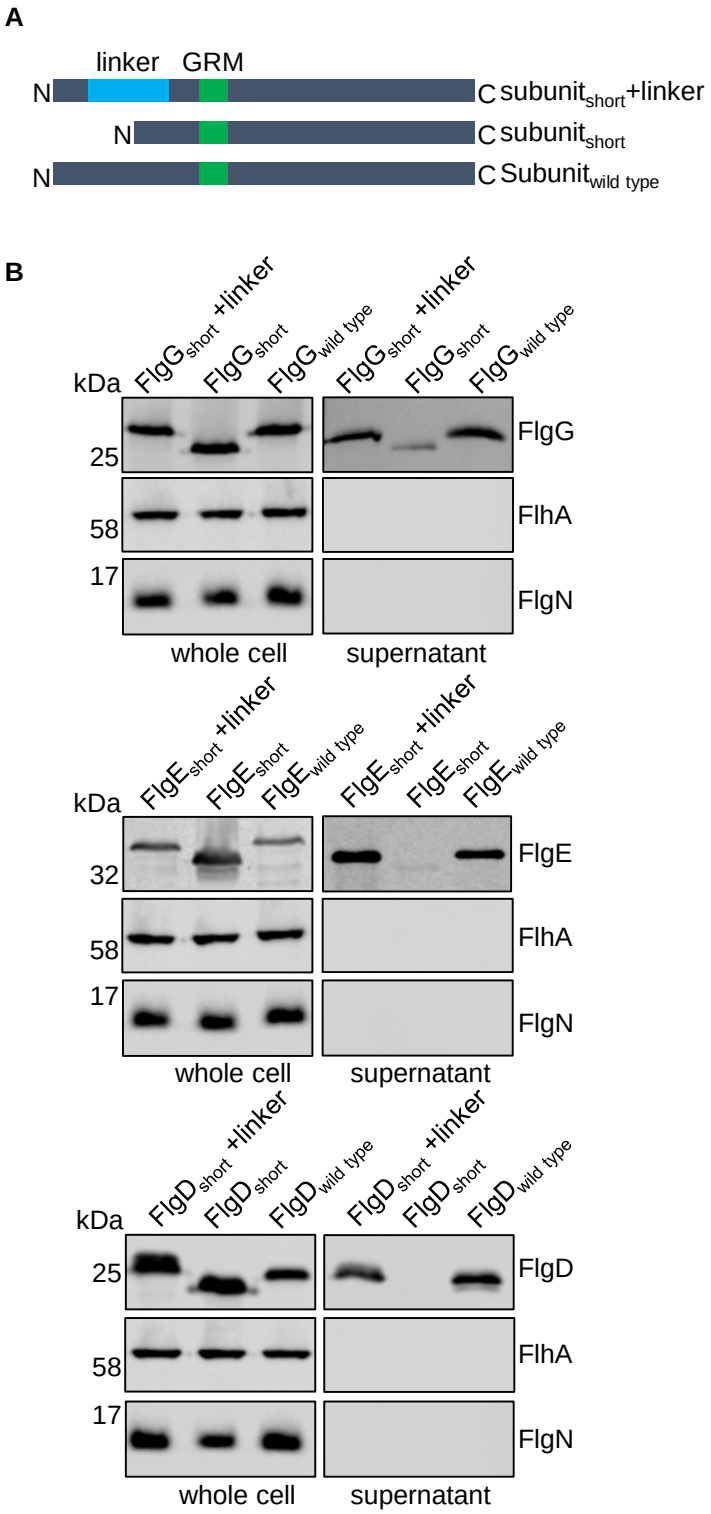

Figure 3.9. Effect of distance between the N-terminus and GRM of rod, hook and cap subunit on export

(**A**) Schematic representation of wild type subunit, subunit$_{short}$ (containing a deletion between the N-terminus and GRM (green)) and subunit$_{short}$+linker (deletion replaced by Gly-Ser-Thr-Asn-Ala-Ser repeats, blue)

(**B**) Secretion analysis of a *Salmonella* Δ*flgD* strain transformed with recombinant pTrc99a plasmids carrying wild type subunit or its variants (subunit$_{short}$, subunit$_{short}$+linker). FlgG (rod) subunit (top), FlgE (hook) subunit (middle) and FlgD (hook cap) subunit (bottom) were engineered to contain an internal 3xFLAG tag for immunodetection. Whole cell (whole cell) and culture supernatant (supernatant) fractions were prepared and immunoblotted with anti-FLAG, anti-FlhA or anti-FlgN sera.

stall at the FlhBc export gate. To test whether the $FlgD_{short}$ variant stalls at a key stage in the export pathway to produce a dominant negative effect on subunit export and cell motility, pTrc99a plasmids encoding $FlgD_{short}$, $FlgD_{short}$ΔGRM, FlgDΔGRM or wild type FlgD were transformed into a *Salmonella* Δ*recA* strain and overexpression of the FlgD variants was induced with 100 μM IPTG. Subunit export and swimming motility assays were assayed as described previously (section 2.15 and 2.16). Proteins in whole cells and supernatants were separated by SDS-PAGE and analysed by immunoblotting with antisera against representative early (FlgD and FliK) and late (FlgK and FliD) subunits, as well as FlhA and FlgN as loading, expression and lysis controls (Figure 3.10). In *Salmonella*, *in trans* expression of $FlgD_{short}$ attenuated export of non-cognate subunits compared to cells expressing wild type FlgD, FlgDΔGRM or $FlgD_{short}$ΔGRM (Figure 3.10). Consistent with the export phenotypes, cells expressing $FlgD_{short}$ were less motile than cells expressing wild type FlgD or the other variants (Figure 3.10). The data indicate that, like the FlgDΔ2-5 variant, $FlgD_{short}$ stalls at FlhBc giving rise to dominant negative effects on subunit export and cell motility, and that deletion of the GRM prevents this stalling, relieving the negative dominance.

3.6.2 Overexpression of $FlgE_{short}$ has a dominant negative effect on motility and export

To investigate whether the distance between the N-terminal hydrophobic export signal and the GRM is important in early subunits other than FlgD, a recombinant pTrc99a plasmid encoding a FlgE variant that lacks residues 9 to 32 but retains the first 8 residues of FlgE and the GRM (FlgEΔ9-32, hereon $FlgE_{short}$) was constructed and transformed into a *Salmonella* Δ*recA* strain. In addition, pTrc99a plasmids encoding $FlgE_{short}$ΔGRM, FlgEΔGRM or wild type FlgE were also constructed as controls. All recombinant FlgE variants were engineered to contain a triple FLAG tag (3xFLAG) between residues 234 and 235 to aid their detection in whole cells and culture supernatants. FlgE and its variants were overexpressed *in trans* in a *Salmonella* Δ*recA* strain by induction with 100 μM IPTG. Subunit export into culture supernatants and cell swimming motility were

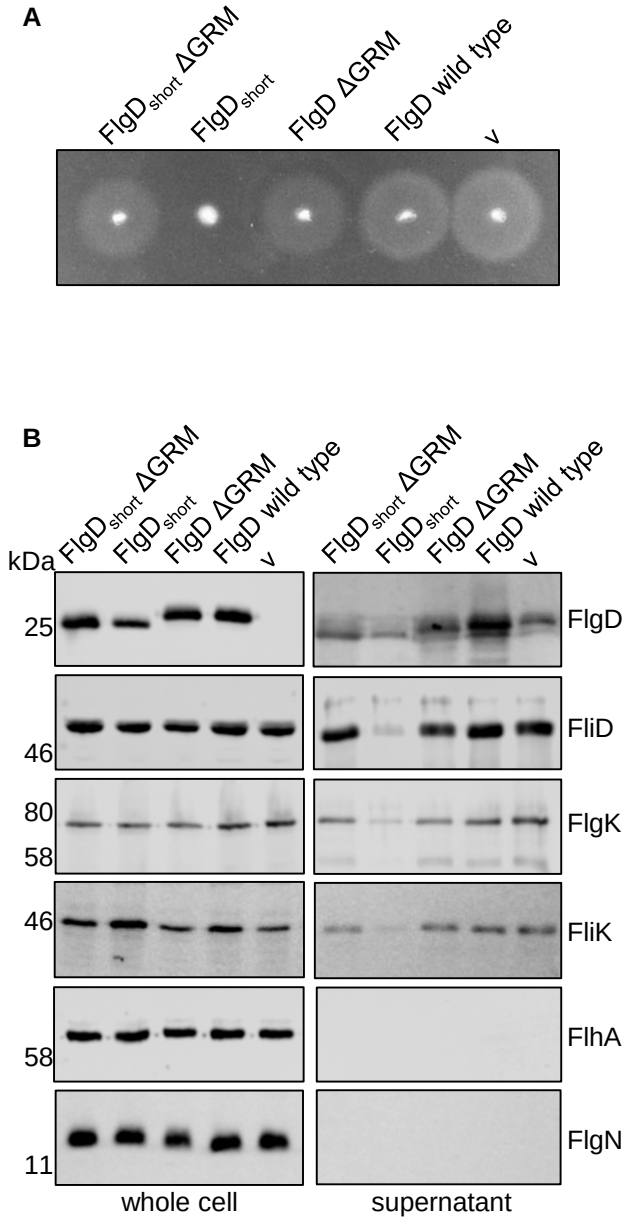

Figure 3.10. Overexpression phenotypes of $FlgD_{short}$ and its variants
(A) Swimming motility assays of a *Salmonella* Δ*recA* strain transformed with recombinant pTrc99a plasmids carrying wild type FlgD or its variants ($FlgD_{short}$ΔGRM, $FlgD_{short}$, FlgDΔGRM) or empty pTrc99a vector (V). Cells were inoculated into 0.3% soft-tryptone agar containing 100 μg/ml ampicillin and 100 μM IPTG and incubated for 3-6 hours at 37°C.
(**B**) Secretion analysis of the above cells by immunoblotting of whole cell (whole cell) and culture supernatant (supernatant) fractions prepared from the above cells with anti-FlgD, anti-FliD, anti-FlgK, anti-FliK, anti-FlhA and anti-FlgN sera.

assayed as described previously (section 2.15 and 2.16). Proteins in whole cell and supernatants were separated by SDS-PAGE and analysed by immunoblotting with antisera against representative early (FlgD and FliK) and late (FlgK and FliD) subunits, anti-FLAG antisera to detect the FlgE(3xFLAG) variants, as well as FlhA and FlgN as loading, expression and lysis controls. As expected, the $FlgE_{short}$ and $FlgE_{short}$ΔGRM variants were not exported into culture supernatants as efficiently as wild type FlgE (3.11). Furthermore, their levels in whole cells appeared to be higher than for wild type FlgE and the other FlgE variants, which would be consistent with their accumulation in the cell (Figure 3.11). Expression of $FlgE_{short}$ attenuated export of non-cognate subunits compared to wild type FlgE and the other FlgE variants, including $FlgE_{short}$ΔGRM. Consistent with the export phenotypes, cells expressing $FlgE_{short}$ were less motile than cells expressing the other FlgE variants (Figure 3.11). This suggests that, in a manner similar to FlgDΔ2-5 and $FlgD_{short}$, the $FlgE_{short}$ variant stalls at the FlhBc export gate and that deletion of the GRM (the FlhBc binding signal) suppresses the dominant negative effects on export and cell motility.

3.7 Mutations in the FliP export gate component suppress the $FlgD_{short}$ motility defect

The minimum distance requirement between the N-terminal hydrophobic 2-5 signal and the GRM suggests that the subunit 2-5 signal binds a site on the export machinery that is positioned at a distance equivalent to the length of a 20-24 residue polypeptide from the FlhBc GRM binding site. This corresponds to a length of 67-88 Å if the subunit N-terminus is in an extended conformation or 29-38 Å for an α-helix. Placement of the flagellar FliPQR export gate structure in the tomographic reconstruction of the *Salmonella* SPI-1 type III secretion system indicates that FlhBc is in the cytoplasm immediately beneath the inner membrane (Figure 3.12)[253]. Mapping the distance between the base of $FlhB_N$-FliPQR and the subunit docking site on FlhBc indicates that these structures are ~62 Å apart[253] (Figure 3.12). It is feasible that subunits docked at FlhBc could contact the base of $FlhB_N$-FliPQR or alternatively contact $FlhA_N$ and/or $FlhB_{CN}$, which lie directly below the $FlhB_N$-FliPQR complex.

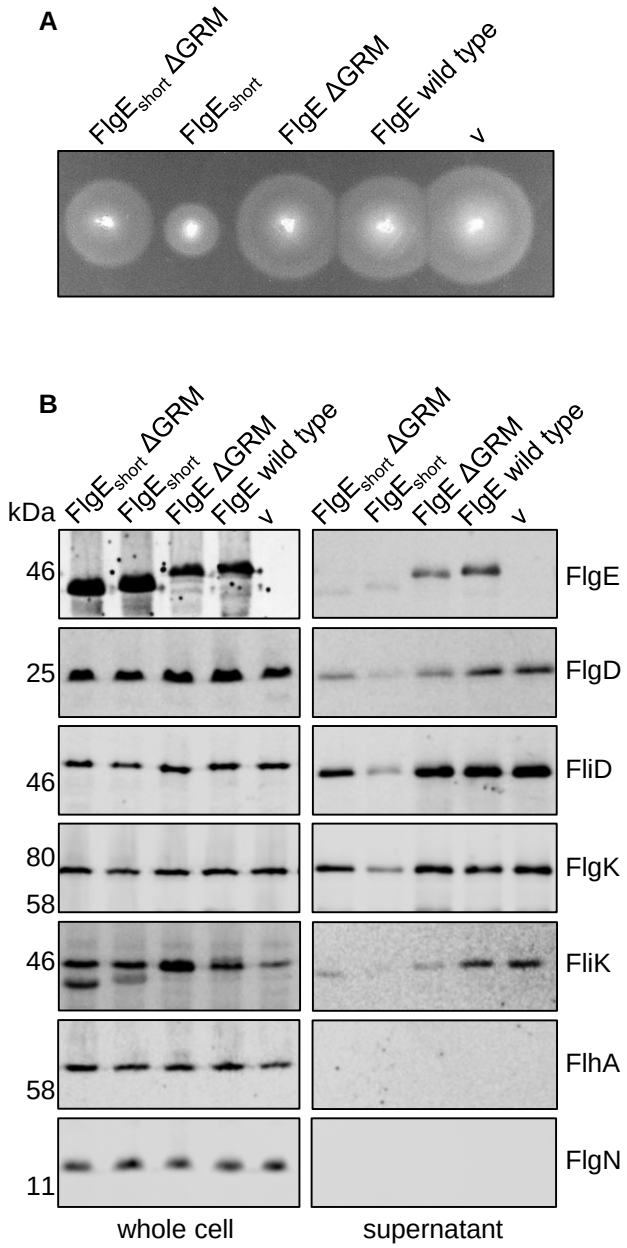

Figure 3.11. Overexpression phenotypes of FlgD$_{short}$ and its variants
(A) Swimming motility assays of a *Salmonella* Δ*recA* strain transformed with recombinant pTrc99a plasmids carrying FlgE containing an internal 3xFLAG tag or its variants (FlgE$_{short}$ΔGRM, FlgE$_{short}$, FlgEΔGRM) or empty pTrc99a vector (V). Cells were inoculated into 0.3% soft-tryptone agar containing 100 μg/ml ampicillin and 100 μM IPTG and incubated for 3-6 hours at 37°C.
(**B**) Secretion analysis of the above cells by immunoblotting of whole cell (whole cell) and culture supernatant (supernatant) fractions prepared from the above cells with anti-FLAG, anti-FlgD, anti-FliD, anti-FlgK, anti-FliK, anti-FlhA and anti-FlgN sera.

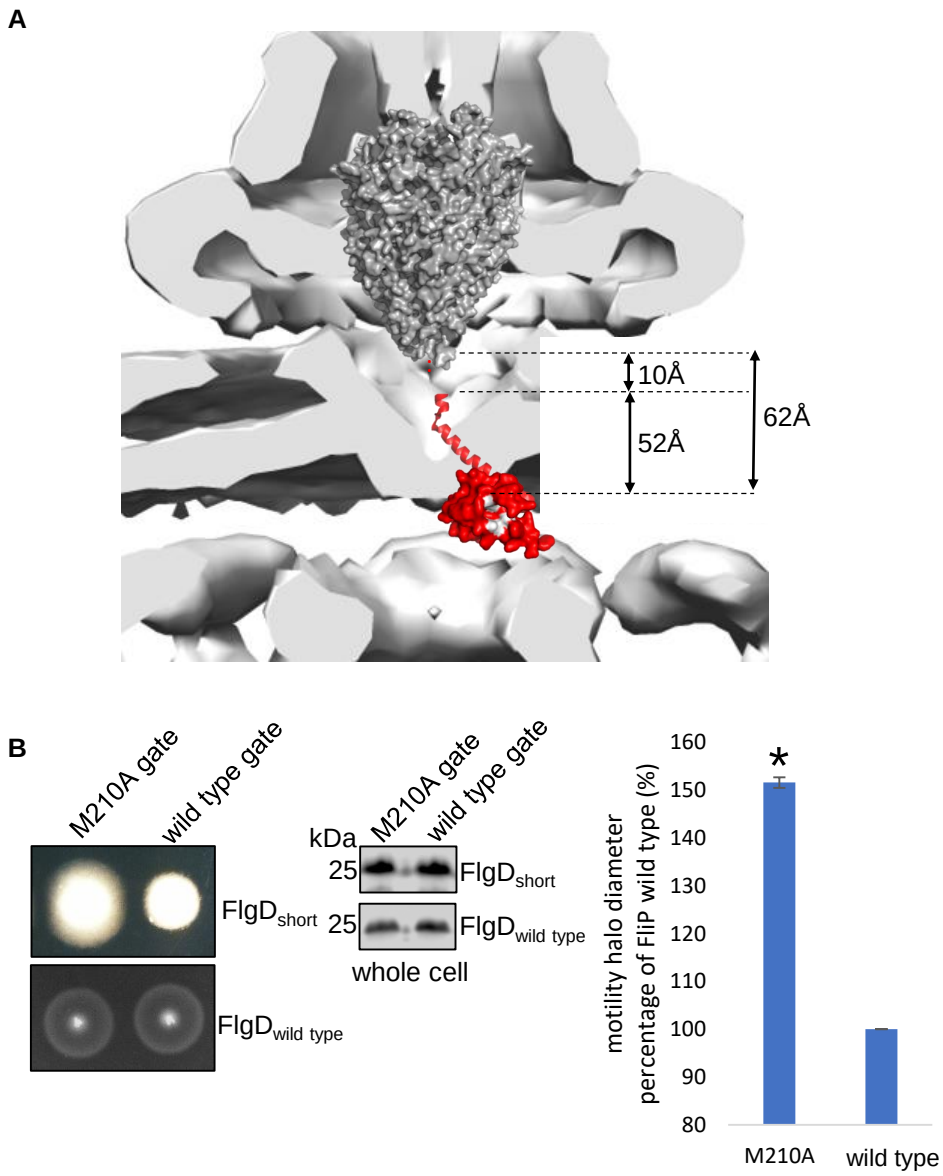

Figure 3.12. Mutations in FliP suppress the $FlgD_{short}$ motility defect
(**A**) Placement of the crystal structure of FlhBc (PDB:3BOZ) and the cryo-EM structure of FliPQR (PDB:6F2D) in a tomographic reconstruction of the *Salmonella* SPI-1 injectisome (EMD-8544). Distance from the GRM binding site on FlhBc (grey) to residue D229 of FlhBc (52Å) and the minimum distance (based on linear alpha helix) between residue D229 in the crystal structure of FlhBc and FlhB residue K221 (*Vibrio mimicus*, equivalent to R221 in *Salmonella* FlhB) from the cryo-EM structure (10Å)[253].
(**B**) Swimming motility assays of *Salmonella fliP*(M210A) Δ*flgD* and Δ*flgD* strains transformed with recombinant pTrc99a plasmids carrying the $FlgD_{short}$ variant. Cells were inoculated into 0.3% soft-tryptone agar containing 100 µg/ml ampicillin and incubated for 12-16 hours at 37°C (left). Whole cell fractions were immunoblotted with anti-FlgD sera (middle). Motility halo diameter of each strain expressing the $FlgD_{short}$ variant were plotted as a percentage of motility of the wild type gate strain expressing $FlgD_{short}$ (right). The error bars represent the standard error of the mean calculated from at least the biological replicates. * indicates a p-value < 0.05.

In considering potential functions for the subunit N-terminal hydrophobic 2-5 export signal, one possibility is that it may be involved in triggering a conformational change in the ABPQR export gate from an energetically favourable closed conformation to the open conformation, allowing subunit translocation into the export channel. If this were the case, I reasoned that introduction of mutations into the export gate to destabilise the closed conformation might allow cells to 'bypass' the absence of the subunit N-terminal hydrophobic 2-5 export signal. One such mutation in the ABPQR export gate, FliP-$M_{210}A$, has been shown to increase ion conductance across the bacterial inner membrane, indicating that efficient gate closure has been disrupted[246]. To test whether destabilising the ABPQR export gate closed state could suppresses the cell motility defects observed for the FlgDΔ2-5 or $FlgD_{short}$ subunits, I constructed a Δ*flgD* strain in which the chromosomal *fliP* gene was replaced with a functional internally HA-tagged variant of FliP designated 'wild type gate' and a second Δ*flgD* strain with a chromosomally-encoded HA-tagged FliP containing the methionine-210 to alanine substitution, designated '$M_{210}A$ gate'. These strains were transformed with pTrc99a encoding FlgDΔ2-5 or $FlgD_{short}$ and cells were grown to A_{600} 1.0 before being inoculated into 0.3% soft-tryptone motility agar and incubated for 12-16 hours at 37ºC. Strains expressing FlgDΔ2-5 were non-motile whereas limited swimming motility was observed, to different extents, in strains producing $FlgD_{short}$, with motility being consistently better in the opened gate strain (Δ*flgD* $M_{210}A$ gate) compared to the strain producing the wild type gate (Δ*flgD* wild type gate; Figure 3.12). The diameter of the motility halo produced by the Δ*flgD* $M_{210}A$ gate strain expressing $FlgD_{short}$ was 50% larger than for the Δ*flgD* wild type gate strain expressing $FlgD_{short}$, indicating a moderate but significant increase in swimming motility (Figure 3.12). These data indicate that the motility defect caused by the incorrect positioning of the N-terminal hydrophobic 2-5 signal relative to the GRM in $FlgD_{short}$ can be partially rescued by introducing mutations that enable the export gate to adopt an open conformation without sensing an export signal from docked subunit. Taken together, the data presented in this chapter suggest that docking of early

subunits *via* the GRM at FlhBc positions the subunit N-terminal hydrophobic signal to trigger opening of the ABPQR export gate (Figure 3.13).

3.8 Discussion

How the type III export machinery recognises and exports only a subset of all the proteins produced in the cell remains poorly understood. It has been recognised for some time that substrates for flagellar and virulence T3SS contain signals which facilitate their export[138,139,140,141,142]. However, not all export signals have been identified and it remains unclear how they target subunits to the export machinery and facilitate their export[8,9]. Furthermore, for subunits that contain several discrete export signals, the relative contribution of each signal to directing subunit export is not known. Work presented in this chapter aimed to further characterise previously identified export signals within the hook capping protein FlgD, and further understand how these signals, and the equivalent signals in other early subunits, direct subunit export through the flagellar T3SS.

A previous study had shown that the first 70 residues of *E.coli* FlgD were sufficient to direct the transport of a reporter protein into the periplasm[254]. This is in agreement with other studies that showed export signals are situated within the N-terminus flagellar subunits[138,139,140,141,142]. The flagellar export signals reside in an extensive region of the subunit N-terminus that is often unstructured or disordered in solution, and this intrinsic disorder may be an essential feature of the export signal[255]. Unstructured N-terminal export signals are a common attribute of substrates recognised by other export systems[103,96]. For example, substrates of the Sec export system possess a tripartite N-terminal signal that is largely unstructured in solution[103]. Similarly, substrates for the TAT export pathway contain unstructured N-terminal signals, even though this pathway transports folded proteins [96]. These unstructured export signals may facilitate multiple interactions with different binding partners during export and/or, in the case of export systems that transport unfolded proteins, aid initial entry into narrow export channels.

A

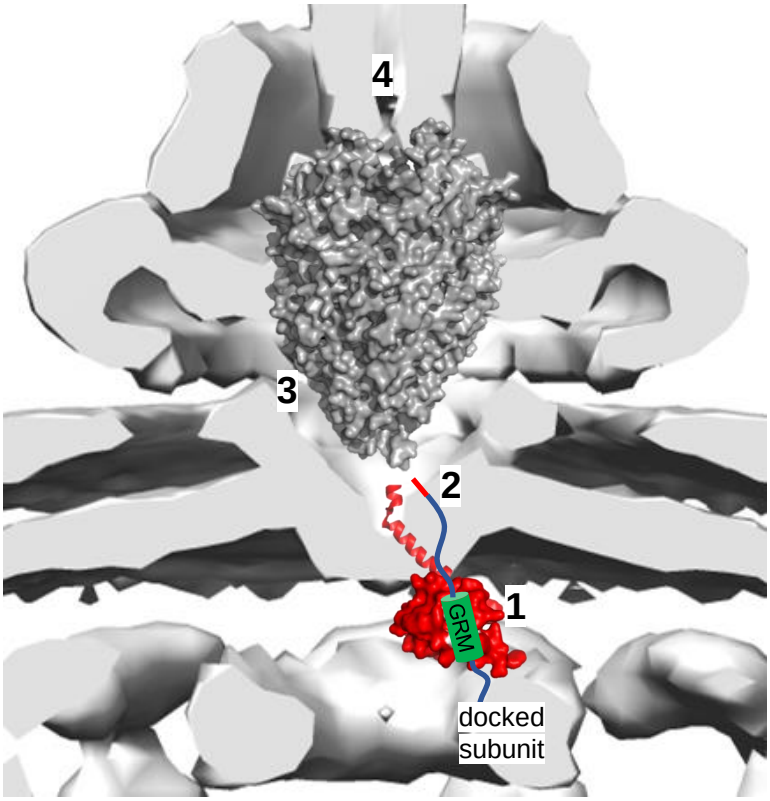

Figure 3.13. A proposed model for the sequence of binding events between early subunits and the export machinery
(**A**) Placement of the crystal structure of FlhBc (PDB:3BOZ) and the cryo-EM structure of FliPQR (PDB:6F2D) in a tomographic reconstruction of the *Salmonella* SPI-1 injectisome (EMD-8544). Subunits dock at the FlhBc gate via their gate-recognition motif (GRM) (**1**) positioning the N-terminal non-polar signal (**2**) to trigger opening of the export gate complex (**3**). Subunits are subsequently translocated into the export channel at the centre of flagellum (**4**) where they transit to the filament tip and refold into the nascent structure.

The FlgDΔ2-5 variant was not exported efficiently into culture supernatants and this export defect was greater than for the FlgD variant lacking the GRM (FlgDΔGRM), the signal that binds the FlhBc export gate component, suggesting that the 2-5 signal is more important for FlgD export than the GRM signal. Screens for suppressors of the export and motility defects associated with FlgDΔ2-5 identified two classes of intragenic suppressors. The first class of suppressor mutations caused the introduction of small non-polar residues at positions between three and seven residues away from the new FlgDΔ2-5 N-terminus. The second class of suppressor mutations introduced duplications or insertions between the FlgDΔ2-5 N-terminus and the GRM, repositioning valine-15 relative to the GRM. Intragenic suppressors isolated from a FlgDΔ2-5-^{19}(GSGSMT)^{20}-V_{15}A variant all caused the introduction of small non-polar residues at the subunit N-terminus, supporting the view that N-terminal small hydrophobic residues are a requirement for early subunit export. Only certain small non-polar residues were isolated in the new FlgDΔ2-5 N-terminus, however this bias is likely based on the fact that all isolated suppressors contained a single nucleotide change and therefore only certain residues can be selected for. For example, asparagine-8 has the codon AAU and the suppressor N_8I was isolated multiple times which required a single nucleotide change (AAU to AUU) whereas an N_8V mutation would require at least a two-nucleotide change (*e.g.* AAU to GUU). Two of the suppressors (M_7I and M_7V) resulted in a change from a large non-polar methionine to a smaller non-polar residue, supporting the view that the residue side chain must be small as well as non-polar.

The FlgDΔ2-5 variant had a dominant negative effect on flagellar export and cell motility when expressed in a *Salmonella* Δ*recA* strain. This suggests that FlgDΔ2-5 stalls at the export machinery, perhaps sequestering one or more export components into a non-functional complex and/or preventing other subunits from docking at the export machinery. Dominant negative phenotypes have been observed for other flagellar subunits or export components, for example, a FlgN chaperone variant lacking the C-terminal 20 residues stalls at the FliI component of the flagellar export ATPase, sequestering FliI and

preventing other components from interacting with it[176]. Furthermore, GST-tagged FliJ (stalk component of the flagellar ATPase) associates with the export gate component FlhA but does not interact properly with FliI and prevents wild type FliJ from forming productive interactions with FlhA[256]. These dominant negative phenotypes can be reversed if additional mutations are introduced that disrupt the 'stalling' interaction. If the FlgDΔ2-5 variant was binding and stalling at FlhBc, then combining the 2-5 deletion with a GRM deletion such that FlgD can no longer bind FlhBc should reverse the dominant negative phenotype. Indeed, the FlgDΔ2-5ΔGRM variant was not dominant negative, indicating that FlgDΔ2-5 stalls at FlhBc. FlhBc is likely positioned within or just below the plane of the membrane. This suggests that when subunits are docked at FlhBc, the N-terminal hydrophobic 2-5 signal, which is positioned ~30 residues upstream of the GRM, could be positioned further along the export pathway, close to export components in the plane of the inner membrane, and could contact the base of the $FlhB_N$-FliPQR complex.

All early flagellar subunits contain a GRM signal which allows them to dock at FlhBc[141]. One interesting feature is that in all early subunits the GRM is positioned at least 30 residues from the start methionine (Figure 3.3). Furthermore, all early subunits contain small non-polar residues at the extreme N-terminus, but FlgD is unique in that its extreme N-terminus contains three small non-polar residues and following these residues there are very few small non-polar residues until the GRM (amino acids 36-40), which is why the FlgD 2-5 deletion variant produced a non-motile phenotype (Figure 3.3). Deletion of the extreme N-terminus of other early subunits generates a new N-terminus containing small non-polar residues that can function as an export signal, so in these subunits deletion variants equivalent to FlgDΔ2-5 would not produce a non-motile phenotype.

The second class of FlgDΔ2-5 suppressors introduced duplications or insertions within the FlgDΔ2-5 N-terminal region upstream of the GRM, suggesting that the distance between the N-terminal hydrophobic 2-5 signal and the GRM is

important for function. By replacing the region between these two signals with four GSTNAS repeats and then sequentially reducing the number of repeats, I observed that export was attenuated when the number of GSTNAS repeats dropped below three. Further refinement showed that a minimum of 20 residues was required between the N-terminal hydrophobic 2-5 signal and the GRM to enable cell motility, with 24 residues restoring motility to wild type levels.

Early subunits bind the FlhBc export gate with micromolar affinities, indicating that these interactions are transient[141,257]. The GRM is essential for this interaction and, in particular, the first phenylalanine of this highly conserved motif (Fxxxϕ, where ϕ is any hydrophobic residue) is critical for binding a surface exposed hydrophobic patch on FlhBc[141]. Unlike the GRM, functionality of the N-terminal hydrophobic 2-5 signal does not require absolute conservation of specific residues. Moreover, we do not know which export component the 2-5 signal contacts to promote subunit export. The data discussed so far indicate that this N-terminal signal constitutes small non-polar residues and that its position relative to the GRM is critical. I anticipate that, like the GRM, any interactions of the N-terminal hydrophobic 2-5 signal with the export machinery will be transient, and that the local environment will influence binding affinity.

When early subunits bind *via* the GRM to FlhBc, they are likely positioned in or just below the plane of the membrane. Our data indicate that the N-terminal hydrophobic 2-5 signal needs to be positioned at least 20-24 residues away from the GRM. The distance separating the 2-5 signal from the GRM will depend on the structure of the subunit N-terminus. It is not known whether the N-terminus of early subunits assume structure whilst docked at FlhBc. In substrates of the TAT export pathway, the N-terminal export signal switches conformations between α-helical and unstructured in response to the hydrophobicity of its environment[258]. It is possible that the local environment within the T3SS machinery might influence the conformation of subunits docked at the export machinery. Furthermore, conformational changes in the export machinery that take place during export may alter the local environment and influence the

conformation of subunit termini[113,105]. If the 24 residues between the N-terminal hydrophobic 2-5 signal and the GRM are unstructured and extended, this would correspond to a polypeptide contour length of approximately 86 Å (where the length of one amino acid is ~3.6 Å), whereas if these residues adopt α-helical structure they would span approximately 36 Å (where one amino acid rises every ~1.5 Å). Without further structural information on the core components of the fT3SS and the precise location of the FlhBc domain, it is difficult to determine where the N-terminal hydrophobic 2-5 signal might contact the export machinery.

The fT3SS must be gated to ensure that the export channel isn't always open, which would compromise the function of the inner membrane as a 'tight' permeability barrier. The extreme N-terminus may be the first region of a flagellar subunit to contact the components of the ABPQR export gate that cross the plane of the inner membrane and/or reside in the periplasm. The recent atomic resolution structure of the FliPQR components of the gate complex identified three gating regions: FliR provides a loop which sits within the core of the gate complex (the R-plug), below which five copies of FliP each provide three methionine residues that together form a methionine-rich ring and, below this, ionic interactions between FliQ residues hold the base of the structure shut (the Q-latch)[105]. I reasoned that one possibility is that the subunit N-terminal hydrophobic 2-5 signal could trigger opening of this export gate. If this were the case, destabilising the closed conformation of the export gate should suppress the export defect associated with FlgDΔ2-5 or $FlgD_{short}$. FlgDΔ2-5 could not restore swimming motility to Δ*flgD* cells producing the destabilised export gate. However, Δ*flgD* cells producing $FlgD_{short}$ were motile, albeit severely reduced compared to wild type cells. Destabilising the export gate closed state by introducing a $M_{210}A$ substitution in FliP improved swimming motility in Δ*flgD* cells producing $FlgD_{short}$, indicating that loss of the subunit N-terminal signal could be bypassed by mutations that allow the gate to open in the absence of this signal. Although destabilising the export gate suppressed the $FlgD_{short}$ motility defect, swimming motility only improved by 50%. This isn't a large improvement in motility, however, the gate opening mutation (FliP $M_{210}A$) may only partially bias

gate conformation towards the open state. Complete opening of the export gate is likely to be lethal as the membrane permeability barrier would be disrupted[246]. This may explain why none of the suppressors of the motility defects associated with FlgDΔ2-5 and $FlgD_{short}$ were located in the export gate complex. Potential suppressors that would only partially/infrequently open the gate (such as FliP $M_{210}A$) would only partially restore motility, whereas suppressors that fully open the gate would presumably be lethal or at least cause a growth defect. The data in this chapter indicate a selectivity process in which a protein is only selected for export and the export gate only opened if a polypeptide contains two specific optimally spaced export signals.

Early subunits for the related virulence T3SS also contain a GRM, suggesting their mode of interaction with the export gate is similar[141,157]. Consistent with this, the binding pocket on FlhBc identified by Evans *et al* is well conserved in the injectisome homologue, SctU[259]. Furthermore, the predicted GRM signals in all four injectisome early subunits (SctI, SctF, SctP, OrgC) are at least 30 residues away from the subunit N-terminus and all early subunits contain small non-polar residues at their extreme N-terminus. Therefore, it is plausible that the subunit export signals and proposed gate opening mechanism may be conserved among flagellar and injectisome T3SSs.

How do other export systems open their export channels? In many cases, the presence of a substrate triggers opening or assembly of the export channel. The outer membrane chitin transporter in *Vibrio* species adopts a closed conformation whereby the N-terminus of a neighbouring subunit acts as a pore plug[99]. Chitin binding to the transporter ejects the plug, opening the transport channel and allowing chitin transport[99]. The SecYEG pore of the SEC machinery switches from a closed energetically favourable state to an open state *via* interactions between the SecYEG pore and the SecA ATPase or a ribosome that is actively translating a substrate. Both of these interactions induce conformational changes within the plug and gate domains of SecYEG, stabilising the open conformation[100,101,102,103]. Furthermore, in the TAT system which

transports folded substrates across the inner membrane, substrate binding to a TatBC complex triggers association of TatA with the TatBC-substrate complex[104,96]. This induces TatA to polymerise, which is required to for the physical transport of the protein. However, this TatA polymer only assembles when a substrate is present[104,96]. These mechanisms serve both to conserve energy use and prevent disruption of the membrane permeability barrier.

The data in this chapter indicates that small non-polar residues within the N-terminus of early subunits trigger opening of the export gate. How do late flagellar export subunits trigger gate opening? The mechanism must differ in some aspects. To start with, late export subunits do not bind FlhBc. Following the export specificity switch, early export subunits can no longer interact with FlhBc, whereas late export subunits can now be recognised and translocated across the membrane by the export machinery. This specificity switch involves FlhB and the molecular 'tape measure' FliK, which is proposed to induce major conformational changes in FlhBc, effectively removing the early subunit binding site on FlhBc[257,63,65]. Late export subunits must therefore find a different path through the export machinery. Much less is known about the specific export signals in late flagellar export subunits except that they reside within the N-terminus[138,142]. Late export subunits must still open the export gate and it is reasonable that one of the export signals within the N-terminus of late export subunits trigger gate opening. A recent publication showed that efficient export of a late export subunit (FliC) requires a spacer segment of at least 15 amino acids within a certain region of the N-terminus[142]. Whether these distance requirements are to provide a similar docking and gate opening activity is unknown.

What happens once a subunit has triggered opening of the export gate? Subunits must be translocated into the export channel which is presumably achieved using some energy source[234]. The chain mechanism model of subunit transit provided experimental evidence indicating that subunits docked at FlhBc are captured by the C-terminus of the preceding subunit already in the channel and pulled from

the export gate into the channel[141]. Genetic evidence indicates that the C-termini of early subunits do not capture subunits from FlhBc (see chapter 5). Furthermore, the opening of the export gate by the N-terminal export signal suggests that the gate may shut between each subunit entering the channel, suggesting a chain might not span this region of the export machinery. If subunits do chain, they might do so following their passage through the export gate. What energises opening of the export gate? Based on the structure of the FliPQR complex, the gate is in a closed conformation[105]. Multiple interactions maintain this closed conformation, suggesting that some energy source must be provided to open the gate[105]. The next chapter explores how opening of the export gate is energised.

Chapter 4

Proton motive force driven opening of the type III secretion export gate

4.1 Introduction

Proton motive force (PMF) is utilized by many export systems to translocate substrates across membrane barriers[260,51,52,96,103]. Type III secretion systems (T3SS) utilise both the PMF and ATP hydrolysis to energise protein export, although the mechanistic basis of how PMF is coupled to protein export is unknown[51,52,111]. The use of PMF by the flagellar export machinery is facilitated by a cytoplasmic ATPase complex - composed of FliH, FliI and FliJ - and is structurally related to the F_1-ATPase, sharing mechanistic similarities: ATP hydrolysis is thought to drive rotation of the central stalk subunit FliJ, allowing it to make sequential interactions with all nine subunits of the FlhA export gate component, converting the export machinery into a highly efficient $\Delta\psi$ driven export machine[111,224,122,107,261]. Deletion of the ATPase complex abrogates motility and export, however, mutations in other components of the export machinery can suppress these export and motility defects[51,218]. The FlhB $P_{28}T$ mutation is one such mutation that allows the export machinery to bypass the need for a productive FlhA-FliJ interaction[111]. Mutations within FlhA (FlhA $V_{404}M$) also overcome the need for a productive FlhA-FliJ interaction by increasing the ability of the export machinery to use sodium motive force (SMF) instead of PMF to energise subunit export[111,110]. These data indicate that the primary energy source for export *via* T3SS is the ion gradient across the inner membrane and that the ATPase complex facilitates use of this gradient[51,52,111].

Data presented in chapter 3 showed that early export subunits that assemble to form the flagellar rod and hook substructures contain an N-terminal export signal that triggers opening of the export gate complex, ensuring that gate opening only occurs once subunits have docked and are primed for export. The recent cryo-EM structure of the FliPQR complex shows that multiple interactions within the core of structure stabilise a closed export gate conformation, indicating that some

energy source must be provided to break these interactions and open the export channel to permit subunit export[105]. I reasoned that as the BPQR components of the export gate are positioned adjacent to the proposed FlhA proton channel, FlhA may use the energy derived from the PMF to promote gate opening. I set out to test this experimentally.

4.2 Mutations within FliR destabilise the closed conformation of the flagellar export gate

The flagellar export machinery must allow the passage of export subunits across the inner membrane without compromising its function as a permeability barrier[246]. Based on the cryo-EM structure of the closed conformation of the FliPQR export gate components, this barrier might, in part, be maintained by the multiple interactions within the core of this structure, including a central plug formed by FliR residues 106-120, a methionine rich loop or "gasket" formed by FliP residues, and ionic interactions between adjacent FliQ subunits[105]. The gate's closed conformation would physically prevent the movement of flagellar subunits out of the cell and also prevents the passage of small molecules across the inner membrane[246].

I aimed to engineer the export gate to destabilise the closed conformation and favour the open state, reasoning that mutations in contact points between adjacent subunits within the gate would reduce the energy barrier required for gate opening. To screen for potential gate opening mutants, the $FlgD_{short}$ subunit (chapter 3), which is unable to efficiently trigger opening of the export gate, was used. As residues within the FliR plug make multiple interactions within the core of the structure and the FliR plug must be displaced to achieve gate opening, I reasoned that the FliR plug would be a good target to screen for gate opening variants. I predicted that mutations within the FliR plug that destabilise the gate closed state would also supress the motility defect associated with $FlgD_{short}$. To test this, the following Δ*flgD* strains were constructed, each containing single/double mutations within the chromosomally-encoded FliR plug loop: *fliR* $F_{110}A$, *fliR* $F_{113}A$, *fliR* $F_{110}A$ $F_{113}A$, and *fliR* $G_{117}D$. These strains were transformed

with pTrc99a encoding $FlgD_{short}$ and single colonies were used to inoculate an overnight culture. Cells were grown to A_{600} 1.0 in LB containing ampicillin before being inoculated into 0.3% soft-tryptone agar containing ampicillin. Plates were incubated for 12-16 hours at 37ºC. Whole cells were collected, lysed and proteins separated by SDS-PAGE and analysed by immunoblotting to confirm that $FlgD_{short}$ levels were the same in all strains (Figure 4.1). All of the engineered FliR variants suppressed the $FlgD_{short}$ motility defect. The diameters of motility halos were measured from three experimental repeats and quantified, and the data showed that the $F_{110}A$, $F_{113}A$ and double $F_{110}A$ $F_{113}A$ mutants were the best suppressors (Figure 4.1). All FliR variants displayed a moderate but significant increase in swimming motility, similar to the improvement in motility observed for the FliP $M_{210}A$ suppressor (chapter 3, Figure 3.12). The data indicate that disrupting interactions in the FliR plug loop and in other components of the export gate can destabilise the closed gate conformation. The FliR $G_{117}D$ mutant was previously proposed to rescue an interaction between FliR and FlhA, but the data presented here indicate that FliR $G_{117}D$ and our FliR and FliP mutants destabilise the closed conformation of the export gate[262].

To test whether the mutations in the FliR plug loop affect cognate subunit export or swimming motility when wild type FlgD is present, I engineered strains that replaced the chromosomal *fliR* gene with mutant *fliR* genes encoding FliR variants with mutations in the plug loop region: *fliR* $F_{110}A$, *fliR* $F_{113}A$, *fliR* $F_{110}A$ $F_{113}A$, and *fliR* $G_{117}D$ (Figure 4.2). Subunit export into culture supernatants and swimming motility assays were performed as previously described (section 2.15 and 2.16). Swarming motility assays were also performed as defects in motility are often magnified when assessing swarming, which requires upregulation of flagella biogenesis in swarmer cells[263,1]. Proteins in whole cells and supernatants were immunoblotted for the presence of representative early (FlgD) and late (FliC, FliD and FlgK) subunits, and for FlhA and FlgN as loading, expression and lysis controls (Figure 4.2). The mutations in FliR did not alter swimming or swarming motility or subunit export, indicating that these mutations do not disrupt the membrane permeability barrier sufficiently to cause a

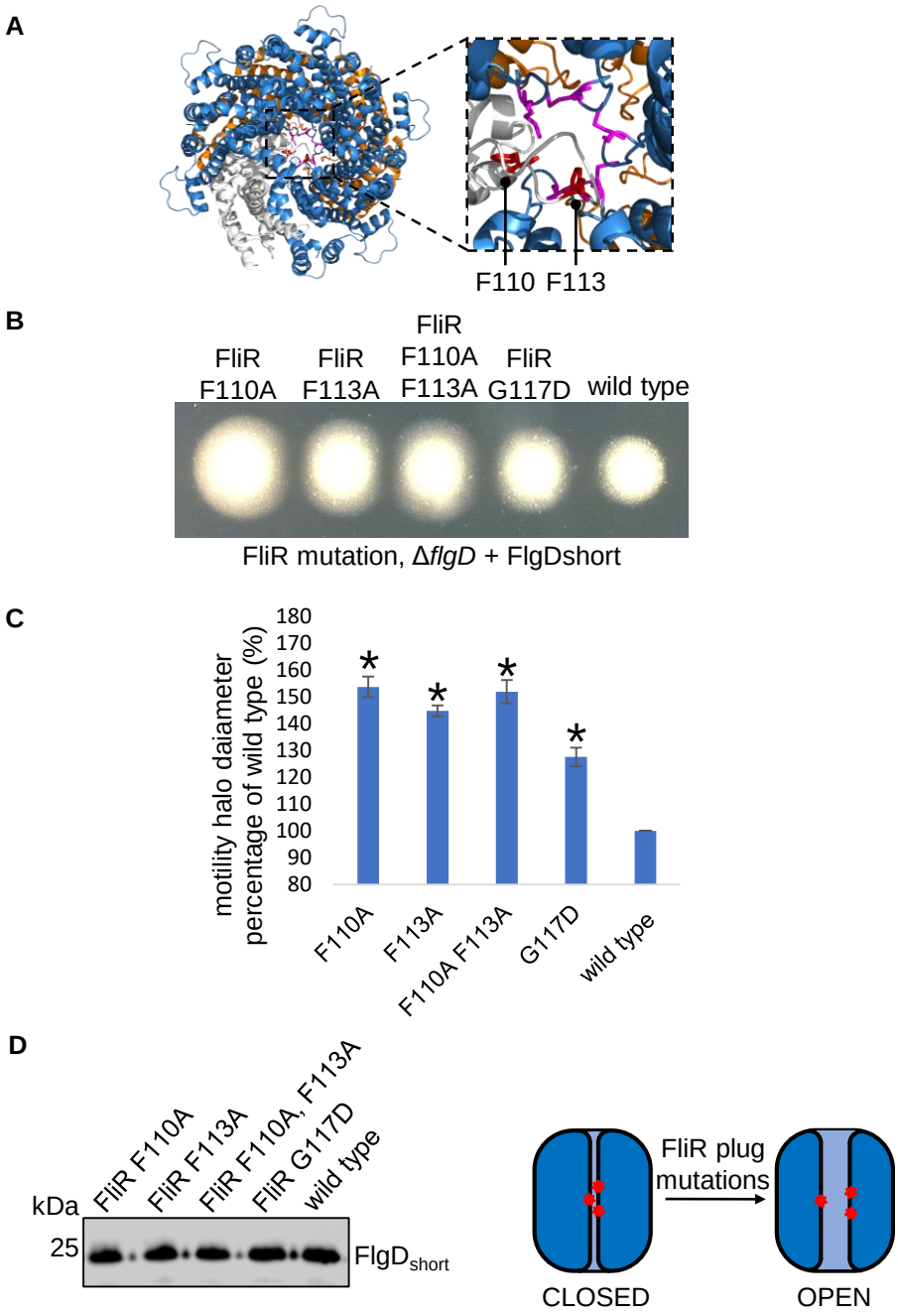

Figure 4.1. Mutations within the FliR plug destabilise the closed export gate conformation

(**A**) Cryo-EM structure of FliPQR (PDB:6F2D) highlighting FliR (grey) residues Phe-110 and Phe-113 (red), FliP (blue) residue Met-210 (purple) and FliQ (orange).

(**B**) Swimming motility assays of a *Salmonella* Δ*flgD* strain and Δ*flgD* strains containing mutations in the *fliR* gene (F110A, F113A, FF10A+F113A or G117D) transformed with recombinant pTrc99a plasmids carrying the $FlgD_{short}$ variant. Cells were inoculated into 0.3% soft-tryptone agar containing 100 µg/ml ampicillin and incubated for 12-16 hours at 37°C.

(**C**) Motility halo diameter of each strain expressing the $FlgD_{short}$ variant were plotted as a percentage of motility of the wild type gate strain expressing $FlgD_{short}$. The error bars represent the standard error of the mean calculated from at least the biological replicates. * indicates a p-value < 0.05.

(**D**) Whole cell fractions from the above strains expressing the $FlgD_{short}$ variant were immunoblotted with anti-FlgD sera (left). Illustration of the gate opening mutations (red) which destabilise the closed export gate (blue) conformation (right).

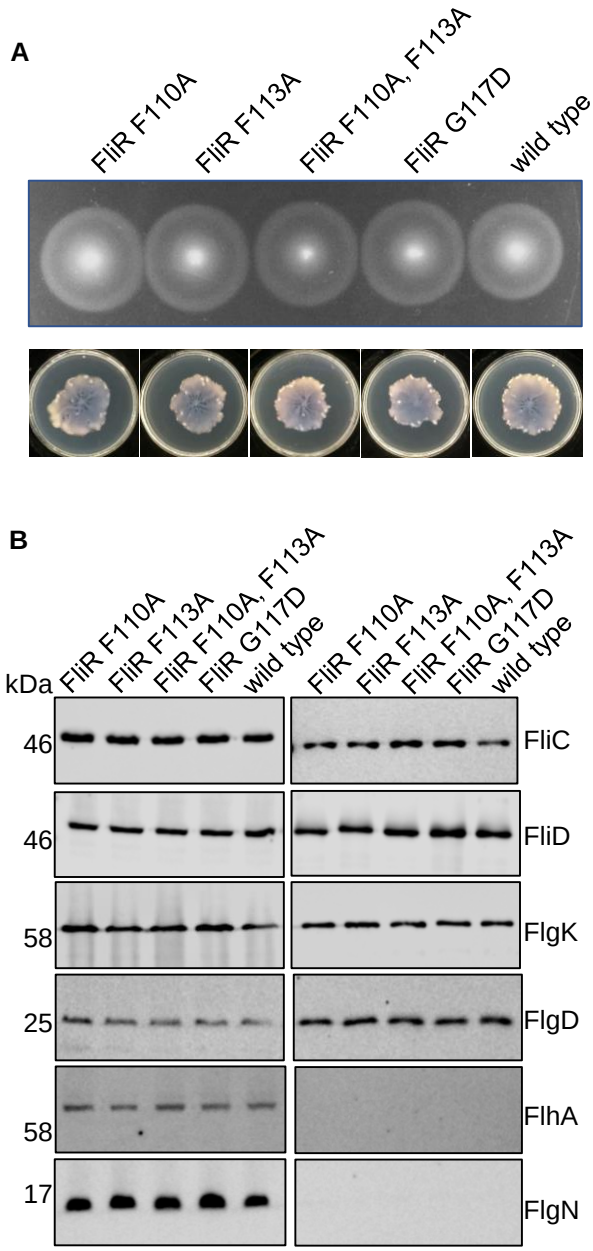

Figure 4.2. Mutations in the FliR plug do not effect subunit export in strains encoding wild type FlhA

(A) Swimming motility assays of wild type *Salmonella* and *Salmonella* strains containing the gate opening mutations in the *fliR* gene (F110A, F113A, F110A+F113A and G117D). Cells were inoculated into 0.3% soft-tryptone agar and incubated for 3-6 hours at 37°C (top).

Swarming motility of the same strains was assessed by centrally inoculating 1µl of stationary phase broth culture on 0.6% agar-tryptone plates supplemented with 0.5% glucose and incubating plates at 30°C for 12-16 hours (bottom).

(**B**) Secretion analysis of the above strains by immunoblotting of whole cell (whole cell) and culture supernatant (supernatant) fractions prepared from the above cells with anti-FliC, anti-FliD, anti-FlgK, anti-FlgD, anti-FlhA and anti-FlgN sera.

swimming or swarming defect, nor do these mutations increase subunit export by reducing the energy barrier required to open the export gate (Figure 4.2).

The FliR plug is reminiscent of the plug loop found in the SecYEG translocon which occludes the channel in combination with several hydrophobic amino acids that come together to form a seal at the centre[264]. Electrophysiology experiments indicated that deleting the plug in SecY caused the channel to alternate between an open and closed state[265]. Furthermore, molecular dynamic simulations indicate that the force required for opening the Sec gate is reduced in SecY plug deletion mutants[266].

By analogy with the Sec system, the FliR plug loop could contribute to maintaining a closed gate conformation. I hypothesised that deletion of the FliR plug loop would destabilise the closed state and promote the open gate conformation. To test this, a strain in which the chromosomal *fliR* gene was replaced with a mutant *fliR* gene that encodes a FliR variant lacking plug loop residues 110-116 was constructed (Figure 4.3). A previous study has shown that cells that fail to maintain the permeability barrier across the inner membrane are more sensitive to a number of chemical agents such as choline[246]. Therefore, if the *fliR* Δ110-116 strain was unable to maintain the permeability barrier then choline should arrest cell growth. The *fliR*Δ110-116 strain was grown at 32ºC with 200 rpm shaking in terrific broth (TB) medium to A_{600} 1.0. The culture was diluted in the same media containing increasing concentrations of choline. The A_{600} of each culture was measured following a further 4.5 hours growth at 32ºC. The *fliR*Δ110-116 strain was more sensitive to choline than the wild type strain, indicating that the FliR plug is important for forming a tight membrane barrier to small molecules and maintaining the closed conformation of the export gate complex (Figure 4.3).

A previous study showed that FliP containing the $M_{210}A$ mutation sensitises cells to a variety of chemical agents[246]. This sensitivity could be reversed by trapping a subunit in the export channel, suggesting that the export gate can form an effective seal around a substrate during transit. I wanted to test whether deletion

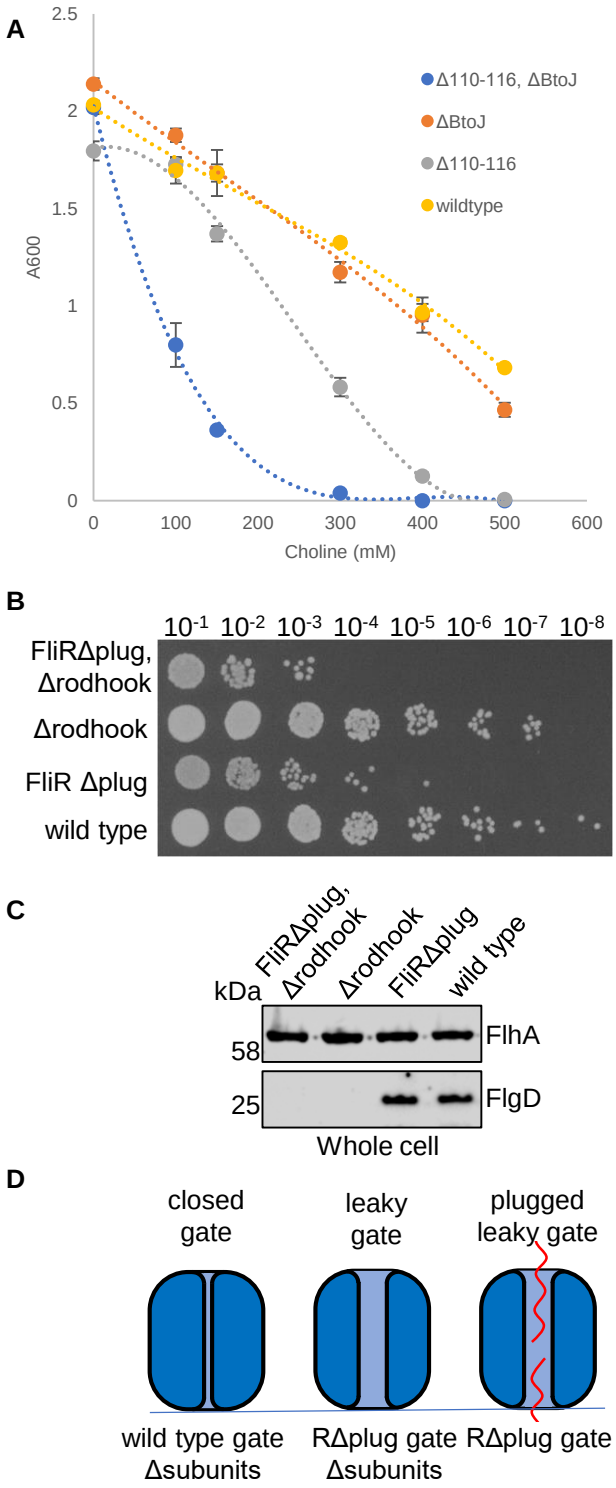

Figure 4.3. Sensitisation of cells to choline in FliR plug and subunit deletion backgrounds

(**A**) Choline sensitisation in wild type cells or cells deleted for early subunits (FlgBCDEFGHIJ, labelled Δrodhook) and/or containing deletions in the FliR plug loop (FliRΔ110-116, labelled Δplug). A600 of strains grown in TB containing varying concentrations of choline (as indicated) following 4.5 hours.

(**B**) Miles and Misra method for determining the colony forming units for the above strains grown for 4.5 hours in TB containing 300 mM choline.

(**C**) Whole cell fractions from the above strains were immunoblotted with anti-FlhA and anti-FlgD sera.

(**D**) Illustration of the FliPQR-FlhB_N export gate in different strains.

of the genes for most of the early flagellar subunits (*flgB*, *flgC*, *flgD*, *flgE*, *flgF*, *flgG*, *flgH*, *flgI*, *flgJ)* would exacerbate the cell growth defect displayed by the *fliR*Δ110-116 strain. Removing most of the flagellar early subunits would mean that, at any given time, there would be fewer subunits transiting through the export gate. The choline sensitivity assay would therefore tell us two things: firstly, if actively transiting subunits seal the gate then a strain exporting fewer subunits should be more sensitive to choline and, secondly, a greater sensitivity to choline would suggest that the gate shuts when there are no subunits actively transiting through it. I generated a strain deleted for the genes that encode most of the early subunits by replacing a large portion of the *flgB-J* operon with a kanamycin cassette: This strain was designated Δ*rodhook.* A second strain combining the *fliR*Δ110-116 deletion and Δ*rodhook* was also constructed (Figure 4.3).

The choline sensitivity assay was performed using the wild type, Δ*rodhook* and Δ*rodhook-fliR*Δ110-116 strains (Figure 4.3). The Δ*rodhook* strain was no more sensitive to choline than wild type, suggesting that fewer available subunits for transit does not interfere with the gating function of the wild type export gate. However, the *fliR*Δ110-116 deletion in combination with the Δ*rodhook* deletion was more sensitive to choline than the *fliR*Δ110-116 deletion strain, indicating that actively transiting subunits partially plug the export gate when it is biased towards the open conformation (Figure 4.3).

4.3 Mutations that promote gate opening suppress the FlhA K_{203}A export defect

A previous study used a genetic screen to identify suppressors of the weakly motile phenotype of a Δ*fliH-fliI, flhB*(P_{28}T), *flhA*(K_{203}W) strain and identified the FliR G_{117}D suppressor mutation, which partially restored motility. This led the authors to suggest that the FliR Gly-117 and FlhA Lys-203 regions may interact. Based on the recent cryo-EM structure of FliPQR, FliR residue Gly-117 is positioned within the core of the structure and is unlikely to directly contact any portion of FlhA[105]. I postulate that replacement of Gly-117 with a bulky aspartate

side chain in the FliR plug likely prevents the export gate from closing fully, as supported by our data showing that FliR $G_{117}D$ partially suppresses the $FlgD_{short}$ motility defect (Figure 4.1). This, together with the fact that the BPQR export gate is located above FlhA and may interact with it, suggests that conformational changes in FlhA may be involved in opening the export gate. I set out to test whether our engineered gate opening mutants could also suppress the motility and export defects caused by the Lysine-203 to Alanine mutation within FlhA. I generated a strain replacing the chromosomal *flhA* gene with a mutant *flhA* gene that encodes a FlhA variant containing the lysine-203 to alanine substitution (FlhA $K_{203}A$). A further two strains were generated that carried the gene encoding the FlhA $K_{203}A$ variant in combination with mutant genes encoding FliR variants predicted to promote gate opening; FliR $F_{113}A$ and FliR $G_{117}D$. Subunit export into culture supernatants and swimming motility assays were performed as previously described (section 2.15 and 2.16). Proteins in whole cells and supernatants were immunoblotted for the presence of FlgD, FliC, FliD and FlgK as representative early (FlgD) and late (FliC, FliD and FlgK) subunits, as well as for FlhA and FlgN as loading, expression and lysis controls. The FliR $F_{113}A$ and FliR $G_{117}D$ variants suppressed the export and motility defects caused by FlhA $K_{203}A$, subunit export restored to wild type levels and motility restored to 60% of wild type (Figure 4.4). It is not clear why cell motility was not fully restored to wild type levels: perhaps the mutations affected the export of a small subset of flagellar subunits or affected cellular fitness, reducing the cell's ability to swim efficiently. The data presented here suggest that FlhA may play an active role in opening the export gate and that FlhA $K_{203}A$ interferes with efficient gate opening. By introducing mutations in the gate that favour the open conformation, this might lower the energy barrier for gate opening by FlhA.

4.4 FlhA uses PMF to energise opening of the export gate

FlhA has been proposed to couple proton motive force to subunit export by functioning as a proton conducting channel[113,262,111,110]. I hypothesised that FlhA may use the PMF to energise opening of the $FlhB_N$-FliPQR portion of the export gate, by directly or indirectly promoting and stabilizing the open conformation.

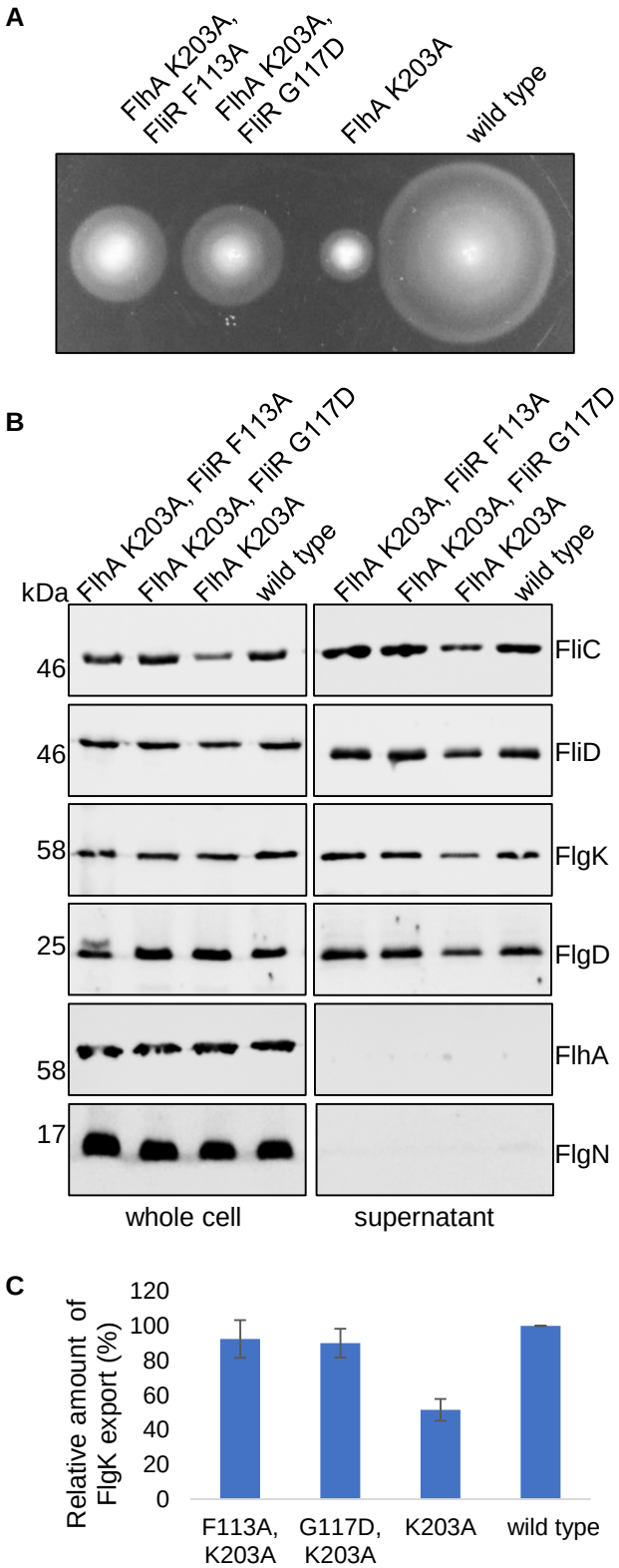

Figure 4.4. Mutations in the FliR plug suppress the FlhA K203A motility and export defects

(**A**) Swimming motility assays of wild type *Salmonella* and *Salmonella* strains containing the gate opening mutations in the *fliR* gene (F113A and G117D) and/or the K203A mutation in the *flhA* gene. Cells were inoculated into 0.3% soft-tryptone agar and incubated for 3-6 hours at 37°C.

(**B**) Secretion analysis of the above strains by immunoblotting of whole cell (whole cell) and culture supernatant (supernatant) fractions prepared from the above cells with anti-FliC, anti-FliD, anti-FlgK, anti-FlgD, anti-FlhA and anti-FlgN sera.

(**C**) Levels of FlgK in culture supernatants from Immunoblots were quantified using ImageStudiolite and plotted as a percentage of FlgK exported by the wild type strain. The error bars represent the standard error of the mean calculated from at least the biological replicates.

The export defect associated with FlhA $K_{203}A$ might be caused by an inability of this FlhA variant to efficiently harness the PMF and couple it to gate opening. To test this, I artificially increased the PMF across the bacterial inner membrane by driving intracellular proton consumption (Figure 4.5). Cells supplemented with arginine convert intracellular protons and arginine to agmatine and CO_2 through the action of the cytoplasmic enzyme arginine decarboxylase, effectively acting as a proton sink within the cell and therefore increasing the PMF[267]. The *flhA* $K_{203}A$ strain and wild type *Salmonella* were grown to A_{600} 1.0 in LB, washed, resuspended in LB or LB containing freshly prepared 20 mM arginine and incubated at 37°C with 200 RPM shaking. Whole cells and culture supernatants were collected after 30 minutes and proteins separated by SDS-PAGE. Proteins in whole cells and supernatants were immunoblotted for the presence of representative early (FlgD) and late (FlgK) subunits, and for FlhA and FlgN as loading, expression and lysis controls. Addition of arginine to the culture of the FlhA $K_{203}A$ strain increased subunit export by 40%, whereas subunit export by the wild type strain was unchanged (Figure 4.5). Addition of arginine did not alter the whole cell levels of subunits or export components (Figure 4.5).

To test whether the arginine-driven increase in subunit export was caused by activity of the two arginine decarboxylase's encoded by *Salmonella*, a strain in which the *speA* and *adiA* genes encoding the arginine decarboxylases were replaced with kanamycin and a spectinomycin resistance cassettes, respectively, was constructed (Δ*speA*, Δ*adiA*). In addition, a strain carrying the *flhA* $K_{203}A$ mutation and the arginine decarboxylase gene deletions (*flhA* $K_{203}A$, Δ*speA*, Δ*adiA*) was constructed. Deletion of two of the *Salmonella* arginine decarboxylases (*speA* and *adiA*) abolished the increase in subunit export in the FlhA $K_{203}A$ cells supplemented with arginine (Figure 4.5). The data indicate that the limiting step in subunit export by the FlhA $K_{203}A$ strain is the ability to utilise the proton gradient.

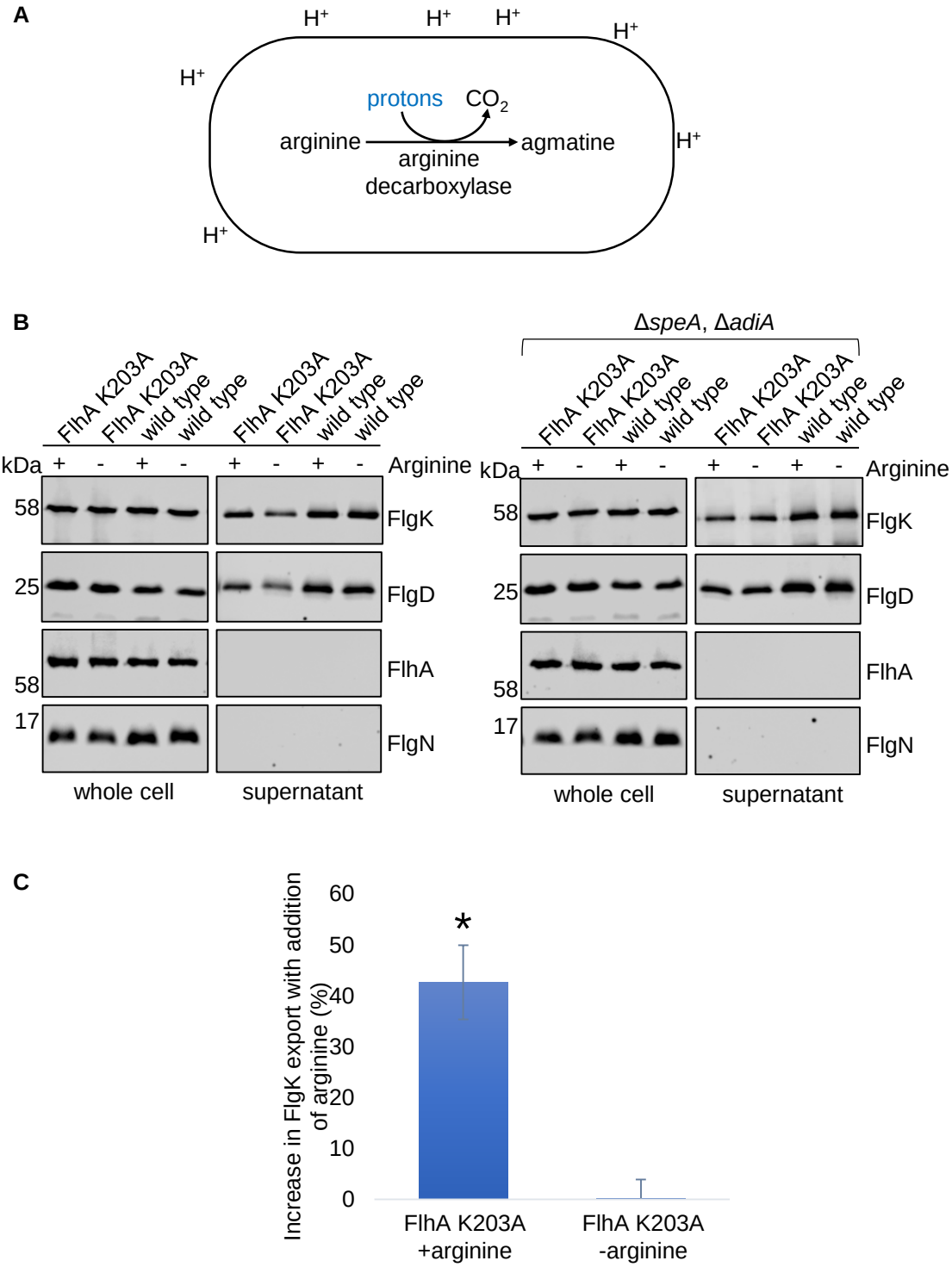

Figure 4.5. Increasing the proton-motive force suppresses the FlhA K203A export defect

(A) An illustration of a cell containing arginine decarboxylase enzyme converting arginine and protons to agmatine and carbon dioxide.

(**B**) Secretion analysis of wild type *and* FlhA(K203A) *Salmonella* strains supplemented with (+) or without (-) 20 mM arginine. Whole cell (whole cell) and culture supernatant (supernatant) fractions were prepared from the above cells and immunoblotted with anti-FlgK, anti-FlgD, anti-FlhA and anti-FlgN sera.

(**C**) Levels of FlgK in culture supernatants from the Immunoblots were quantified using ImageStudiolite and plotted as a percentage of FlgK exported by the wild type strain. The error bars represent the standard error of the mean calculated from at least the biological replicates. * indicates a p-value < 0.05.

4.5 A screen for mutations that suppress the cell motility defect associated with the FlhA $K_{203}A$ variant

The *flhA* $K_{203}A$ strain is poorly motile, I therefore set out to isolate motile suppressors in which export, and therefore motility, was restored. The *flhA* $K_{203}A$ strain was grown to A_{600} 1.0 and inoculated into 0.3% soft-tryptone agar. Plates were incubated at 30ºC for 1-2 days until spurs of motile cells began to swim away from the site of inoculation. Cells were taken from spurs and streaked onto LB agar plates. Arising single colonies were used as template to perform PCR with primers flanking the *flhA* gene and PCR products were sent for sequencing. Six suppressor mutations were identified (Figure 4.6 and 4.7). The suppressor mutations in *flhA* caused the following amino acid replacements; $A_{113}E$, $G_{115}C$, $V_{134}L$ (isolated twice) and $A_{181}T$ (isolated twice). To ensure that the suppressor phenotype did not result from mutations in genes other than *flhA*, strains were generated in which the *flhA* gene was replaced with a mutant *flhA* gene containing one of the identified intragenic suppressor mutations together with the missense mutation encoding $K_{203}A$. All strains gave the same motility phenotype as that observed for the initial suppressor strains, indicating no other extragenic suppressor mutations were present (Figure 4.6 and 4.7). The suppressor mutations were categorised into two classes based on their position in the predicted transmembrane region of FlhA. The first two suppressor mutations, $A_{113}E$ and $G_{115}C$, were positioned in a predicted periplasmic loop connecting transmembrane helices 3 and 4, and both replace a small residue with a bulky side chain (Figure 4.6). These suppressors restored subunit export to wild type levels (Figure 4.6). Furthermore, the $A_{113}E$ and $G_{115}C$ suppressors improved motility to 80% and 70% of wild type, respectively, which is greater than the motility defect suppression observed for the gate opening mutations in FliR ($F_{113}A$ or $G_{117}D$).

The FlhA periplasmic loop containing $A_{113}E$ and $G_{115}C$ is predicted to be directly adjacent to base of the $FlhB_N$-FliPQR export gate substructure[105]. It is possible that these suppressors promote the export gate open conformation. To test this, the ability of these mutations to suppress the $FlgD_{short}$ motility defect was

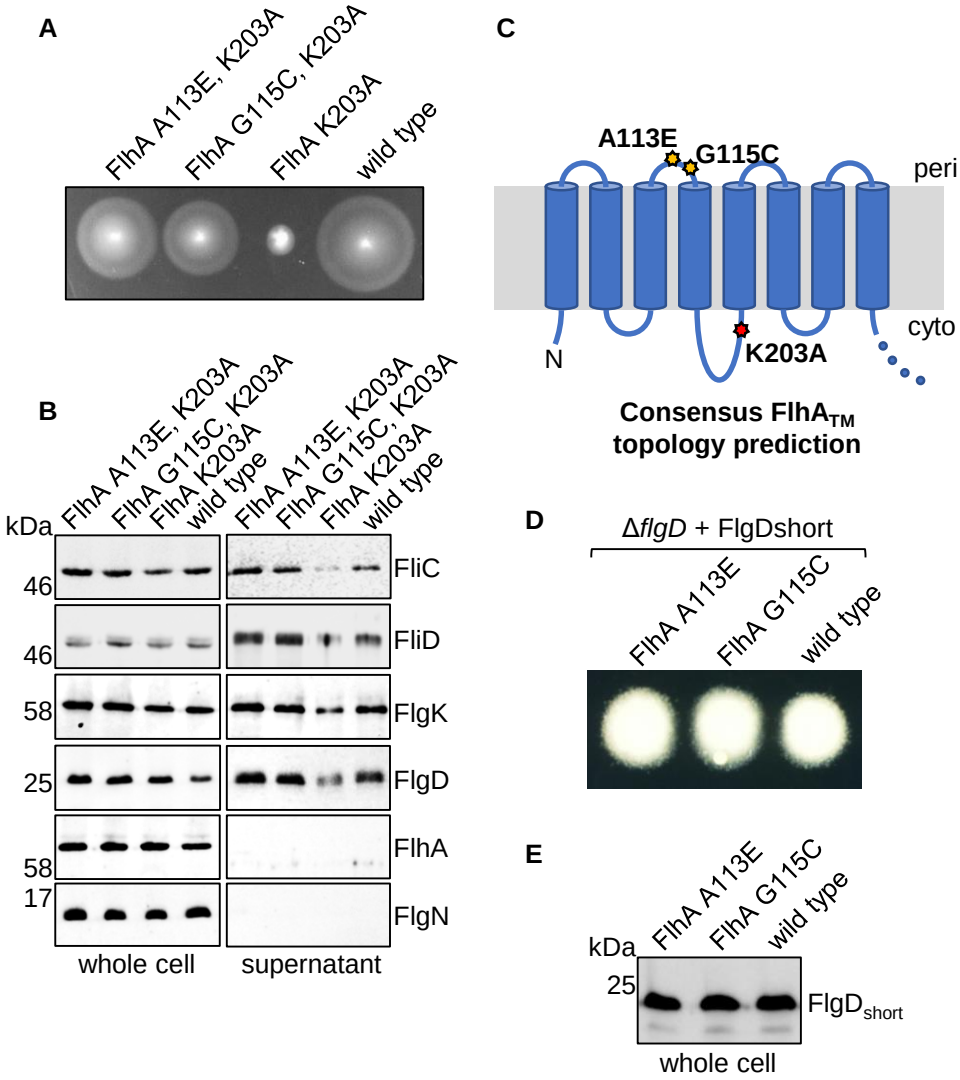

Figure 4.6. Isolated motile suppressors of FlhA K203A

(**A**) Swimming motility assays of wild type *Salmonella* and a strain containing the K203A mutation in the *flhA* gene and its gain of function mutants (FlhA K203A, A113E and FlhA K203A, G115C). Cells were inoculated into 0.3% soft-tryptone agar and incubated for 3-6 hours at 37°C.

(**B**) Secretion analysis of whole cell (whole cell) and culture supernatant (supernatant) fractions of the above strains by immunoblotting with anti-FliC, anti-FliD, anti-FlgK, anti-FlgD, anti-FlhA and anti-FlgN sera.

(**C**) Topology prediction of the transmembrane region of FlhA. The predicted locations of the K203A mutation (red) and gain of function mutations (A113E and G115C, yellow) are highlighted with an asterisk.

(**D**) Swimming motility assays of a *Salmonella* Δ*flgD* strain and Δ*flgD* strains containing mutations in the *flhA* gene (A113E or G115C) transformed with recombinant pTrc99a plasmids carrying the FlgD$_{short}$ variant. Cells were inoculated into 0.3% soft-tryptone agar containing 100 µg/ml ampicillin and incubated for 12-16 hours at 37°C.

(**E**) Whole cell fractions from the above strains were immunoblotted with anti-FlgD sera.

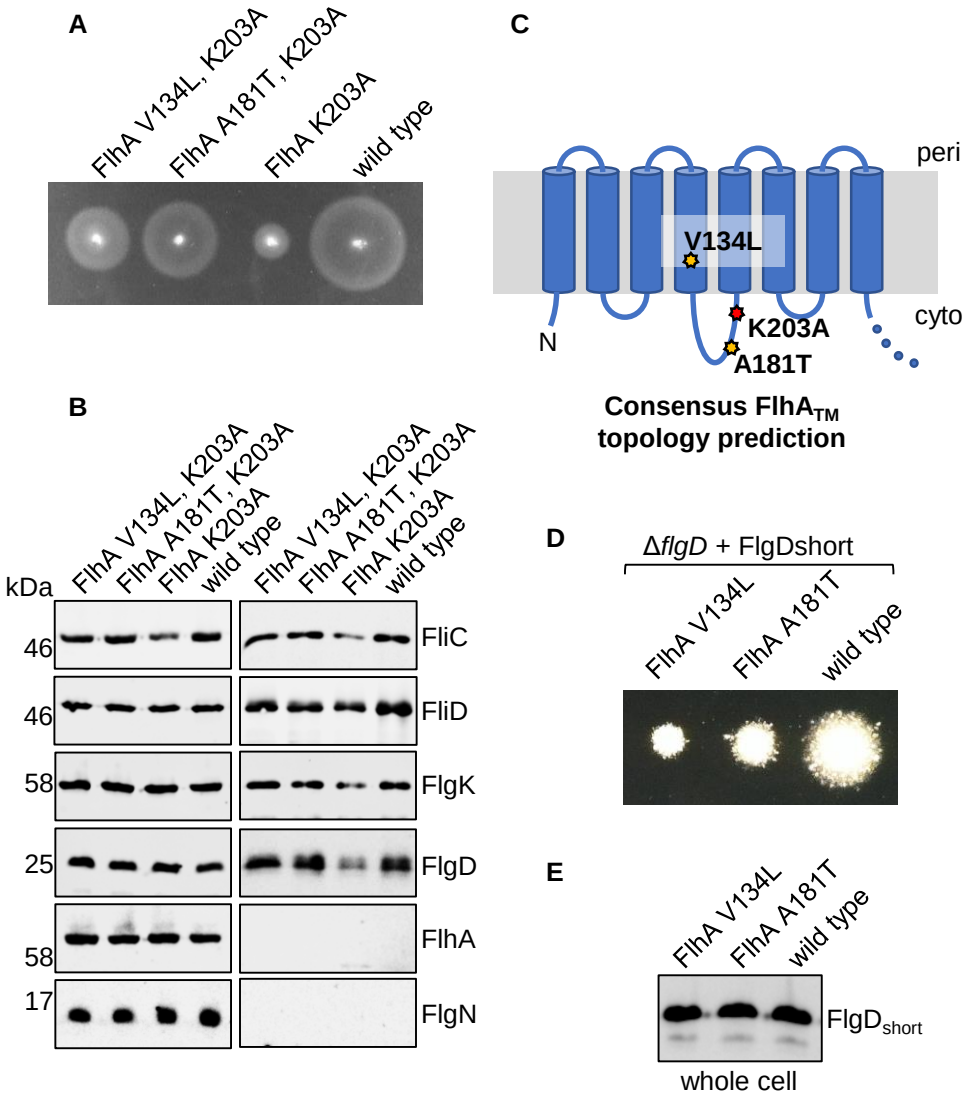

Figure 4.7. Isolated motile suppressors of FlhA K203A

(**A**) Swimming motility assays of wild type *Salmonella* and a strain containing the K203A mutation in the *flhA* gene and its gain of function mutants (FlhA K203A, V134L and FlhA K203A, A181T). Cells were inoculated into 0.3% soft-tryptone agar and incubated for 3-6 hours at 37°C.

(**B**) Secretion analysis of whole cell (whole cell) and culture supernatant (supernatant) fractions of the above strains by immunoblotting with anti-FliC, anti-FliD, anti-FlgK, anti-FlgD, anti-FlhA and anti-FlgN sera.

(**C**) Topology prediction of the transmembrane region of FlhA. The predicted locations of the K203A mutation (red) and gain of function mutations (V134L and A181T, yellow) are highlighted with an asterisk.

(**D**) Swimming motility assays of a *Salmonella* Δ*flgD* strain and Δ*flgD* strains containing mutations in the *flhA* gene (V134L or A181T) transformed with recombinant pTrc99a plasmids carrying the FlgD$_{short}$ variant. Cells were inoculated into 0.3% soft-tryptone agar containing 100 µg/ml ampicillin and incubated for 12-16 hours at 37°C.

(**E**) Whole cell fractions from the above strains were immunoblotted with anti-FlgD sera.

assessed. A Δ*flgD* strain in which the chromosomal *flhA* gene was replaced with mutant *flhA* genes encoding FlhA variants containing either the $A_{113}E$ or the $G_{115}C$ suppressor mutations were constructed. These strains were transformed with pTrc99a carrying $FlgD_{short}$ and motility assays were carried out as previously described (section 2.16). Both *flhA* mutations marginally, but insignificantly, suppressed the $FlgD_{short}$ motility defect, suggesting that these mutations do not suppress the phenotypes associated with the FlhA $K_{203}A$ mutation by promoting the open conformation of the export gate (Figure 4.6).

The other two suppressor mutations isolated from the *flhA* $K_{203}A$ strain ($V_{134}L$ and $A_{181}T$) were positioned in or near the cytoplasm. $V_{134}L$ resides close to the base of transmembrane helix 3, and $A_{181}T$ resides in a predicted cytoplasmic loop adjacent to a region of FlhA termed FHIPEP (flagellum/hypersensitive response/invasion protein export pore, residues 147-170), located between transmembrane helices 4 and 5. Both suppressors restored subunit export to wild type levels. Furthermore, the $V_{134}L$ and $A_{181}T$ suppressors improved motility to 65% and 75% of wild type, respectively. To test the ability of these mutations to suppress the $FlgD_{short}$ motility defect, a Δ*flgD* strain was constructed in which the chromosomal *flhA* gene was replaced with mutant *flhA* genes encoding variants containing either the $V_{134}L$ or the $A_{181}T$ suppressor mutations. These strains were transformed with pTrc99a encoding $FlgD_{short}$ and motility assays were performed as described previously (section 2.16). Rather than suppressing the $FlgD_{short}$ motility defect, these suppressor mutations attenuated motility of cells producing $FlgD_{short}$ compared to the isogenic strain encoding wild type FlhA, indicating that the $V_{134}L$ and $A_{181}T$ mutations do not promote the open conformation of the export gate, but may instead modulate the conformation of FlhA, compensating for any conformational change caused by the $K_{203}A$ mutation (Figure 4.7).

To test whether the $A_{113}E$, $G_{115}C$, $V_{134}L$ or $A_{181}T$ changes in FlhA affected cognate subunit export or swimming motility in the absence of the *flhA* $K_{203}A$ mutation, strains were constructed in which the chromosomal *flhA* gene was

replaced with mutant *flhA* genes encoding these variants. Subunit export, swimming and swarming motility were assayed as previously described (section 2.15, 2.16 and 2.17). Proteins in whole cells and supernatants were immunoblotted for representative early (FlgD) and late (FliC, FliD and FlgK) subunits, and for FlhA and FlgN as loading, expression and lysis controls. Strains producing FlhA variants carrying the $A_{113}E$, $G_{115}C$, or $A_{181}T$ mutations displayed subunit export and motility phenotypes similar to wild type (Figure 4.8). However, the strain producing FlhA $V_{134}L$ exhibited decreased swimming and swarming motility compared to wild type motility, though there was no discernible decrease in subunit export (Figure 4.8). This is perhaps because the FlhA $V_{134}L$ variant causes only a small decrease in the export of each subunit, with the combined effect of producing an observable decrease in motility. Alternatively, the FlhA $V_{134}L$ mutation may affect cellular fitness, which could interfere with the cells ability to swim efficiently. The data indicates that the FlhA $K_{203}A$ mutation induces a conformational change in the export gate preventing efficient gate opening.

4.6 Two distinct signals are required to activate the PMF-driven export machinery

Having provided evidence that FlhA facilitates opening of the export gate (Section 6.3 and Figure 4.4), I wanted to investigate further the mechanistic basis of FlhA-mediated export gate opening. Previous studies have shown that interaction of the ATPase stalk component FliJ with FlhA activates the export machinery so that it can efficiently use the $\Delta\psi$ component of the PMF to drive subunit export, suggesting that this binding event is one 'signal' required to open the export gate[111]. In addition, data presented in chapter 3 show that the extreme N-terminus of early flagellar subunits contains a signal that triggers opening of the export gate, and it is possible that this signal is transmitted *via* FlhA to energise opening of the export gate. Furthermore, loss of either of these proposed signals - the FliJ-FlhA interaction or the subunit N-terminal signal - can be overcome by compensatory mutations in genes encoding components of the export machinery. Specifically, loss of the FliH-FliI-FliJ ATPase can be overcome by mutations in *flhA* or *flhB* (FlhA $V_{404}M$, FlhB $P_{28}T$)[111,218], and data presented in

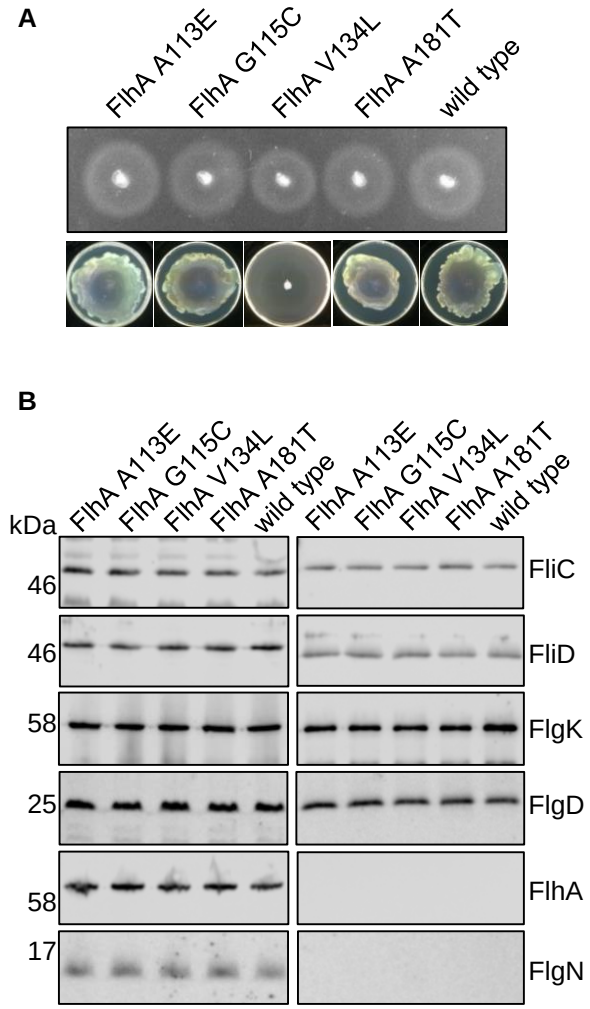

Figure 4.8. motility and export phenotypes of mutations within FlhA
(**A**) Swimming motility assays of wild type *Salmonella* and *Salmonella* strains containing the gate opening mutations in the *flhA* gene (A113E, G115C, V134L and A181T). Cells were inoculated into 0.3% soft-tryptone agar and incubated for 3-6 hours at 37°C (top).
Swarming motility of the same strains was assessed by centrally inoculating 1µl of stationary phase broth culture on 0.6% agar-tryptone plates supplemented with 0.5% glucose and incubating plates at 30°C for 12-16 hours (bottom).
(**B**) Secretion analysis of the above strains by immunoblotting of whole cell (whole cell) and culture supernatant (supernatant) fractions prepared from the above cells with anti-FliC, anti-FliD, anti-FlgK, anti-FlgD, anti-FlhA and anti-FlgN sera.

chapter 3 and this chapter shows that loss of the subunit N-terminal signal (as in $FlgD_{short}$) can be overcome by mutations in the FliP or FliR export gate components.

To determine whether mutations predicted to promote the open conformation of the export gate could restore motility and subunit export in a strain lacking key components of the ATPase complex, strains were constructed in which the chromosomal *fliR* gene was replaced with mutant *fliR* genes encoding variants with 'gate opening' mutations ($F_{113}A$ or $G_{117}D$) in combination with deletions in genes encoding the ATPase components FliH and FliI. These strains were also deleted for the gene encoding the secreted FlgM flagellar anti-sigma factor. Deletion of *flgM* uncouples flagellar export activity from flagellar gene expression[84]. The engineered strains were designated *fliR($F_{113}A$)-ΔfliHI-ΔflgM* and *fliR($G_{117}D$)-ΔfliHI-ΔflgM*. As a positive control, a *flhB($P_{28}T$)-ΔfliHI-ΔflgM* strain was constructed, and a *ΔfliHI-ΔflgM* strain was used as a negative control (Figure 4.9). Subunit export and swimming motility were assayed as previously described (section 2.15 and 2.16). Whole cell lysates and culture supernatants were immunoblotted for representative early (FlgD) and late (FliD) subunits, and for FlhA and FlgN as loading, expression and cell lysis controls. The data indicate that the proposed 'gate opening' mutations in *fliR* ($F_{113}A$, $G_{117}D$) were unable to recover the defects in motility and subunit export caused by deletion of the genes encoding the FliH and FliI components of the export ATPase (figure 4.9).

To test whether the FlhB $P_{28}T$ variant, which allows cells to bypass the loss of the flagellar ATPase, can suppress the motility defect associated with $FlgD_{short}$, a strain was constructed in which the *flgD* gene was replaced with a kanamycin cassette and the *flhB* gene was replaced with a mutant *flhB* encoding FlhB $P_{28}T$: *flhB($P_{28}T$)-ΔflgD*. A *ΔflgD* strain was used as a control. The *flhB($P_{28}T$)-ΔflgD* strain and a *ΔflgD* negative control strain were transformed with pTrc99a encoding $FlgD_{short}$ and motility assays were performed as previously described (section 2.15 and 2.16). The FlhB $P_{28}T$ mutation did not suppress the $FlgD_{short}$ motility defect (Figure 4.9).

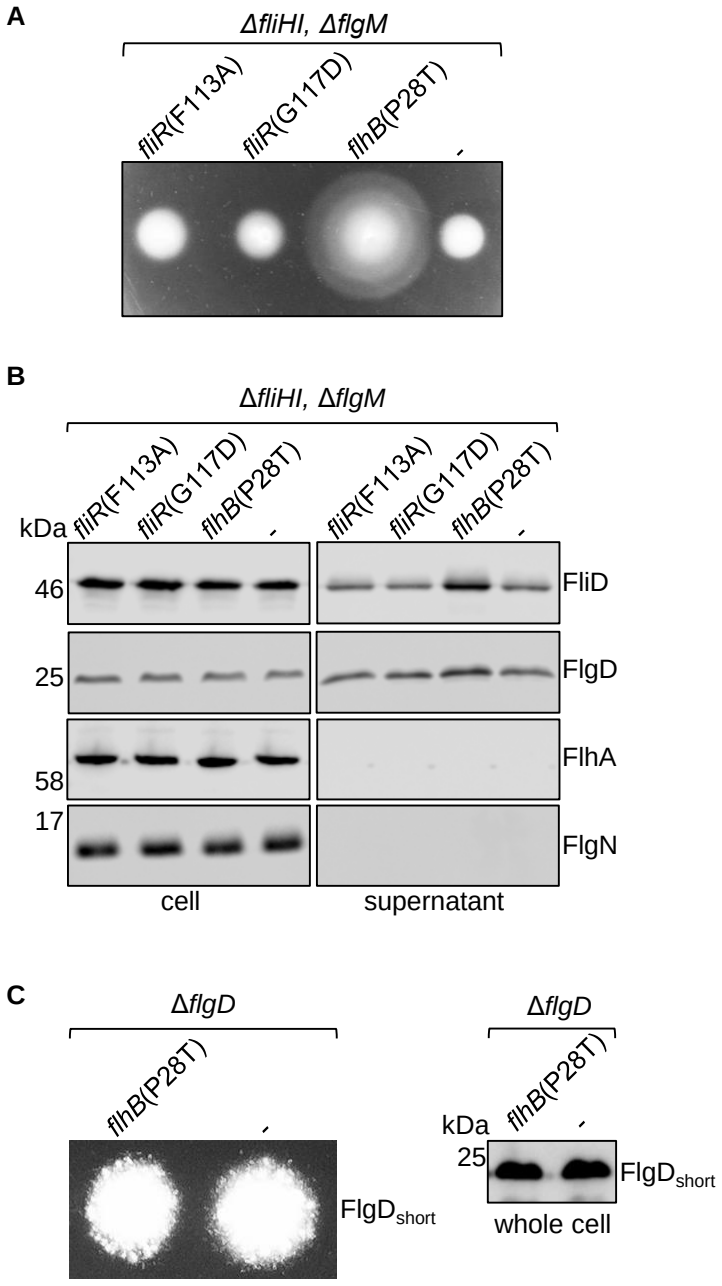

Figure 4.9. Mutations in the FliR plug do not suppress export and motility defects caused by deletion of the ATPase complex

(**A**) Swimming motility assays of a *Salmonella* Δ*flgM* strain and Δ*flgM*Δ*fliH*Δ*fliI* strains containing mutations in the *fliR* gene (F113A or G117D) or a P28T mutation in the *flhB* gene. Cells were inoculated into 0.3% soft-tryptone agar and incubated for 3-6 hours at 37°C.

(**B**) Secretion analysis of whole cell (whole cell) and culture supernatant (supernatant) fractions of the above strains by immunoblotting with anti-FliD, anti-FlgD, anti-FlhA and anti-FlgN sera.

(**C**) Swimming motility assays of a *Salmonella* Δ*flgD* strain and Δ*flgD* strains containing the P28T mutation in the *flhB* gene transformed with recombinant pTrc99a plasmids carrying the $FlgD_{short}$ variant. Cells were inoculated into 0.3% soft-tryptone agar containing 100 μg/ml ampicillin and incubated for 12-16 hours at 37°C (left). Whole cell fractions from the above strains were immunoblotted with anti-FlgD sera (right).

The data in this section indicate that mutations that bypass loss of the subunit extreme N-terminal signal or loss of the FliJ-FlhA interaction cannot compensate for each other, indicating that these two signals are mechanistically separate and that both are required to activate PMF-driven export gate opening by FlhA (Figure 4.10).

4.7 Discussion

Transport of substances across the bacterial inner membrane is highly selective, thereby maintaining the transmembrane electrochemical gradients that drive numerous processes at the cell membrane, including ATP synthesis and protein export[93,268,103]. Many protein export systems, such as the fT3SS, contain a translocation pore in the inner membrane through which proteins are translocated[75,264,105,246]. One important requirement of these transporters is to maintain the membrane permeability barrier while facilitating efficient protein export. One of these barriers in the injectisome and flagellar T3SS is the $FlhB_N$-FliPQR export gate substructure, which contain three constriction points that are believed to help maintain the gate in a closed conformation[105,253]. These interactions between subunits in the core of $FlhB_N$-FliPQR need to be broken to allow channel opening, and this is likely to require energy.

Like many processes that occur at the membrane, T3SS utilise the proton motive force to energise protein export[260,51,52,188]. This is facilitated by an ATPase complex and, specifically, the interaction of the FliJ stalk subunit of the ATPase with FlhA, which turns the export machinery into a highly efficient $\Delta\psi$ driven export machine[111]. This interaction is analogous to that between the stalk component of the F_1/F_0 ATPase and its membrane localised proton channel that drives proton translocation across the inner membrane[261,268]. Like many processes that occur at the membrane, the activity of the F_1/F_0 ATPase must be regulated to ensure proton transduction only occurs when needed, minimising wasteful transport[269,270].

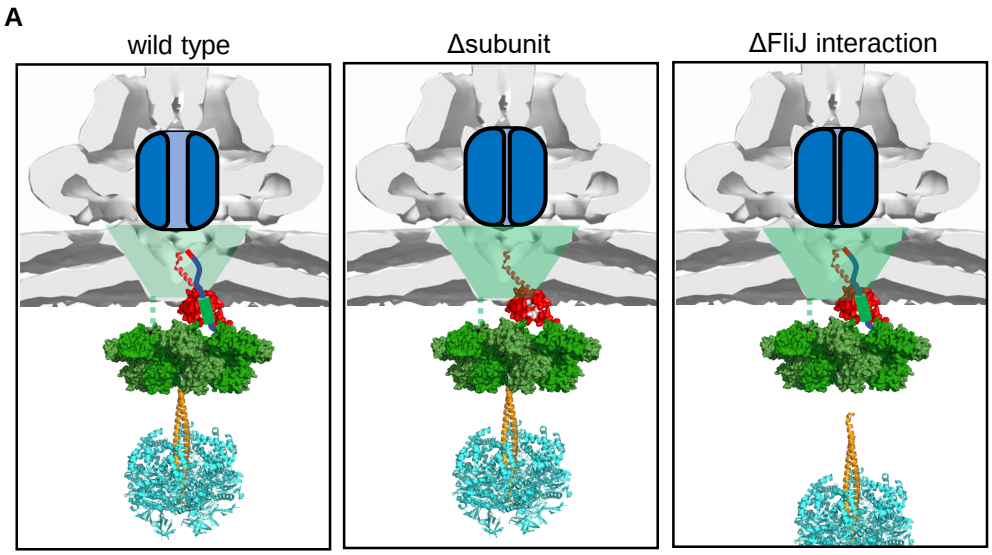

Figure 4.10. A proposed model for the opening of the export gate
(**A**) FliJ (orange, PDB: 3AJW) interactions with FlhA (green, PDB: 3A5I) together with the N-terminal non-polar early subunit signal triggers PMF-driven opening of the export gate (left). The absence of subunits at the export machinery (middle) or the absence of the FliJ-FlhA interaction (right) renders the export machinery unable to utilise the PMF to drive opening of the export gate.

Over 35 years ago it was discovered that the fT3SS requires the proton motive force for subunit export, yet little is known about how the PMF is coupled to subunit export[260]. The PMF could be required at any stage of the export cycle *e.g.* to power protein unfolding, drive translocation, open the export gate or for a combination of these. Based on the hypothesis that the export gate requires some form of energy to drive channel opening, I set out to test whether the PMF provides this energy.

Data presented in chapter 3 showed that the $M_{210}A$ mutation in FliP, which I propose destabilises the closed conformation of the export gate, could suppress the motility defect associated with the $FlgD_{short}$ subunit, which lacks a wild type N-terminal export signal. Using the recent atomic resolution structure of the FliPQR complex, I identified further mutations that are predicted to promote the open conformation of the export gate[105]. These mutations reside in a hydrophobic loop of FliR that forms a plug within the secretion channel[105]. Based on the structure, two phenylalanine residues in FliR (F_{113} and F_{115}) make hydrophobic interactions with a concentric ring of conserved methionine residues that form a constriction point below the FliR plug, stabilising the closed conformation[105]. To allow the passage of unfolded subunits through the export channel, the FliR plug must be displaced. Deletion of the hydrophobic plug (residues 110-116) sensitized cells to choline, consistent with the plug forming a tight seal and being essential for maintaining the membrane permeability barrier (Figure 4.3). Similar gating mechanisms have been observed in other protein conducting channels, such as the SecY channel which similarly contains a constriction formed by ring of hydrophobic residues and a central plug forming a seal[264]. Deletion of the central plug or ring of hydrophobic residues in SecY results in increased permeability of the channel[265,266].

A previous study showed that a substrate trapped in the flagellar export channel of a Δ*fliP* strain expressing FliP $M_{210}A$ could de-sensitize cells to choline, suggesting that the export gate forms a tight seal around subunits in the channel[246]. I showed that in cells lacking the FliR plug, deletion of the genes

encoding the majority of early subunits (*flgB*, *flgC*, *FlgD*, *flgE*, *flgF*, *flgG* and *flgJ)* caused cells to become hyper-sensitised to extracellular choline. However, cells encoding the wild type export gate lacking the early subunits were no more sensitive to choline than wild type *Salmonella*. It has been previously suggested that FliE, which assembles on top of the FliP component of the export gate, may stabilise the open gate conformation[7]. However, the data presented in this chapter indicate that the export gate alternates between an open and closed state depending on the presence or absence of subunit, either in the channel or docked at the export machinery.

Data from the choline sensitivity experiments indicate that the T3SS export gate maintains the membrane permeability barrier, sustaining electrochemical gradients and preventing entry of harmful molecules that bacteria may encounter in the environment (including in the host), especially when the export machinery is not actively transporting protein. When might the machinery reduce subunit export? This could occur when the cell reduces flagellar gene expression, *e.g.* upon host cell invasion or in response to certain environmental cues[86,47,87,88]. Any reduction in flagellar gene expression would result in fewer subunits being produced and available for export. Therefore, it is vital that opening and/or closing of the export gate is regulated in response to subunit availability.

The FlhA component of the ABPQR export gate is the export component that most likely harnesses the energy of the PMF to power export and I hypothesise that this might be through gate opening. A previous study identified suppressor mutations in *fliR* that rescued the motility defect of the *flhB(P$_{28}$T)-ΔfliHI-flhA(K$_{203}$W)* strain and the authors proposed that the suppressor mutations restored an interaction between FliR and FlhA[262]. One of these suppressor mutations (FliR G$_{117}$D) is positioned within the core of the FlhB$_N$-FliPQR complex and introduces a bulky side chain, indicating that this suppressor mutation may instead prevent the FlhB$_N$-FliPQR complex from closing fully[105]. As for the FliR G$_{117}$D suppressor, I found that our engineered 'gate opening' mutations (F$_{113}$A or G$_{117}$D) could enhance the motility and flagellar subunit export of a strain

producing FlhA K_{203}A. Export was restored to wild type levels whereas motility was restored to 60% of wild type. It is unclear why motility was only partially restored, but it may be that the FlhA K_{203}A mutation causes a conformational change in the export machinery that might influence flagellar rotation, either by causing proton leakage and a local drop in PMF or by affecting function of the flagellar switch. Another possibility is that the FlhA K_{203}A mutation causes an export defect for a structural subunit that I have not analysed.

The 'gate opening' mutations can suppress the motility and export defects caused by FlhA K_{203}A, indicating that FlhA might function to open the export gate. The proposed function of FlhA as a proton channel and the proximity of FlhA to the FlhB and FliPQR components of the export gate suggest that FlhA might couple proton translocation to gate opening[113, 262, 111, 110]. In support of this, data showing that supplementation of cultures with arginine to increase the PMF enhanced subunit export by 40% in the *flhA(K_{203}A)* strain (Figure 4.5). A negative control strain lacking the SpeA and AdiA arginine decarboxylases, showed no increase in subunit export confirming that the arginine supplementation effect on subunit export was caused by an increase in the PMF. The data suggest that the *flhA(K_{203}A)* strain might be limited in its ability to efficiently couple PMF to export gate opening (Figure 4.4 and 4.5). The enhancement of subunit export caused by increasing the PMF was smaller than that observed in strains carrying suppressor mutations that promote the open conformation of the export gate (Figure 4.4 and 4.5). Taken together, these data suggest that while the reduced ability of FlhA K_{203}A to harness the energy in the PMF might partially contribute to defects in cell motility and subunit export, the main cause of these defects is the inability of FlhA K_{203}A to trigger opening of the export gate.

The screen for suppressors of the motility and export defects associated with the *flhA(K_{203}A)* strain identified six intragenic suppressor mutations. It is unclear why no mutations were isolated in *fliR* despite such suppressors having been isolated in a previous study[262]. Specifically, a screen for suppressors of the motility defect of the *flhB(P_{28}T)-ΔfliHI-flhA(K_{203}W)* strain identified suppressor mutations in *fliR*,

but no suppressors were found in *flhA* [262]. One possible reason for this is that mutations in *flhA* often cannot be tolerated in combination with deletion of the flagellar ATPase[262].

I reasoned that if FlhA lysine-203 directly binds protons, any intragenic suppressors isolated from the FlhA $K_{203}A$ strain would likely re-introduce a lysine or similarly charged residue at, or close to, position 203. Whereas, if the $K_{203}A$ mutation stabilises an 'export off' conformation of FlhA, such that proton binding residues are no longer optimally positioned to form a proton conducting channel, then any intragenic suppressors might restore the wild type FlhA conformation or alternatively stabilise an 'export on' FlhA conformation that promotes opening of the export gate. In this study, none of the suppressors ($A_{113}E$, $G_{115}C$, $V_{134}L$, $A_{181}T$) of the FlhA $K_{203}A$ mutation were located near to Lysine-203. Moreover, none of the suppressor mutations could suppress the motility defect associated with the $FlgD_{short}$ subunit, suggesting that the suppressors do not promote gate opening. This indicates that the effect of the suppressors of the of the FlhA $K_{203}A$ mutation may instead be to restore the 'wild type' conformation of FlhA. Notably, one of these suppressors ($A_{181}T$) has been shown to suppress numerous mutations within the cytoplasmic FHIPEP region of FlhA (residues 147-170), a highly conserved region that doesn't tolerate mutations[271, 112]. Furthermore, one study showed that a mutation (FlhA $D_{158}N$) that mimics the protonation of a key acidic residue within the FHIPEP region of FlhA (Asp-158) triggers a global conformational change that alters its susceptibility to proteolysis, suggesting that conformational changes in FlhA occur during the export process[113].

One of the signals that the export machinery requires for efficient subunit export is the FliJ-FlhA interaction[272]. FliJ binding to FlhA converts the export machinery into a highly efficient $\Delta\psi$-driven export machine, indicating that FliJ binding to FlhA modulates its proton conducting ability and, therefore, gate opening activity[111]. Suppressor mutations in genes encoding other components of the export machinery (FlhA $V_{404}M$ or FlhB $P_{28}T$) can bypass loss of the ATPase complex and, therefore, the need for the FliJ-FlhA interaction[111, 218]. The data

presented in chapters 3 and 4 indicate that the export machinery requires an additional signal located at the extreme N-terminus of early subunits to trigger opening of the export gate. I wanted to test whether suppressor mutations that compensate for loss of the ATPase could also suppress the motility defect associated with loss of the subunit N-terminal signal. I found that the FlhB $P_{28}T$ mutation cannot suppress the $FlgD_{short}$ motility defect. Furthermore, suppressor mutations that promote the open conformation of the export gate could not compensate for loss of the ATPase complex. This indicates that mutations that suppress the export defect caused by loss of the ATPase do not act by opening the export gate, but function by some other mechanism. Moreover, mutations that do compensate for loss of the ATPase *e.g.* FlhB $P_{28}T$ mutation cannot suppress the FlhA $K_{203}A$ export defect[262]. Taken together, the data indicate that two mechanistically distinct signals – the subunit N-terminal signal and the FliJ-FlhA interaction - are required to open the export gate.

I propose that the FliJ interaction with FlhA and the presence of a subunit at the export machinery act together to induce conformational changes in FlhA that render the export machinery competent to use the PMF and open the export gate. Without either the FliJ signal or the subunit signal, the export gate remains closed, maintaining the membrane permeability barrier. This requirement for two distinct signals, or checkpoints, decreases the probability of the export gate opening when subunits are not available or when the export machinery is not ready for export. Neither signal alone is sufficient to allow efficient subunit export. Based on the current data, it is likely that the subunit N-terminal gate opening signal is more important than the FliJ-FlhA interaction signal. Loss of the FliJ-FlhA interaction can be suppressed by mutations in the export machinery without any apparent effect on the cell growth rate[51]. However, the mutations in the export gate that promote gate opening do not suppress the $FlgD_{short}$ motility defect to a large extent (Figure 4.1). This is compatible with the view that mutations that promote the open conformation of the export gate increase permeability of the inner membrane, which would reduce the fitness of the cell.

Based on the high structural and functional similarities between the core components of the injectisome and flagellar type III secretion systems, it is probable that the PMF-driven export gate opening mechanism is conserved in both secretion systems. How do other export systems maintain the membrane permeability barrier and open the channel when required? As discussed in chapter 3, many export systems trigger opening of their export channel when a substrate binds the export machinery[99, 100, 104, 96]. The Sec system, which is probably the best-studied protein export system, contains many features similar to the gating mechanism employed by T3SS[264, 105.] The SecYEG translocon is maintained in an energetically favourable closed state, a constriction formed by ring of hydrophobic residues (analogous to the FliP methionine ring) and a central plug (analogous to the FliR plug loop) forms a seal and physical plug within the pore[264]. Molecular dynamic simulations of the SecY protein conducting channel indicate that the plug is displaced from the channel whilst the ring of hydrophobic residues forms a seal around the translocating subunit[273, 274, 275]. Electrophysiology experiments showed that deleting the plug in SecY causes the channel to alternate between an open and closed state[265]. Furthermore, molecular dynamic simulations indicated that the force required to open the gate is reduced in SecY plug deletion mutants[266]. In fact, the data showed that the plug serves to maintain a closed conformation and that the primary role of the hydrophobic ring is to prevent the flow of ions or water molecules through the channel[266]. In the export gate complex of the fT3SS, the FliR plug and the FliP methionine ring interact with each other, which may be why mutations in the FliR plug or in the FliP methionine ring can suppress the $FlgD_{short}$ motility defect, indicating that these suppressor mutations promote gate opening. Mutations in the FliP methionine ring would disrupt interactions with FliR and therefore decrease the energy barrier required for displacement of the FliR plug.

Another parallel between the Sec machinery and the T3SS is the mechanism of Sec translocon activation. In *E.coli*, the SecYEG complex, which forms the protein conducting channel, associates with the cytosolic ATPase, SecA[276]. SecA ATPase activity increases upon binding the SecYEG complex[276]. Protein

substrates are targeted to the SecYEG-SecA complex by the chaperone SecB, and the binding of SecB to functional signal peptides promotes its interaction with SecA, which in turn increases SecA ATPase activity and transport efficiency[277, 278, 279]. In other words, efficient activity of the Sec system is dependent on substrate availability at the machinery.

Based on the data in this chapter and in chapter 3, opening of the export gate is triggered by the N-terminus of early subunits, and this is dependent on subunit docking at FlhBc. Therefore, gate opening is regulated by the presence of subunits at the export machinery. How FliJ activation of the export machinery is regulated is less clear. One possibility is that the ATPase activity of FliI is regulated and its activity is dependent on substrate availability or, alternatively, the localisation of FliI at the machinery. Another possibility is that the FliJ-FlhA interaction is regulated such that the interaction only takes place when subunits are available for export. Regulation of the FliJ-FhA interaction is explored in chapter 7.

In summary, the data in this chapter demonstrate that FlhA is involved in opening the export gate. I propose that proton transport through FlhA induces conformational changes that are transmitted to the adjacent $FlhB_N$-FliPQR components of the export gate, stabilising the open conformation. I demonstrate that FlhA requires at least two signals to promote gate opening; a FliJ-dependent activation step, and a subunit docked at the export machinery. The data suggest that there is a multi-signal control system that acts *via* FlhA to ensure that use of the PMF and export channel opening only occur when a FliJ-activation signal is received and a subunit is available for export.

Chapter 5

The C-terminus of early flagellar subunits contains an export signal required for subunit targeting to the flagellar export machinery

5.1 Introduction

To achieve efficient subunit export, T3SS substrates must be post-translationally targeted from their site of synthesis at the ribosome to the export machinery. One way this is achieved is by targeting signals in the subunit or targeting signals in the chaperones that aid subunit delivery to the export machinery[207,226,238,156,141,138,177,116.] The late flagellar export subunits are an example of subunits that are targeted to the machinery with the aid of dedicated chaperones that sequentially interact with different components of the export machinery[207,226,177,116]. How the early export subunits that assemble to form the rod and hook substructures are targeted to the export machinery is less clear[141]. Unlike late subunits, the early flagellar subunits are not chaperoned to the export machinery, therefore, all targeting signals are presumably contained within the subunit[141].

Our laboratory has previously shown that early subunits dock at the FlhBc export gate using a small hydrophobic motif termed the gate recognition motif (GRM) that is localised within the N-terminus of all early subunits[141]. The FlhBc export gate is proposed to be positioned within or just below the plain of the membrane[105]. Early subunits presumably contain targeting signals for other components of the export machinery to aid their delivery to the FlhBc export gate. However, interactions between early flagellar subunits and other components of the export machinery positioned below FlhBc have not been identified.

Our laboratory previously proposed that the C-terminus of early subunits are involved in early subunit export[141]. It was proposed that early subunits docked at the FlhBc are captured *via* the C-terminus of the preceding subunit already in the export channel. It was proposed that these subunit capture events could result in a multi-subunit chain that spans from the FlhBc export gate to the filament tip.

Evidence for this was obtained by *in vitro* capture assays, whereby subunits docked at the $FlhB_C$ gate could be captured by the C-terminus of other early subunits. Furthermore, it was shown that export of the hook subunit (FlgE) variant lacking its C-terminal helix was attenuated[141,9,8]. One discrepancy between this model and the evidence in chapter 4 suggests that if subunit chaining does occur, then it is unlikely to occur from FlhBc but instead chains must form after subunits have passed through the export gate complex and into the central channel within the rod/hook/filament. As discussed in chapter 4, the export gate must transition from a closed to open conformation to allow subunit transit into the export channel[105]. Data from experiments with early subunit depleted strains (Chapter 4, Figure 4.2) indicate that the gate reverts to a closed conformation if subunits are not present at the export machinery and that subunits passing through the export gate seal the channel when the FliR plug is deleted. If a chain were formed at FlhBc (positioned below the $FlhB_N$-FliPQR components of the export gate) and extended to the filament tip, then there would always be subunit present, spanning the export gate, and therefore the gate would always be sealed by subunit.

To investigate whether subunit capture from FlhBc occurs *in vivo*, I sought to determine whether subunit variants that failed to capture *in vitro* interfere with subunit capture *in vivo*, which would induce stalling of subunits at the export machinery[141]. Refinement of the export signal and a screen for suppressors, indicated an alternative role for early subunit C-termini in subunit export. The data establish key events in the export mechanism of the flagellar Type III secretion systems; targeting of subunits and their sequential interactions with key components of the export machinery.

5.2. The dominant negative phenotype caused by FlgE overexpression is suppressed by deletion of its C-terminus

Having provided direct evidence that an export signal at the subunit extreme N-terminus triggers export channel opening after subunit docking at $FlhB_C$ (chapter 3), I set out to investigate the role of the C-terminus of early flagellar subunits in

promoting export. Our laboratory has previously proposed that subunits docked at the $FlhB_C$ export gate are captured from FlhBc by the C-terminus of the preceding subunit already in the export channel[141]. Evidence for this was obtained by *in vitro* capture assays, whereby subunits docked at the $FlhB_C$ gate could be captured from $FlhB_C$ by other early subunits and this capture was dependent on their C-terminus. Furthermore, it was shown that export of the hook subunit (FlgE) lacking its C-terminal helix was attenuated[141]. I envisaged that if subunits are captured from the $FlhB_C$ export gate by a specific sequence at the C-terminus of the preceding subunit already in the channel then a subunit variant lacking this C-terminal 'capture' sequence would display a dominant negative phenotype. Subunits lacking the specific C-terminal 'capture' sequence would themselves be captured from $FlhB_C$ but would be unable to capture the next newly docked subunit, resulting in subunit stalling at $FlhB_C$.

To test this, I constructed recombinant pTrc99a plasmids encoding a FlgE variant lacking residues 360 to 403 (termed FlgEΔCt) or wild type FlgE. All recombinant FlgE variants contained a triple FLAG-tag (3xFLAG) between residues 234 and 235 to aid detection by immunoblotting. Plasmids were transformed into a *Salmonella* Δ*recA* strain and FlgE variants were expressed at either endogenous levels (by induction with 50 μM IPTG) or overexpressed by induction with 1 mM IPTG. Cells were grown under inducing conditions to A_{600} 1.0 before being inoculated into 0.3% soft-tryptone agar containing IPTG and ampicillin. Plates were incubated at 37ºC for 4-6 hours. At endogenous expression levels, wild type FlgE caused a slight attenuation in swimming motility compared to the FlgEΔCt variant (Figure 5.1). However, overexpression of wild type FlgE attenuated swimming motility considerably more than overexpression of the FlgEΔCt variant (Figure 5.1). To determine, whether this was caused by a reduction in subunit export, I performed subunit export assays as previously described (section 2.15) at the higher level of expression using 1 mM IPTG. Proteins in whole cells and supernatants were immunoblotted for the presence of representative early (FlgD) and late (FliC and FlgL) subunits, and for FlhA and

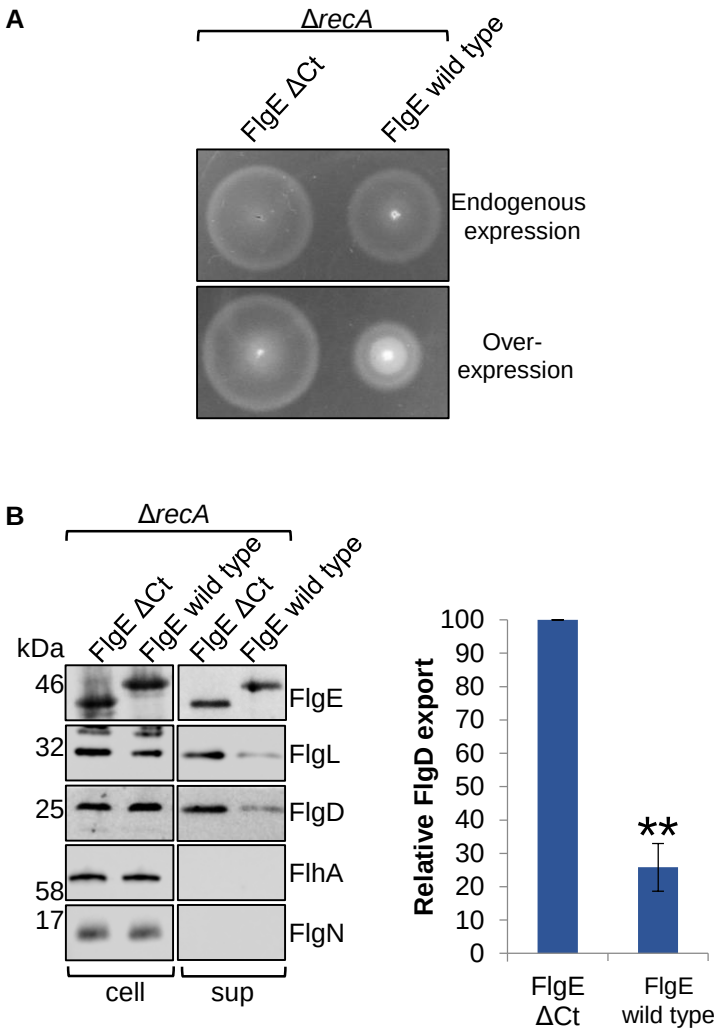

Figure 5.1. Dominant negative phenotype of wild type FlgE
(**A**) Swimming motility assays of a *Salmonella* Δ*recA* strain transformed with recombinant pTrc99a plasmids carrying a FlgE variant containing an internal 3xFLAG tag (FlgE wild type) or its variant deleted for residues 360-403 (FlgEΔCt). Cells were inoculated into 0.3% soft-tryptone agar containing 100 µg/ml ampicillin and either 50 µM IPTG (top panel) or 1 mM IPTG (bottom panel) and incubated for 3-6 hours at 37°C.
(**B**) Secretion analysis of whole cell (cell) and culture supernatant (sup) fractions from the above cells grown in LB containing 100 µg/ml ampicillin and 1 mM IPTG. Proteins were separated by SDS-PAGE and immunoblotted with anti-FliC, anti-FLAG, anti-FlgL, anti-FlgD, anti-FlhA and anti-FlgN sera (left). Levels of FlgD in culture supernatants from the Immunoblots were quantified using ImageStudiolite and plotted as a percentage of FlgD exported by the cells overexpressing FlgEΔCt. The error bars represent the standard error of the mean calculated from at least the biological replicates. ** indicates a p-value < 0.005.

FlgN as loading, expression and lysis controls. Wild type FlgE attenuated subunit export to 25% of that observed for cells expressing FlgEΔCt variant (Figure 5.1). This suggests that the export defect resulting from deletion of the subunit C-terminus is not caused by loss of a specific 'capture' sequence required for subunit release from FlhBc.

5.3 Overexpression of FlgEΔCt restores export

To test whether increasing the expression level of the FlgEΔCt variant could restore its export, a Δ*flgD* strain was transformed with pTrc99a encoding FlgEΔCt or wild type FlgE and export assays were performed as previously described (section 2.15) at endogenous expression levels (50 μM IPTG) or at overexpression levels (1 mM IPTG). A Δ*flgD* strain cannot assemble the hook substructure and therefore all FlgE subunits exported out of the cell are released into the culture supernatant. Overexpression of FlgEΔCt restored its export to levels comparable to that of wild type FlgE (Figure 5.2). This suggests that the export defect of FlgEΔCt is caused by a reduction in FlgE availability at the export machinery and this could be compensated for by increasing the amount of FlgEΔCt in the cell, which increased the probability of FlgEΔCt reaching the export machinery.

5.4 Deletion of the FlgD C-terminus does not attenuate export

To determine whether a similar export signal resides within the C-terminus of FlgD, plasmids encoding wild type FlgD or a FlgD variant lacking the C-terminal 42 amino acids (FlgDΔCt) was constructed. The recombinant plasmid-encoded FlgD variants were engineered to contain a triple FLAG-tag (3xFLAG) between residues 172 and 173 to differentiate them from chromosomally encoded FlgD. Plasmids were transformed into a *Salmonella* Δ*flgE* strain and FlgD variants were expressed at endogenous levels. In contrast to the FlgEΔCt variant, FlgDΔCt was exported into culture supernatants at wild type levels (Figure 5.3). Similarly, swimming motility of *Salmonella* Δ*recA* strains overexpressing FlgDΔCt or wild type FlgD was comparable (figure 5.3). The data indicate that, unlike FlgE, FlgD does not contain a C-terminal export signal (Figure 5.3). Why

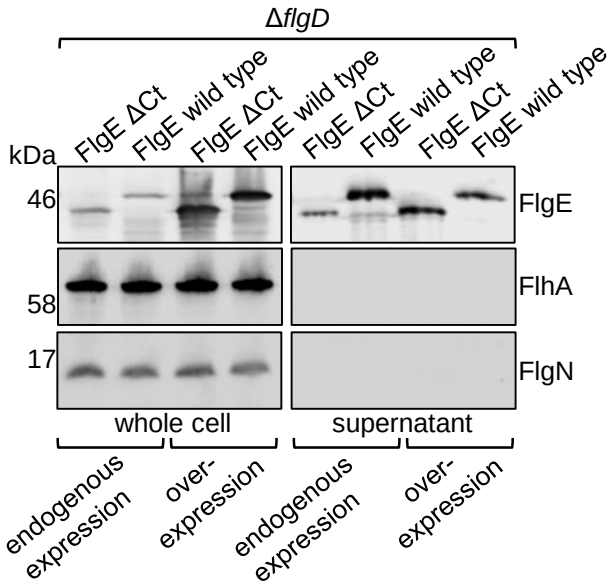

Figure 5.2. Overexpression of FlgEΔCt suppresses its export defect
Secretion analysis of a *Salmonella* Δ*flgD* strain transformed with recombinant pTrc99a plasmids carrying a FlgE variant containing an internal 3xFLAG tag (FlgE wild type) or its variant deleted for residues 360-403 (FlgEΔCt). Whole cell (whole cell) and culture supernatant (supernatant) fractions were prepared from the above cells grown in LB containing 100 μg/ml ampicillin and either 50 μM IPTG (endogenous expression) or 1 mM IPTG (overexpression). Proteins were separated by SDS-PAGE and immunoblotted with anti-FLAG, anti-FlhA and anti-FlgN sera.

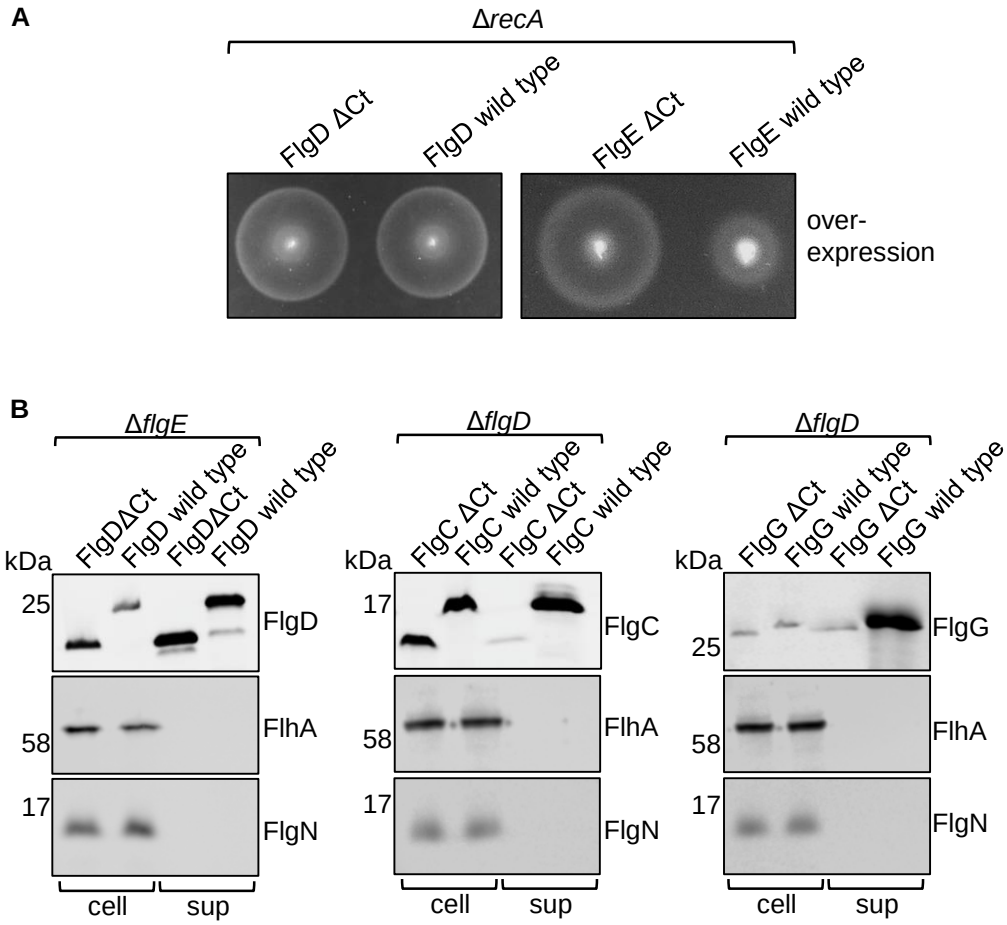

Figure 5.3. Deletion of the FlgD C-terminus does not attenuate FlgD export
(**A**) Swimming motility assays of a *Salmonella* Δ*recA* strain transformed with recombinant pTrc99a plasmids carrying either a FlgD variant containing an internal 3xFLAG tag (FlgD wild type) or its variant deleted for residues 191-232 (FlgDΔCt) (left) or pTrc99a plasmid carrying a FlgE variant containing an internal 3xFLAG tag (FlgE wild type) or its variant deleted for residues 360-403 (FlgEΔCt). Cells were inoculated into 0.3% soft-tryptone agar containing 100 µg/ml ampicillin and 1 mM IPTG and incubated for 3-6 hours at 37°C.
(**B**) Secretion analysis of whole cell (cell) and culture supernatant (sup) fractions from a Δ*flgE* strain transformed with recombinant pTrc99a plasmids carrying a FlgD variant containing an internal 3xFLAG tag (FlgD wild type) or its variant deleted for residues 191-232 (FlgDΔCt) (left panels). A Δ*flgD* strain was transformed with recombinant pTrc99a plasmids carrying a FlgC variant containing an internal 3xFLAG tag (FlgC wild type) or its variant deleted for residues 91-134 (FlgCΔCt) (middle panels) or transformed with with recombinant pTrc99a plasmids carrying a FlgG variant containing an internal 3xFLAG tag (FlgG wild type) or its variant deleted for residues 218-260 (FlgGΔCt) (right panels). The above transformed cells were grown in LB containing 100 µg/ml ampicillin and 50 µM IPTG. Proteins were separated by SDS-PAGE and immunoblotted with anti-FLAG, anti-FlhA and anti-FlgN sera.

FlgE contains a C-terminal export signal but FlgD does not is unclear. One possibility is that because FlgE is present at higher levels in the flagellum than FlgD (~100 FlgE subunits, 5 FlgD subunits), FlgE might require an additional export signal to promote its export over other subunits that are present at lower copy number in the flagellar structure. To test this hypothesis, recombinant plasmids were constructed that encoded wild type or C-terminally deleted variants of two rod subunits - FlgG and FlgC, which are present in the flagellum at approximately 26 and six copies, respectively[53]. All recombinant FlgG and FlgC variants were engineered to contain an internal triple FLAG tag (3xFLAG; Table A1.2) and were expressed in a Δ*flgD* strain with 50 μM IPTG. Deletion of the C-terminus in both FlgG and FlgC attenuated export into culture supernatants indicating that both subunits contain a C-terminal export signal (Figure 5.3).

5.5 Overexpressed FlgE has a dominant negative effect on export in strains deleted for the ATPase and C-ring

I reasoned that the C-terminus of FlgE may function as a binding site for a component of the export machinery, and that the dominant negative effect on export caused by overexpression of FlgE would be lost in an export competent strain deleted for the binding partner of the FlgE C-terminus. To test whether the flagellar ATPase was a binding partner, I overexpressed FlgEΔCt and wild type FlgE in a motile strain of *Salmonella* that contained deletions in the genes that encode the FliH and FliI components of the ATPase in combination with mutations that bypass the need for the ATPase complex (*flhB*P_{28}T-*ΔfliHI-ΔflgM)*. Swimming motility and export were assayed as previously described (section 2.15 and 2.16). Whole cell lysates and supernatants were immunoblotted for the presence of FlgD subunit, as well as for FlhA and FlgN as loading, expression and lysis controls. Overexpression of wild type FlgE attenuated subunit export and deletion of the FlgE C-terminus suppressed the overexpression phenotype (Figure 5.4). Consistent with the export phenotype, cells expressing wild type FlgE were less motile than cells expressing FlgEΔCt (Figure 5.4). This indicates that the FlgE C-terminus does not bind and stall at the ATPase complex.

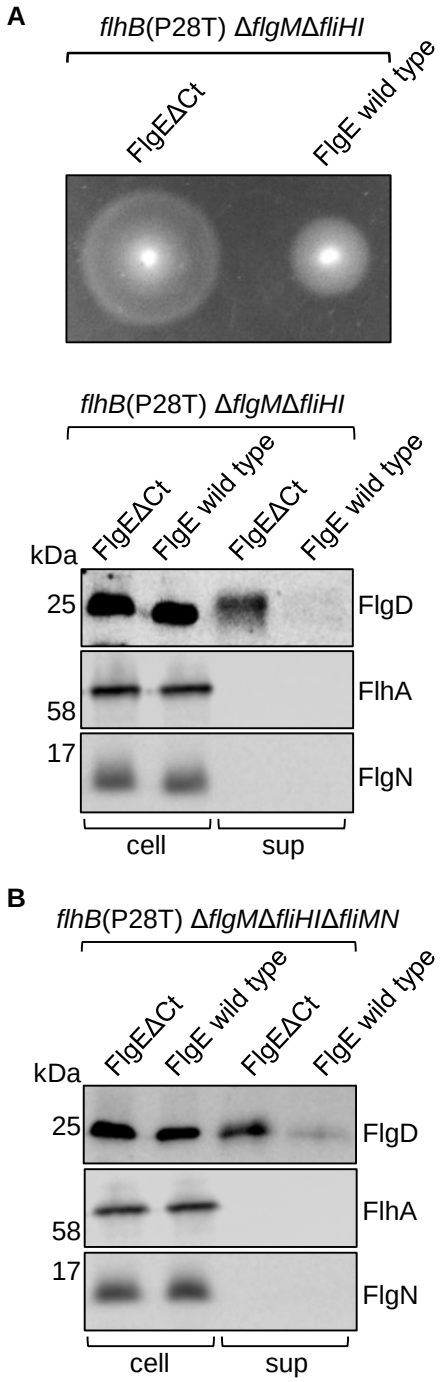

Figure 5.4. The FlgE dominant negative overexpression phenotype is retained in strains deleted for the ATPase and C-ring

(**A**) Swimming motility assays of a *Salmonella* Δ*flgM*Δ*fliH*Δ*fliI* strain containing the ATPase deletion suppressor mutation in the *flhB* gene (P28T) transformed with recombinant pTrc99a plasmids carrying a FlgE variant containing an internal 3xFLAG tag (FlgE wild type) or its variant deleted for residues 360-403 (FlgEΔCt). Cells were inoculated into 0.3% soft-tryptone agar containing 100 μg/ml ampicillin and 1 mM IPTG and incubated for 3-6 hours at 37°C (top panel). Secretion analysis of whole cell (cell) and culture supernatant (sup) fractions from the above cells grown to mid-log phase in LB containing 100 μg/ml ampicillin and 1 mM IPTG. Proteins were separated by SDS-PAGE and immunoblotted with anti-FlgD, anti-FlhA and anti-FlgN sera (bottom panel).

(**B**) Secretion analysis of whole cell (cell) and culture supernatant (sup) fractions from a *Salmonella* Δ*flgM*Δ*fliH*Δ*fliI*Δ*fliM*Δ*fliN* strain containing the ATPase deletion suppressor mutation in the *flhB* gene (P28T) transformed with recombinant pTrc99a plasmids carrying a FlgE variant containing an internal 3xFLAG tag (FlgE wild type) or its variant deleted for residues 360-403 (FlgEΔCt). Cells were grown to mid-log phase in LB containing 100 μg/ml ampicillin and 1 mM IPTG. Proteins were separated by SDS-PAGE and immunoblotted with anti-FlgD, anti-FlhA and anti-FlgN sera.

No interactions have been identified between flagellar subunit or flagellar chaperones and the C-ring. However, interactions between the injectisome chaperones and the injectisome C-ring have been identified[280,228]. To test whether the flagellar C-ring is a possible binding partner of the FlgE C-terminus, I constructed a strain deleted for genes encoding the C-ring (*fliM* and *fliN*) and deleted for the genes encoding the FliH and FliI components of the ATPase complex in combination with mutations that bypass the need for the ATPase complex (*flhB*P_{28}T-*ΔfliHI-ΔfliMN-ΔflgM)*. This strain is non-motile due to the loss of the C-ring, however, subunits are still exported into culture supernatants. To test whether the dominant negative overexpression phenotype of FlgE is retained, I transformed this strain with pTrc99a encoding FlgEΔCt or wild type FlgE and induced expression with 1 mM IPTG. Export assays were performed as previously described (section 2.15). The dominant negative overexpression phenotype of wild type FlgE was observed in this strain, indicating that neither the ATPase nor the C-ring is the binding site for the FlgE C-terminus (Figure 5.4). This leaves only the cytoplasmic domains of the core components of the export machinery, FlhA and FlhB as the potential binding partner for the FlgE C-terminus.

5.6 Isolation of FlgE variants that do not exhibit a dominant negative overexpression effect on export

To help find the potential binding partner of the FlgE C-terminal export signal, I aimed to identify the specific region of the C-terminus responsible for the FlgE overexpression phenotype. Although numerous conserved residues are located within the C-terminus, these residues may be conserved because they are required for assembly rather than being part of a C-terminal export signal. To identify specific sequences in the C-terminus of FlgE required for efficient export, internal ten-residue scanning deletions were made within the C-terminal 63 residue region, with the exception of FlgEΔ391-403, which removes 13 residues. These in frame deletions were generated by overlap-extension PCR and were inserted into pTrc99a. Plasmids were transformed into a *Salmonella* Δ*recA* strain and FlgE variants were overexpressed by induction with 1 mM IPTG. Cells were

grown to A_{600} 1.0 with inducing agent and ampicillin before being inoculated into 0.3% soft-tryptone agar. Plates were incubated at 37ºC for 4-6 hours. The data showed that the FlgEΔ371-380 deletion suppressed the overexpression phenotype, whereas the other deletion variants retained the overexpression phenotype (Figure 5.5). Whole cell lysates were immunoblotted for the presence of FlgE subunit with anti-FLAG sera as an expression control (Figure 5.5). This data indicates that the C-terminal signal resides between residues 371-380.

5.7 Characterisation of the FlgEΔ371-380 export signal

Residues 371-380 contain three fully conserved residues (V373, N374 and R380) and four partially conserved residues (E371, L372, I376 and Q379; Figure 5.5). To identify which residues contribute to the FlgE overexpression phenotype, these residues and two further fully conserved residues (V376 and Y382) located just outside the 371-380 region were substituted with alanine and the variant *flgE* genes were inserted into pTrc99a. Plasmids were transformed into a *Salmonella* Δ*recA* strain and FlgE variants were overexpressed by induction with 1 mM IPTG. Cells were grown to A_{600} 1.0 with inducing agent and ampicillin before being inoculated into 0.3% soft-tryptone agar. Plates were incubated at 37ºC for 4-6 hours. Whole cell lysates were immunoblotted for the presence of FlgE subunit with anti-FLAG sera as an expression control (Figure 5.6). The FlgE-I_{376}A, FlgE-R_{380}A and FlgE-Y_{382}A variants suppressed the overexpression motility phenotypes of wild type FlgE, indicating that these residues constitute part of the export signal (Figure 5.6).

To test whether these FlgE variants were exported less efficiently into culture supernatants, plasmids encoding the FlgE variants were transformed into a Δ*flgE* strain and the FlgE variants were expressed at endogenous levels by induction with 50 μM IPTG. Export assays were performed as described previously (section 2.15). Whole cell lysates and culture supernatants were immunoblotted for the presence of FlgE subunit using anti-FLAG and anti-FliC sera. Levels of FliC export by cells expressing FlgE I_{376}A or FlgE R_{380}A were reduced, consistent with delayed hook assembly and a reduced number of cells switching to late

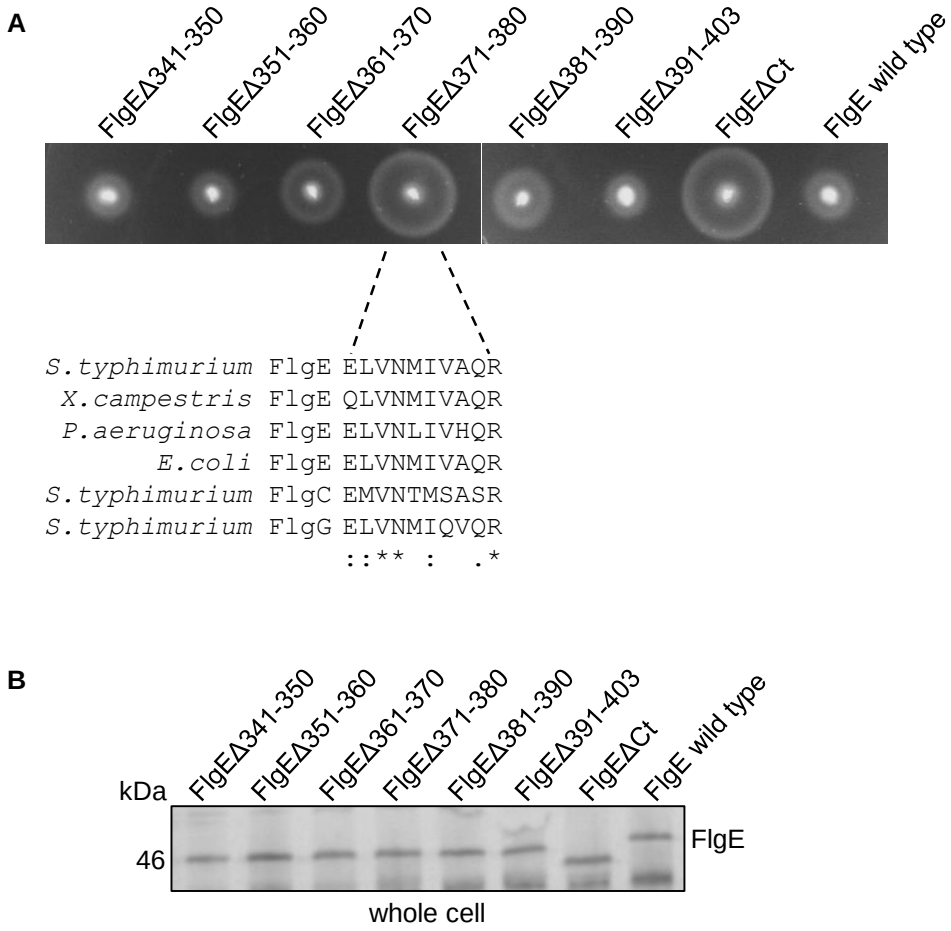

Figure 5.5. Dominant negative overexpression phenotypes of FlgE C-terminal deletion variants

(**A**) Swimming motility assays of a *Salmonella* Δ*recA* strain transformed with recombinant pTrc99a plasmids carrying a FlgE variant containing an internal 3xFLAG tag (FlgE wild type) or its variants (as indicated). Cells were inoculated into 0.3% soft-tryptone agar containing 100 µg/ml ampicillin and 1 mM IPTG and incubated for 3-6 hours at 37°C (top panel). An amino acid sequence alignment was performed for *Salmonella* FlgE amino acids 370-380 with homologous regions in FlgE from other bacterial species and with *Salmonella* FlgC and FlgG subunits (bottom). An * (asterisk) indicates a position which contains a fully conserved residue, a : (colon) indicates a position with conservation between groups of similar property and a . (period) indicates conservation between groups of weakly similar property.

(**B**) Whole cell fractions were collected from the above cells grown to A_{600} 1.0 in LB containing 100 µg/ml ampicillin and 1 mM IPTG. Proteins were separated by SDS-PAGE and immunoblotted with anti-FLAG sera.

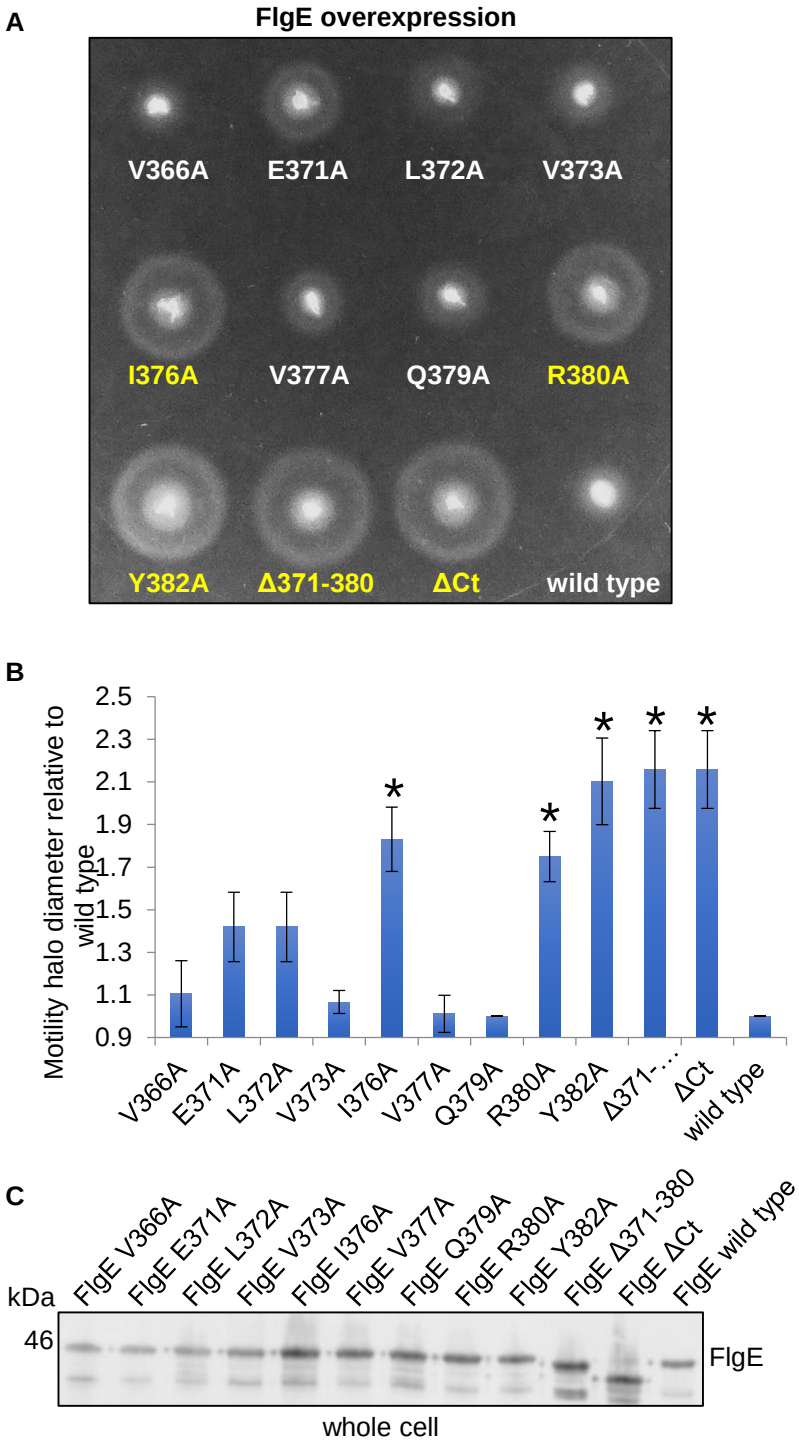

Figure 5.6. Dominant negative overexpression phenotypes of FlgE point mutants in a *Salmonella* Δ*recA* strain

(**A**) Swimming motility assays of a *Salmonella* Δ*recA* strain transformed with recombinant pTrc99a plasmids carrying a FlgE variant containing an internal 3xFLAG tag (FlgE wild type) or its variants (as indicated). Cells were inoculated into 0.3% soft-tryptone agar containing 100 µg/ml ampicillin and 1 mM IPTG and incubated for 3-6 hours at 37°C (top panel). FlgE mutants or variants that suppress the overexpression phenotype are colored yellow (**B**) Motility halo diameters from the above cells expressing the FlgE point mutants were plotted as a percentage of cells expressing wild type FlgE. The error bars represent the standard error of the mean calculated from at least the biological replicates. * indicates a p-value < 0.05.

(**C**) Whole cell fractions were collected from the above cells grown to A_{600} 1.0 in LB containing 100 µg/ml ampicillin and 1 mM IPTG. Proteins were separated by SDS-PAGE and immunoblotted with anti-FLAG sera.

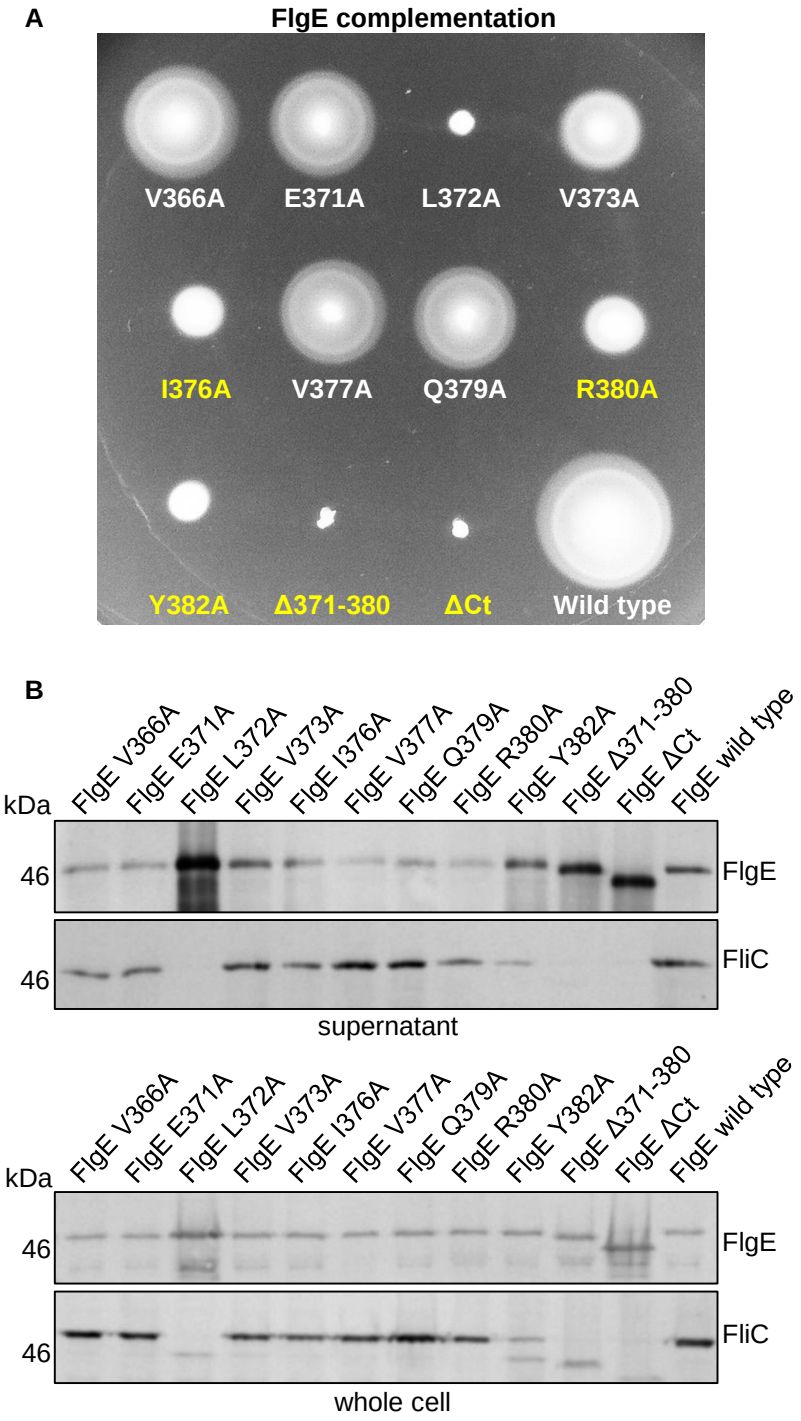

Figure 5.7. Motility and export phenotypes of Δ*flgE* strain complemented with FlgE point mutants

(**A**) Swimming motility assays of a *Salmonella* Δ*flgE* strain transformed with recombinant pTrc99a plasmids carrying a FlgE variant containing an internal 3xFLAG tag (FlgE wild type) or its variants (as indicated). Cells were inoculated into 0.3% soft-tryptone agar containing 100 µg/ml ampicillin and 50 µM IPTG and incubated for 3-6 hours at 37°C (top panel). (**B**) Secretion analysis of culture supernatant (supernatant, top panels) and whole cell (whole cell, bottom panels) fractions from the above cells. Cells were grown to mid-log phase in LB containing 100 µg/ml ampicillin and 50 µM IPTG. Proteins were separated by SDS-PAGE and immunoblotted with anti-FLAG and anti-FliC sera.

subunit export (Figure 5.7). Cells expressing the FlgE L_{372}A, FlgE Y_{382}A, FlgEΔ371-380 or FlgEΔCt variants contained increased levels of FlgE in culture supernatants compared to wild type and displayed little or no FliC expression, consistent with these variants being unable to assemble the flagellar hook (Figure 5.7). Consistent with the export phenotypes, the Δ*flgE* strain expressing the FlgE I_{376}A and R_{380}A variants were less motile than the wild type FlgE variant. These two variants were not exported into culture supernatants at higher levels than wild type FlgE, indicating that unlike the FlgE L_{372}A, FlgE Y_{382}A, FlgEΔ371-380 or FlgEΔCt variants, the FlgE I_{376}A and FlgE R_{380}A are able to assemble into the nascent structure and are not released directly into the culture supernatant. The location of the residues replaced with alanine were mapped onto the C-terminus of the cryo-EM structure of FlgE (Figure 5.8). The location of the residues substituted with alanine that disrupt hook assembly (red) form key interactions between adjacent subunits in the assembled hook explaining why they are unable to assemble to form the flagellar hook (Figure 5.8). Plotting this FlgE region using a helical wheel shows that the FlgE I376 and FlgE R380 residues are positioned on the same face of the FlgE C-terminal helix, however the Y382 residue is not (Figure 5.8).

5.8 Screening for suppressors of the motility defect associated with FlgE I_{376}A and FlgE R_{380}A

As FlgE I_{376}A and FlgE R_{380}A appear to assemble, screening for motile suppressors might identify suppressors that overcome the export defect. A Δ*flgE* strain was transformed with pTrc99a encoding FlgE I_{376}A or FlgE R_{380}A and single colonies were inoculated into LB broth and grown to A_{600} 1.0, before being inoculated into 0.3% soft-tryptone agar containing ampicillin and 50 μM IPTG. Plates were incubated at 30°C for 1-2 days until spurs of motile cells began to swim away from the site of inoculation. Cells from these spurs were streaked onto LB agar plates, single colonies were isolated and used to inoculate overnight cultures and plasmids were extracted and sequenced. Five plasmids containing suppressor mutations were characterised for each FlgE variant. Sequencing revealed that none of the plasmids contained mutations within the

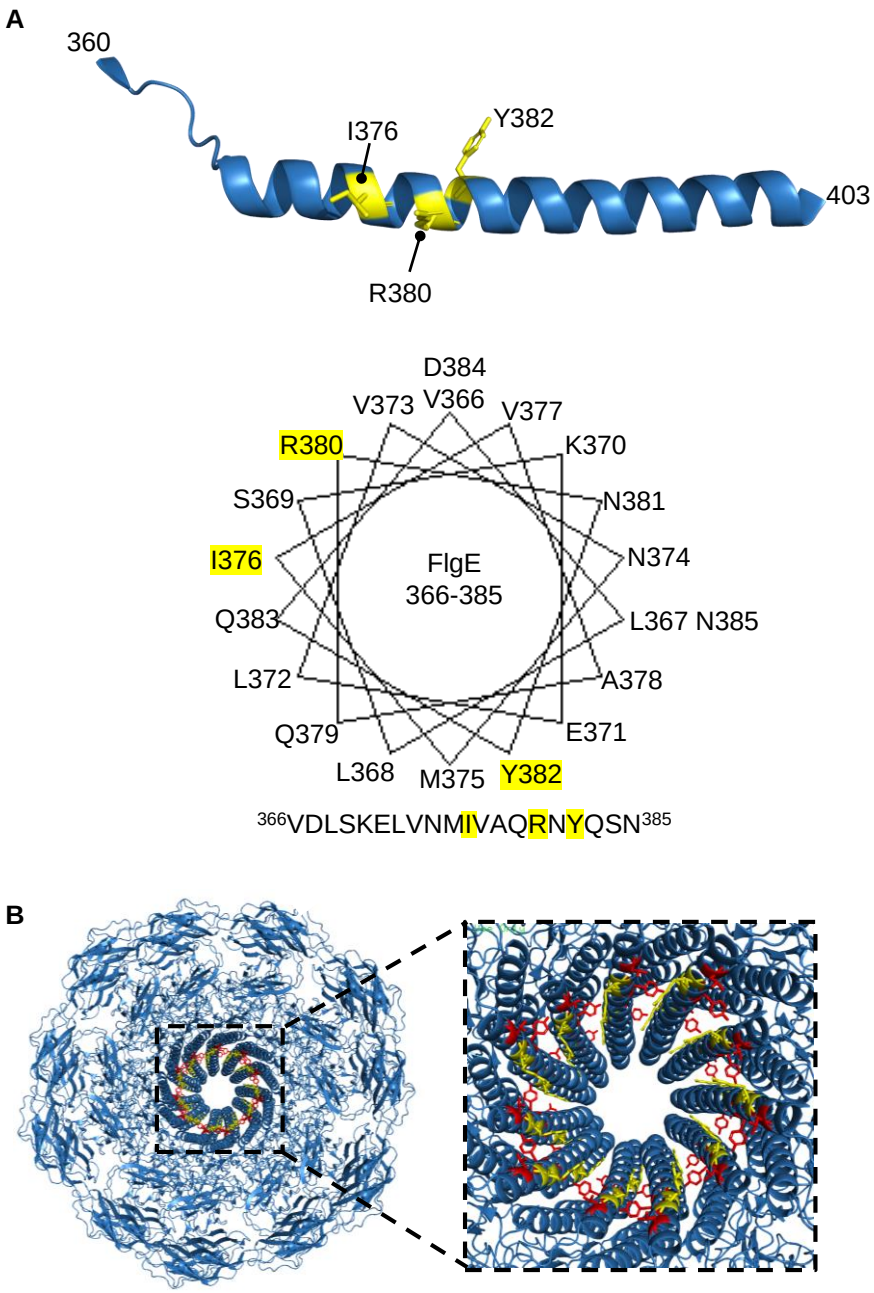

Figure 5.8. Location of the loss-of-function mutants in the structure of FlgE

(**A**) Amino acids 360-403 (blue) of the cryo-EM structure of *Salmonella* FlgE (PDB:6jzt) form predominantly alpha helical structure in the assembled flagellar hook (top). Helical wheel of FlgE amino acids 366-385 (bottom). FlgE amino acids that suppress the overexpression phenotype when replaced with alanine are colored yellow (I376, R380 and Y382). (**B**) Location of the FlgE amino acids in the cryo-EM structure of FlgE (PDB: 6jzt) that strongly suppress the overexpression phenotype when replaced with alanine are colored yellow (I376, R380). The FlgE amino acids that prevent flagellar hook assembly when mutated to alanine are colored red (L372 and Y382).

coding region of FlgE. In fact, all suppressors contained an adenine deletion upstream of the *flgE* start site within the *lacI* operator region, likely disrupting the interaction between the LacI repressor protein and the operator, increasing *flgE* expression (Figure 5.9). This indicates that increasing the expression level of FlgE suppresses the export defect. To test this further, I performed motility assays with a Δ*flgE* strain transformed with pTrc99a encoding the FlgE I_{376}A or FlgE R_{380}A variants or wild type FlgE at endogenous expression levels (50 μM IPTG) and at higher levels of IPTG induction (100 μM IPTG; Figure 5.9). Increasing the level of IPTG increased swimming motility by the two FlgE variants whereas swimming motility did not change significantly in cells expressing wild type FlgE (Figure 5.9), suggesting that increasing the expression level of the FlgE variants suppresses the export defect. This is in agreement with the data in figure 5.2 where overexpression increased FlgEΔCt export into culture supernatants.

5.9 Ribosome profiling of an 'early locked' fT3SS strain

Previous work from our laboratory showed that the binding affinities of early subunits for the FlhBc gate are in the micromolar range[257]. This suggests that the binding affinities of early rod and hook subunits for the FlhBc gate do not reflect the order of export or their stoichiometry in the assembled rod and hook substructures. Having identified a C-terminal export signal that targets early subunits to the export machinery, I cannot rule out a contribution of the C-terminus in promoting ordered export or ensuring that the correct number of each subunit is targeted to the export machinery to reflect their stoichiometry in the final structure. To determine the amount of each early subunit that is produced during peak flagellar gene expression I performed ribosome profiling, which provides a global snapshot of all the ribosomes in the cell that are engaged with a particular mRNA. Importantly, ribosome profiling in combination with RNA-seq can allow us to determine which genes are being translated and how efficiently they are being translated. I constructed a strain in which the export specificity switch from early to late flagellar subunits does not occur so that all cells are locked in 'early' export mode, such that they are expressing and exporting only

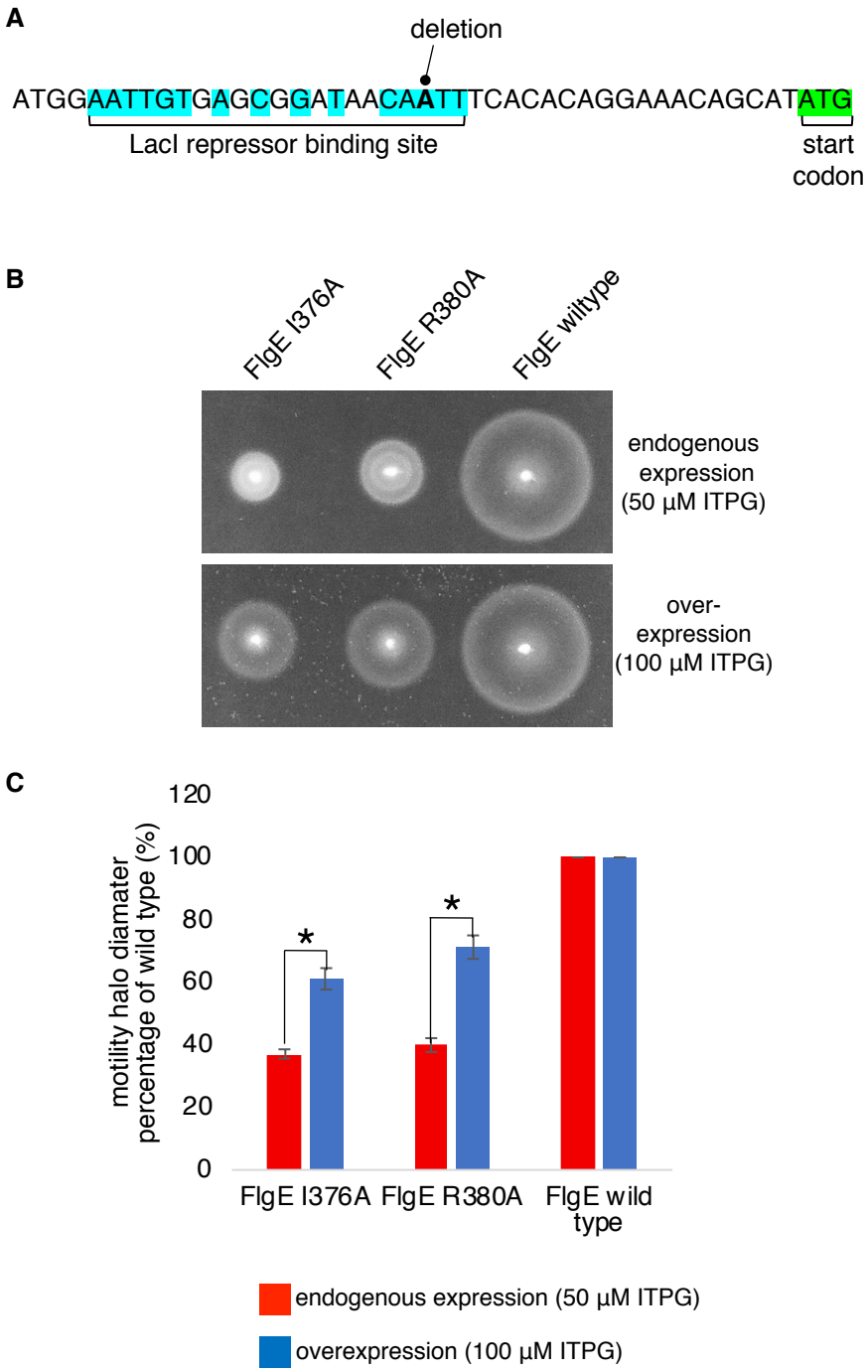

Figure 5.9. Increasing expression levels of FlgE I376A or FlgE R380A suppress their motility defect

(**A**) Location of the FlgE I376A and FlgE R380A suppressor mutations in the trc promoter of pTrc99a vector. The binding site for the LacI repressor is colored blue, the start codon is colored green and the adenine nucleobase that is deleted in the isolated suppressors is in bold.

(**B**) Swimming motility assays of a *Salmonella* Δ*flgE* strain transformed with recombinant pTrc99a plasmids carrying a FlgE variant containing an internal 3xFLAG tag (FlgE wild type) or its variants (as indicated). Cells were inoculated into 0.3% soft-tryptone agar containing 100 µg/ml ampicillin and 50 µM IPTG (top panel) or 100 µM IPTG (bottom panel) and incubated for 3-6 hours at 37°C (top panel).

(**C**) Motility halo diameters from the above cells expressing the FlgE point mutants were plotted as a percentage of cells expressing wild type FlgE. The error bars represent the standard error of the mean calculated from at least the biological replicates. * indicates a p-value < 0.05.

early flagellar subunits. Mutations in the *flhB* gene that prevent FlhB autocleavage ($P_{239}A$, $N_{269}A$) prevent the export specificity switch[281,282]. A *Salmonella* strain producing chromosomally encoded FlhB $P_{238}A$, $N_{269}A$ was grown to A_{600} 1.0 and lysed in cryogenic conditions in the presence of the bacterial translation inhibitor chloramphenicol and treated with ribonuclease to degrade portions of mRNA that are not protected by ribosome. These samples were passed through a Sephacryl S-400 column to separate monosomes from smaller RNA fragments. Protected fragments were collected by phenol/chloroform extraction. The protected fragments were gel purified, Illumina compatible 5' and 3' adapters were ligated and the fragments were amplified by reverse-transcription PCR. The major component of the libraries corresponds to ribosomal RNA contamination, decreasing the amount of useful sequence data in a sequencing experiment[283]. Therefore, prior to the ligation steps, rRNA was removed using a RiboZero kit that hybridises rRNA to biotinylated antisense strand oligonucleotides. rRNA contamination was further depleted at the library stage using duplex specific nuclease (DSN)[284]. Computational analysis of the sequencing data was performed by Betty Chung using the SL1344 genome assembly (ASM21085v2) and GenBank annotation (FQ312003.1). The number of ribosome protected fragments that correspond to each mRNA can effectively tell us how much of that mRNA is being translated and therefore tell us how much of each protein is being produced in the cell. Ribosome profiling revealed that the amount of each early flagellar subunit being produced correlated with the predicted stoichiometry in the final structure (Figure 5.10) with the exception of the FlgD hook cap subunit. This indicates that the expression level of early flagellar subunits reflects their stoichiometry in the final structure with the exception of FlgD. The higher levels of FlgD being produced can be explained by the observation that FlgD doesn't contain a C-terminal targeting signal and that increasing the expression level of early subunits lacking the C-terminal signal supresses their export defect. Therefore, FlgD may be produced at higher levels as it is not targeted as efficiently as other early subunits to the export machinery.

A

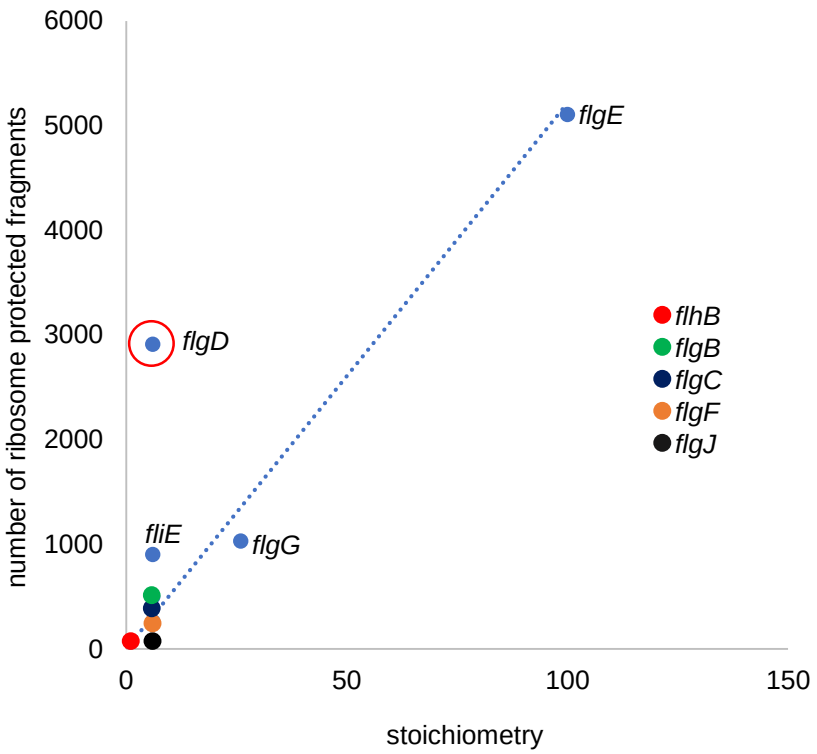

Figure 5.10. Ribosome profiling reveals the amount of each early subunit produced by a *Salmonella flhB* P238A, N269A strain
The number of ribosome protected fragments in the coding region of each early flagellar subunit and *flhB* were determined by ribosome profiling of an early subunit locked strain containing the P238A and N269A mutations in the *flhB* gene. *flgD* is circled in red.

5.10 Comparison of dominant negative phenotypes of FlgE$_{short}$, FlgEΔGRM, FlgEΔCt and their variants

I reasoned that if the FlgE C-terminal export signal is used after subunits have docked at FlhB$_C$ then a FlgE variant lacking the GRM (FlhBc binding signal) would display a weaker dominant negative overexpression phenotype than wild type FlgE (containing the C-terminal signal) as the FlgEΔGRM variant would not be able to reach the export machinery to allow the C-terminal export signal to be used. If the C-terminal signal is used before the GRM, then I would envisage that a FlgE variant lacking the GRM would have a greater dominant negative overexpression effect. To test this, I transformed a ΔrecA strain with pTrc99a encoding all three known export defective FlgE variants identified so far: FlgEΔ9-32 (or FlgE$_{short}$), FlgEΔGRM or FlgEΔCt. As a control I used wild type FlgE and for the FlgE$_{short}$ variant, I constructed a FlgE variant where amino acids 9-32 were replaced with four tandem repeats 4x(GSTNAS) to restore the length of the N-terminus. Wild type FlgE and its variants were overexpressed by induction with 1 mM IPTG. Export assays and motility assays were performed as previously described (section 2.15 and 2.16). Whole cell lysates and culture supernatants were immunoblotted for the presence of FlgE subunit using anti-FLAG sera and immunoblotted for FlgD and FlgL as representative early and late subunits, respectively, and for FlhA and FlgN as loading, expression and lysis controls. FlgEΔGRM did not suppress the overexpression phenotype caused by the presence of the FlgE C-terminus. The FlgEΔCt, FlgEΔGRM and FlgE$_{short}$ variants displayed progressively greater dominant negative overexpression phenotypes (Figure 5.11). In fact, the increasing strength of the dominant negative overexpression phenotypes appear to represent the likely order in which the export signals are used. Early subunits could be targeted initially to the export machinery by their C-terminal export signal, subunits subsequently dock at FlhBc *via* the GRM and this docking event positions the N-terminal export signal to be used efficiently (Chapter 3; Figure 5.12).

The data presented in this section indicate that early subunits interact sequentially with components of the export machinery although the precise role

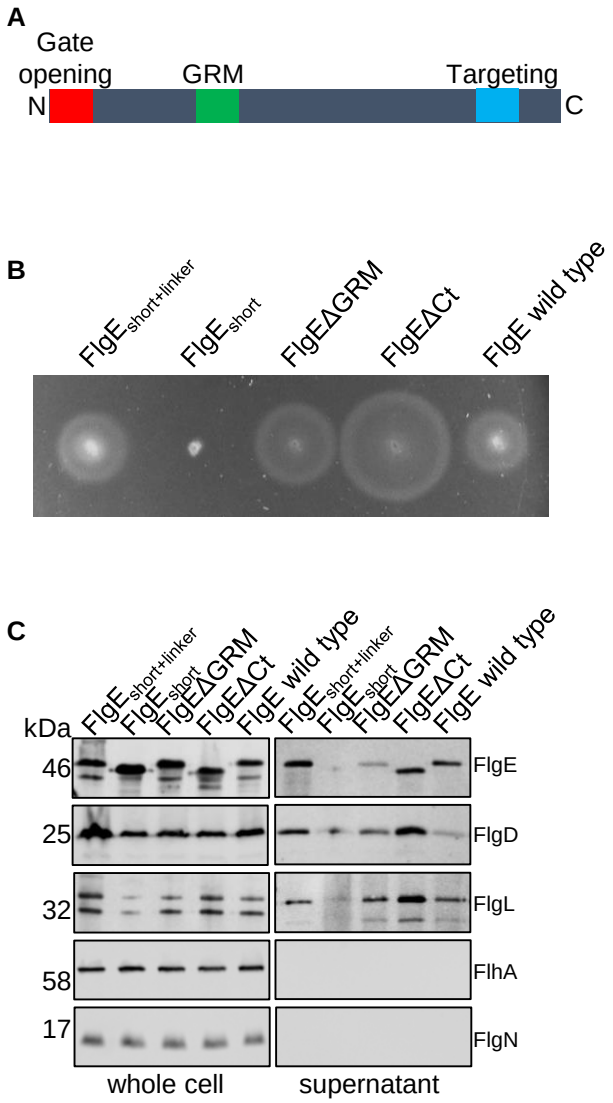

Figure 5.11. Overexpression phenotypes of $FlgE_{short}$, FlgE ΔGRM, FlgEΔCt and their variants

(**A**) Schematic representation of wild type FlgE highlighting the gate opening signal (red), gate recognition motif (GRM, green) and C-terminal targeting signal (blue).

(**B**) Swimming motility assays of a *Salmonella* Δ*recA* strain transformed with recombinant pTrc99a plasmids carrying FlgE containing an internal 3xFLAG tag or its variants ($FlgE_{short}$+linker, $FlgE_{short}$, FlgEΔGRM, FlgEΔCt). Cells were inoculated into 0.3% soft-tryptone agar containing 100 µg/ml ampicillin and 1 mM IPTG and incubated for 3-6 hours at 37°C.

(**C**) Secretion analysis of whole cell (whole cell) and culture supernatant (supernatant) fractions from the above cells grown to mid-log phase in LB containing 100 µg/ml ampicillin and 1 mM IPTG. Proteins were separated by SDS-PAGE and immunoblotted with anti-FLAG, anti-FlgD, anti-FlgL, anti-FlhA and anti-FlgN sera.

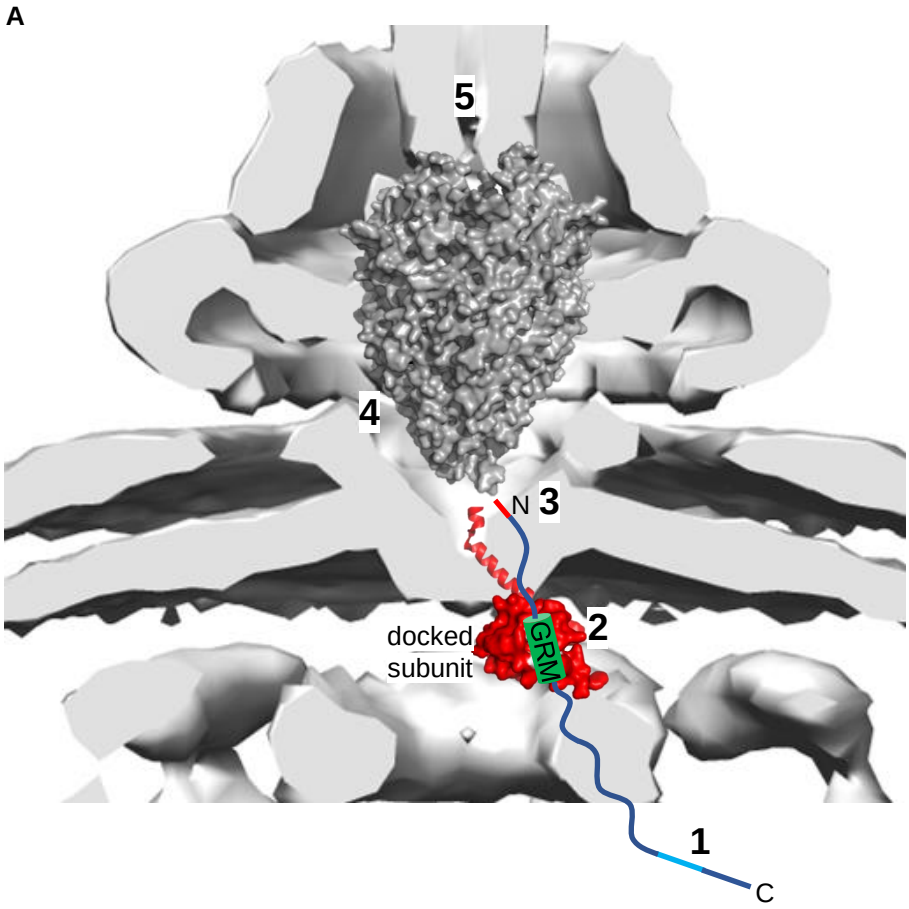

Figure 5.12. A proposed model for the sequence of binding events between early subunits and the export machinery
Placement of the crystal structure of FlhBc (PDB:3BOZ) and the cryo-EM structure of FliPQR (PDB:6F2D) in a tomographic reconstruction of the *Salmonella* SPI-1 injectisome (EMD-8544). A C-terminal signal in a subset of early subunits aids their targeting to the export machinery (**1**).
Subunits subsequently dock at the FlhBc gate via their gate-recognition motif (GRM) (**2**) positioning the N-terminal non-polar signal (**3**) to trigger opening of the export gate complex (**4**). Subunits are subsequently translocated into the export channel at the centre of flagellum (**5**) where they transit to the filament tip and refold into the nascent structure.

of the C-terminal export signal is unclear. Based on data suggesting that it mediates the first binding event, it is reasonable to assume that the C-terminal signal facilitates subunit entry into the export pathway by aiding initial recruitment of subunits to the export machinery. Second site mutations that restored motility to cells producing FlgE $I_{376}A$ or $R_{380}A$ mapped to the LacI repressor binding site of the heterologous *flgE* promoter region in pTrc99a, indicating that increasing the expression level compensates for the loss of subunit targeting to the export machinery and likely increases the chance of subunits reaching the export machinery to subsequently bind the FlhBc export gate.

5.11 Discussion

The aim of this study was to elucidate the role of the C-terminus of early subunits in export. The prevailing model is that early subunits docked at the FlhBc gate are captured by the C-terminus of the preceding subunit already in channel. Linked subunits are then thought to be pulled from the export gate into the channel, freeing the binding site on FlhBc for the subsequent subunit to dock, repeating the cycle[141]. The first piece of evidence provided in support of subunit capture from FlhBc was that *in vitro*, early subunits docked at FlhBc could be captured by the C-terminus of free subunits in a concentration dependent manner. These capture assays were all performed with FlgD (hook cap) subunit docked at FlhBc and challenged with FlgE, FlgD or FliK subunits. One criticism is that all of these challenge subunits are known to interact with FlgD either in the assembled structure or during export[240,239]. Therefore, capture of FlgD from FlhBc could be due to other weak interactions taking place between subunits rather than a capture event that reflects what happens at the export machinery *in vivo*. The second piece of evidence comes from *in vitro* and *in vivo* cysteine crosslinking experiments, whereby early or late flagellar subunits could form intermolecular crosslinks when cysteine residues were placed in their termini. The final piece of evidence was that hook subunit export into culture supernatants was attenuated when the C-terminus was deleted. This led authors to propose that this was due to a loss of both subunit capture from the FlhBc gate and the ability to form a subunit chain within the flagellar channel. Subunits

lacking a C-terminus would be captured from $FlhB_C$ but unable to capture newly docked subunits from $FlhB_C$, resulting in subunit stalling at $FlhB_C$. This would therefore result in a dominant negative phenotype, whereby subunits would not be captured from FlhBc, preventing other subunits from docking at FlhBc and being exported. However, FlgE lacking its C-terminus did not display a dominant negative phenotype when expressed at endogenous levels. In fact, when overexpressed, wild type FlgE (which contains the C-terminal region) attenuated subunit export and motility to a greater degree than FlgEΔCt. Furthermore, increasing the expression level of FlgEΔCt improves its export into culture supernatants indicating that the C-terminus of FlgE is not required for subunit capture from FlhBc and may instead contain an alternative export signal.

To test whether the hook cap subunit FlgD also contains a C-terminal export signal, I performed export assays with FlgD variants containing or lacking its C-terminus. Surprisingly, FlgDΔCt was exported into culture supernatants at the same level as wild type FlgD. Furthermore, neither FlgDΔCt or wild type FlgD displayed a dominant negative phenotype when overexpressed in a Δ*recA* strain, indicating that FlgD does not contain a C-terminal export signal. Based on the crystal structure of FlgD from *Pseudomonas aeruginosa,* the C-terminal deletion (equivalent to *Pseudomonas* FlgD amino acids 193-237) results in the deletion of four beta sheets and a small alpha helix[285]. Based on this structure, this deletion is likely to cause a considerable structural perturbation such that FlgD is unlikely to assemble into a pentameric cap[285]. This may explain why the FlgDΔCt variant was unable to capture subunits in the *in vitro* capture assay in Evans et al., 2013[141]. Wild type FlgD may be able to interact with the FlgD subunit docked at the FlhBc gate and 'capture' FlgD, whereas the deletion in FlgDΔCt may prevent these interactions from occurring. Why FlgD doesn't contain the C-terminal export signal is unclear. The C-terminus of FlgD is structurally different to the other early subunits that assemble to form the rod and hook[286,66,68,56]. Similarly, the C-terminus of the hook length ruler FliK also has a very different structure and shares no amino acid sequence homology to the early subunits that assemble to form the rod and hook[287]. Therefore, FliK is

unlikely to contain a C-terminal export signal (although this will need to be tested to confirm). This suggests that both FliK and FlgD must be produced at higher levels to compensate for the lack of a C-terminal export signal to aid their delivery to the export machinery.

Export of two other early subunits FlgC and FlgG was attenuated when their C-terminus was deleted, indicating that these subunits also contain a C-terminal export signal. Unlike FlgD and FliK, all other early subunits are thought to have a C-terminal D0 domain which could contain a C-terminal export signal, similar to those in FlgC, FlgE and FlgG, although I cannot be certain without testing all other early subunits.

A previous study showed that early subunits have a dominant negative effect on export and cell motility when overexpressed (FlgD and FliK were not tested in this study)[55]. Here I show that deletion of the FlgE C-terminus suppresses this overexpression effect, indicating that the C-terminal export signal causes the dominant negative phenotype. This could be simply caused by competition of the plasmid encoded subunit with chromosomally encoded early subunits for export through the channel. However, levels of exported FlgEΔCt and wild type FlgE were comparable, indicating that the phenotype is not caused by more wild type FlgE being exported. The phenotype could instead be caused by FlgE subunit docking at one of the components of the export machinery and preventing other early subunits from docking at this component. However, export of FlgD (which doesn't contain a C-terminal export signal) was also attenuated when wild type FlgE was overexpressed, indicating that the phenotype isn't due to direct competition for a binding site with other early subunits. Another possibility is that FlgE is docking at a component of the export machinery and physically prevents other early subunits from entering the export pathway. Whether overexpression of wild type FlgE directly affects export of late subunits is less clear as late subunit export depends on completion of the early substructures and therefore attenuation of early subunit export indirectly reduces levels of late subunit export in culture supernatants.

The data so far indicate that the C-terminal export signal may in fact be a subunit targeting signal to aid early subunit entry into the export pathway. In some species, dedicated export chaperones have been identified for the injectisome needle subunit, SctF – a subunit that assembles to form the injectisome needle, which is a substructure that is equivalent to the flagellar hook[184,186]. Deletion of the SctF chaperone attenuates needle subunit export, and this chaperone binds the C-terminus of the needle subunit and, presumably like other T3SS chaperones, delivers SctF to FlhA[177,115]. Unlike SctF, the early flagellar subunits do not have dedicated export chaperones. However, the late flagellar subunits are chaperoned to the export machinery[172,173,183]. The chaperones for the late flagellar subunits also bind the subunit C-terminus and deliver them to various components of the export machinery[207,177,115]. Deletion of flagellar export chaperones can be suppressed by overexpressing the cognate subunit(s) of the deleted chaperone, indicating that loss of chaperone-mediated targeting can be suppressed by increasing the amount of available subunit in the cell, analogous to suppression of the FlgEΔCt export defect by overexpression of FlgE[288].

Another interesting feature of the chaperoned flagellar subunits is that docking of chaperone-subunit complexes at the cytoplasmic domain of FlhA is thought to promote subunit unfolding[230]. Based on the predicted location of FlhB within/below the plane of the membrane, early subunits must transit beyond the FlhAc nonameric ring to reach and dock at FlhBc[105]. Therefore, if early subunits are also unfolded at FlhAc then early subunits may need to be anchored at or nearby FlhAc for unfolding to occur in a similar manner to the chaperoned late subunits[230]. The C-terminus of FlgE may carry out this role by docking subunits at or near to FlhAc.

The FlgN and FliT export chaperones dock at the cytoplasmic ATPase complex[176]. To test whether the ATPase is required for the dominant negative overexpression phenotype of wild type FlgE, I overexpressed FlgEΔCt and wild type FlgE in a strain that was deleted for the ATPase and that contained

mutations that bypass the need for the ATPase. Overexpression of wild type FlgE attenuated subunit export to a greater amount than FlgEΔCt. A similar phenotype was observed in a strain lacking the ATPase and the C-ring components, indicating that the binding site of the FlgE C-terminus is not the C-ring or ATPase complex but may instead be one of the core components of the export machinery – FlhA or FlhB.

To identify the region of the FlgE C-terminus that is responsible for the dominant negative overexpression phenotype, I performed motility assays with a *recA* null strain overexpressing FlgE variants containing ten-residue scanning deletions. I found that amino acids 371-380 of FlgE were required to give the dominant negative phenotype of FlgE. Further refinement showed that amino acids isoleucine-376, arginine-380 and tyrosine-382 are the key residues involved. Chaperone binding sites on subunits often cover an extended region of the subunit, sometimes up to 100 amino acids[249,149]. This screen shows that a relatively small portion of the FlgE C-terminus is responsible for the motility and export defect, indicating that the mode of interaction of the subunit C-terminus with a potential binding partner is different to the way T3SS chaperones interact with their cognate subunits. A screen for suppressors in cells expressing FlgE $I_{376}A$ or FlgE $R_{380}A$ identified six suppressor mutations, all of which increased FlgE expression, indicating that increasing the amount of FlgE in the cell increases the probability of it entering the export pathway.

One of the other roles of T3SS export chaperones is to protect their cognate subunit from degradation in the cell. As early flagellar subunits do not have dedicated chaperones, it is possible that their termini are more sensitive to degradation in the cytoplasm. Having a C-terminal export signal could prevent the entry of subunits that do not contain a functional C-terminus into the export pathway, favouring subunits that do contain a functional C-terminus and therefore can assemble into the nascent structure.

If subunits are not captured from FlhBc, where could subunits begin forming a subunit chain? The data in chapter 4 indicates that the export gate transitions from a closed to open conformation whilst subunits are transiting through the gate and returns to a closed state when there are no subunits available to transit through the gate. This indicates that subunit chaining must occur after subunits have passed through the export gate, otherwise a chain of subunits would always be spanning the export gate and seal the leaky FliRΔ110-116 phenotype observed in chapter 4 (Figure 4.2).

Interestingly, FlhAc can adopt an open or closed conformation, whereby the closed conformation reduces the binding affinity of FlhAc for the export chaperones[232]. Formation of the open conformation is required for chaperone binding and efficient late subunit export[232]. This indicates that the closed FlhAc conformation may be adopted during early subunit export. It is feasible that this closed FlhAc conformation allows the C-terminus of early subunits to bind FlhAc or to another component of the export machinery, and following the export specificity switch, the adoption of the open FlhAc conformation may prevent early subunits from being efficiently targeted to the export machinery[232].

Comparing the dominant negative overexpression phenotypes of FlgE variants ($FlgE_{short}$, FlgEΔGRM, FlgEΔCt) revealed that the dominant negative overexpression phenotypes appear to reflect the sequence of early subunit interactions with the export machinery with subunit variants that are able to pass further down the export pathway displaying a more dominant negative overexpression phenotype. This suggests that as early subunits pass down the export pathway they become more committed for export and therefore display a greater dominant negative phenotype.

A picture emerges where the early subunits interact sequentially with the export machinery with the export signals carrying out distinct roles for subunit targeting, docking at the machinery and triggering opening of the export gate. In summary, I have presented evidence to support the view that the C-terminal export signal

of early subunits does not capture subunits from the FlhBc gate as predicted by the chain mechanism model but instead functions as a targeting export signal to aid subunit delivery into the export pathway. Refinement of the C-terminal signal identified key residues required for efficient subunit export and motility. I propose that the C-terminal signal aids early subunit targeting to the export machinery by providing a binding site for a core component of the flagellar type III secretion machinery.

Chapter 6
Sequential interactions of flagellar chaperones with the flagellar export machinery

6.1 Introduction

Over a third of bacterial proteins synthesised at the ribosome need to be targeted to the bacterial membrane and either inserted into the membrane or exported out of the cell[289]. One of the issues with preprotein synthesis in the cytosol is their tendency to aggregate or degrade before they reach the translocation machinery[289,183,172,103]. Two strategies have evolved to circumvent this problem: coupling translation with translocation or employing cytosolic chaperones[103,163,195]. There is no evidence that the flagellar export machinery utilises co-translational export, in fact the initial rate of protein export by the flagellum is greater than the rate of translation by the ribosome[174,175]. However, a subset of flagellar subunits are recognised by a group of export chaperones[183,172,173]. The late flagellar subunits are delivered to the export machinery by specific chaperones that bind the C-terminus of their cognate subunit[183,172,173,178,249]. Three cytosolic chaperones - the FlgN chaperone for hook-filament junction proteins, the FliT chaperone for filament cap subunits and the FliS chaperone for flagellin - prevent premature association between subunits in the cytosol and delivering subunits to the export machinery[13,46,60,59,60].

The chaperones FlgN and FliT in complex with their cognate subunits initially dock at the FliI component of the cytoplasmic ATPase complex[176,290]. Chaperone-subunit complexes are then thought to interact with the cytosolic domain of FlhA ($FlhA_C$) which is proposed to act as an export gate for the late structural subunits in a similar manner to $FlhB_C$ is for early structural subunits[176,177,116,115,227]. Furthermore, in the absence of bound subunit, unladen chaperones are able to bind to the FliJ stalk component of the ATPase complex[226]. This FliJ-chaperone interaction has been proposed to recruit chaperones to the export machinery and transfer them to subunits[226]. The fact that only the chaperones for the minor filament substructures (FlgN and FliT) can

dock at FliJ led authors to propose that this selective binding may offer a mechanism to promote assembly of the hook-filament junction complex and the filament cap substructures required for filament assembly[226,225]. The sequence in which these binding events between chaperones and the export machinery occurs is unclear. In this chapter I provide evidence indicating that the FlgN chaperone interacts sequentially with components of the export machinery.

6.2 Characterisation of a FlgN variant defective in chaperone activity

The sequence of chaperone binding events at the export machinery has not been fully determined. To assess this, I set out to identify variants of the chaperone FlgN that were defective in binding components of the flagellar export machinery *in vitro,* and went on to test their ability to bind export components *in vivo*. Specifically, I assessed whether, in *Salmonella*, the inability of FlgN to bind one export component hindered subsequent access to other binding partner(s) in the export machinery, revealing the order of transient binding events in the chaperone export cycle. A previous graduate student in the laboratory (Sangita Ahmed) identified an export defective FlgN chaperone variant (FlgNΔ112-121)[291]. The previously observed motility defect of FlgNΔ112-121 may be caused by loss of one or more interactions between the chaperone variant and its cognate subunits or components of the export machinery. To assess which components of the export machinery the FlgNΔ112-121 can interact with, I used an *in vitro* affinity pull down assay. I also tested whether previously identified chaperone variants (FlgN $Y_{122}A$, FlgNΔ90-100 and FlgNΔ120-140) can interact with their cognate subunits and components of the export machinery. The FlgN $Y_{122}A$ variant has been shown to be defective in FlhAc binding, FlgNΔ90-100 variant is unable to interact with both FliJ and its cognate subunits, whilst FlgNΔ120-140 has been shown to stall at the FliI component of the ATPase complex[115,176]. It is important to note that there are a few limitations to using affinity pull down assays to screen for protein-protein interactions. First, the affinity tag can affect the function of the protein of interest. Second, many flagellar proteins associate with other proteins as part of a large protein complex, whereas the affinity purification assays performed in this section are performed

with tagged proteins in isolation. Therefore, these proteins will contain exposed regions that are not normally exposed when part of a protein complex. These exposed regions could interact non-specifically with other proteins. Another factor to consider is that proteins can non-specifically interact with the resin rather than the resin-immobilised protein of interest. Where possible, I utilised protein variants that are defective in target protein binding as negative controls and wild type proteins as positive controls.

A pGEX-4T3 vector encoding glutathione-S-transferase tagged components of the export machinery (GST-FlhAc or GST-FliJ) or cognate subunits (GST-FlgK or GST-FlgL) were introduced into *E.coli* C41 and the GST-tagged proteins were overexpressed. Cells were harvested, resuspended in lysis buffer A (Table A1.1) and lysed. The lysed cells were clarified by centrifugation and bound to glutathione-sepharose resin before washing the resin. *E.coli* cell extracts containing overexpressed untagged wild type FlgN and its variants (FlgN $Y_{122}A$, FlgNΔ112-121, FlgNΔ90-100, FlgNΔ120-140) were incubated with the resin bound GST-tagged proteins and washed extensively. Proteins were boiled off the resin, separated by SDS-PAGE and stained with InstantBlue. The FlgNΔ112-121 variant failed to bind FlhAc but could still bind other components of the export machinery (Figure 6.1). The 112-121 deletion lies adjacent to FlgN Y122, a residue that has previously been shown to be critical for FlgN binding to FlhA[115], and I confirmed that the FlgN $Y_{122}A$ variant failed to bind GST-$FlhA_C$, but could bind GST-tagged cognate subunits and GST-FliJ (Figure 6.1). FlgNΔ120-140 could still bind GST tagged FlgK and FlgL. Unexpectedly, FlgNΔ120-140 showed reduced binding to GST-FliJ, despite the 120-140 deletion being outside the region required for FlgN binding to FliJ (Figure 6.1)[226]. These data indicate that large deletions in the C-terminal region of FlgN cause considerable structural perturbations that disrupt interactions with multiple binding partners. I failed to develop a method to detect chaperone-subunit interactions with FliI, possibly due to the very weak association between FliI and chaperone-subunit complexes[176,292]. Therefore, I was unable to determine which FlgN variants could associate with FliI.

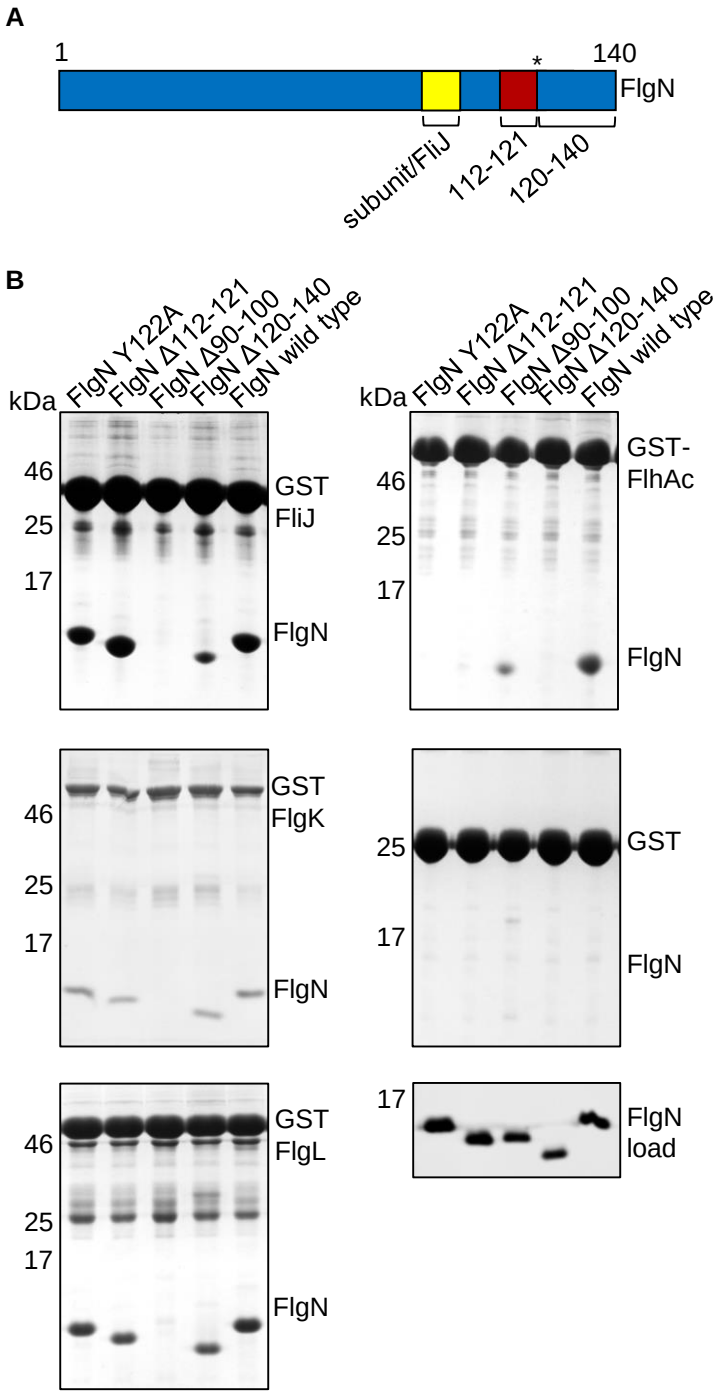

Figure 6.1. *In vitro* interactions of wild type FlgN and its variants with components of the export machinery

(**A**) Schematic representation of the 140-residue *Salmonella* FlgN) indicating the subunit/FliJ binding region (residues 90-100; yellow), the uncharacterized 112-121 deletion region (red), and the position of tyrosine-122 (Y122, red), which is essential for FlhA binding.

(**B**) Affinity chromatography of cell lysates of *E.coli* C41 expressing GST-tagged flagellar export components (GST-FliJ, GST-$FlhA_C$), cognate subunits (GST-FlgK, GST-FlgL) or GST alone were incubated with glutathione sepharose resin and washed. Cell lysates containing full-length wild type FlgN or its variants (Y122A, Δ112-121, Δ90-100, Δ120-140) were incubated with the resin-bound GST-tagged proteins, washed extensively and proteins were eluted by boiling the resin in SDS-loading buffer. Proteins were separated by SDS-PAGE and visualized by staining with Coomassie Brilliant Blue. Levels of FlgN and its variants in the input cell lysates (FlgN load, bottom right hand panel) were assessed by immunoblotting with anti-FlgN polyclonal antisera. Apparent molecular weights are in kilodaltons (kDa).

6.3 FlgNΔ120-140, FlgNΔ112-121 and FlgN Y_{122}A fail to bind FliJ in vivo

I reasoned that FlgN variants that failed to bind one or more components of the export machinery might not be able to interact with subsequent binding partner at the export machinery. Previous studies indicate that chaperone-subunit complexes initially dock at the FliI component of the ATPase before docking at FlhAc[176,177,116]. At what stage of the export cycle unladen chaperones bind to the FliJ component of the export machinery is unknown. To test this, I assessed whether the FlgNΔ120-140, FlgNΔ112-121and FlgN Y_{122}A variants that can bind FliJ *in vitro* and are defective in binding FlhAc *in vitro* can access the FliJ component *in vivo*. To assess this, an *in vivo* FliJ pull down assay was developed using a *Salmonella* Δ*flgN* strain in which the *fliJ* chromosomal locus had been replaced with a recombinant gene encoding His_6-tagged FliJ. A *Salmonella* strain containing wild type FlgN and the chromosomally encoded His_6-tagged FliJ displayed wild type motility, indicating that that His_6-FliJ is functional (Figure 6.2). The *Salmonella his-fliJ* Δ*flgN* strain was transformed with pTrc99a encoding wild type FlgN or its variants (Y_{122}A, Δ112-121, Δ90-100, Δ120-140) and expressed at wild type (physiological) levels (Figure 6.2). Cells were grown to A_{600} 1.0, harvested and resuspended in buffer D (table A1.1). Cells were disrupted mechanically to release membrane-associated flagellar components to the soluble fraction, from which His_6-FliJ-FlgN complexes were affinity purified using HisPur cobalt resin. The resin was washed extensively with buffer D (table A1.1) and proteins were boiled off the resin. Proteins were separated by SDS-PAGE and immunoblotted for the presence of FlgN and FliJ using anti-FlgN and anti-His sera. Load fractions were also immunoblotted for FlgN and FliJ to ensure all components were expressed at equivalent levels (Figure 6.2). The amount of protein in the resin fractions corresponding to the FlgN variants were compared to wild type FlgN levels (Figure 6.2). The standard error of the mean was calculated for each sample and is represented as error bars (Figure 6.2). The data revealed that the three FlgN variants (FlgN Y_{122}A, FlgN Δ112-121 and FlgN Δ120-140) that can bind FliJ but not FlhAc *in vitro* displayed reduced binding to FliJ *in vivo* (Figure 6.2). Levels of FliJ-bound FlgN Y_{122}A and FlgN Δ112-121 (variants that fail to bind FlhA) were 50% lower *in vivo* than *in vitro*. Furthermore,

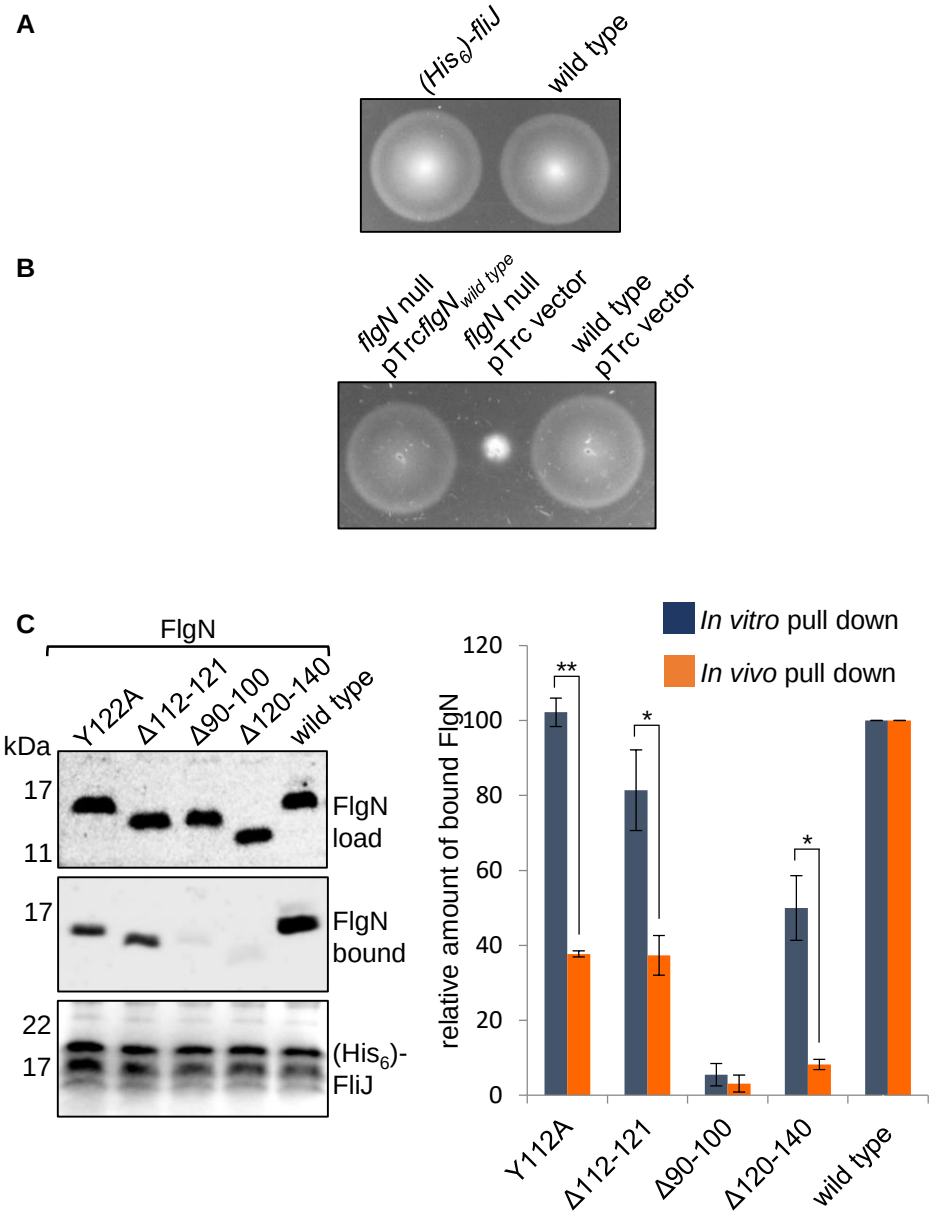

Figure 6.2. FlgN variants that bind FliJ *in vitro* do not interact efficiently with FliJ *in vivo*

(**A**) Swimming motility assays of wild type *Salmonella* and a strain in which the *fliJ* gene is replaced with an N-terminal hexa-histidine tagged variant. Cells were inoculated into 0.3% soft-tryptone agar and incubated for 3-6 hours at 37°C (top panel).

(**B**) Swimming motility assays of wild type *Salmonella* transformed with empty pTrc99a vector and a *Salmonella* Δ*flgN* strain transformed with empty pTrc99a vector or pTrc99a carrying wild type FlgN. Cells were inoculated into 0.3% soft-tryptone agar containing 100 µg/ml ampicillin and 50 µM IPTG and incubated for 3-6 hours at 37°C.

(**C**) *A Salmonella* Δ*flgN* strain containing a chromosomally-encoded (His_6)-FliJ transformed with pTrc99a carrying wild type FlgN (wild type) or its variants (Y122A, Δ112-121, Δ90-100, Δ120-140) were grown to A_{600} 1.0 and mechanically lysed. Soluble fractions (FlgN load) were incubated with Cobalt-nitriloacetic acid (NTA) agarose, washed and proteins were eluted by boiling the resin in SDS-loading buffer. Proteins were separated by SDS-PAGE and detected by immunoblotting with anti-FlgN (FlgN bound) or anti-FliJ ((His_6)-FliJ) antisera. Apparent molecular weights are in kilodaltons (kDa) (Left panels). Relative levels of FliJ-bound FlgN (WT) or its variants (Y122A, Δ112-121, Δ90-100, Δ120-140) from the *in vitro* (blue) and *in vivo* (orange) affinity chromatography assays were quantified using Image Studio Lite and plotted as a percentage of wild type FlgN bound levels (right). Error bars show standard error of the mean from at least three biological replicates. * indicates a p-value < 0.05, ** indicates a p-value < 0.005.

levels of FlgN Δ120-140 (unable to bind FlhA and stalls at FliI) bound to FliJ was 80% lower *in vivo* than *in vitro* (Figure 6.2). These data indicate that FlgN binds FliJ after docking at the cytoplasmic domain of FlhA.

6.4 FlgN variants fail to restore subunit export or motility to a flgN null strain

To compare the ability of the different chaperone variants in facilitating the export of cognate subunits, I performed motility and export assays as described previously (sections 2.15 and 2.16). A Δ*flgN* strain was transformed with pTrc99a encoding wild type FlgN or its variants ($Y_{122}A$, Δ112-121, Δ90-100, Δ120-140). Whole cell lysates and supernatants were immunoblotted for the presence of FliC, FlgK and FlgL subunits, and also for FlgN as an expression and lysis control. None of the FlgN variants restored motility to the Δ*flgN* strain (Figure 6.3). Similarly, export of cognate subunits (FlgK and FlgL) into culture supernatants was attenuated to the same level as in the Δ*flgN* strain. Levels of the non-cognate subunit FliC in culture supernatants was greater than for wild type *Salmonella* which corresponds to the inability to assemble the hook-filament junction and therefore results in the release of unassembled FliC directly into the culture supernatants (Figure 6.3). These data indicate that all the chaperone variants are defective in their chaperone activity.

6.5 ATPase-dependent dominant negative phenotypes associated with FlgN variants

I wanted to assess whether any of the chaperone variants displayed a dominant negative phenotype when expressed in wild type *Salmonella*, which might be indicative of sequestration of a key export component and/or blocking of the export machinery to prevent docking and export of other substrates. The previously identified chaperone variant FlgNΔ120-140 was shown to be dominant negative as a result of stalling at the FliI component of the ATPase[207]. Whether the other FlgN variants display dominant negative phenotypes is unknown. Negative dominance could be caused by a combination of stalling

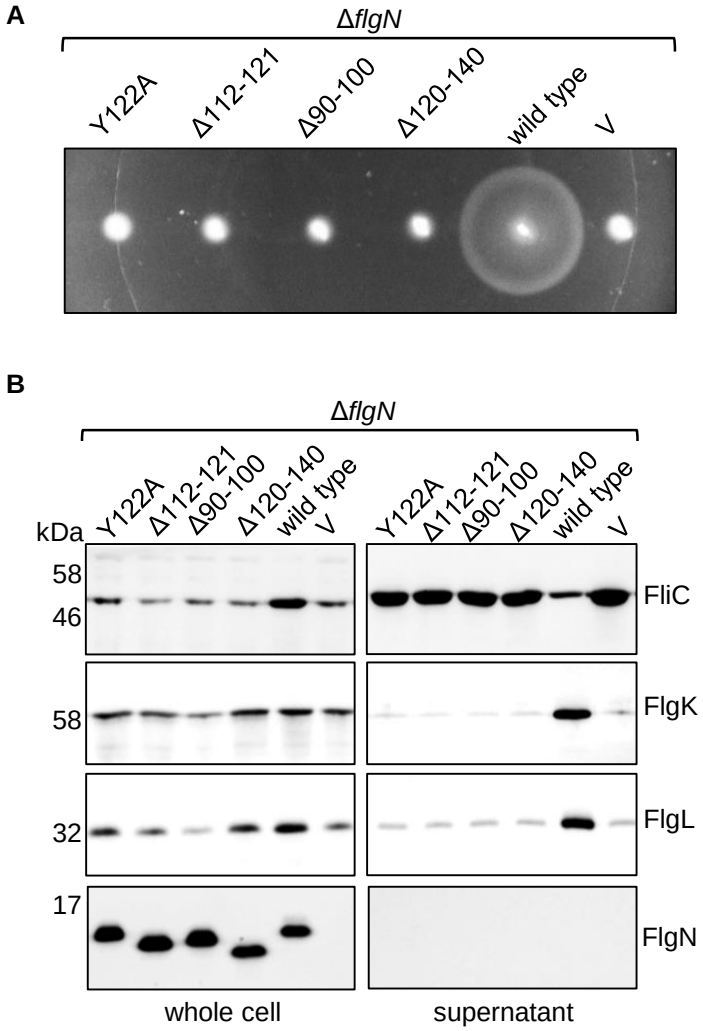

Figure 6.3. Motility and export phenotypes of a Δ*flgN* strain complemented with wild type FlgN and its variants

(**A**) Swimming motility assays of a *Salmonella* Δ*flgN* strain transformed with recombinant pTrc99a plasmids carrying wild type FlgN or its variants (Y122A, Δ112-121, Δ90-100, Δ120-140). Cells were grown to A600 1.0 in LB containing 100 μg/ml ampicillin and 50 μM IPTG, inoculated into 0.3% soft-tryptone agar containing 100 μg/ml ampicillin and 50 μM IPTG and incubated for 3-6 hours at 37°C.

(**B**) Secretion analysis of whole cell (whole cell) and culture supernatants (supernatant) fractions from the above cells. Cells were grown to mid-log phase in LB containing 100 μg/ml ampicillin and 50 μM IPTG. Proteins were separated by SDS-PAGE and immunoblotted with anti-FliC, anti-FlgK, anti-FlgL and anti-FlgN sera.

interactions at different components of the export machinery or by sequestration of cognate subunits.

To assess negative dominance, wild type *Salmonella* was transformed with pTrc99a encoding wild type FlgN or its variants (FlgN Y_{122}A, FlgNΔ112-121 and FlgNΔ90-100, FlgNΔ120-140). Cells were grown with ampiciilin and overexpression of *flgN* was induced with 100 μM IPTG. Cell motility and subunit export were assayed as described previously (sections 2.15 and 2.16). Both the FlgN Y_{122}A and FlgNΔ120-140 variants attenuated motility and export to the same degree, suggesting that FlgN Y_{122}A stalls at the FliI component of the ATPase complex, as has been shown for FlgNΔ120-140[176]. Both FlgN Y_{122}A and FlgNΔ120-140 are defective in FlhA binding (Figure 6.1). Stalling at FliI by these two FlgN variants might represent the inability of FlgN Y_{122}A and FlgNΔ120-140 to be passed to FlhAc and therefore they remain bound at FliI. FlgNΔ112-121, like FlgN Y_{122}A and FlgNΔ120-140, failed to bind to FlhAc *in vitro* but could still interact with the other binding partners that were tested (Figure 6.1). Unlike FlgN Y_{122}A and FlgNΔ120-140, FlgNΔ112-121 was not dominant negative (Figure 6.4). This suggests that FlgNΔ112-121 may no longer be able to interact with FliI. The FlgNΔ90-100 displayed the least dominant negative phenotype and this may be caused by a combination of factors. FlgNΔ90-100 cannot bind cognate subunit and therefore would not be able to sequester cognate subunits into complexes incompetent for export. Furthermore, as FlgNΔ90-100 cannot bind subunit it cannot interact with FliI (FliI only binds chaperones that are in complex with subunit) and therefore FlgNΔ90-100 stalling at FliI cannot occur.

6.6 Attenuation of flagellar subunit export by FlgN variants in a Salmonella flhBP_{28}*T-ΔfliHI-ΔflgM strain*

If FlgNΔ112-121 has lost the ability to bind and stall at FliI then the dominant negative phenotypes of the FlgN variants that stall at FliI (FlgN Y_{122}A and FlgNΔ120-140) should match that of FlgNΔ112-121 in a motile strain deleted for the genes that encode FliI and FliH. I constructed a strain in which the *fliH* and *fliI* genes were deleted in combination with mutations that bypass the need for

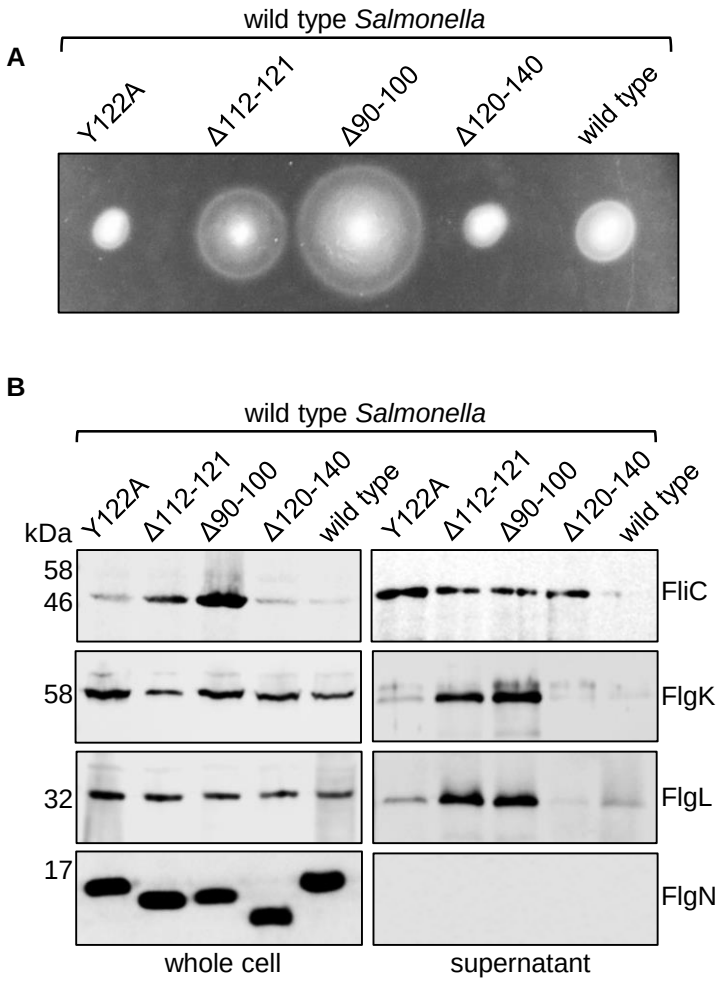

Figure 6.4. Dominant negative overexpression phenotypes of wild type FlgN and its variants in wild type *Salmonella*

(**A**) Swimming motility assays of wild type *Salmonella* strain (SJW1103) transformed with recombinant pTrc99a plasmids carrying wild type FlgN or its variants (Y122A, Δ112-121, Δ90-100, Δ120-140). Cells were grown to A600 1.0 in LB containing 100 μg/ml ampicillin and 100 μM IPTG, inoculated into 0.3% soft-tryptone agar containing 100 μg/ml ampicillin and 100 μM IPTG and incubated for 3-6 hours at 37°C.

(**B**) Secretion analysis of whole cell (whole cell) and culture supernatants (supernatant) fractions from the above cells. Cells were grown to mid-log phase in LB containing 100 μg/ml ampicillin and 100 μM IPTG. Proteins were separated by SDS-PAGE and immunoblotted with anti-FliC, anti-FlgK, anti-FlgL and anti-FlgN sera.

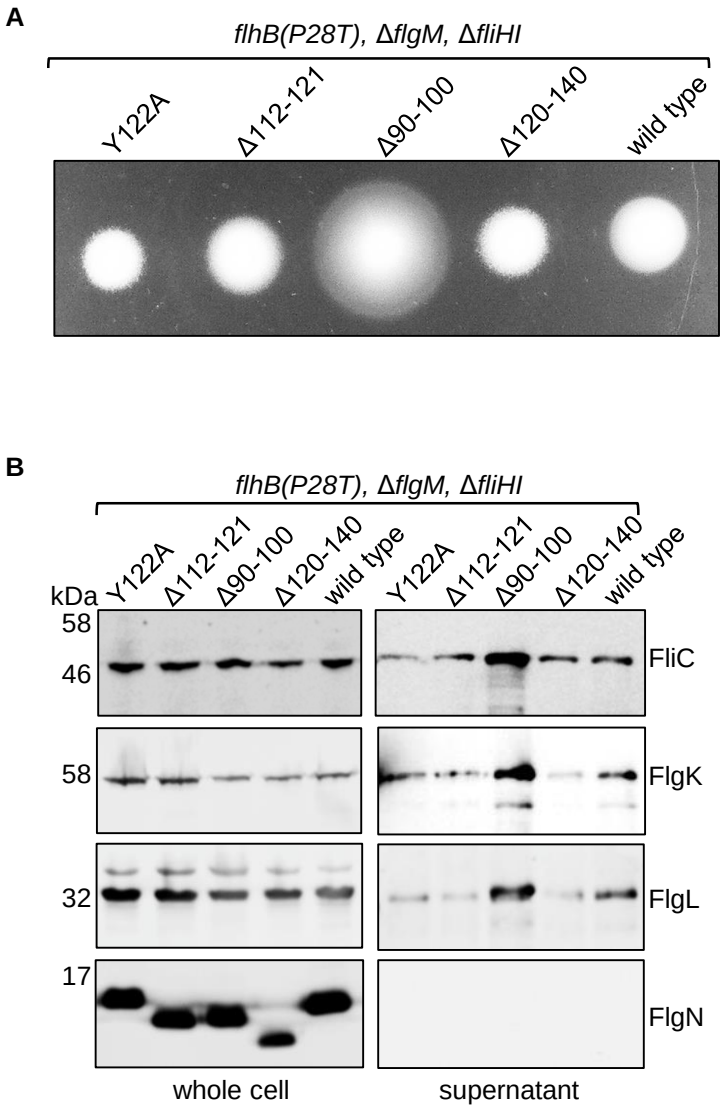

Figure 6.5. Dominant negative overexpression phenotypes of wild type FlgN and its variants in a *Salmonella* strain deleted for genes encoding FlgM, FliH and FliI and containing the ATPase deletion suppressor mutation *flhB*P28T

(**A**) Swimming motility assays of a *Salmonella flhB*P28T, Δ*flgM,* Δ*fliHI* strain transformed with recombinant pTrc99a plasmids carrying wild type FlgN or its variants (Y122A, Δ112-121, Δ90-100, Δ120-140). Cells were grown to A600 1.0 in LB containing 100 µg/ml ampicillin and 100 µM IPTG, inoculated into 0.3% soft-tryptone agar containing 100 µg/ml ampicillin and 100 µM IPTG and incubated for 3-6 hours at 37°C.

(**B**) Secretion analysis of whole cell (whole cell) and culture supernatants (supernatant) fractions from the above cells. Cells were grown to mid-log phase in LB containing 100 µg/ml ampicillin and 100 µM IPTG. Proteins were separated by SDS-PAGE and immunoblotted with anti-FliC, anti-FlgK, anti-FlgL and anti-FlgN sera.

the ATPase (*flhB*P$_{28}$T-*ΔfliHI-ΔflgM)*. This strain was transformed with pTrc99a encoding wild type FlgN or its variants (FlgN Y$_{122}$A, FlgNΔ112-121, FlgNΔ90-100, FlgNΔ120-140). Cell motility and export were assayed as previously described (sections 2.15 and 2.16). Whole cell lysates and supernatants were immunoblotted for the presence of FliC, FlgK and FlgL subunits, as well as for FlgN as an expression and lysis control. The diameter of the motility halos and levels of cognate and non-cognate subunit export in cells expressing FlgNΔ112-121, FlgN Y$_{122}$A or FlgNΔ120-140 were equivalent, suggesting that the FlgNΔ112-121 variant that is unable to bind FlhAc (like the FlgNΔ112-121 and FlgN Y$_{122}$A variants) is defective in binding FliI (Figure 6.5). The FlgNΔ90-100 variant was more motile and exported more cognate subunit than the other FlgN variants indicating that the motility and export defects caused by the other chaperone variants may be due to sequestration of cognate subunits, preventing their export (Figure 6.5).

*6.7 Attenuation of flagellar subunit export by FlgN variants in a Salmonella flhB*P$_{28}$T*-ΔfliHIJ-ΔflgM strain*

Some of the FlgN variants may stall at FliJ, preventing it from carrying out its function. Deletion of the genes encoding FliH and FliI prevents FliJ from localising at the export machinery, although FliJ can still promote subunit export but much less efficiently than if *fliHI* were present[51,111]. To test whether FlgN docking at FliJ affects flagellar subunit export and swimming motility, I constructed a strain lacking the ATPase complex (which includes deletion of the *fliJ* gene) in combination with the ATPase bypass mutations (*flhB*P$_{28}$T-*ΔflgM).* This strain (*flhB*P$_{28}$T-*ΔfliHIJ-ΔflgM)* was transformed with pTrc99a encoding wild type FlgN or its variants (FlgN Y$_{122}$A, FlgNΔ112-121, FlgNΔ90-100, FlgNΔ120-140). Cell motility and export were assayed as previously described (sections 2.15 and 2.16). Whole cell lysates and supernatants were immunoblotted for the presence of FliC, FlgK and FlgL subunits, as well as for FlgN as an expression and lysis control. Cells expressing FlgN Y$_{122}$A, FlgNΔ112-121 or FlgNΔ120-140 produced motility halos with equivalent diameter (Figure 6.6). However, unlike in the Δ*fliHI* strain, when wild type FlgN was overexpressed in the Δ*fliHIJ* strain,

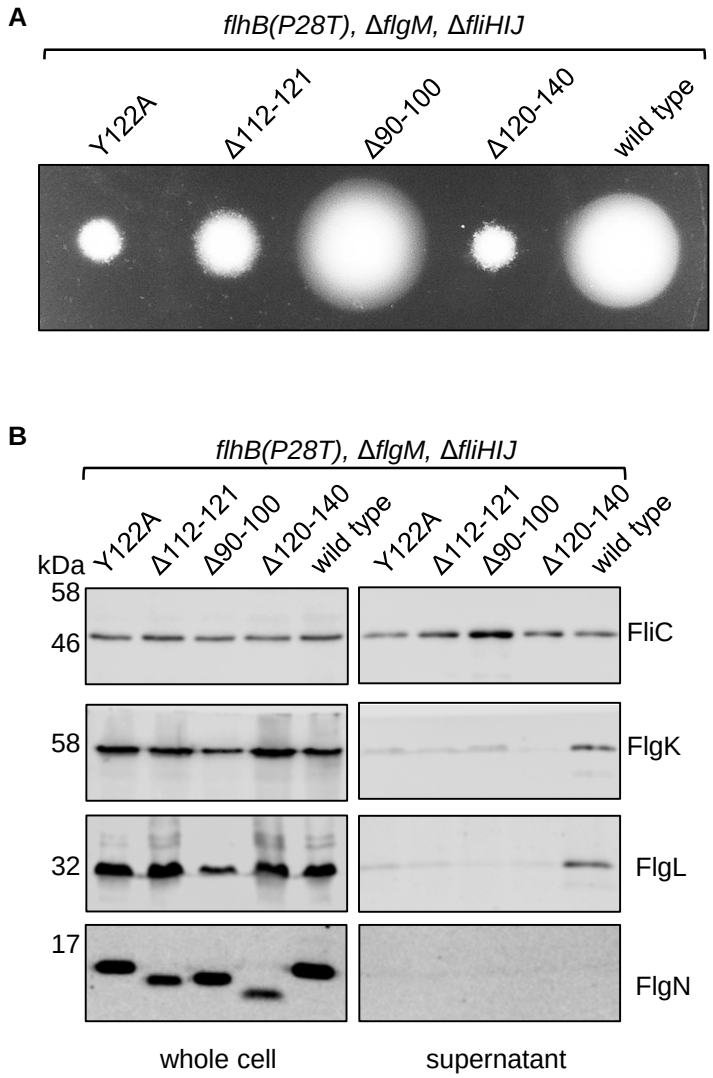

Figure 6.6. Dominant negative overexpression phenotypes of wild type FlgN and its variants in a *Salmonella* strain deleted for genes encoding FlgM, FliH, FliI and FliJ and containing the ATPase deletion suppressor mutation *flhB*P28T

(**A**) Swimming motility assays of a *Salmonella flhB*P28T*, ΔflgM, ΔfliHIJ* strain transformed with recombinant pTrc99a plasmids carrying wild type FlgN or its variants (Y122A, Δ112-121, Δ90-100, Δ120-140). Cells were grown to A600 1.0 in LB containing 100 µg/ml ampicillin and 100 µM IPTG, inoculated into 0.3% soft-tryptone agar containing 100 µg/ml ampicillin and 100 µM IPTG and incubated for 3-6 hours at 37°C.

(**B**) Secretion analysis of whole cell (whole cell) and culture supernatants (supernatant) fractions from the above cells. Cells were grown to mid-log phase in LB containing 100 µg/ml ampicillin and 100 µM IPTG. Proteins were separated by SDS-PAGE and immunoblotted with anti-FliC, anti-FlgK, anti-FlgL and anti-FlgN sera.

the motility halo was of greater diameter than for cells overexpressing FlgN Y_{122}A, FlgNΔ112-121 and FlgNΔ120-140 variants (Figure 6.6). This indicates that overexpressing wild type FlgN also interferes with FliJ activity, possibly by preventing a productive interaction between FliJ and FlhA. In the Δ*fliHIJ* strain, the three FlgN variants (FlgN Y_{122}A, FlgNΔ112-121 and FlgNΔ120-140) that display the greatest dominant negative effects cannot bind FlhAc. Furthermore, in this strain no other components of the export machinery are available for these FlgN variants to bind. This indicates that the dominant negative overexpression phenotypes caused by these FlgN variants in are due to the sequestration of cognate subunits FlgK and FlgL by the FlgN variants, preventing their export and therefore attenuating motility (Figure 6.6).

6.8 Discussion

Over the past two decades, significant progress has been made in understanding the interactions between flagellar structural subunits, their export chaperones and components of the flagellar export machinery. However, our knowledge of the sequence of binding events of chaperones and chaperoned subunits with the export machinery is incomplete. Furthermore, the molecular mechanisms by which the export machinery components regulate and promote flagellar protein translocation across the inner membrane are not fully understood. I screened a suite of chaperone variants that are defective in binding one or more components of the export machinery or cognate subunits. Three of these chaperone variants that are defective in binding FlhAc but able to bind FliJ *in vitro*, failed to interact with FliJ *in vivo*. Two FlgN variants FlgN Y_{122}A and FlgNΔ112-121 displayed 50% reduced binding to FliJ *in vivo* than *in vitro*. A third FlgN variant FlgNΔ120-140 that also is unable to bind FlhA but also stalls at the FliI component of the ATPase displayed 80% lower binding to FliJ *in vivo* than *in vitro*. The data in this chapter support the view that chaperones interact sequentially with components of the export machinery. Specifically, the inability of chaperone variants to bind the FlhA export component seems also to prevent these chaperone variants from reaching the FliJ component of the ATPase complex *in vivo*, even though these

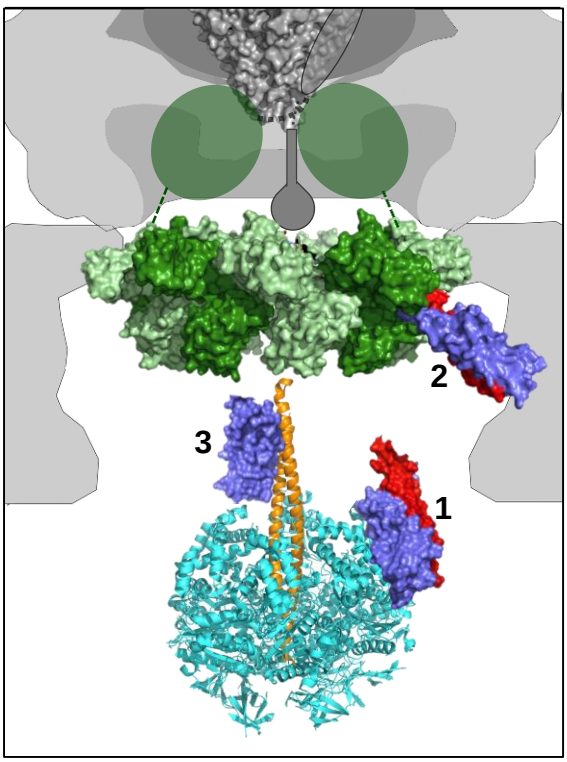

Figure 6.7. Proposed sequential steps in the chaperone-mediated subunit export cycle
Chaperone-subunit complexes (chaperone, blue; subunit, red) initially dock at the FliI (cyan) component of the ATPase complex (1). ATP hydrolysis by FliI releases the docked chaperone-subunit complex, which then binds the cytoplasmic domain of FlhA (green; 2). Subunits are then unfolded, released from cognate chaperone and translocated into the export channel. Unladen chaperones are free to bind FliJ (orange) before being captured by newly synthesized subunits to repeat the export cycle (3).

chaperone variants can bind FliJ *in vitro*. This suggests that *in vivo* FlgN interacts with FliJ only after it has bound FlhA (Figure 6.7).

Various roles have been assigned to FliJ. FliJ was initially thought to be an export chaperone because of its small size and because early publications predicted it to have an extended alpha helical structure[293]. However this was later found not to be the case, instead, empty chaperones for the minor subunit specific chaperones (FliT and FlgN) were found to interact directly with FliJ, whereas subunits or chaperoned-subunits did not[226,225]. Later, Evans et al. (2006) proposed that FliJ recruits empty chaperones to the export machinery and transfers them to subunits[226]. FliJ shows strong structural similarity to the γ-subunit of the F_1-ATPase and has been proposed to rotate within the FliI hexameric ring[106,261,108]. The close proximity between FliJ and FlhAc and the weak interactions that occur between FliJ and FlhA mean it is possible to envisage a mechanism whereby rotation of FliJ allows it to access all nine binding sites of the nonameric ring of FlhA[294,256,108]. Rotation of FliJ may allow it to sequentially remove empty chaperones from FlhA, freeing FlhA for new chaperone-subunit complexes to dock.

The reduced motility and export phenotypes of all of the chaperone variants tested (FlgN Y_{122}A, FlgNΔ112-121, FlgNΔ90-100, FlgNΔ120-140) highlight how essential the interactions of chaperone-subunit complexes with the export machinery are for promoting efficient subunit export. All chaperone variants failed to restore cognate subunit export in a Δ*flgN* strain, whilst the amount of unpolymerized FliC released into culture supernatants increased, corresponding to a delay in hook-filament junction assembly and therefore the inability of FliC to polymerise.

To test whether any of the chaperone variants displayed a dominant negative overexpression phenotype, FlgN variants were overexpressed in wild type *Salmonella*. FlgNΔ120-140 has previously been shown to display a dominant negative phenotype as a result of stalling at the FliI component of the ATPase

complex[176]. This stalling prevents both cognate and non-cognate subunits from being exported by either blocking subunits from engaging with the export machinery or possibly by sequestering FliI away from the export machinery. Cells expressing FlgNΔ120-140 did display a stronger dominant negative overexpression phenotype than wild type FlgN, similarly, cells overexpressing FlgN Y_{122}A displayed the same phenotype as FlgNΔ120-140, indicating that FlgN Y_{122}A may also stall at FliI. Cells expressing FlgNΔ112-121 displayed a less dominant negative overexpression phenotype than wild type FlgN. However, like FlgN Y_{122}A and FlgNΔ120-140, FlgNΔ112-121 is unable to interact with FlhA. This suggests that FlgNΔ112-121 has lost the ability to bind an additional binding partner. FlgNΔ112-121 bound all other binding partners tested *in vitro* at wild type levels, suggesting that FlgNΔ112-121 may have lost its ability to bind and stall at FliI.

I used a range of methods to try and identify a direct interaction between chaperone-subunit complexes and FliI. A previous study showed that subunits and chaperones accumulate in the membrane of a strain that produces a catalytically inactive variant of FliI[221]. I constructed two strains that encoded FliI with a C-terminal His tag with either wild type ATPase activity or with a mutation in the active site (E_{211}A) that results in stalling of chaperone-subunit complexes at FliI[221,223]. I expressed the FlgN variants in this strain and pulled down FliI with cobalt HisPur resin, however, the assay didn't produce consistent results. Similarly, expressing FliI *in vitro* and performing affinity co-purifications failed to consistently detect interactions between chaperone-subunit complexes and FliI. The addition of non-hydrolyzable ATP (Adenosine 5′-(β,γ-imido)triphosphate) to trap FliI in a conformation that increases the affinity for chaperone-subunit complexes also failed to produce consistent results. The FliI interaction with chaperones is thought to be very weak and transient, possibly explaining why these assays failed to reliably detect chaperone interactions with FliI[176]. Therefore, I couldn't directly detect chaperone-subunit interactions with FliI but instead used genetics to infer whether chaperone variants display similar phenotypes to the FliI stalling chaperone variant, FlgNΔ120-140.

The dominant negative overexpression phenotype of FlgN Y_{122}A and FlgNΔ120-140 was lost when expressed in a motile *Salmonella* strain deleted for *fliH* and *fliI*. In fact, cells expressing FlgNΔ112-121 displayed export and motility phenotypes comparable to that of cells expressing FlgN Y_{122}A or FlgNΔ120-140, suggesting that FlgNΔ112-121 has lost its ability to bind and stall at FliI. I also assessed whether wild type FlgN and its variants also display similar dominant negative overexpression phenotypes in a strain deleted for the whole ATPase complex (Δ*fliHIJ*). Swimming motility and subunit export by cells overexpressing wild type FlgN was greater relative to cells producing FlgN Y_{122}A, FlgNΔ112-121 or FlgNΔ120-140 suggesting that wild type FlgN interferes with FliJ activity. The role of chaperone binding to FliJ is explored further in Chapter 7.

The *flhB*P_{28}T-*ΔfliHIJ-ΔflgM* strain overexpressing three of the FlgN variants (FlgN Y_{122}A, FlgNΔ112-121 or FlgNΔ120-140) displayed a greater dominant negative overexpression phenotype than cells expressing wild type FlgN or FlgNΔ90-100. These three FlgN variants can bind cognate subunit but are defective in binding FlhAc and, in this strain, the genes encoding their other binding partners are deleted. Therefore, the dominant negative overexpression phenotype is likely caused by the sequestering of cognate subunits in the cytoplasm in chaperone complexes that cannot dock at the export machinery.

The data indicate that FlgNΔ112-121 is unable to interact with FliI. A previous study has shown that FlgNΔ120-140 stalls at FliI, therefore residues 120-140 are not directly involved in the interaction with FliI. Residues 80-100 of FlgN are required for subunit binding therefore this region is unlikely directly interacting with FliI as subunits will be occluding this region of FlgN. Furthermore, residues 1-65 of FlgN can be replaced with GST, restoring subunit export, indicating that the N-terminal region of FlgN is not required for FliI binding. This leaves residues 66-80 and residues 100-120 which may be required for chaperone-subunit docking at FliI.

How chaperone-subunit complexes are released from FliI is not known. As mentioned previously, the ATP-bound state increases the affinity of FliI for chaperone-subunit complexes indicating that conformational changes induced by ATP hydrolysis may release chaperone-subunit complexes from FliI allowing subsequent chaperone-subunit binding to the cytoplasmic domain of FlhA[221]. Sequential interactions of cargo at the export machinery of secretion systems is often driven by increasing binding affinities as cargo moves from one binding partner to the next[103,295]. This certainly is the case with chaperone-subunit transfer from FliI to FlhAc. The FlgN/FlgK complex and FliT/FliD complex bind to FlhAc with dissociation constants of 37 and 43 nM, respectively[115]. Whilst the FliS/FliC complex binds FlhAc with a 14-fold lower affinity with a dissociation constant of 500 nM[115]. The reason why the affinity for the FlgN and FliT subunit-chaperone complexes is 14-fold higher is unclear, although it has been proposed that this may promote export of the minor subunits over the FliC to ensure the filament cap and hook-filament junction assembles rapidly before filament assembly can begin and may also serve to establish a strict assembly order[115]. These chaperone-FlhAc affinities are thought to be greater than for the affinity of chaperone-subunit complexes and FliI, therefore handover of chaperone-subunit complexes at this stage of the export cycle appears to occur along a path of increasing affinity for the export machinery.

Once chaperone-subunit complexes have docked at FlhAc, subunits are thought to be unfolded and released from their cognate chaperone before being translocated into the export channel[8,9]. The FliS and FliT chaperones are unable to bind FlhAc unless they are bound to cognate subunit, therefore, once subunits have been released from these chaperones, they presumably dissociate from FlhAc[177]. However, the FlgN chaperone can bind FlhAc independently of its cognate subunits, although the affinity of FlgN for FlhAc reduces by about 3-fold to 100 nM. Therefore, once subunits have been released from FlgN, FlgN could remain bound to FlhAc, and therefore prevent other chaperone-subunit complexes from docking at FlhAc. How, FlgN is released from FlhAc is unclear.

FliJ could aide capture of FlgN from FlhAc and therefore free the binding sites on FlhAc for new chaperone-subunit complexes to dock.

The data in this chapter support the view that chaperone-subunit complexes interact sequentially with components of the export machinery. I propose that chaperone-subunit complexes initially dock at the FliI component of the ATPase. Chaperone-subunit complexes then dock at FlhAc where subunits are unfolded and released from their cognate chaperone. These free chaperones then bind FliJ which frees the binding site on FlhAc for the subsequent chaperone-subunit complexes to dock at FlhAc. Chaperones bound to FliJ are then captured by free subunits, which could subsequently dock at FliI, repeating the cycle.

Chapter 7

Chaperone-mediated coupling of subunit availability to activation of proton motive force-driven flagellar type III secretion

7.1 Introduction

In the previous chapter I provided evidence supporting the view that the FlgN chaperone interacts sequentially with components of the export machinery. Specifically, FlgN interacts with FliJ after it has interacted with FlhAc. In this chapter, I present work that investigates the importance of the chaperone-FliJ interaction for flagella biogenesis. The cytoplasmic chaperones FlgN, FliT and FliS bind the C-terminal domains of their cognate structural subunits (FlgK and FlgL for FlgN, FliD for FliT, and FliC for FliS) and deliver them to the specialized type III export machinery at the base of each flagellum[173,172,183]. The export machinery then unfolds subunits and translocates them across the inner membrane into a narrow channel that spans the length of the growing flagellum[9,8]. Subunit export is powered by the PMF and by a cytoplasmic ATPase complex comprising FliH, FliI and FliJ, which are evolutionarily-related to components of the F_1-ATPase[51,52,121,261].

As well as binding their cognate subunit(s), chaperones also interact with other components in the cell[176,177,115,226,290,296]. As discussed in Chapter 6, FlgN can interact with FliI, FliJ and FlhAc as well as its two cognate subunits FlgK and FlgL. The chaperone for the filament cap (FliT) also interacts with the FlhC component of the FlhDC master regulator and promotes its degradation, therefore regulating gene expression[166,296]. Furthermore, the FliS chaperone interacts with the anti-sigma factor FlgM and therefore modulates late flagella gene expression[167].

In chapter 4, I provided evidence indicating that the PMF energises opening of the export gate and that a signal in the extreme N-terminus of early subunits can trigger opening of the export gate when early subunits are docked at FlhBc. This is therefore one way in which the export machinery can regulate use of the PMF

such that opening of the export gate only occurs when subunits are docked at the machinery and ready for transit through the gate. How activation of the export machinery by the flagellar ATPase is regulated is unknown. The FliJ component of the flagellar ATPase interacts with FlhA, which converts the export machinery into a highly efficient ΔΨ driven export machine[224,272]. How this FliJ-FlhA interaction is regulated to prevent constitutive activation of the export machinery is unknown. It is known that two of the flagellar export chaperones (FlgN and FliT) bind FliJ and are then later captured from FliJ by their cognate subunits[226]. It is feasible that chaperone binding to FliJ could regulate FliJ activation of FlhA. To test this, I screened for chaperone variants that are specifically defective for binding to FliJ and used these variants to assess the importance of the chaperone-FliJ interaction for subunit export, and whether these interactions regulate the FliJ-FlhA interaction required for ΔΨ driven activation of the export machinery.

7.2 Screening for FlgN chaperone variants defective in binding FliJ

I sought to identify a FlgN variant that is specifically defective in FliJ binding but retains the ability to bind cognate subunits and other components of the export machinery. Deletion of residues 80-100 of FlgN results in the loss of binding to both FliJ and to cognate subunit. No FlgN variants have been identified that specifically disrupt the FlgN-FliJ interaction but retain FlgN-subunit interactions. A previous screen identified a chaperone variant, FlgNΔ76-78, that had specifically lost the ability to bind FliJ but retained the ability to bind cognate subunits[291]. FlgN variants containing internal three-residue scanning deletions were generated between residues 70 and 102 and their ability to bind FliJ and cognate subunit was assessed by affinity chromatography pull down assays. It is important to note that there are a few limitations to affinity chromatography pull down assays as discussed in section 6.2. To confirm the results from the previous screen, I constructed the FlgN variants containing the three-residue scanning deletions by overlap extension PCR and inserted them into a pACT7 expression vector. The pACT7 plasmids encoding wild type FlgN or its variants were transformed into *E.coli* C41 and overexpressed by induction with 0.5 mM

IPTG. Cells were harvested, resuspended in lysis buffer A (Table A1.1) and lysed. The lysed cells were clarified by centrifugation and were added to glutathione resin that contained pre-bound GST-FliJ, GST-FlgK or GST alone, before washing extensively. Proteins were boiled off the resin, separated by SDS-PAGE and stained with InstantBlue. The data showed that three-residue deletions between amino acids 76 and 99 reduced FlgN binding to FliJ, indicating an extensive region of FlgN is required for FliJ binding (Figure 7.1). The FlgNΔ76-78 variant was defective in FliJ binding but retained the ability to bind its cognate subunit, FlgK (Figure 7.1). Interestingly, tryptophan-78 which is contained within amino acids 76-78 is well conserved in FlgN. To test whether Trp-78 is required for FlgN binding to FliJ, I generated a FlgN W_{78}A variant by overlap extension PCR. To assess whether FlgN W_{78}A and FlgNΔ76-78 are specifically unable to bind FliJ but can still bind their other binding partners, I performed an affinity chromatography pull down assay with GST-tagged components of the export machinery (GST-FliJ and GST-FlhAc) and GST-tagged subunits (GST-FlgK and GST-FlgL). Both FlgN W_{78}A and FlgNΔ76-78 were defective in binding FliJ whereas interactions with other components of the export machinery were retained (Figure 7.2). The FlgNΔ90-100 variant was used as a subunit and FliJ binding control and wild type FlgN was used as a positive control (Figure 7.2).

7.3 Disruption of the FlgN-FliJ interaction attenuates motility and subunit export

To assess the importance of the FlgN-FliJ interaction for subunit export and cell motility, I constructed strains to express chromosomally-encoded FlgN variants (FlgN W_{78}A, FlgNΔ76-78 and FlgNΔ90-100). Wild type *Salmonella* and a Δ*flgN* strain were used as controls. Export and swimming motility assays were performed as described in section 2.15 and 2.16. The strains encoding FlgN W_{78}A and FlgNΔ76-78 had a slight swimming motility defect compared to wild type (Figure 7.3), indicating that the loss of the FlgN-FliJ interaction might reduce the efficiency of cognate subunit export, as previously postulated[226]. Whole cell lysates and supernatants were immunoblotted for the presence representative

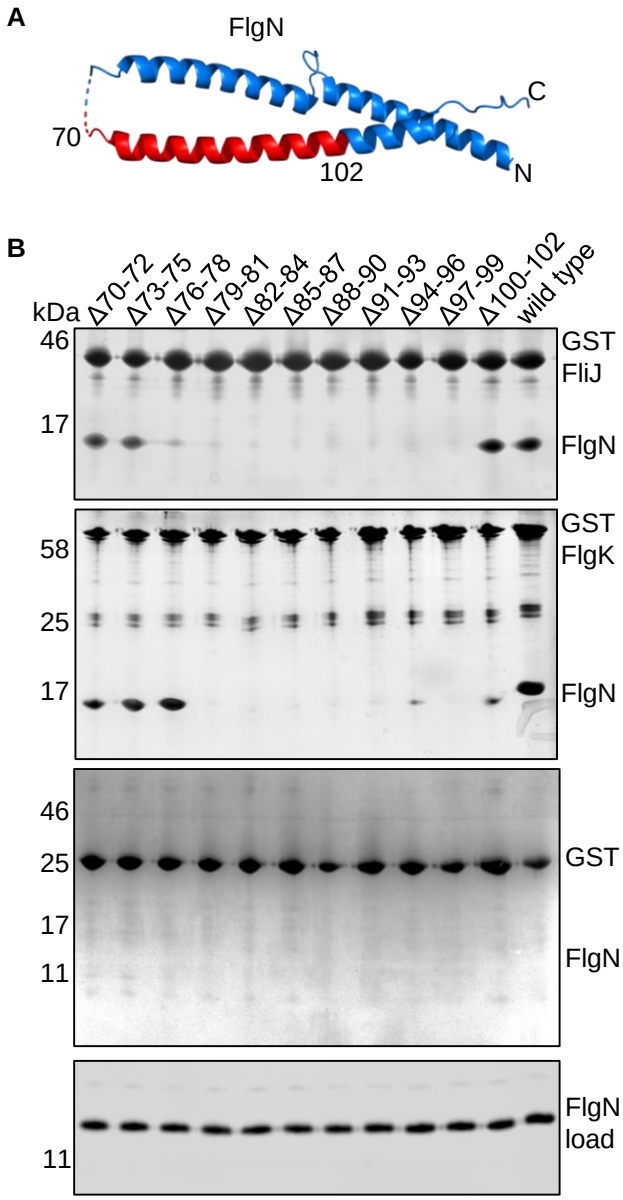

Figure 7.1. Screening for FlgN variants defective in binding FliJ
(**A**) Atomic resolution structure of the 140-residue *Salmonella* FlgN (PDB:5b3d) indicating the region of FlgN (red) that was screened by three-residue deletions for FlgN variants defective in FliJ binding.
(**B**) Affinity chromatography of cell lysates of *E.coli* C41 expressing GST-tagged FliJ, GST-tagged FlgK (subunit) and GST alone were incubated with glutathione sepharose resin and washed. Cell lysates containing wild type wild type FlgN (wild type) or its variants (as indicated) were incubated with resin bound GST-FliJ, GST-FlgK or GST alone and washed extensively. Proteins were eluted by boiling the resin in SDS-loading buffer. Proteins were separated by SDS-PAGE and visualized by staining with Coomassie Brilliant Blue. Levels of FlgN and its variants in the input cell lysates (FlgN load, bottom) were assessed by immunoblotting with anti-FlgN polyclonal antisera. Apparent molecular weights (MW) are in kilodaltons (kDa).

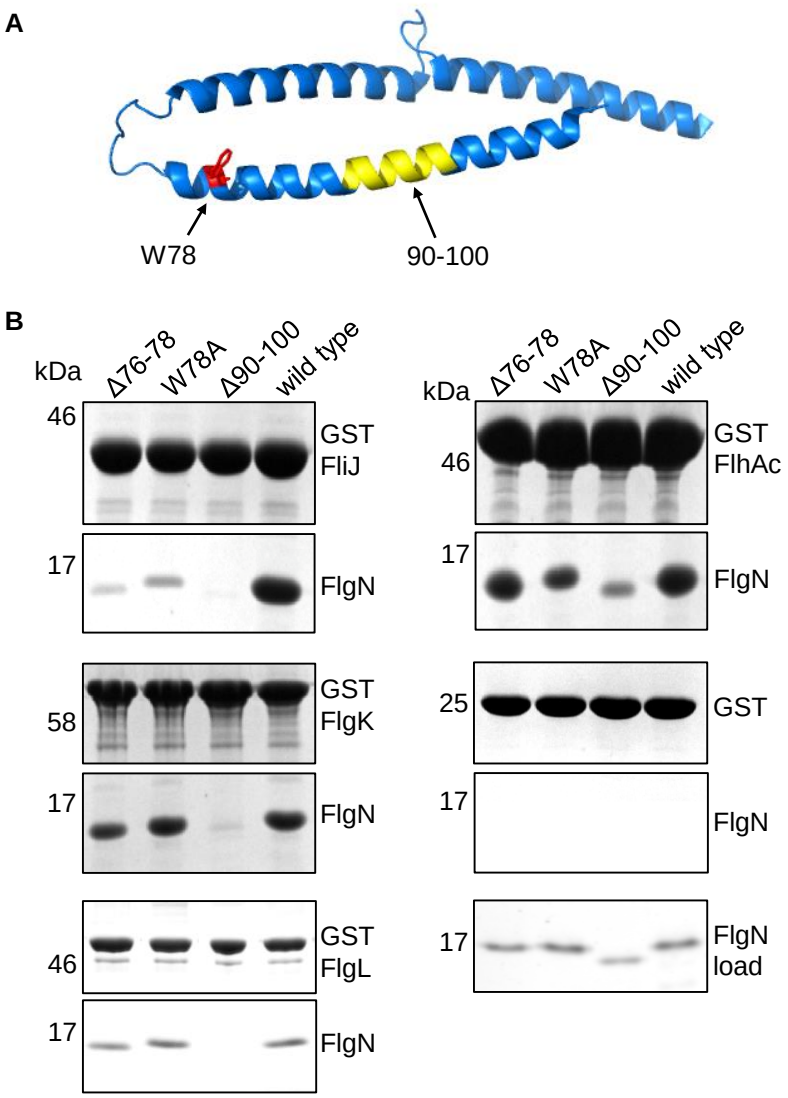

Figure 7.2. *In vitro* interactions of wild type FlgN and its variants with components of the export machinery

(**A**) Atomic resolution structure of the 140-residue *Salmonella* FlgN (PDB:5b3d) indicating the subunit/FliJ binding region (residues 90-100; yellow), and the position of tryptophan-78 (W78, red).

(**B**) Affinity chromatography of cell lysates of *E.coli* C41 expressing GST-tagged flagellar export components (GST-FliJ, GST-$FlhA_C$), cognate subunits (GST-FlgK, GST-FlgL) or GST alone were incubated with glutathione sepharose resin and washed. Cell lysates containing full-length wild type FlgN or its variants (Δ76-78, W78A, Δ90-100) were incubated with the resin-bound GST-tagged proteins, washed extensively and proteins were eluted by boiling the resin in SDS-loading buffer. Proteins were separated by SDS-PAGE and visualized by staining with Coomassie Brilliant Blue. Levels of FlgN and its variants in the input cell lysates (FlgN load, bottom right hand panel) were assessed by immunoblotting with anti-FlgN polyclonal antisera. Apparent molecular weights are in kilodaltons (kDa).

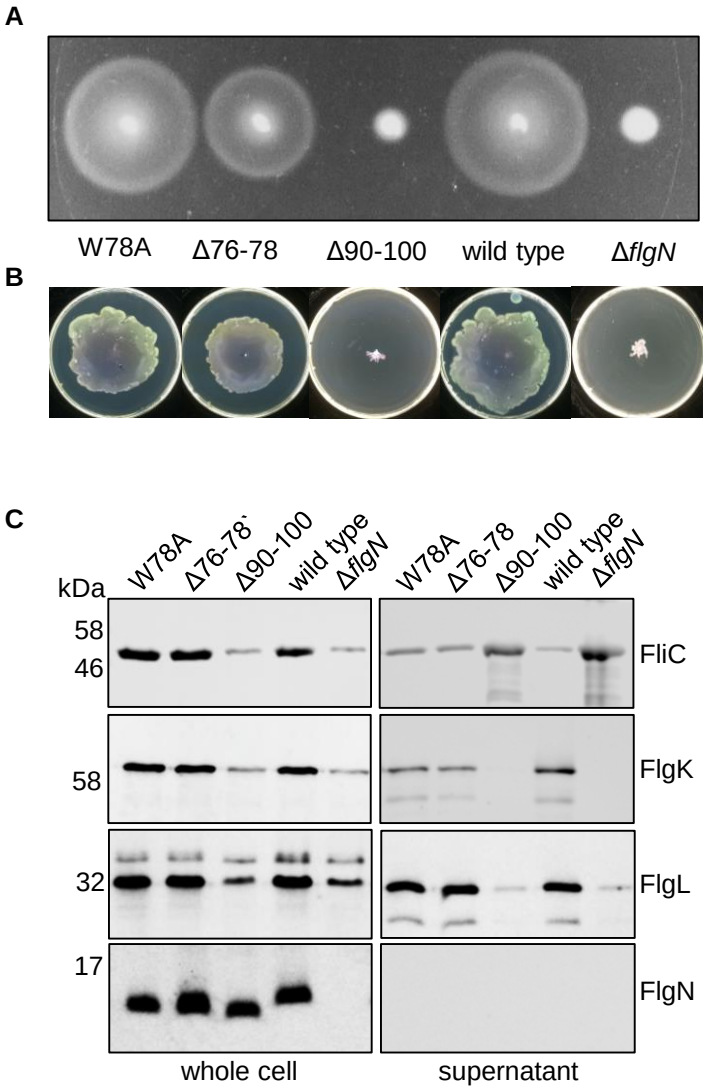

Figure 7.3. FlgN binding to FliJ is required for efficient swarming but not swimming motility

(**A**) Swimming motility of *Salmonella* strains producing chromosomally-encoded FliT variants (FlgN W78A, FlgNΔ76-78, FlgNΔ90-100), the *Salmonella* SJW1103 (WT) and the *Salmonella flgN* null strain (Δ*flgN*). Motility was assessed in 0.3% soft tryptone agar and incubated at 37°C for 4-6 hours.

(**B**) Swarming motility of the same strains was assessed by centrally inoculating 1 µl of stationary phase broth culture on 0.6% agar-tryptone plates supplemented with 0.5% glucose and incubating plates at 30°C for 12-16 hours.

(**C**) Secretion analysis of culture supernatant (supernatant) and whole cell (whole cell) fractions of the above strains by immunoblotting with anti-FliC, anti-FlgK, anti-FlgL and anti-FlgN sera.

cognate (FlgK) and non-cognate (FliC) subunits, and for FlgN as an expression and lysis control. Consistent with the motility phenotypes, the level of FlgK exported into culture supernatants by the strains encoding FlgN $W_{78}A$ and FlgNΔ76-78 was reduced (Figure 7.3).

Swarming motility assays were also performed for the above strains (Figure 7.3). Swarming motility tends to magnify any swimming motility defect due to the need for upregulation of flagellar gene regulation and the need for more efficient subunit export by swarmer cells[1]. Strains encoding FlgN $W_{78}A$ and FlgNΔ76-78 showed a marginal reduction in swarming motility compared to wild type (Figure 7.3). Although the reduction in swarming motility by the strains encoding FlgN $W_{78}A$ and FlgNΔ76-78 was not larger than the reduction observed in the swimming motility assay, there was still a reduction in swarming motility compared to wild type, supporting the view that the FlgN-FliJ interaction increases the efficiency of export of subunits chaperoned by FlgN.

7.4 Screening for FliT chaperone variants defective in binding FliJ

I wanted to identify a FliT chaperone variant that like FlgNΔ76-78 and FlgN $W_{78}A$ can bind subunit but not FliJ. FliT, the chaperone for the filament cap subunit (FliD) interacts with four additional flagellar proteins involved in export or gene regulation[290,296,115,226]. Three of these - FliI (ATPase), FliJ (ATPase stalk) and FlhC (master transcriptional regulator subunit) - compete with each other and with FliD subunit for binding to the same binding site on FliT (amino acids 42-94 on the α3 helix)[249]. I sought to identify a FliT variant that could bind FliD and components of the export machinery but not FliJ. To identify a FliT variant that is defective in FliJ binding I initially targeted seven conserved residues within the FliJ binding site on the FliT α3 helix for site directed mutagenesis to alanine (Figure 7.4). Two of these FliT variants ($E_{75}A$ and $K_{79}A$) have been previously shown to reduce FliT binding to FliD, whilst the other FliT variants ($I_{68}A$, $L_{72}A$, $N_{74}A$, $L_{78}A$ and $L_{81}A$) displayed wild type levels of binding to FliD[180]. These point mutations were introduced into a FliT variant (FliT94) lacking the α4 helix that occludes the FliJ binding site on FliT[297]. Affinity chromatography pull-down

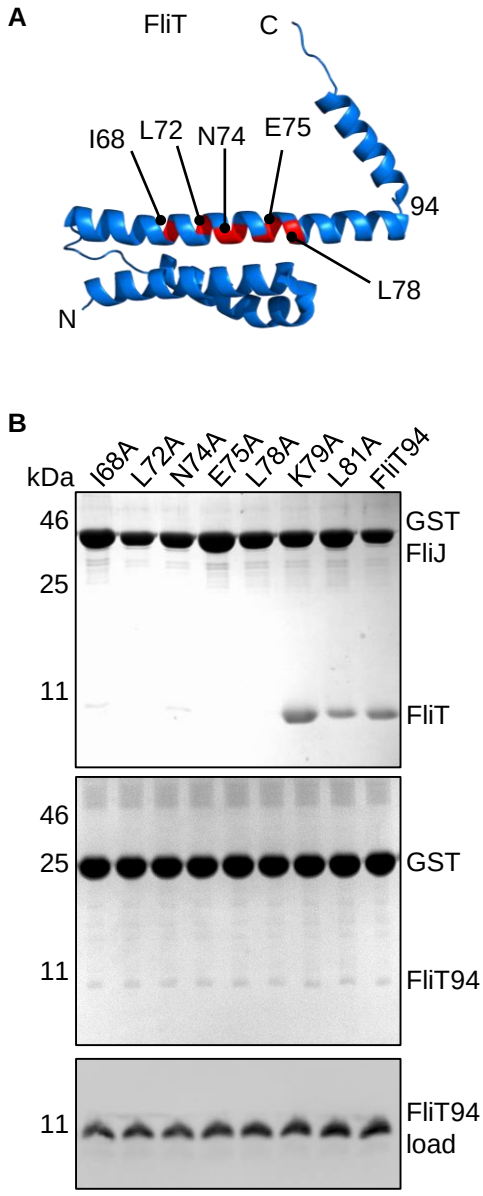

Figure 7.4. Screening for FliT variants defective in binding FliJ
(**A**) Atomic resolution structure of the 122-residue *Salmonella* FliT (PDB:3A7M) indicating the position of conserved residues (red) within the region essential for both FliJ and FliD binding.
(**B**) Affinity chromatography of cell lysates of *E.coli* C41 expressing GST-tagged FliJ and GST alone were incubated with glutathione sepharose resin and washed. Cell lysates containing wild type FliT94 (missing its C-terminal inhibitory helix) or its variants (as indicated) were incubated with resin bound GST-FliJ or GST alone, washed extensively and proteins eluted by boiling the resin in SDS-loading buffer. Proteins were separated by SDS-PAGE and visualized by staining with Coomassie Brilliant Blue. Levels of FliT94 and its variants in the input cell lysates (FliT load, bottom) were assessed by immunoblotting with anti-FliT polyclonal antisera. Apparent molecular weights are in kilodaltons (kDa).

assays showed that five of the seven FliT point mutant variants (I_{68}A, L_{72}A, N_{74}A, E_{75}A and L_{78}A) showed severely reduced binding to GST-FliJ (Figure 7.4). I chose to further investigate the FliT L_{72}A variant to assess whether it could interact with its other binding partners by affinity chromatography pull down assays using GST-tagged components of the export machinery (GST-FliJ, GST-FlhAc and GST-FliI) and GST-tagged subunit (GST-FliD). As a control, I also assessed the binding of subunits and components of the export components to the FliT Y_{106}A variant, previously shown to be critical for FlhA binding[177]. I found that although FliT L_{72}A is defective in binding FliJ it retained the ability to bind its other partners (Figure 7.5). The data indicate that binding of FliT to FliJ can be dissected from binding to other FliJ partners, allowing investigation of the role of the FliT-FliJ interaction in subunit export.

7.5 Disruption of the FliT-FliJ interaction attenuates motility and subunit export

To assess the importance of the FliT-FliJ interaction for subunit export and cell motility, I constructed strains to express chromosomally-encoded FliT variants (L_{72}A or Y_{106}A) and compared these to a *Salmonella fliT* null strain and wild type *Salmonella*. Export and swimming motility assays were performed as described in sections 2.15, 2.16 and 2.17. The FliT L_{72}A strain displayed wild type swimming motility, whereas FliT Y_{106}A and the *fliT* null strain showed a marginal reduction is swimming motility (Figure 7.6). However, the FliT L_{72}A had a significant swarming defect compared to wild type, whereas the FliT Y_{106}A strain had a partial swarming defect, whilst the *fliT* null strain swarmed similar to wild type, indicating that the FliT-FliJ interaction is required for hyper-flagellation.

Whole cell lysates and supernatants were immunoblotted for the presence of representative cognate (FliD) and non-cognate (FliC, FlgK, FlgL and FlgD) subunits, as well as for FlhA and FliT as expression and lysis controls. Levels of cognate subunit (FliD) export by the FliT L_{72}A strain were reduced compared to wild type, with a concomitant increase in unpolymerized FliC being released into the culture supernatant (Figure 7.6). Export of cognate subunit (FliD) was further

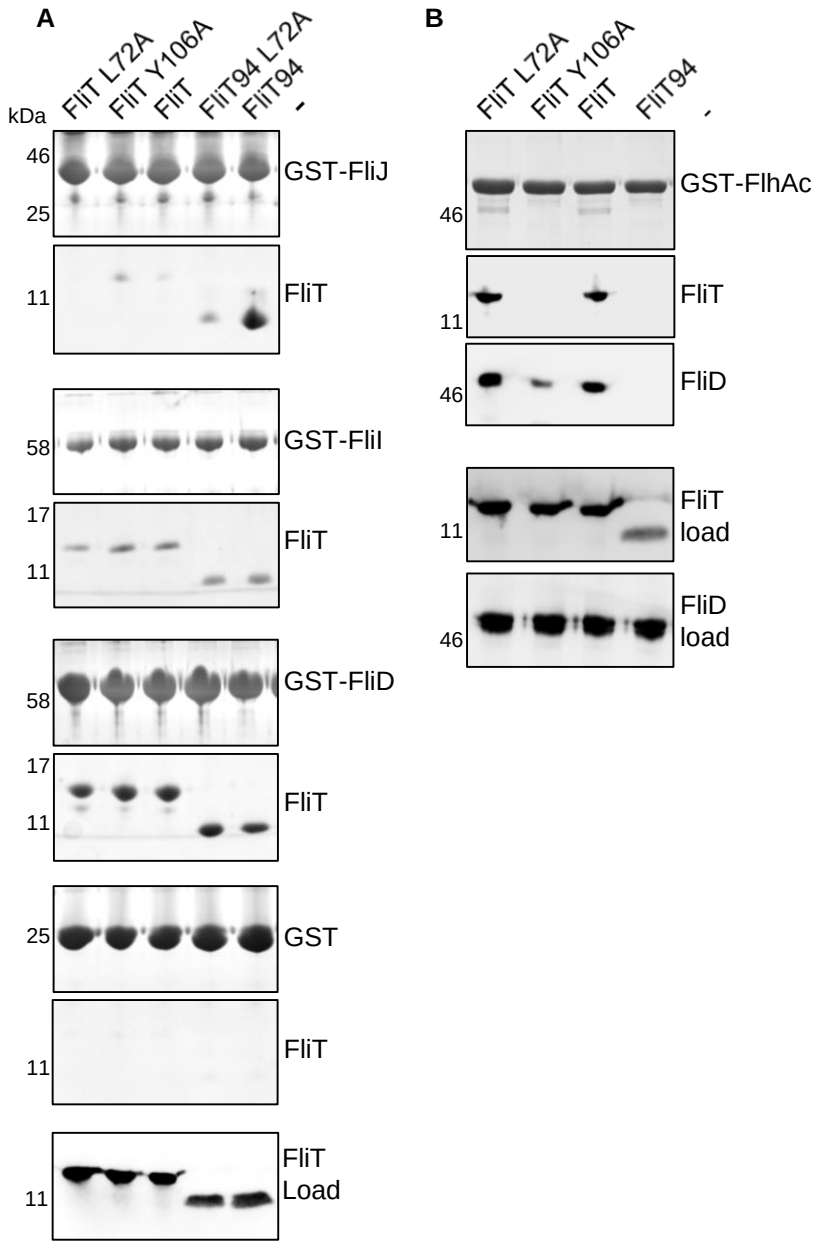

Figure 7.5. *In vitro* interactions of wild type FliT and its variants with components of the export machinery

(**A**) Affinity chromatography of cell lysates of *E.coli* C41 expressing GST-tagged flagellar export components (GST-FliJ, GST-FliI), cognate subunit (GST-FliD) or GST alone were incubated with glutathione-sepharose resin and washed. Cell lysates containing full length or residues 1-94 (FliT94) of wild type FliT or its variants (FliT L72A, FliT Y106A, FliT94 L72A) were incubated with resin bound GST-tagged proteins, washed extensively and proteins were eluted by boiling the resin in SDS-loading buffer. Proteins were separated by SDS-PAGE and stained with Coomassie Brilliant Blue. Levels of FliT and its variants in the input cell lysates (FliT load, bottom panel) were assessed by immunoblotting with anti-FliT polyclonal antisera. Apparent molecular weights (MW) are in kilodaltons (kDa).

(**B**) Affinity chromatography of *E.coli* C41 expressing GST-tagged $FlhA_C$ was performed as above but in the presence cell lysate containing FliD. Resin was washed extensively and proteins eluted by boiling off the resin. Proteins were separated by SDS-PAGE and stained with coomassie Brilliant Blue. Input cell levels (FliT Load and FliD load, bottom panels) were assessed by immunoblotting. Apparent molecular weights are in kilodaltons (kDa).

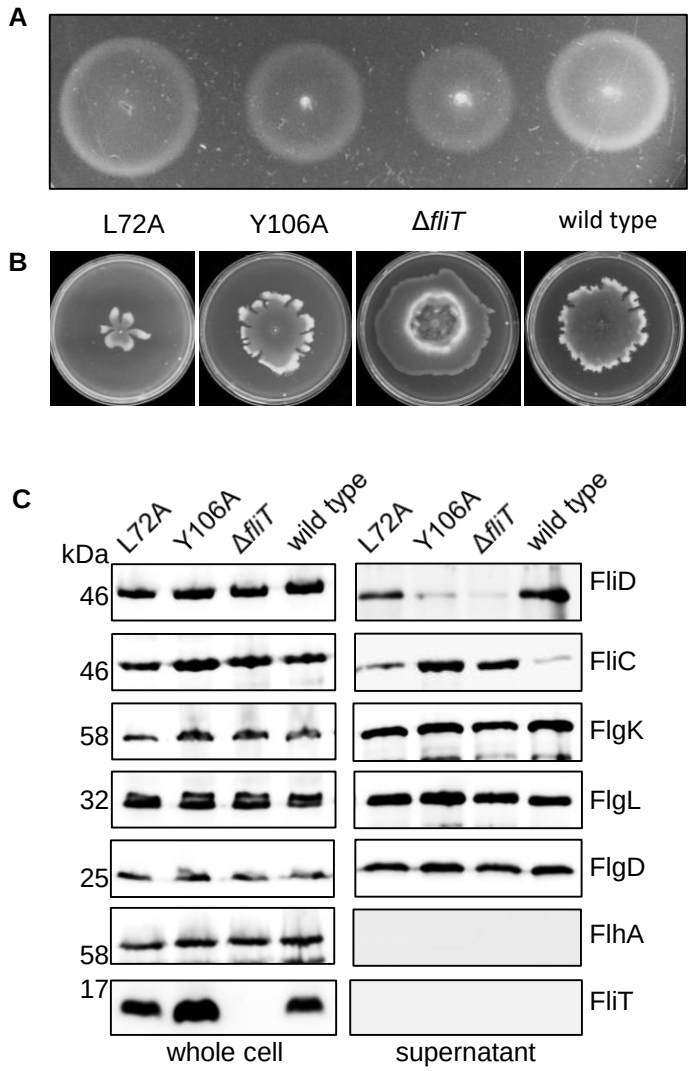

Figure 7.6. FliT binding to FliJ is required for efficient swarming but not swimming motility

(**A**) Swimming motility of *Salmonella* strains producing chromosomally-encoded FliT variants (FliT L72A and FliT Y106A), the *Salmonella* SJW1103 (wild type) and the *Salmonella fliT* null strain (Δ*fliT*). Motility was assessed in 0.3% soft tryptone agar and incubated at 37°C for 4-6 hours.

(**B**) Swarming motility of the same strains was assessed by centrally inoculating 1µl of stationary phase broth culture on 0.6% agar-tryptone plates supplemented with 0.5% glucose and incubating plates at 30°C for 12-16 hours.

(**C**) Secretion analysis of culture supernatant (supernatant) and whole cell (whole cell) fractions of the above strains by immunoblotting with anti-FliD, FliC, FlgK, FlgL, FlgD, FlhA or FliT sera.

attenuated in the FliT Y_{106}A and *fliT* null strains and levels of FliC in culture supernatants were increased relative to wild type *Salmonella* and the FliT L_{72}A strain, consistent with an increase in unpolymerized FliC being released into the culture supernatant. The cellular levels of FlhA, FliC, FlgK and FlgL were higher in the *fliT* null strain, consistent with FlhC not being targeted by FliT for degradation. Similarly, the cellular levels of FlhA, FliC, FlgK and FlgL were higher in the FliT Y_{106}A strain, likely due to the inability of FliT Y_{106}A to dock at FlhAc and therefore FliD subunits remain bound to FliT Y_{106}A, preventing it from binding FlhC for targeting it degradation. This may explain why the FliT Y_{106}A and *fliT* null strains only display a marginal decrease in swimming motility as flagellar gene expression is increased in these strains, compensating for the loss of FliT chaperone activity. Levels of FlhA, FliC, FlgK and FlgL in the strain encoding FliT L_{72}A were not greater than wild type, indicating that FliT L_{72}A retains the ability to bind and target FlhC for degradation. These data also indicate that the FliT-FliJ interaction increases the efficiency of FliD subunit export.

7.5 Chaperones FliT and FlgN compete with FlhA for binding to FliJ

I reasoned that when cellular levels of subunit are depleted, activation of the FlhA export gate by FliJ is unnecessary and potentially a waste of cellular energy reserves. I set out to experimentally test whether unladen chaperones docked at FliJ inactivate the FlhA export gate by blocking the FliJ-FlhA interaction. To do this, I developed an *in vitro* competition assay, in which I assessed $FlhA_C$ binding to cobalt bead-immobilized $(His)_6$-FliJ in the presence of wild type chaperone or chaperone variants defective in binding FliJ (Figure 7.7). As predicted, the chaperone variants defective for FliJ binding did not block the FliJ interaction with FlhAc (Figure 7.7). However, I found that in the presence of 'wild type' FliT94, the amount of $FlhA_C$ interacting with FliJ was significantly reduced (Figure 7.7). Similarly, FlgN competed with $FlhA_C$ for binding to FliJ (Figure 7.7) and the amount of FlhAc interacting with FliJ was reduced (Figure 7.7). These chaperones were engineered such that they could only dock at FliJ and were unable to bind $FlhA_C$ (FliT94 - no C-terminus, FlgN Y_{122}A – mutation of critical tyrosine). The data indicated that chaperones can, indeed, prevent interaction of

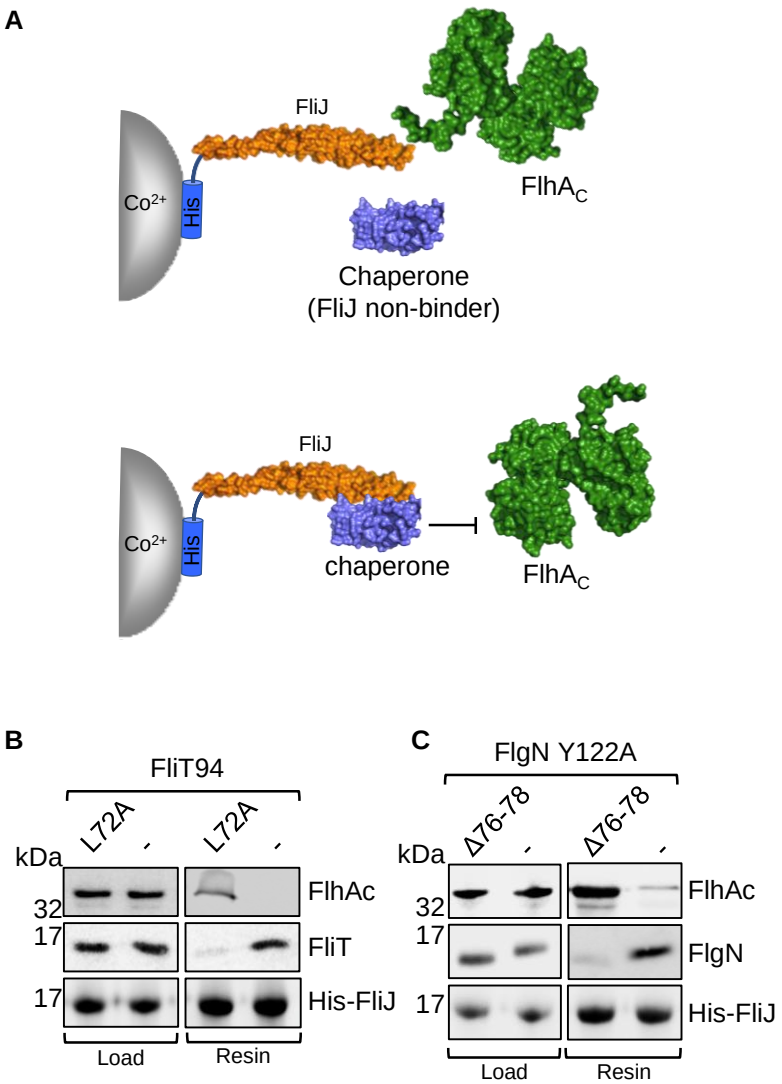

Figure 7.7. The chaperones FlgN and FliT compete with $FlhA_C$ for binding to FliJ

(**A**) Competition assay to assess $FlhA_C$ binding to cobalt bead immobilized $(His)_6$-FliJ in the presence of the flagellar chaperones FlgN or FliT.

(**B**) Cell lysates of *E.coli* C41 expressing wild type FliT94 or FliT94 L72A (defective in binding FliJ) and $FlhA_C$ (input, left panels, immunoblot) were incubated with cobalt bead immobilized $(His)_6$-FliJ, washed extensively and proteins were eluted by boiling the resin in SDS loading dye. Proteins were separated by SDS-PAGE and immunoblotted with anti-FlhA, FliT or FliJ sera. Apparent molecular weights are in kilodaltons (kDa).

(**C**) Competition assay between $FlhA_C$ and FlgN Y122A (defective in binding $FlhA_C$) or FlgN Y122A, Δ76-78 (defective in binding FliJ and FlhAc) for binding to FliJ. Proteins were eluted by boiling the resin, separated by SDS (15%)-PAGE and immunoblotted with anti-FlhA, FlgN or FliJ sera. Apparent molecular weights (MW) are in kilodaltons (kDa).

FliJ with FlhAc. I hypothesised that in the absence of cognate subunits *in vivo*, the unladen FliT and FlgN chaperones would disrupt the FliJ-FlhA interaction and block FliJ activation of the export gate, inhibiting export. Direct support for this view was obtained using an *in vivo* competition assay. In an 'early locked' strain (Δ*flgE*), in which the 'late' cognate subunits for FlgN are expressed at very low levels, overexpression of plasmid-encoded wild type FlgN resulted in a 4-fold reduction in FlgD subunit export compared to the FlgN variant defective in binding FliJ (Figure 7.8). An *in vivo* competition assay using FliT was not carried out because of the FliT-dependent downregulation of flagellar gene expression that would occur when FliT is expressed *in trans*. In the Δ*flgE* strain these FlgN variants (FlgN Y_{122}A and FlgN Δ76-78-Y_{122}A) will predominantly interact wth FliJ, as cognate subunits are present at very low levels and both FlgN variants were engineered to contain the Y_{122}A mutation – preventing chaperone interactions with FlhAc. The data indicates that in the absence of cognate subunits FlgN can prevent the FliJ-FlhA interaction *in vivo* and prevents FliJ-dependent activation of the export machinery.

7.6 Ribosome profiling reveals cellular levels of chaperones and subunits

The above data indicate that in the absence of cognate subunits, FliT and FlgN prevent the FliJ-dependent activation of the flagellar export machinery and therefore prevents flagellar export when subunit levels are low (Figure 7.8). However, one might expect an excess of subunits relative to their cognate chaperone in wild type cells during peak flagellar gene expression. To determine how much of each chaperone and subunit are produced during peak flagellar gene expression, I performed ribosome profiling as described in Chapter 5 (Figure 7.9).

Ribosome profiling was performed on wild type *Salmonella* grown to A_{600} 1.0 as described in section 2.21. The data indicate that all three flagellar chaperones (FlgN, FliT and FliS) are expressed at similar levels with the number of protected fragments corresponding to FlgN, FliT and FliS being 5616, 8127 and 6837, respectively (Figure 7.9). However, the number of ribosome protected fragments

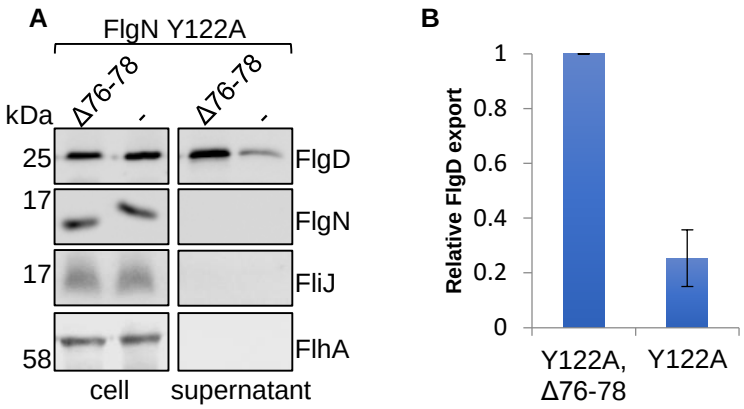

Figure 7.8. The chaperone FlgN competes with $FlhA_C$ for binding to FliJ *in vivo*

(**A**) FlgD export is attenuated by expression of the FlgN variant capable of binding FliJ (FlgN Y122A) compared to the FlgN variant defective in binding FliJ (FlgN Y122A, Δ76-78). A *Salmonella* Δ*flgE* strain transformed with pTrc99a carrying FlgN Y122A or FlgN Y122A, Δ76-78 were grown to mid-log phase in LB containing 100 μg/ml ampicillin and 50 μM IPTG. Whole cell (whole cell) and secreted proteins (supernatant) from late exponential-phase cultures were separated by SDS-PAGE and immunoblotted with anti-FlgD, anti-FlgN, anti-FliJ or anti-FlhA sera.

(**B**) Relative levels of FlgD in culture supernatants by cells expressing FlgN Y122A or FlgN Y122A, Δ76-78 were quantified using Image Studio Lite and plotted as a percentage of cells expressing FlgN Y122A, Δ76-78. Error bars show standard error of the mean from at least three biological replicates. * indicates a p-value < 0.05.

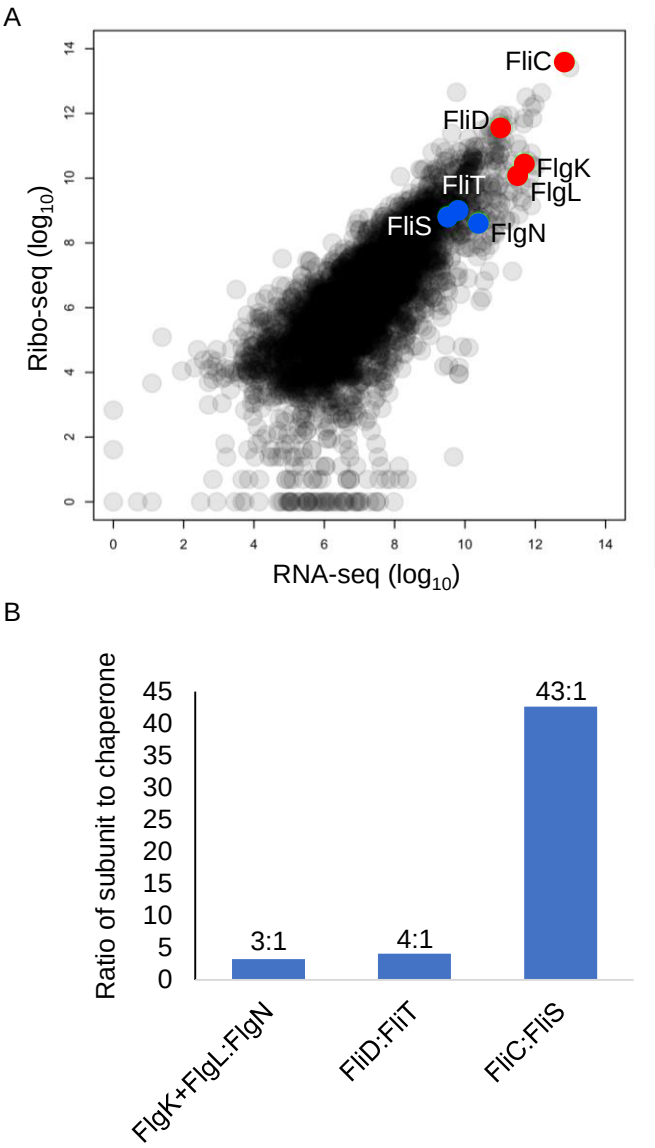

Figure 7.9. Ribosome profiling reveals the amount of chaperones and cognate subunits produced in *Salmonella*

(**A**) Comparison of the total mRNA transcripts (RNA-seq) and ribosome protected fragments (Ribo-seq) for each gene in *Salmonella*. Chaperones are colored blue, subunits are colored red.

(**B**) The ratio of counts of ribosome protected fragments to gene length corresponding to subunit(s) to counts of ribosome protected fragments of their cognate chaperone.

corresponding to their cognate subunits differs greatly (Figure 7.9). The number of cognate subunits produced per chaperone can tell us how likely it is that a particular chaperone is bound to cognate subunit at any one time. The ratio of FlgN chaperone to its cognate subunits (FlgK and FlgL) was ~3. Similarly, the ratio of FliT chaperone to its cognate subunit (FliD) was ~4. However, the ratio of FliS chaperone to its cognate subunit (FliC) was 43. This indicates that it is much less likely for free FliS chaperone to be present in the cell than for the FlgN and FliT chaperones. This may explain why FlgN and FliT are more suited to detect a drop in cellular subunit levels and bind FliJ because the ratio of chaperone to subunit for FlgN and FliT is >10 fold lower than for FliS. These data indicate that the minor subunit chaperones, FliT and FlgN, regulate FliJ-dependent activation of the export gate and couple cellular subunit levels to efficient protein export (Figure 7.10).

7.7 Discussion

The $(FliI)_6$-FliJ complex is structurally related to the $\alpha_3\beta_3$-γ complex of F-type ATPases[121,261,106]. Rotation of the central stalk of the F-type ATPase is driven by sequential ATP binding and hydrolysis at its three catalytic sites located at the interface between the alternating α and β subunits[268]. In the flagellar ATPase, conformational changes in FliI during the catalytic cycle are similarly thought to drive FliJ rotation, which is transmitted to the FlhA export gate protein *via* a specific interaction between FliJ and FlhA, allowing the export gate to efficiently use the potential energy from the electrical component of the proton motive force to drive protein export[111].

Upon assembly of the membrane export components and associated ATPase, the T3SS export apparatus is competent to export subunits[10]. The virulence T3SS is poised for export until an appropriate signal such as host cell contact activates export, whereby efficiency of export increases[7,298,299]. It is unclear how T3SS ATPase activity is regulated to prevent ATP hydrolysis when export of substrates is reduced. Constitutive ATP hydrolysis by FliI and a continual influx

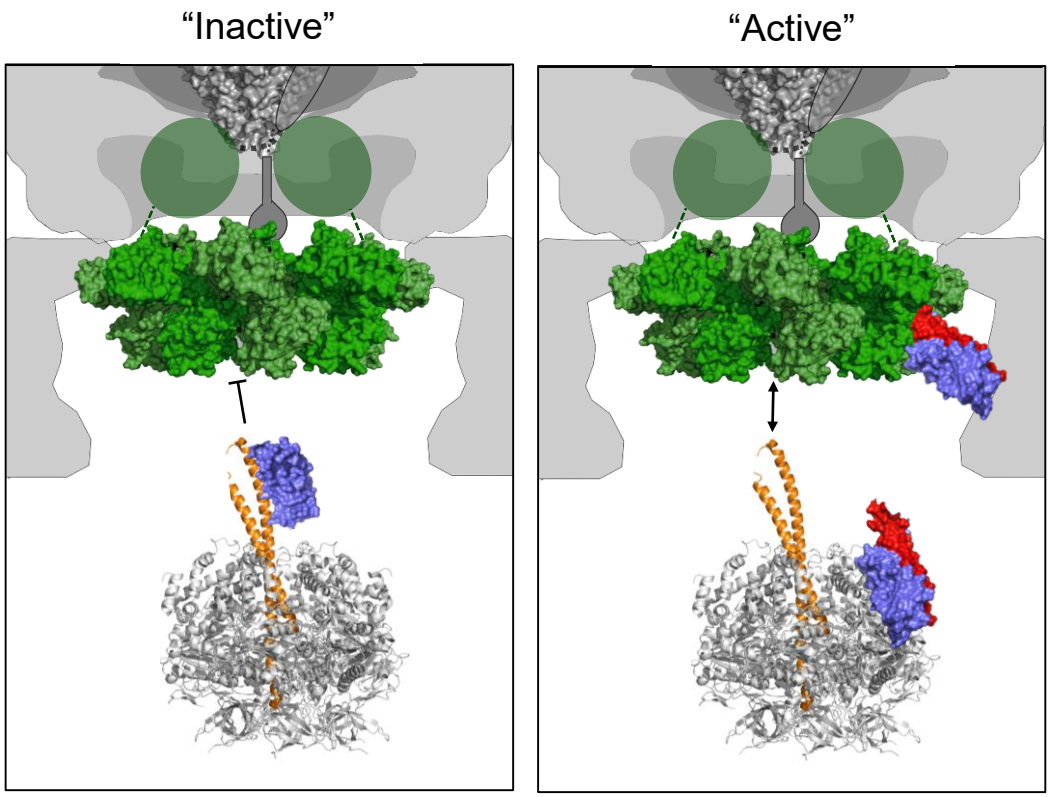

Figure 7.10. A proposed model for inactivation of the export machinery by depletion of cellular subunit levels
FlgN or FliT chaperone-subunit complexes initially dock at the FliI ATPase complex (grey) before docking at the cytoplasmic domain of FlhA ($FlhA_{C,}$ green). Subunits (red) are then thought to be released from their cognate chaperone (blue) at $FlhA_C$ and translocated into the export channel. Unladden chaperones bind newly synthesized subunits before repeating the export process (right). Under limiting subunit availability, increased levels of unladen FlgN and FliT are available to bind FliJ, blocking FliJ from binding to FlhA and therefore preventing the export machinery from being activated by FliJ (left).

of protons in the absence of subunit export would be wasteful. Although FliH reduces FliI ATPase activity to some extent *in vitro*, FliH is required to link FliI to the C-ring/sorting platform at the export apparatus and is needed to correctly promote the specific interaction between FliJ and FlhA[300,218,111].

Various mechanisms of regulation have been identified for the related F-type and V-type ATPases[268,269]. The mitochondrial ATPase IF1 inhibitor protein forms a complex with the F_1F_0 ATPase when the pH drops below pH 6.7, and is thought to prevent wasteful ATP hydrolysis under anaerobic conditions[301,270]. IF1 binds to a catalytic interface between the α and β subunits preventing ATP hydrolysis and simultaneously contacts the γ subunit (equivalent to FliJ)[301,270]. α-Proteobacteria produce an alternative inhibitor protein (ξ-subunit) that similarly prevents ATP hydrolysis. The crystal structure of inhibited F_1F_0-ATPase from *Paracoccus denitrificans* shows that the ξ-subunit binds to the α and β subunits in a similar mode to IF1[302,303]. The ξ-subunit functions as a ratchet and pawl, allowing clockwise rotation of the ATPase, preventing ATP hydrolysis without affecting ATP synthase activity[304]. Intriguingly, some bacteria and chloroplasts produce another ATPase inhibitor protein known as the epsilon (ε) subunit[305]. The ε subunit inhibits both the F_1 complex and the full F_1F_0 ATPase complex[306]. In the active state, the ε subunit adopts a contracted conformation and may play a role in ensuring efficient coupling between ATP hydrolysis and proton pumping[307]. A conformational change in the C-terminal domain of the ε subunit from a contracted hairpin-like structure to an extended conformation allows it to reach the ATPase hexamer, inhibiting ATPase activity and is thought to also prevent efficient coupling between the F_1 and F_0 components[307]. The ε subunit in some bacterial species directly binds ATP indicating it may function as an ATP sensor[308,309]. The epsilon subunit becomes extended in the presence of ADP, therefore when the ATP/ADP ratio is low, ATPase activity is thought to be inhibited[309]. Two important ways V-type ATPases regulate activity is by reversibly dissociating the V_0 and V_1 components upon nutrient depletion or by modulating the efficiency of coupling between the V_0 and V_1 components, thereby conserving ATP[269,310]. These studies highlight the importance of

regulating ATPase activity but also demonstrate the number of mechanisms that have evolved to achieve this regulation. It is feasible that the flagellar and injectisome ATPases are regulated at two levels; by regulating ATP hydrolysis and by regulating the FliJ-FlhA interaction that is required to convert the export machinery into a highly efficient ΔΨ driven export machine. In this chapter, I explored how the FliJ-FlhA interaction can be regulated to prevent unnecessary activation of the export machinery when subunits are not present for export by the flagellar T3SS. I have shown that FlgN W_{78}A and FlgNΔ76-78) are defective in binding to FliJ but are still able to interact with their other binding partners; FlgK, FlgL and FlhAc (Figure 7.2). These FlgN variants allowed us to unpick the role of the FlgN interaction with FliJ from its other binding partners. Motility of strains encoding FlgN W_{78}A and FlgNΔ76-78 was marginally reduced compared to wild type (Figure 7.3). Furthermore, export of cognate subunits FlgK and FlgL was marginally reduced, suggesting that the loss of the FlgN-FliJ interaction reduces the efficiency of cognate subunit export (Figure 7.3). FlgN Tryptophan-78 is positioned at the N-terminal region of helix-3. FlgN has been shown to bind the N-helix-1 of FliJ[226]. Interestingly two conserved residues in helix-1 of FliJ (Tyrosine-45 and Tyrosine-49) are positioned at the C-terminal end of FliJ and would be exposed when FliJ is in complex with FliI. These two conserved tyrosine residues are well positioned to potentially interact with Tryptophan-78 of FlgN.

In this study, I showed that an extensive number of highly conserved, surface exposed residues along the length of the substrate binding site on FliT are critical for FliT to interact with FliJ (Figure 7.6). I showed that a FliT variant in which Leucine-72 was replaced with alanine displayed reduced binding to FliJ but was able to interact with its other binding partners; FliD, FliI and $FlhA_c$ (Figure 7.5). This allowed us to unpick the role of FliT binding to FliJ from its other functions. Interestingly, the strain encoding FliT L_{72}A did not display a swimming motility defect compared to wild type *Salmonella* (Figure 7.6). However, a marginal export defect for its cognate subunit FliD was observed (Figure 7.6). The strain encoding FliT L_{72}A displayed reduced swarming motility, indicating

that the FliT-FliJ interaction is required for hyperflagellation. These data indicate that the like FlgN, the FliT-FliJ interaction is required for promoting efficient subunit export.

Flagellar export chaperones also dock at the cytoplasmic domain of FlhA ($FlhA_c$)[177,116,115]. Docking of chaperone-subunit complexes at $FlhA_c$ is essential for efficient subunit export[177,116,115]. The highly conserved Tyrosine residue at position 106 in FliT is required for its interaction with FlhA[115]. The *Salmonella* strain containing the chromosomally encoded FliT $Y_{106}A$ had a marginal swimming and swarming motility defect (Figure 7.6), whereas the level of FliD exported into culture supernatants was significantly reduced at levels comparable to the *fliT* null strain (Figure 7.6). Furthermore, the expression level of all components appeared to be increased in the FliT $Y_{106}A$ strain at similar levels to the FliT null, most likely caused by the binding of FliT $Y_{106}A$ to FliD but not being able to dock at FlhAc and therefore unable to release FliD. FliD subunits would therefore remain bound to FliT $Y_{106}A$ and prevent FliT $Y_{106}A$ from targeting FlhC for degradation, resulting in higher FlhDC levels and therefore higher flagellar gene expression.

FliJ interacts with the export chaperones but also interacts with FlhA[226,294]. I wanted to test whether the FliJ-FlhA interaction can occur whilst export chaperones are bound to FliJ or whether chaperones compete with FlhA for binding to FliJ. Deletion of residues 21-50 in FliJ prevents FliJ binding to FlgN, whilst deletion of residues 61-100 in FliJ prevents FliJ binding to FliT, suggesting that both FlgN and FliT bind different regions of FliJ[226]. Two conserved residues in the FliT binding region of FliJ (Phe-72 and Leu-76) are also required for FliJ binding to FlhA[256]. This suggests that FliT may compete with FlhA for FliJ binding. FlgN doesn't bind the same region of FliJ and therefore unlikely directly competes with FlhA for FliJ binding. However, FlgN binding to FliJ may physically prevent FliJ from being able to contact FlhA. The *in vitro* competition assay showed that both FlgN and FliT compete with FlhA for binding to FliJ (Figure 7.7). To test whether this competition occurs *in vivo*, I expressed wild type FlgN

and its variant that was defective in FliJ binding in a strain that does not encode the FlgN cognate subunits (FlgK and FlgL) and assessed whether FlgN interfered with non-cognate subunit export. FlgN variants were also engineered such that they were unable to bind to FlhA (FlgN $Y_{122}A$ – mutation of critical tyrosine). Expression of FlgN attenuated subunit export compared to the FlgN variant defective in FliJ binding, suggesting that FlgN binds to FliJ *in vivo*, preventing subunit export. I did not test whether FliT also displayed the same phenotype *in vivo* because of the reduced flagellar gene expression that would occur by producing additional FliT protein which would increase degradation of FlhC. This data supports a model whereby when subunits are at low levels in the cell, unladen FlgN and FliT bind to FliJ, preventing the FliJ-FlhA interaction and activation of the export gate. Ribosome profiling revealed how much of each chaperone and cognate subunit(s) are produced by the cell. Although all three flagellar chaperones are produced at similar levels (Figure 7.9), the ratio of subunit to chaperone is lower for the FlgN and FliT chaperones compared to the FliS chaperone. FlgN and FliT are therefore a better proxy for subunit availability in the cell as they are more likely to become free when subunit levels drop in the cell. This may explain why FliS does not bind FliJ.

A reduction in subunit levels in the cell could occur if FlhDC levels drop, resulting in a decrease in flagellar gene expression. When flagellar gene expression decreases, fewer subunits are produced and available for export. As subunit availability decreases, the amount of free FlgN and FliT chaperones in the cell would increase, increasing the chance of a chaperone-FliJ interaction and therefore preventing FliJ from binding FlhA and activating the export machinery. *Salmonella* encounters a multitude of stress conditions in the environment and during pathogenesis and modulates its flagellar gene expression accordingly. Some stress conditions such as cell envelope stress or low pH induce downregulation of flagellar gene expression[311,312]. Under these conditions, free FlgN and FliT chaperones would therefore prevent unnecessary activation of the export machinery and conserve energy reserves for other essential cellular functions. Furthermore, FliC is highly immunogenic and therefore during the

early stages of infection by *Salmonella* Typhimurium, flagellar gene expression decreases, avoiding immune recognition by the NRLC4/NAIP5/6 inflammasome[313,47]. A reduction in flagellar gene expression would reduce the amount of subunit produced by the cell, as the ratio of subunit to chaperone is lower for the FlgN and FliT chaperones, it is feasible that they would become free and bind FliJ, preventing further FliC export, therefore decreasing the amount of FliC being exported and available for immune recognition by the host cell.

Our laboratory has previously shown that FlgN and FliT bind to FliJ[226]. This selective binding was proposed to promote export of the hook-filament junction and filament cap subunits by recruiting their cognate chaperones to the export machinery by binding to FliJ[226]. Similarly, the FliJ homologues from *Salmonella* and *Yersinia* injectisome T3SS were also shown to bind a subset of export chaperones, specifically the chaperones for the translocon subunits[225]. Chaperones docked at FliJ could be captured by cognate subunits *in vitro*, suggesting that FliJ transfers unladen chaperones to cognate subunits[226]. These observations led authors to propose an escort model whereby unladen chaperones can be cycled after subunit release and transferred to new subunits[226]. The data in this chapter support this view and also indicate that the FlgN and FliT chaperones compete with FlhA for binding to FliJ, supporting a model in which these export chaperones regulate FliJ dependent activation of the export machinery.

Chaperone binding to FliJ would prevent activation of the export machinery. However, how ATP hydrolysis is prevented when subunits are not available or when the ATPase is not localised at the membrane is unclear. Chaperone binding to FliJ may also inhibit ATPase activity, or another component may regulate ATPase activity. Further work will need to be carried out to determine how ATP hydrolysis by the flagellar ATPase complex is regulated *in vivo*.

These data indicate that chaperone binding at the flagellar export machinery also serves to regulate the export machinery as well as aiding subunit delivery to components of the export machinery. This data together with previous data suggest that all of the flagellar export chaperones are specialised to perform distinct regulatory functions at the machinery or within the cytoplasm. FliS binds to the anti-sigma factor FlgM, preventing it from binding to the sigma factor (FliA) and therefore modulates late flagellar gene expression[92]. FliT promotes FlhC degradation and therefore modulates global flagellar gene expression in response to free FliT within the cell[296]. Here I provide evidence to support the view that both FlgN and FliT chaperones prevent FliJ activation of the export machinery in response to low subunit availability within the cell.

Based on the current data I propose a model whereby a FlgN-FlgK complex or a FliT-FliD complex initially docks the FliI component of the ATPase complex[176]. The chaperone-subunit complex is released from FliI and transferred to the FlhAc docking platform through interactions between the chaperone and FlhAc[177,116,115,227]. Subunits are released from their cognate chaperone, unfolded and translocated into the export channel. Free FlgN or FliT chaperones then interact with FliJ. Subunits subsequently capture chaperones from FliJ and the cycle re-starts[226]. If subunits are not available to capture FlgN or FliT from FliJ then these chaperones remain bound to FliJ, preventing FliJ from activating the FlhA export machinery such that it cannot efficiently use the $\Delta\Psi$ component of the PMF[111].

In summary, I have presented evidence that FlgN and FliT chaperones interact with FliJ to prevent FliJ from making a productive interaction with FlhA. I propose that when subunit levels in the cell are low, the FlgN and FliT chaperones remain bound to FliJ, preventing activation of the export machinery.

Chapter 8
Concluding remarks

In this chapter, I provide a general overview of the thesis, drawing together the data presented and discussing how these findings might feed into future investigations.

During flagellar Type III secretion, structural and some regulatory components are exported from the cytoplasm into the narrow central export channel where they transit to the flagellar tip and assemble into the nascent structure or are released into the extracellular environment[8,9]. The majority of previous studies have addressed the mechanism of targeting of the chaperoned late export subunits to the export machinery. This study has explored the nature of the signals of the unchaperoned early flagellar subunits and how these signals allow early flagellar subunits to be targeted to the export machinery and promote their export. In addition, this thesis has extended the knowledge of how the export gate complex comprising FlhA, FlhB, FliP, FliQ and FliR is gated and the signals required to convert the export gate from a closed to open conformation. Furthermore, the role of the flagellar export chaperones in regulating activity of the flagellar export machinery was also investigated.

Early subunits dock at the FlhBc component of the export gate *via* a five amino acid sequence found in all early flagellar subunits termed the gate recognition motif (GRM)[141]. Previous unpublished work in our laboratory identified a new export signal at the extreme N-terminus of the hook capping protein, FlgD (amino acids 2-5)[252]. Deletion of this signal attenuated FlgD export and when overexpressed in wild type cells the FlgDΔ2-5 subunit had a dominant negative overexpression phenotype. However, a FlgD variant containing the 2-5 deletion in combination with the GRM deletion was no longer dominant negative, indicating that the FlgDΔ2-5 variant stalls at FlhBc. A screen for suppressor mutations of the export defect associated with the FlgDΔ2-5 variant showed that the introduction of small hydrophobic amino acids within the FlgD N-terminus

could supress the motility and export defects. In addition, mutations that introduced insertions or duplications that increased the distance between valine-15 and the FlgD GRM suppressed the FlgDΔ2-5 motility and export defects. Amino acid sequence analysis and hydrophobicity plots show that all the early flagellar subunits contain small hydrophobic residues within their N-termini. FlgD is unusual compared to the other early flagellar subunits in that the 2-5 deletion removes most of the small hydrophobic residues from the N-terminus (upstream of the GRM), creating a new polar N-terminus. Decreasing the number of residues between the 2-5 signal and the GRM showed that below a threshold of 20-24 amino acids, FlgD export was attenuated. This distance requirement between the extreme N-terminus and the GRM was also found to be true for the rod (FlgG) and hook (FlgE) subunits, suggesting that the mechanism is conserved among all early subunits. The FlgE and FlgD variants (termed $subunit_{short}$ variants) containing deletions that decrease the distance between the N-terminus and GRM to below the minimum threshold displayed a dominant negative overexpression phenotype analogous to that of the FlgD 2-5 deletion variant. Deletion of the GRM signal in the $subunit_{short}$ variants relieved the dominant negative overexpression phenotype indicating that these variants stall at FlhBc, preventing other subunits from docking, and possibly preventing the N-terminal small hydrophobic residues from making the appropriate interactions with the export machinery to allow $subunit_{short}$ export. Mutations within the FliP and FliR components of the export gate that are predicted to destabilise the closed gate conformation, suppressed the motility defect of $FlgD_{short}$, indicating that the 2-5 signal triggers opening of the export gate. The data indicates that early subunits dock at FlhBc to correctly position the 2-5 export signal to trigger opening of the export gate. Gating mechanisms in membrane transport systems ensure that the permeability barrier across the inner membrane is not compromised, and export systems have evolved various mechanisms to trigger gate opening or transporter assembly once a substrate is present for export. The Sec system switches from a closed to open conformation based on substrate availability at the export machinery whilst the TAT export system assembles a functional transporter when a substrate has docked at certain Tat

components[103,96,104]. The data discussed so far indicate a selectivity process in which an early flagellar subunit is only selected for export and the export gate only opened if a substrate contains two specific optimally spaced export signals. It is not clear which component of the export machinery the N-terminus of early subunits contacts to trigger gate opening, though information on the precise location of FlhBc in the export machinery could aid in identifying which components the Subunit N-terminal signal may contact. One possible way of determining the location of FlhBc would be to construct a *Salmonella* strain encoding the non-cleavable FlhB variant (FlhB-P238A-N269A) and performing single particle cryo-EM on intact purified basal bodies or attempt to obtain high resolution cryo-electron tomography (cryo-ET) of the *in situ* flagellar export machinery. A cleavage event in wild type FlhB between Asn-269 and Pro-270 occurs and there is evidence indicating that the cleaved $FlhB_{CC}$ portion dissociates from $FlhB_{CN}$ following the export specificity switch, therefore, purified or *in situ* structures may not contain the FlhBcc domain if the T3SS have switched substrate specificity, hence the need to perform cryo-EM or cryo-ET with strains encoding a non-cleavable FlhB variant[282,257].

Whether the N-termini of early substrates of the virulence T3SS also trigger export gate opening in a similar manner to the early flagellar substrates is not known. Early vT3SS substrates also contain a GRM-like export signal and bind to the FlhB homologue in a similar manner to early flagellar substrates, furthermore, the core components of the vT3SS machinery share sequence and structural similarity to the equivalent flagellar components[158,106,121,105,251,108,109]. To test whether the early substrates for the vT3SS also contain an N-terminal export signal it would necessary to engineer early subunit variants equivalent to the $subunit_{short}$ variants described in chapters 3 and 4 and assess their export in a *Salmonella* strain in which the virulence T3SS is locked in the early substrate export phase.

Having identified the signals within early flagellar subunits required for export gate opening, I sought to characterise how export gate opening is energised.

Two energy sources are known to be required to power flagellar type III secretion. The first is the ATPase complex which that hydrolyses ATP, which is proposed to drive rotation of the FliJ component of the ATPase complex so that it can make interactions with all nine copies of FlhA[122,224,272,124]. The second energy source is the PMF, and FlhA is thought to be the proton conducting component of the export machinery[52,51,262,113]. Mutations within FliR that are predicted to destabilise the closed gate conformation suppressed the motility and export defects of a strain encoding the FlhA K_{203}A mutation, suggesting that FlhA is involved in export gate opening. Increasing the PMF also improved subunit export by the FlhA K_{203}A strain indicating that the export machinery uses the PMF to open the export gate. It is unclear how the FlhA K_{203}A variant prevents efficient export gate opening. It is possible that the K_{203}A mutation alters the conformation of FlhA and that the intragenic suppressor mutations isolated from the strain encoding FlhA K_{203}A restore a wild type conformation. Structures of wild type, the K_{203}A variant and K_{203}A suppressor variants of full length FlhA would confirm this. A key finding was that the FliR mutations that open the export gate cannot suppress the export and motility defects caused by deletion of the FliH and FliI components of the ATPase complex, indicating that the ATPase does not directly open the export gate. Rather, the PMF is the main energy source required for gate opening. Taken together, the data suggests that FlhA requires two mutually exclusive signals before it can commit to export gate opening: the subunit N-terminal signal and the interaction between FliJ and FlhA.

The FlhB-P_{28}T variant suppresses the motility and export defects associated with deletion of the FliHIJ ATPase components of the export machinery and our data indicate that the FlhB-P_{28}T does not stabilise an open gate confirmation but instead likely modulates the conformation of FlhA[111]. Cryo-EM of the export gate complex containing FlhA or high resolution cryo-ET of a strain encoding FlhB-P_{28}T could allow us to determine whether the FlhB P_{28}T modulates the conformation of the ABPQR export gate.

In the course of this study it was found that deletion of the FliR plug loop sensitised cells to choline, indicating that this loop plays an important role in gating the export gate, analogous to the plug loop within the Sec machinery[273,274,264,266]. Deletion of genes encoding the majority of the early flagellar subunits further increased sensitivity of the FliR plug deletion strain to choline, indicating that subunits transiting through the export gate partially plug the export gate containing the leaky FliR variant. A strain encoding the wild type export gate in combination with deletions in the genes encoding the majority of the early flagellar subunits was not more sensitive to choline than wild type *Salmonella,* indicating that the export gate returns to a closed conformation when there are no subunits present at the export machinery to be exported through the export gate.

Another aim of this study was to elucidate the role of the C-terminus of early flagellar subunits in subunit export. Our laboratory previously proposed that the C-terminus of an early flagellar subunit in the channel can 'capture' the N-terminus of the preceding subunit docked at FlhBc and pull it into the flagellar export channel[141]. The N- and C-termini were proposed to remain associated during subunit transit, whereby subunits form a multi-subunit chain in the channel from the export machinery to the flagellar tip where the subunits assemble into the nascent structure. Our laboratory showed that deletion of the FlgE C-terminus attenuated its export into culture supernatants, which was used as evidence to support the role of the C-terminus of early subunits capturing the preceding subunit docked at FlhBc[141]. A key finding from this study was that a FlgE variant lacking its C-terminus (amino acids 360-403) did not display a dominant negative phenotype as would be predicted if a specific C-terminal signal was required for capture of subunits into a chain. Furthermore, the wild type FlgE variant containing a functional C-terminus displayed a greater dominant negative overexpression phenotype than the FlgEΔCt variant. The data indicate that that early flagellar subunits are not captured from the FlhBc export gate through sequence-specific interactions between subunit N- and C-termini. Furthermore, the data from chapter 4 showing that strains deleted for the

majority of early subunits increases the choline sensitivity of a FliR plug deletion strain indicates that the export gate closes when no subunit are present for export. This data indicates that early flagellar subunits are not captured into a multi-subunit chain from FlhBc and that a chain does not span through the export gate and into the central export channel within the rod. If a multi-subunit chain does exist in the central channel, subunit termini would need to associate after they have passed though the export gate and into the rod portion of the channel.

In the course of this study it was found that deletion of a ten-residue sequence (amino acids 371-380) within FlgE alleviated the defects in motility and flagellar eexport seen in cells overexpressing FlgE. Amino acids within the FlgE C-terminus were substituted to alanine, three of which ($I_{376}A$, $R_{380}A$ and $Y_{382}A$) were found to alleviate the FlgE overexpression phenotype. Suppressor mutations isolated from cells producing FlgE $I_{376}A$ and FlgE $R_{380}A$ caused an increase in the expression level of these FlgE variants, suggesting that the C-terminal signal functions to recruit subunits into the flagellar export pathway, analogous to the C-termini of late flagellar export subunits which bind export chaperones that target subunits to the flagellar export machinery[176,177,115].

I found that a FlgD variant that lacked its C-terminus (amino acids 191-232) did not display reduced export into culture supernatants, furthermore, this variant did not inhibit motility or export when overexpressed in wild type cells, indicating that FlgD does not contain a C-terminal export signal. Ribosome profiling revealed that the amount of each early flagellar subunit (except for FlgD) produced in the cell correlated with its stoichiometry in the rod/hook. FlgD was produced at higher levels than other flagellar subunits with similar stoichiometry, which can be explained by the observation that FlgD does not contain a C-terminal export signal and increasing the expression levels of early flagellar subunits deleted for their C-terminal export signal suppresses the export defect.

Further experiments are required to identify the potential binding partner of the FlgE C-terminus. Affinity chromatography purification assays were attempted

using full length FlgE and the FlgEΔCt variant with FlhAc and FlhBc but any potential interaction may have been too weak to detect using affinity chromatography as might be expected for a transient interaction. Affinity chromatography assays with FlhAc variants that stabilise the 'open' or 'closed' conformations, which are proposed to modulate early subunit binding to FlhAc could increase an early subunit-FlhAc interaction to a level that can be detected by affinity chromatography[232]. Alternatively, *in vitro* and *in vivo* crosslinking studies by introducing photo-crosslinking unnatural amino acids adjacent to the I376, R380 and Y238 residues could be used to identify a potential binding partner, as long as appropriate negative controls are used (for example the $I_{376}A$, $R_{380}A$ or $Y_{382}A$ mutations).

How subunits with an intact C-terminal export signal inhibit flagellar export when they are overexpressed in wild type cells is unclear. As discussed in Chapter 5, having excess subunits in the cell that contain the C-terminal export signal could result in subunits sequestering a component of the export machinery and acting as a physical barrier that prevents other subunits from docking at the export machinery. Cryo-ET of wild type *Salmonella* overexpressing full length FlgE could reveal increased electron density at a particular component of the export machinery, corresponding to FlgE subunits docking at the export machinery.

Overall the analyses presented for the early subunits provide evidence for a tripartite organisation of export signals that are used sequentially. The C-terminal signal is likely required for the delivery of early flagellar subunits to the export machinery, increasing the number of subunits at the export machinery to go on and dock at FlhBc *via* their GRM signal. Subunits docked at FlhBc position the N-terminal non-polar signal to trigger opening of the export gate energised by the PMF, facilitated by interactions between the FliJ component of the ATPase complex and FlhA.

Another aim of this study was to determine the sequence in which the export chaperones for the late flagellar subunits bind to components of the export

machinery. The FlgN and FliT chaperones bind to the FliI and FliJ components of the ATPase complex and the cytoplasmic domain of FlhA (FlhAc)[176,226,177]. Chaperone-subunit complexes are thought to initially dock at FliI, followed by FlhAc[176,177,115,116,227]. However, the precise sequence of interactions of FlgN and FliT chaperones with the FliJ and FlhAc components is unclear. In this study it was found that chaperone variants that are defective in binding FlhAc did not interact efficiently with FliJ *in vivo*, indicating that chaperones dock at FliJ after docking at FlhAc. Previous unpublished work in our laboratory identified a FlgN variant that was defective in binding to FliJ[291]. Cells producing this variant displayed a small motility defect and partially attenuated FlgK export, suggesting that chaperone docking at FliJ improves the efficiency of cognate subunit export as proposed by Evans et al.[226]. An *in vitro* competition assay showed that the FlgN and FliT chaperones compete with FlhAc for docking at FliJ. Expression of FlgN in an early locked strain (Δ*flgE*) that produces little FlgK or FlgL attenuated non-cognate subunit export, indicating that when FlgN is competent to bind FliJ (when FlgN is not bound to subunit) it prevents FliJ from binding to FlhA, preventing efficient ΔΨ driven subunit export by the flagellar export machinery. This ensures the export machinery is only active when subunits are present for export. If late export subunits are present within the cytosol, they can bind their cognate chaperone, occluding the FliJ binding site on their cognate chaperone. When subunit levels within the cell become depleted, FlgN and FliT chaperones are able to bind FliJ, preventing activation of the export machinery. How the ATPase activity of FliI is regulated at this stage is unclear, it is conceivable that chaperone binding to FliJ may also attenuate FliI ATPase activity and therefore prevent unnecessary ATP hydrolysis.

In summary, this thesis has increased our knowledge of the export signals that reside within early flagellar subunits and how these signals aide early flagellar subunit export. Furthermore, the role of the PMF has been explored and how export signals trigger opening of the export gate. Finally, the flagellar export chaperones were shown to play an accessory role other than subunit targeting, coupling flagellar subunit availability to activation of the export machinery. A

number of unanswered questions remain *e.g.* What component(s) of the export machinery does the N-terminal non-polar signal within early flagellar subunits contact? What signals within late export subunits achieve export gate opening? How are subunits unfolded and translocated into the export channel? How does FlhA open the export gate? Higher resolution *in vitro* and *in vivo* structures of intact flagellar basal bodies could in part help answer some of these questions and improve our understanding of flagellar assembly.

References

1. Kearns, D. B. A field guide to bacterial swarming motility. *Nat. Rev. Microbiol.* **8**, 634–644 (2010).
2. Yao, J. & Allen, C. Chemotaxis is required for virulence and competitive fitness of the bacterial wilt pathogen *Ralstonia solanacearum*. *J. Bacteriol.* **188**, 3697-708 (2006).
3. Boin, M. A. *et al*. Chemotaxis in *Vibrio cholerae*. *FEMS Microbiol. Lett.* **239**, 1-8 (2004).
4. Bolton, D. J. *Campylobacter* virulence and survival factors. *Food Microbiol.* **48**, 99-108 (2015).
5. Aihara, E. *et al.* Motility and Chemotaxis Mediate the Preferential Colonization of Gastric Injury Sites by *Helicobacter pylori*. *PLoS Pathog.* **10**, e1004275 (2014).
6. Dongre, M. *et al.* Flagella-mediated secretion of a novel *Vibrio cholerae* cytotoxin affecting both vertebrate and invertebrate hosts. *Commun. Biol.* **1**, 59 (2018).
7. Wagner, S. *et al.* Bacterial type III secretion systems: A complex device for the delivery of bacterial effector proteins into eukaryotic host cells. *FEMS Microbiol. Lett.* **365**, 19 (2018).
8. Evans, L. D. B. *et al*. Building a flagellum in biological outer space. *Microb. cell.* **1**, 64-66 (2014).
9. Evans, L. D. B. *et al*. Building a flagellum outside the bacterial cell. *Trends Microbiol.* **22**, 566-572 (2014).
10. Macnab, R. Genetics and Biogenesis of Bacterial Flagella. *Annu. Rev. Genet.* **26**, 131-158(1992).
11. Lambert, C. *et al.* Characterizing the flagellar filament and the role of motility in bacterial prey-penetration by *Bdellovibrio bacteriovorus*. *Mol. Microbiol.* **60**, 274-286 (2006).
12. Rodgers, F. G. *et al*. Electron microscopic evidence of flagella and pili on *Legionella pneumophila*. *J. Clin. Pathol.* **33**, 1184-1188 (1980).
13. Leifson E. *et al*. Morphological characteristics of flagella of *Proteus* and

related bacteria. *J. Bacteriol.* **69**, 73-82 (1955).

14. Taylor, B. L. & Koshland, D. E. Reversal of flagellar rotation in monotrichous and peritrichous bacteria: generation of changes in direction. *J. Bacteriol.* **119**, 640-642 (1974).
15. Macnab, R. M. & Koshland, D. E. The gradient-sensing mechanism in bacterial chemotaxis. *Proc. Natl. Acad. Sci. U.S.A.* **69**, 2509-2512 (1972).
16. Hess, J. F. *et al*. Phosphorylation of three proteins in the signaling pathway of bacterial chemotaxis. *Cell.* **53**, 79-87 (1988).
17. Hess, J. F. *et al*. Histidine phosphorylation and phosphoryl group transfer in bacterial chemotaxis. *Nature.* **336**, 139-143 (1988).
18. Ravid, S. *et al*. Restoration of flagellar clockwise rotation in bacterial envelopes by insertion of the chemotaxis protein CheY. *Proc. Natl. Acad. Sci. U.S.A.* **83**, 7157-7161 (1986).
19. Magariyama, Y. *et al*. Genetic and behavioral analysis of flagellar switch mutants of *Salmonella* typhimurium. *J. Bacteriol.* **172**, 4359-4369 (1990).
20. Togashi, F. *et al*. An extreme clockwise switch bias mutation in fliG of *Salmonella* typhimurium and its suppression by slow-motile mutations in motA and motB. *J. Bacteriol.* **179**, 2994-3003 (1997).
21. Larsen, S. H. *et al*. Chemomechanical coupling without ATP: the source of energy for motility and chemotaxis in bacteria. *Proc. Natl. Acad. Sci. U.S.A.* **71**, 1239-1243 (1974).
22. McCarter, L. L. MotY, a component of the sodium-type flagellar motor. *J. Bacteriol.* **176**, 4219-4225 (1994).
23. Asai, Y. *et al*. Hybrid motor with H^+- and Na^+-driven components can rotate *Vibrio* polar flagella by using sodium ions. *J. Bacteriol.* **181**, 6332-6338 (1999).
24. Asai, Y. *et al*. Coupling ion specificity of chimeras between H^+- and Na^+-driven motor proteins, MotB and PomB, in *Vibrio* polar flagella. *EMBO J.* **19**, 3639-3648 (2000).
25. Magariyama, Y. *et al.* Simultaneous measurement of bacterial flagellar rotation rate and swimming speed. *Biophys. J.* **69**, 2154-2162 (1995).
26. Magariyama, Y. *et al.* Very fast flagellar rotation. *Nature.* **27**, 752(1994).

27. Muramoto, K. *et al.* High-speed Rotation and Speed Stability of the Sodium-driven Flagellar Motor in *Vibrio alginolyticus*. *J. Mol. Biol.* **251**, 50-58 (1995).
28. Drake, D. & Montie, T. C. Flagella, motility and invasive virulence of *Pseudomonas aeruginosa*. *J. Gen. Microbiol.* **134**, 43-52 (1988).
29. Marchetti, M. *et al*. Interaction of pathogenic bacteria with rabbit appendix M cells: Bacterial motility is a key feature *in vivo*. *Microbes Infect.* **6**, 521-528 (2004).
30. Krukonis, E. S. & DiRita, V. J. From motility to virulence: Sensing and responding to environmental signals in *Vibrio cholerae*. *Curr. Opin. Microbiol*. **6**, 186-190 (2003).
31. Tobe, T. *et al*. Activation of Motility by Sensing Short-Chain Fatty Acids via Two Steps in a Flagellar Gene Regulatory Cascade in Enterohemorrhagic *Escherichia coli*. *Infect. Immun.* **79**, 1016-1024 (2011).
32. Frymier, P. D. *et al*. Three-dimensional tracking of motile bacteria near a solid planar surface. *Proc. Natl. Acad. Sci. U.S.A.* **92**, 6195-6199 (2006).
33. Misselwitz, B. *et al.* Near surface swimming of *Salmonella* Typhimurium explains target-site selection and cooperative invasion. *PLoS Pathog.* **8**, e1002810 (2012).
34. Roy, K. *et al.* Enterotoxigenic *Escherichia coli* EtpA mediates adhesion between flagella and host cells. *Nature*. **457**, 594-598 (2009).
35. Sampaio, S. C. F. *et al.* Flagellar Cap Protein FliD Mediates Adherence of Atypical Enteropathogenic *Escherichia coli* to Enterocyte Microvilli. *Infect. Immun.* **84**, 1112-1122 (2016).
36. Kirov, S. M. *et al*. *Aeromonas* Flagella (Polar and Lateral) Are Enterocyte Adhesins That Contribute to Biofilm Formation on Surfaces. *Infect. Immun.* **72**, 1939-1945 (2004).
37. Lemon, K. P. *et al*. Flagellar motility is critical for *Listeria monocytogenes* biofilm formation. *J. Bacteriol.* **189**, 4418-4424 (2007).
38. Serra, D. O. *et al*. Microanatomy at Cellular Resolution and Spatial Order of Physiological Differentiation in a Bacterial Biofilm. *MBio* **4**, e00103-13

(2013).

39. Ghelardi, E. *et al.* Requirement of flhA for swarming differentiation, flagellin export, and secretion of virulence-associated proteins in *Bacillus thuringiensis*. *J. Bacteriol.* **184**, 6424-6433 (2002).
40. Samuelson, D. R. *et al.* The *Campylobacter jejuni* CiaD effector protein activates MAP kinase signaling pathways and is required for the development of disease. *Cell Commun. Signal.* **11**, 79 (2013).
41. Konkel, M. E. *et al.* Secretion of virulence proteins from *Campylobacter jejuni* is dependent on a functional flagellar export apparatus. *J. Bacteriol.* **186**, 3296-3303 (2004).
42. Neal-McKinney, J. M. & Konkel, M. E. The *Campylobacter jejuni* CiaC virulence protein is secreted from the flagellum and delivered to the cytosol of host cells. *Front. Cell. Infect. Microbiol.* **2**, 31 (2012).
43. Hayashi, F. *et al.* The innate immune response to bacterial flagellin is mediated by Toll-like receptor 5. *Nature.* **410**, 1099-1103 (2001).
44. Roy, C. R. & Zamboni, D. S. Cytosolic detection of flagellin: A deadly twist. *Nat. Immunol.* **7**, 549-551 (2006).
45. Feuillet, V. *et al.* Involvement of toll-like receptor 5 in the recognition of flagellated bacteria. *Proc. Natl. Acad. Sci. U.S.A.* **103**, 12487-12492 (2006).
46. Anderson, K. V. Toll signaling pathways in the innate immune response. *Curr. Opin. Immunol.* **12**, 13-19 (2000).
47. Ilyas, B. *et al.* Regulatory Evolution Drives Evasion of Host Inflammasomes by *Salmonella* Typhimurium. *Cell Rep.* **25**, 825-832 (2018).
48. Hanuszkiewicz, A. *et al.* Identification of the flagellin glycosylation system in *Burkholderia cenocepacia* and the contribution of glycosylated flagellin to vasion of human innate immune responses. *J. Biol. Chem.* **289**, 19231-19244 (2014).
49. Merino, S. *et al.* Role of *Aeromonas hydrophila* flagella glycosylation in adhesion to hep-2 cells, biofilm formation and immune stimulation. *Int. J. Mol. Sci.* **15**, 21935-21946 (2014).

50. Bonifield, H. R. & Hughes, K. T. Flagellar phase variation in *Salmonella enterica* is mediated by a posttranscriptional control mechanism. *J. Bacteriol.* **185**, 3567-3574 (2003).
51. Minamino, T. & Namba, K. Distinct roles of the FliI ATPase and proton motive force in bacterial flagellar protein export. *Nature.* **451**, 485–488 (2008).
52. Paul, K. *et al*. Energy source of flagellar type III secretion. *Nature.* **451**, 489-492 (2008).
53. Jones, C. J. *et al*. Stoichiometric analysis of the flagellar hook-(basal-body) complex of *Salmonella* Typhimurium. *J. Mol. Biol.* **212**, 377-387 (1990).
54. DePamphilis, M. L. & Adler, J. Fine structure and isolation of the hook-basal body complex of flagella from *Escherichia coli* and *Bacillus subtilis*. *J. Bacteriol.* **105**, 384-395 (1971).
55. Hirano, T. *et al*. Substrate specificity classes and the recognition signal for *Salmonella* type III flagellar export. *J. Bacteriol.* **185**, 2485-2492 (2003).
56. Fujii, T. *et al.* Identical folds used for distinct mechanical functions of the bacterial flagellar rod and hook. *Nat. Commun.* **8**, 14276 (2017).
57. Muller, V. *et al*. Characterization of the fliE genes of *Escherichia coli* and *Salmonella* Typhimurium and identification of the FliE protein as a component of the flagellar hook-basal body complex. *J. Bacteriol.* **174**, 2298-2304 (1992).
58. Diepold, A. *et al*. Composition, Formation, and Regulation of the Cytosolic C-ring, a Dynamic Component of the Type III Secretion Injectisome. *PLoS Biol.* **13**, e1002039 (2015).
59. Cohen, E. J. *et al*. Nanoscale-length control of the flagellar driveshaft requires hitting the tethered outer membrane. *Science.* **356**,197-200 (2017).
60. Cohen, E. J. & Hughes, K. T. Rod-to-Hook transition for extracellular flagellum assembly is catalyzed by the L-ring-dependent rod scaffold removal. *J. Bacteriol.* **196**, 2387-2395 (2014).

61. Spöring, I. *et al.* Hook length of the bacterial flagellum is optimized for maximal stability of the flagellar bundle. *PLoS Biol.* **16**, e2006989 (2018).
62. Erhardt, M. *et al*. An infrequent molecular ruler controls flagellar hook length in *Salmonella enterica*. *EMBO J.* **30**, 2948-2961 (2011).
63. Hirano, T. *et al*. Roles of FliK and FlhB in determination of flagellar hook length in *Salmonella* Typhimurium. *J. Bacteriol.* **176**, 5439-5449 (1994).
64. Williams, A. W. *et al.* Mutations in fliK and flhB affecting flagellar hook and filament assembly in *Salmonella* Typhimurium. *J. Bacteriol.* **178**, 2960-2970 (1996).
65. Aizawa, S.-I. Mystery of FliK in Length Control of the Flagellar Hook. *J. Bacteriol.* **194**, 4798-4800 (2012).
66. Samatey, F. A. *et al.* Structure of the bacterial flagellar hook and implication for the molecular universal joint mechanism. *Nature.* **431**, 1062-1068 (2004).
67. Fujii, T. *et al*. Specific Arrangement of α-Helical Coiled Coils in the Core Domain of the Bacterial Flagellar Hook for the Universal Joint Function. *Structure.* **17**, 1485-1493 (2009).
68. Matsunami, H. *et al*. Complete structure of the bacterial flagellar hook reveals extensive set of stabilizing interactions. *Nat. Commun.* **7**, 13425 (2016).
69. Brown, M. T. *et al.* Flagellar hook flexibility is essential for bundle formation in swimming *Escherichia coli* cells. *J. Bacteriol.* **194**, 3495-3501 (2012).
70. Ikeda, T. *et al*. Localization and stoichiometry of hook-associated proteins within *Salmonella* Typhimurium flagella. *J. Bacteriol.* **169**, 1168-1173 (1987).
71. Homma, M. *et al*. Hook-associated proteins essential for flagellar filament formation in *Salmonella* Typhimurium. *J. Bacteriol.* **157**, 100-108 (1984).
72. Hong, H. J. *et al.* Crystal structure of FlgL and its implications for flagellar assembly. *Sci. Rep.* **8**, 14307 (2018).
73. Yonekura, K. *et al*. Complete atomic model of the bacterial flagellar filament by electron cryomicroscopy. *Nature.* **424**, 643-650 (2003).

74. Kamiya, R. *et al*. Transition of bacterial flagella from helical to straight forms with different subunit arrangements. *J. Mol. Biol.* **131**, 725-742 (1979).
75. Samatey, F. A. *et al.* Structure of the bacterial flagellar protofilament and implications for a switch for supercoiling. *Nature.* **410**, 331-337 (2001).
76. Yamashita, L. *et al.* Structure and switching of bacterial flagellar filaments studied by X-ray fiber diffraction. *Nat. Struct. Biol.* **5**, 125-132 (1998).
77. Macnab, R. M. & Ornston, M. K. Normal-to-curly flagellar transitions and their role in bacterial tumbling. Stabilization of an alternative quaternary structure by mechanical force. *J. Mol. Biol.* **112**, 1-30 (1977).
78. Vogel, R. & Stark, H. Rotation-induced polymorphic transitions in bacterial flagella. *Phys. Rev. Lett.* **110**, 158104 (2013).
79. Ikeda, T. *et al*. 'Cap' on the tip of *Salmonella* flagella. *J. Mol. Biol.* **184**, 735-737 (1985).
80. Yonekura, K. *et al.* The bacterial flagellar cap as the rotary promoter of flagellin self-assembly. *Science.* **290**, 2148-2152 (2000).
81. Postel, S. *et al.* Bacterial flagellar capping proteins adopt diverse oligomeric states. *Elife.* **5**, e18857 (2016).
82. Cho, S. Y. *et al.* Tetrameric structure of the flagellar cap protein FliD from *Serratia marcescens*. *Biochem. Biophys. Res. Commun.* **489**, 63-69 (2017).
83. Chevance, F. F. V. & Hughes, K. T. Coupling of Flagellar gene expression with assembly in *Salmonella enterica*. *Methods Mol. Biol.* **1593**, 47-71 (2017).
84. Chilcott, G. S. & Hughes, K. T. Coupling of Flagellar Gene Expression to Flagellar Assembly in *Salmonella enterica* Serovar Typhimurium and *Escherichia coli*. *Microbiol. Mol. Biol. Rev.* **64**, 694-708 (2003).
85. Kutsukake, K. *et al*. Transcriptional analysis of the flagellar regulon of *Salmonella* Typhimurium. *J. Bacteriol.* **172**, 741-747 (1990).
86. Wei, B. L. *et al.* Positive regulation of motility and *flhDC* expression by the RNA-binding protein CsrA of *Escherichia coli*. *Mol. Microbiol.* (2001).
87. Singer, H. M. *et al*. The *Salmonella* Spi1 virulence regulatory protein HilD

directly activates transcription of the flagellar master operon *flhDC*. *J. Bacteriol.* **196**, 1448-1457 (2014).

88. Wada, T. *et al.* EAL domain protein YdiV acts as an anti-$FlhD_4C_2$ factor responsible for nutritional control of the flagellar regulon in *Salmonella enterica* serovar typhimurium. *J. Bacteriol.* **193**, 1600-1611 (2011).
89. Liu, X. & Matsumura, P. The FlhD/FlhC complex, a transcriptional activator of the *Escherichia coli* flagellar class II operons. *J. Bacteriol.* **176**, 7345-7351 (1994).
90. Ohnishi, K. *et al*. Gene *fliA* encodes an alternative sigma factor specific for flagellar operons in *Salmonella* Typhimurium. *MGG Mol. Gen. Genet.* **221**, 139-147 (1990).
91. Hughes, K. T *et al*. Sensing structural intermediates in bacterial flagellar assembly by export of a negative regulator. *Science.* **262**, 1277-1280 (1993).
92. Kutsukake, K. & Iino, T. Role of the FliA-FlgM regulatory system on the transcriptional control of the flagellar regulon and flagellar formation in *Salmonella* Typhimurium. *J. Bacteriol.* **176**, 3598-3605 (1994).
93. Costa, T. R. D. *et al.* Secretion systems in Gram-negative bacteria: Structural and mechanistic insights. *Nat. Rev. Microbiol.* **13**, 343-359 (2015).
94. Abby, S. S. & Rocha, E. P. C. Identification of protein secretion systems in bacterial genomes using MacSyFinder. *Methods Mol. Biol.* **1615**, 1-21 (2017).
95. Lycklama a Nijeholt, J. A. & Driessen, A. J. M. The bacterial Sec-translocase: Structure and mechanism. *Philos. Trans. R. Soc. B. Biol. Sci.* **367**, 1016-1028 (2012).
96. Palmer, T. & Berks, B. C. The twin-arginine translocation (Tat) protein export pathway. *Nat. Rev. Microbiol.* **10**, 483-496 (2012).
97. Drobnak, I. *et al*. Multiple driving forces required for efficient secretion of autotransporter virulence proteins. *J. Biol. Chem.* **290**, 10104-10116 (2015).
98. Baclayon, M. *et al.* Mechanical Unfolding of an Autotransporter

Passenger Protein Reveals the Secretion Starting Point and Processive Transport Intermediates. *ACS Nano.* **10**, 5710-5719 (2016).

99. Aunkham, A. *et al.* Structural basis for chitin acquisition by marine *Vibrio* species. *Nat. Commun.* **9**, 220 (2018).
100. Ge, Y. *et al*. Lateral opening of the bacterial translocon on ribosome binding and signal peptide insertion. *Nat. Commun.* **5**, 5263 (2014).
101. Zimmer, J. *et al*. Structure of a complex of the ATPase SecA and the protein-translocation channel. *Nature.* **455**, 936-943 (2008).
102. Voorhees, R. M. *et al*. Structure of the mammalian ribosome-Sec61 complex to 3.4 Å resolution. *Cell.* **157**,1632-43 (2014).
103. Tsirigotaki, A. *et al*. Protein export through the bacterial Sec pathway. *Nat. Rev. Microbiol.* **15**, 21-36 (2017).
104. Mori, H. & Cline, K. A twin arginine signal peptide and the pH gradient trigger reversible assembly of the thylakoid ΔpH/Tat translocase. *J. Cell Biol.* **157**, 205-210 (2002).
105. Kuhlen, L. *et al.* Structure of the core of the type III secretion system export apparatus. *Nat. Struct. Mol. Biol.* **25**, 583-590 (2018).
106. Zarivach, R. *et al*. Structural analysis of a prototypical ATPase from the type III secretion system. *Nat. Struct. Mol. Biol.* **14**, 131–137 (2007).
107. Ibuki, T. *et al.* Common architecture of the flagellar type III protein export apparatus and F- and V-type ATPases. *Nat. Struct. Mol. Biol.* **18**, 277–282 (2011).
108. Abrusci, P. *et al.* Architecture of the major component of the type III secretion system export apparatus. *Nat. Struct. Mol. Biol.* **20**, 99–104 (2012).
109. Saijo-Hamano, Y. *et al.* Structure of the cytoplasmic domain of FlhA and implication for flagellar type III protein export. *Mol. Microbiol.* **76**, 260–268 (2010).
110. Minamino, T. *et al*. The Bacterial Flagellar Type III Export Gate Complex Is a Dual Fuel Engine That Can Use Both H^+ and Na^+ for Flagellar Protein Export. *PLoS Pathog.* **12**, e1005495 (2016).
111. Minamino, T. *et al*. An energy transduction mechanism used in bacterial

flagellar type III protein export. *Nat. Commun.* **2**, 475 (2011).

112. Barker, C. S. *et al*. Function of the conserved FHIPEP domain of the flagellar type III export apparatus, protein FlhA. *Mol. Microbiol.* **100**, 278-288 (2016).
113. Erhardt, M. *et al.* Mechanism of type-III protein secretion: Regulation of FlhA conformation by a functionally critical charged-residue cluster. *Mol. Microbiol.* **104**, 234–249 (2017).
114. Hartmann, N. & Büttner, D. The inner membrane protein HrcV from *Xanthomonas* spp. is involved in substrate docking during type III secretion. *Mol. Plant. Microbe. Interact.* **26**, 1176–89 (2013).
115. Kinoshita, M. *et al*. Interactions of bacterial flagellar chaperone-substrate complexes with FlhA contribute to co-ordinating assembly of the flagellar filament. *Mol. Microbiol.* **90**, 1249–1261 (2013).
116. Minamino, T. *et al.* Interaction of a bacterial flagellar chaperone FlgN with FlhA is required for efficient export of its cognate substrates. *Mol. Microbiol.* **83**, 775–788 (2012).
117. Van Arnam, J. S. *et al*. Analysis of an Engineered *Salmonella* Flagellar Fusion Protein, FliR-FlhB. *J. Bacteriol.* **186**, 2495-2498 (2004).
118. Eichelberg, K. *et al*. Molecular and functional characterization of the *Salmonella* Typhimurium invasion genes invB and invC: Homology of InvC to the F_0F_1 ATPase family of proteins. *J. Bacteriol.* **176**, 4501–4510 (1994).
119. Woestyn, S. *et al*. YscN, the putative energizer of the Yersinia Yop secretion machinery. *J. Bacteriol.* **176**, 1561–1569 (1994).
120. Akeda, Y. & Galán, J. E. Genetic Analysis of the *Salmonella enterica* Type III Secretion-Associated ATPase InvC Defines Discrete Functional Domains. *J. Bacteriol.* **186**, 2402–2412 (2004).
121. Imada, K. *et al*. Structural similarity between the flagellar type III ATPase FliI and F1-ATPase subunits. *Proc. Natl. Acad. Sci. U.S.A.* **104**, 485–90 (2007).
122. Claret, L. *et al*. Oligomerization and activation of the FliI ATPase central to bacterial flagellum assembly. *Mol. Microbiol.* **48**, 1349–1355 (2003).

123. Pallen, M. J. *et al*. Evolutionary links between FliH/YscL-like proteins from bacterial type III secretion systems and second-stalk components of the F_oF_1 and vacuolar ATPases. *Protein Sci.* **15**, 935–941 (2006).
124. Baba, M. *et al.* Rotation of artificial rotor axles in rotary molecular motors. *Proc. Natl. Acad. Sci. U.S.A.* **113**, 11214-11219 (2016).
125. Collazo, C. M. & Galán, J. E. Requirement for exported proteins in secretion through the invasion- associated type III system of *Salmonella* Typhimurium. *Infect. Immun.* **64**, 3524–3531 (1996).
126. Kaniga, K. *et al*. Homologs of the Shigella IpaB and IpaC invasins are required for *Salmonella* Typhimurium entry into cultured epithelial cells. *J. Bacteriol.* **177**, 3965–3971 (1995).
127. Anderson, D. M. A mRNA Signal for the Type III Secretion of Yop Proteins by *Yersinia enterocolitica*. *Science.* **278**, 1140–1143 (1997).
128. Anderson, D. M. & Schneewind, O. *Yersinia enterocolitica* type III secretion: An mRNA signal that couples translation and secretion of YopQ. *Mol. Microbiol.* **31**, 1139–1148 (1999).
129. Ramamurthi, K. S. & Schneewind, O. *Yersinia enterocolitica* type III secretion: Mutational analysis of the yopQ secretion signal. *J. Bacteriol.* **184**, 3321–3328 (2002).
130. Majander, K. *et al.* Extracellular secretion of polypeptides using a modified *Escherichia coli* flagellar secretion apparatus. *Nat. Biotechnol.* **23**, 475–481 (2005).
131. Mudgett, M. B. *et al.* Molecular signals required for type III secretion and translocation of the *Xanthomonas campestris* AvrBs2 protein to pepper plants. *Proc Natl Acad Sci U.S.A* **97**, 13324–13329 (2000).
132. Rüssmann, H. *et al*. Molecular and functional analysis of the type III secretion signal of the *Salmonella enterica* InvJ protein. *Mol. Microbiol.* **46**, 769–779 (2002).
133. Lloyd, S. A. *et al*. *Yersinia* YopE is targeted for type III secretion by N-terminal, not mRNA, signals. *Mol. Microbiol.* **39**, 520–531 (2001).
134. Lloyd, S. A. *et al*. Molecular characterization of type III secretion signals via analysis of synthetic N-terminal amino acid sequences. *Mol.*

Microbiol. **43**, 51–59 (2002).

135. Wang, Y. *et al*. High-accuracy prediction of bacterial type III secreted effectors based on position-specific amino acid composition profiles. *Bioinformatics* **27**, 777–784 (2011).
136. Wang, Y. *et al*. Effective Identification of Bacterial Type III Secretion Signals Using Joint Element Features. *PLoS One.* **8**, e59754 (2013).
137. Niemann, G. S. *et al.* RNA type III secretion signals that require Hfq. *J. Bacteriol.* **195**, 2119–2125 (2013).
138. Kuwajima, G. *et al.* Export of an N-terminal fragment of *Escherichia coli* flagellin by a flagellum-specific pathway. *Proc. Natl. Acad. Sci. U.S.A.* **86**, 4953-4957 (2006).
139. Minamino, T. & Macnab, R. M. Components of the *Salmonella* flagellar export apparatus and classification of export substrates. *J. Bacteriol.* **181**, 1388-1394 (1999).
140. Kornacker, M. G. & Newton, A. Information essential for cell-cycle-dependent secretion of the 591-residue *Caulobacter* hook protein is confined to a 21-amino-acid sequence near the N-terminus. *Mol. Microbiol.* **14**, 73-85 (1994).
141. Evans, L. D. B. *et al*. A chain mechanism for flagellum growth. *Nature.* **504**, 287–290 (2013).
142. Végh, B. M. *et al*. Localization of the flagellum-specific secretion signal in *Salmonella* flagellin. *Biochem. Biophys. Res. Commun.* **345**, 93-98 (2006).
143. Michiels, T. *et al*. Secretion of Yop proteins by yersiniae. *Infect. Immun.* **58**, 2840–2849 (1990).
144. Miao, E. A. & Miller, S. I. A conserved amino acid sequence directing intracellular type III secretion by *Salmonella* Typhimurium. *Proc. Natl. Acad. Sci. U.S.A.* **97**, 7539–7544 (2000).
145. Sory, M.-P *et al*. Identification of the YopE and YopH domains required for secretion and internalization into the cytosol of macrophages, using the cyaA gene fusion approach. *Microbiology.* **92**, 11998–12002 (1995).
146. Samudrala, R. *et al*. Accurate prediction of secreted substrates and

identification of a conserved putative secretion signal for type iii secretion systems. *PLoS Pathog.* **5**, e1000375 (2009).

147. Löwer, M. & Schneider, G. Prediction of type III secretion signals in genomes of gram-negative bacteria. *PLoS One* **4**, e5917 (2009).
148. Guttman, D. S. A Functional Screen for the Type III (Hrp) Secretome of the Plant Pathogen *Pseudomonas syringae*. *Science.* **295**, 1722–1726 (2002).
149. Stebbins, C. E. & Galán, J. E. Maintenance of an unfolded polypeptide by a cognate chaperone in bacterial type III secretion. *Nature.* **414**, 77–81 (2001).
150. Lilic, M. *et al*. A common structural motif in the binding of virulence factors to bacterial secretion chaperones. *Mol. Cell.* **21**, 653-664 (2006).
151. Stebbins, C. E. & Galán, J. E. Priming virulence factors for delivery into the host. *Nat. Rev. Mol. Cell Biol.* **4**, 738–743 (2003).
152. Namba, K. Roles of partly unfolded conformations in macromolecular self-assembly. *Genes Cells.* **6**, 1–12 (2001).
153. Vonderviszt, F. *et al*. Terminal regions of flagellin are disordered in solution. *J. Mol. Biol.* **209**, 127–133 (1989).
154. Vonderviszt, F. *et al*. Terminal disorder: A common structural feature of the axial proteins of bacterial flagellum. *J. Mol. Biol.* **226**, 575–579 (1992).
155. Wang, Y. *et al.* Differences in the Electrostatic Surfaces of the Type III Secretion Needle Proteins PrgI, BsaL, and MxiH. *J. Mol. Biol.* **371**, 1304–1314 (2007).
156. Evans, L. D. B. *et al. Interactions of flagellar structural subunits with the membrane export machinery*. *Methods. Mol. Biol.* **1593**, 17-35 (2017).
157. Bergeron, J. R. C. *et al.* The Structure of a type 3 secretion system (T3SS) ruler protein suggests a molecular mechanism for needle length sensing. *J. Biol. Chem.* **291**, 1676-1691(2016).
158. Ho, O. *et al.* Characterization of the ruler protein interaction interface on the substrate specificity switch protein in the *Yersinia* type III secretion system. *J. Biol. Chem.* **292**, 3299-3311 (2017).

159. Edqvist, P. J. *et al.* YscP and YscU regulate substrate specificity of the *Yersinia* type III secretion system. *J. Bacteriol.* **185**, 2259-2266 (2003).
160. Journet, L. *et al*. The Needle Length of Bacterial Injectisomes Is Determined by a Molecular Ruler. *Science.* **302**, 1757-1760 (2003).
161. Hughes, K. T. Flagellar Hook Length Is Controlled by a Secreted Molecular Ruler. *J. Bacteriol.* **194**, 4793-4796 (2012).
162. Kinoshita, M. *et al*. The role of intrinsically disordered C-terminal region of FliK in substrate specificity switching of the bacterial flagellar type III export apparatus. *Mol. Microbiol.* **105**, 572-588 (2017).
163. Bennett, J. C. Q. & Hughes, C. From flagellum assembly to virulence: The extended family of type III export chaperones. *Trends Microbiol.* **8**, 202-204 (2000).
164. Wattiau, P. & Cornells, G. R. SycE, a chaperone-like protein of *Yersinia enterocolitica* involved in the secretion of YopE. *Mol. Microbiol.* **8**, 123-131 (1993).
165. d'Enfert, C. Yet another chaperone?. *Trends Microbiol.* **1**, 161-162 (1993).
166. Kutsukake, K. *et al*. Two novel regulatory genes, fliT and fliZ, in the flagellar regulon of *Salmonella*. *Genes Genet. Syst.* **74**, 287–292 (1999).
167. Galeva, A. *et al.* Bacterial flagellin-specific chaperone FliS interacts with anti-sigma factor FlgM. *J. Bacteriol.* **196**, 1215-1221 (2014).
168. Xu, S. *et al.* FliS modulates FlgM activity by acting as a non-canonical chaperone to control late flagellar gene expression, motility and biofilm formation in *Yersinia pseudotuberculosis*. *Environ. Microbiol.* **16**, 1090-1104 (2014).
169. Büttner, D. *et al*. HpaB from *Xanthomonas campestris* pv. vesicatoria acts as an exit control protein in type III-dependent protein secretion. *Mol. Microbiol.* **54**, 755-768 (2004).
170. Porter, S. B. & Curtiss, R. Effect of Inv Mutations on *Salmonella* Virulence and Colonization in 1-Day-Old White Leghorn Chicks. *Avian Dis.* **41**, 45-57 (2006).
171. Plé, S. *et al*. Cochaperone interactions in export of the Type III needle

component PscF of *Pseudomonas aeruginosa*. *J. Bacteriol.* **192**, 3801–3808 (2010).

172. Fraser, G. M. *et al*. Substrate-specific binding of hook-associated proteins by FlgN and FliT, putative chaperones for flagellum assembly. *Mol. Microbiol.* **32**, 569–580 (1999).
173. Gygi, D. *et al*. A motile but non-swarming mutant of *Proteus mirabilis* lacks FlgN, a facilitator of flagella filament assembly. *Mol. Microbiol.* **25**, 597–604 (1997).
174. Renault, T. T. *et al.* Bacterial flagella grow through an injection-diffusion mechanism. *Elife* **6**, e23136 (2017).
175. Young, R. & Bremer, H. Polypeptide-chain-elongation rate in *Escherichia coli* B/r as a function of growth rate. *Biochem. J.* **160**, 185-194 (2015).
176. Thomas, J. *et al*. Docking of cytosolic chaperone-substrate complexes at the membrane ATPase during flagellar type III protein export. *Proc. Natl. Acad. Sci. U.S.A.* **101**, 3945-3950 (2004).
177. Bange, G. *et al.* FlhA provides the adaptor for coordinated delivery of late flagella building blocks to the type III secretion system. *Proc. Natl. Acad. Sci. U.S.A.* **107**, 11295–11300 (2010).
178. Ozin, A. J. *et al*. The FliS chaperone selectively binds the disordered flagellin C-terminal D_0 domain central to polymerisation. *FEMS Microbiol. Lett.* **219**, 219–224 (2003).
179. Evdokimov, A. G. *et al.* Similar modes of polypeptide recognition by export chaperones in flagellar biosynthesis and type III secretion. *Nat. Struct. Biol.* **10**, 789–93 (2003).
180. Imada, K. *et al*. Structural insight into the regulatory mechanisms of interactions of the flagellar type III chaperone FliT with its binding partners. *Proc. Natl. Acad. Sci. U.S.A.* **107**, 8812–8817 (2010).
181. Kinoshita, M. *et al.* Rearrangements of α-helical structures of FlgN chaperone control the binding affinity for its cognate substrates during flagellar type III export. *Mol. Microbiol.* **101**, 656–670 (2016).
182. Yokoseki, T. *et al*. Functional analysis of the flagellar genes in the fliD operon of *Salmonella* Typhimurium. *Microbiology* **141**, 1715–1722

(1995).

183. Auvray, F. *et al*. Flagellin polymerisation control by a cytosolic export chaperone. *J. Mol. Biol.* **308**, 221–229 (2001).
184. Quinaud, M. *et al.* Structure of the heterotrimeric complex that regulates type III secretion needle formation. *Proc. Natl. Acad. Sci. U.S.A.* **104**, 7803–8 (2007).
185. Sun, P. *et al*. Structural Characterization of the *Yersinia pestis* Type III Secretion System Needle Protein YscF in Complex with Its Heterodimeric Chaperone YscE/YscG. *J. Mol. Biol.* **377**, 819-830 (2008).
186. Chatterjee, C. *et al.* Crystal structure of the heteromolecular chaperone, AscE-AscG, from the type III secretion system in *Aeromonas hydrophila*. *PLoS One.* **6**, e19208 (2011).
187. Johnson, S. *et al.* Self-chaperoning of the type III secretion system needle tip proteins IpaD and BipD. *J. Biol. Chem.* **282**, 4035–4044 (2007).
188. Lee, P.-C. *et al*. Control of type III secretion activity and substrate specificity by the cytoplasmic regulator PcrG. *Proc. Natl. Acad. Sci. U.S.A.* **111**, E2027–E2036 (2014).
189. Skrzypek, E. & Straley, S. C. LcrG, a secreted protein involved in negative regulation of the low- calcium response in *Yersinia pestis*. *J. Bacteriol.* **175**, 3520-3528 (1993).
190. DeBord, K. L. *et al*. Roles of LcrG and LcrV during type III targeting of effector Yops by *Yersinia enterocolitica*. *J. Bacteriol.* **183**, 4588-4598 (2001).
191. Matson, J. S. & Nilles, M. L. LcrG-LcrV interaction is required for control of Yops secretion in *Yersinia pestis*. *J. Bacteriol.* **183**, 5082-5091 (2001).
192. Blocker, A. *et al.* The tripartite type III secreton of *Shigella flexneri* inserts IpaB and IpaC into host membranes. *J. Cell Biol.* **147**, 683–693 (1999).
193. Collazo, C. M. & Galán, J. E. The invasion-associated type III system of *Salmonella* Typhimurium directs the translocation of Sip proteins into the host cell. *Mol. Microbiol.* **24**, 747-756 (1997).
194. Neyt, C. & Cornelis, G. R. Insertion of a Yop translocation pore into the

macrophage plasma membrane by *Yersinia enterocolitica*: Requirement for translocators YopB and YopD, but not LcrG. *Mol. Microbiol.* **33**, 971-981 (1999).

195. Ghosh, P. Process of protein transport by the type III secretion system. *Microbiol. Mol. Biol. Rev.* **68**, 771–95 (2004).
196. Bröms, J. E. *et al*. Tetratricopeptide repeats are essential for PcrH chaperone function in *Pseudomonas aeruginosa* type III secretion. *FEMS Microbiol. Lett.* **256**, 57–66 (2006).
197. Schreiner, M. & Niemann, H. H. Crystal structure of the Yersinia enterocolitica type III secretion chaperone SycD in complex with a peptide of the minor translocator YopD. *BMC Struct. Biol.* **12**, 13 (2012).
198. Lunelli, M. *et al.* IpaB-IpgC interaction defines binding motif for type III secretion translocator. *Proc. Natl. Acad. Sci. U.S.A.* **106**, 9661–9666 (2009).
199. Discola, K. F. *et al.* Membrane and Chaperone recognition by the major Translocator Protein PopB of the Type III secretion system of *Pseudomonas aeruginosa*. *J. Biol. Chem.* **289**, 3591-3601 (2014).
200. Job, V. *et al*. Structural basis of chaperone recognition of type III secretion system minor translocator proteins. *J. Biol. Chem.* **285**, 23224-23232 (2010).
201. Thomas, N. A. *et al*. Expanded roles for multicargo and class 1B effector chaperones in type III secretion. *J. Bacteriol.* **194**, 3767–3773 (2012).
202. Birtalan, S. C. *et al*. Three-dimensional secretion signals in chaperone-effector complexes of bacterial pathogens. *Mol. Cell.* **9**, 971-980 (2002).
203. Vujanac, M. & Stebbins, C. E. Context-dependent protein folding of a virulence peptide in the bacterial and host environments: Structure of an SycH-YopH chaperone-effector complex. *Acta Crystallogr. Sect. D Biol. Crystallogr.* **69**, 546–554 (2013).
204. Halavaty, A. S. *et al.* Structure of the Type III Secretion Effector Protein ExoU in Complex with Its Chaperone SpcU. *PLoS One.* **7**, e49388 (2012).
205. Letzelter, M. *et al.* The discovery of SycO highlights a new function for

type III secretion effector chaperones. *EMBO J.* **25**, 3223-3233 (2006).

206. Krampen, L. *et al.* Revealing the mechanisms of membrane protein export by virulence-associated bacterial secretion systems. *Nat. Commun.* **9**, 3467 (2018).
207. Thomas, J. *et al*. Docking of cytosolic chaperone-substrate complexes at the membrane ATPase during flagellar type III protein export. *Proc. Natl. Acad. Sci. U.S.A.* **101**, 3945–3950 (2004).
208. Akeda, Y. & Galán, J. E. Chaperone release and unfolding of substrates in type III secretion. *Nature.* **437**, 911–915 (2005).
209. Jackson, M. W. & Plano, G. V. Interactions between type III secretion apparatus components from *Yersinia pestis* detected using the yeast two-hybrid system. *FEMS Microbiol. Lett.* **186**, 85-90 (2000).
210. Lara-Tejero, M. *et al*. A Sorting Platform Determines the Order of Protein Secretion in Bacterial Type III Systems. *Science.* **331**, 1188–1191 (2011).
211. Francis, N. R. *et al*. Isolation, characterization and structure of bacterial flagellar motors containing the switch complex. *J. Mol. Biol.* **235**, 1261–70 (1994).
212. Hu, B. *et al.* Visualization of the type III secretion sorting platform of *Shigella flexneri*. *Proc. Natl. Acad. Sci. U.S.A.* **112**, 1047–52 (2015).
213. Notti, R. Q. *et al*. A common assembly module in injectisome and flagellar type III secretion sorting platforms. *Nat. Commun.* **6**, 7125 (2015).
214. Morita-Ishihara, T. *et al. Shigella* Spa33 is an essential C-ring component of type III secretion machinery. *J. Biol. Chem.* **281**, 599–607 (2006).
215. Lorenz, C. *et al*. HrcQ Provides a Docking Site for Early and Late Type III Secretion Substrates from Xanthomonas. *PLoS One.* **7**, e51063 (2012).
216. Kato, J. *et al*. Structural Features Reminiscent of ATP-Driven Protein Translocases Are Essential for the Function of a Type III Secretion-Associated ATPase. *J. Bacteriol.* **197**, 3007-3014 (2015).
217. Yoshida, Y. *et al.* Functional characterization of the type III secretion ATPase SsaN encoded by *Salmonella* pathogenicity island 2. *PLoS One.*

9, e94347 (2014).

218. Minamino, T. *et al*. The ATPase FliI can interact with the type III flagellar protein export apparatus in the absence of its regulator, FliH. *J. Bacteriol.* **185**, 3983-3988 (2003).
219. Bai, F. *et al.* Assembly dynamics and the roles of FliI ATPase of the bacterial flagellar export apparatus. *Sci. Rep.* **4**, 1–7 (2014).
220. Diepold, A. *et al.* A dynamic and adaptive network of cytosolic interactions governs protein export by the T3SS injectisome. *Nat. Commun.* **8**, 15940 (2017).
221. Stafford, G. P. *et al.* Sorting of Early and Late Flagellar Subunits After Docking at the Membrane ATPase of the Type III Export Pathway. *J. Mol. Biol.* **374**, 877–882 (2007).
222. Chen, L. *et al.* Substrate-Activated Conformational Switch on Chaperones Encodes a Targeting Signal in Type III Secretion. *Cell Rep.* **3**, 709–715 (2013).
223. Allison, S. E. *et al.* Identification of the docking site between a type III secretion system ATPase and a chaperone for effector cargo. *J. Biol. Chem.* **289**, 23734–23744 (2014).
224. Fraser, G. M. *et al*. Interactions of FliJ with the *Salmonella* type III flagellar export apparatus. *J. Bacteriol.* **185**, 5546-5554 (2003).
225. Evans, L. D. B. *et al*. Selective binding of virulence type III export chaperones by FliJ escort orthologues InvI and YscO. *FEMS Microbiol. Lett.* **293**, 292-297 (2009).
226. Evans, L. D. B. *et al*. An escort mechanism for cycling of export chaperones during flagellum assembly. *Proc. Natl. Acad. Sci. U.S.A.* **103**, 17474–9 (2006).
227. Xing, Q. *et al.* Structures of chaperone-substrate complexes docked onto the export gate in a type III secretion system. *Nat. Commun.* **9**, 1773 (2018).
228. Alegria, M. C. *et al.* New protein-protein interactions identified for the regulatory and structural components and substrates of the type III secretion system of the phytopathogen *Xanthomonas axonopodis*

pathovar citri. *J. Bacteriol.* **186**, 6186–6197 (2004).

229. Büttner, D. *et al*. Targeting of two effector protein classes to the type III secretion system by a HpaC- and HpaB-dependent protein complex from *Xanthomonas campestris* pv. vesicatoria. *Mol. Microbiol.* **59**, 513–527 (2006).
230. Furukawa, Y. *et al.* Structural stability of flagellin subunit affects the rate of flagellin export in the absence of FliS chaperone. *Mol. Microbiol.* **102**, 405–416 (2016).
231. Minamino, T. *et al.* Role of the C-terminal cytoplasmic domain of FlhA in bacterial flagellar type III protein export. *J. Bacteriol.* **192**, 1929–1936 (2010).
232. Inoue, Y. *et al.* Structural Insights into the Substrate Specificity Switch Mechanism of the Type III Protein Export Apparatus. *Structure.* **27**, 965-976 (2019).
233. Rathinavelan, T. *et al.* A repulsive electrostatic mechanism for protein export through the type III secretion apparatus. *Biophys. J.* **98**, 452-461 (2010).
234. Lee, P. C. & Rietsch, A. Fueling type III secretion. *Trends Microbiol.* **23**, 296-300 (2015).
235. Loquet, A. *et al.* Atomic model of the type III secretion system needle. *Nature.* **486**, 276-279 (2012).
236. Demers, J. P. *et al.* High-resolution structure of the *Shigella* type-III secretion needle by solid-state NMR and cryo-electron microscopy. *Nat. Commun.* **5**, 4976 (2014).
237. Singer, H. M. *et al.* Selective purification of recombinant neuroactive peptides using the flagellar type III secretion system. *MBio.* **3**, e00115-12. (2012).
238. Green, C. A. *et al.* Engineering the flagellar type III secretion system: Improving capacity for secretion of recombinant protein. *Microb. Cell Fact.* **18**, 10 (2019).
239. Minamino, T. *et al*. Interaction of FIiK with the bacterial flagellar hook is required for efficient export specificity switching. *Mol. Microbiol.* **74**, 239-

251 (2009).

240. Ohnishi, K. *et al*. FlgD is a scaffolding protein needed for flagellar hook assembly in *Salmonella* Typhimurium. *J. Bacteriol.* **176**, 2272-2281 (1994).
241. Truebestein L. *et al*. Coiled-coils: The long and short of it. *BioEssays.* **38**, 903-916 (2016).
242. O'Shea, E. K. *et al*. X-ray structure of the GCN4 leucine zipper, a two-stranded, parallel coiled coil. *Science.* **254**, 539-544 (1991).
243. Stern, A. S. & Berg, H. C. Single-file diffusion of flagellin in flagellar filaments. *Biophys. J.* **105**, 182-184 (2013).
244. Chen, M. *et al.* Length-dependent flagellar growth of *vibrio alginolyticus* revealed by real time fluorescent imaging. *Elife.* **6**, e22140 (2017).
245. Hoffmann, S. *et al*. Scarless deletion of up to seven methylaccepting chemotaxis genes with an optimized method highlights key function of CheM in *Salmonella* Typhimurium. *PLoS One.* **12**, e0172630 (2017).
246. Ward, E. *et al.* Type-III secretion pore formed by flagellar protein FliP. *Mol. Microbiol.* **107**, 94-103 (2018).
247. Miles, A. A. *et al*. The estimation of the bactericidal power of the blood. *J. Hyg. (Lond).* **38**, 732-749 (1938).
248. Minamino, T. & Macnab, R. M. Domain structure of *Salmonella* FlhB, a flagellar export component responsible for substrate specificity switching. *J. Bacteriol.* **182**, 4906-4914 (2000).
249. Khanra, N. *et al*. Recognition and targeting mechanisms by chaperones in flagellum assembly and operation. *Proc. Natl. Acad. Sci. U.S.A.* **113**, 9798–9803 (2016).
250. Masi, M. & Wandersman, C. Multiple signals direct the assembly and function of a type 1 secretion system. *J. Bacteriol.* **192**, 3861-3869 (2010).
251. Johnson, S. *et al*. The Structure of an Injectisome Export Gate Demonstrates Conservation of Architecture in the Core Export Gate between Flagellar and Virulence Type III Secretion Systems. *MBio.* **10**, e00818-19 (2019).

252. Dhillon, P. Recognition and discrimination of substrates in the flagellar type III secretion pathway. (2010).
253. Kuhlen, L. *et al.* The flagellar substrate specificity switch protein FlhB assembles onto the extra-membrane export gate to regulate type three secretion. *bioRxiv*. preprint at https://doi.org/10.1101/686782 (2019)
254. Weber-Sparenberg, C. *et al.* Characterization of the type III export signal of the flagellar hook scaffolding protein FlgD of *Escherichia coli*. *Arch. Microbiol.* **186**, 307-316 (2006).
255. Aizawa, S. I. *et al*. Termini of *Salmonella* flagellin are disordered and become organized upon polymerization into flagellar filament. *J. Mol. Biol.* **211**, 673-677 (1990).
256. Ibuki, T. *et al.* Interaction between FliJ and FlhA, components of the bacterial flagellar type III export apparatus. *J. Bacteriol.* **195**, 466-473 (2013).
257. Bergen, P. M. Characterisation of the structure and function of the *Salmonella* flagellar export gate protein, FlhB. (2017).
258. San Miguel, M. *et al*. An *Escherichia* coli twin-arginine signal peptide switches between helical and unstructured conformations depending on the hydrophobicity of the environment. *Eur. J. Biochem.* **270**, 3345-3352 (2003).
259. Zarivach, R. *et al.* Structural analysis of the essential self-cleaving type III secretion proteins EscU and SpaS. *Nature.* **453**, 124-127 (2008).
260. Galperin, M. Y. *et al*. ΔμH+ is required for flagellar growth in *Escherichia coli*. *FEBS Lett.* **143**, 319-322 (1982).
261. Kishikawa, J-I. *et al.* Common Evolutionary Origin for the Rotor Domain of Rotary Atpases and Flagellar Protein Export Apparatus. *PLoS One.* **8**, e64695. (2013).
262. Hara, N. *et al*. Genetic characterization of conserved charged residues in the bacterial flagellar type III export protein FlhA. *PLoS One* **6**, (2011).
263. Stafford, G. P. & Hughes, C. *Salmonella* Typhimurium flhE, a conserved flagellar regulon gene required for swarming. *Microbiology.* **153**, 541-547 (2007).

264. Van Den Berg, B. *et al.* X-ray structure of a protein-conducting channel. *Nature.* **427**, 36-44 (2004).
265. Saparov, S. M. *et al.* Determining the Conductance of the SecY Protein Translocation Channel for Small Molecules. *Mol. Cell.* **26**, 501-509 (2007).
266. Gumbart, J. & Schulten, K. The Roles of Pore Ring and Plug in the SecY Protein-conducting Channel. *J. Gen. Physiol.* **132**, 709-719 (2008).
267. Armbruster, C. E. *et al*. Arginine promotes *Proteus mirabilis* motility and fitness by contributing to conservation of the proton gradient and proton motive force. *Microbiologyopen.* **3**, 630-641 (2014).
268. Stock, D. *et al*. The rotary mechanism sf ATP synthase. *Curr. Opin. Struct. Biol.* **10**, 672-679 (2000).
269. Beyenbach, K. W & Wieczorek, H. The V-type H^+ ATPase: molecular structure and function, physiological roles and regulation. *J. Exp. Biol.* **209**, 577-589 (2006).
270. Gledhill, J. R. *et al*. How the regulatory protein, IF1, inhibits F1-ATPase from bovine mitochondria. *Proc. Natl. Acad. Sci. U.S.A.* **104**, 15671-15676 (2007).
271. McMurry, J. L. *et al*. Analysis of the cytoplasmic domains of *Salmonella* FlhA and interactions with components of the flagellar export machinery. *J. Bacteriol.* **186**, 7586-7592 (2004).
272. Minamino, T. *et al*. An energy transduction mechanism used in bacterial flagellar type III protein export. *Nat. Commun.* **2**, 475 (2011).
273. Gumbart, J. & Schulten, K. Molecular dynamics studies of the archaeal translocon. *Biophys. J.* **90**, 2356-2367 (2006).
274. Gumbart, J. & Schulten, K. Structural determinants of lateral gate opening in the protein translocon. *Biochemistry.* **46**, 11147-11157 (2007).
275. Bol, R. *et al*. The active protein-conducting channel of *Escherichia coli* contains an apolar patch. *J. Biol. Chem.* **282**, 29785-29793 (2007).
276. Economou, A. *et al*. SecA membrane cycling at SecYEG is driven by distinct ATP binding and hydrolysis events and is regulated by SecD and SecF. *Cell.* **83**,1171-1181(1995).

277. Zhou, J. & Xu, Z. The structural view of bacterial translocation-specific chaperone SecB: Implications for function. *Mol. Microbiol.* **58**, 349-357 (2005).
278. Hartl, F. U. *et al*. The binding cascade of SecB to SecA to SecY E mediates preprotein targeting to the *E. coli* plasma membrane. *Cell.* **63**, 269-279 (1990).
279. Kim, J. *et al*. Evidence that SecB enhances the activity of SecA. *Biochemistry.* **40**, 3674-3680 (2001).
280. Lara-Tejero, M. *et al*. A sorting platform determines the order of protein secretion in bacterial type III systems. *Science.* **331**, 1188-1191 (2011).
281. Ferris, H. U. *et al.* FlhB regulates ordered export of flagellar components via autocleavage mechanism. *J. Biol. Chem.* **280**, 41236-41242 (2005).
282. Fraser, G. M. *et al.* Substrate specificity of type III flagellar protein export in *Salmonella* is controlled by subdomain interactions in FlhB. *Mol. Microbiol.* **48**, 1043-1057 (2003).
283. Ingolia, N. T. *et al*. The ribosome profiling strategy for monitoring translation in vivo by deep sequencing of ribosome-protected mRNA fragments. *Nat. Protoc.* **7**, 1534-1550 (2012).
284. Chung, B. Y. *et al.* The use of duplex-specific nuclease in ribosome profiling and a user-friendly software package for Ribo-seq data analysis. *RNA.* **21**, 1731-1745 (2015).
285. Zhou, H. *et al.* Crystal structure of a novel dimer form of FlgD from *P. aeruginosa* PAO1. *Proteins.* **79**, 2346-2351 (2011).
286. Kuo, W.-T. *et al*. Crystal structure of the C-terminal domain of a flagellar hook-capping protein from Xanthomonas campestris. *J. Mol. Biol.* **381**, 189-199 (2008).
287. Mizuno, S. *et al*. The NMR structure of FliK, the trigger for the switch of substrate specificity in the flagellar type III secretion apparatus. *J. Mol. Biol.* **409**, 558-573 (2011).
288. Aldridge, P. *et al*. The type III secretion chaperone FlgN regulates flagellar assembly via a negative feedback loop containing its chaperone substrates FlgK and FlgL. *Mol. Microbiol.* **49**, 1333-1345 (2003).

289. Dalbey, R. E. *et al*. Assembly of Bacterial Inner Membrane Proteins. *Annu. Rev. Biochem.* **80**, 161-187 (2011).
290. Minamino, T. *et al*. Interaction between FliI ATPase and a flagellar chaperone FliT during bacterial flagellar protein export. *Mol. Microbiol.* **83**, 168–178 (2012).
291. Ahmed, S. Functional analysis of the *Salmonella* flagellar export chaperone FlgN. Sangita Ahmed (2010).
292. Akeda, Y. & Galán, J. E. Chaperone release and unfolding of substrates in type III secretion. *Nature.* **437**, 911-915 (2005).
293. Minamino, T. *et al*. Role of FliJ in flagellar protein export in Salmonella. *J. Bacteriol.* **182**, 4207–4215 (2000).
294. Fraser, G. M. *et al.* Interactions of FliJ with the *Salmonella* type III flagellar export apparatus. *J. Bacteriol.* **185**, 5546–5554 (2003).
295. Schleiff, E. & Becker, T. Common ground for protein translocation: Access control for mitochondria and chloroplasts. *Nat. Rev. Mol. Cell. Biol.* **12**, 48-59 (2011).
296. Yamamoto, S. & Kutsukake, K. FliT acts as an anti-$FlhD_2C_2$ factor in the transcriptional control of the flagellar regulon in *Salmonella enterica* serovar typhimurium. *J. Bacteriol.* **188**, 6703–6708 (2006).
297. Imada, K. *et al*. Structural insight into the regulatory mechanisms of interactions of the flagellar type III chaperone FliT with its binding partners. *Proc. Natl. Acad. Sci. U.S.A*. **107**, 8812–8817 (2010).
298. Zierler, M. K. & Galan, J. E. Contact with cultured epithelial cells stimulates secretion of *Salmonella* typhimurium invasion protein InvJ. *Infect. Immun.* **63**, 4024-4028 (1995).
299. Lee, P. C. *et al*. Control of type III secretion activity and substrate specificity by the cytoplasmic regulator PcrG. *Proc. Natl. Acad. Sci. U.S.A.* **111**, E2027-E2036 (2014).
300. Minamino, T. & Macnab, R. M. FliH, a soluble component of the type III flagellar export apparatus of *Salmonella*, forms a complex with FliI and inhibits its ATPase activity. *Mol. Microbiol.* **37**, 1494-1503 (2000).
301. Cabezón, E. *et al*. The structure of bovine IF1, the regulatory subunit of

mitochondrial F-ATPase. *EMBO J.* **20**, 6990-6996 (2002).

302. Morales-Ríos, E. *et al.* A novel 11-kDa inhibitory subunit in the F 1 F O ATP synthase of *Paracoccus denitrificans* and related α-proteobacteria. *FASEB J.* **24**, 599-608 (2009).
303. Morales-Rios, E. *et al*. Structure of ATP synthase from *Paracoccus denitrificans* determined by X-ray crystallography at 4.0 Å resolution. *Proc. Natl. Acad. Sci. U.S.A.* **112**, 13231-13236 (2015).
304. Mendoza-Hoffmann, F. *et al.* The Biological Role of the ζ Subunit as Unidirectional Inhibitor of the F_1F_O-ATPase of *Paracoccus denitrificans*. *Cell Rep.* **22**, 1067-1078 (2018).
305. Laget, P. P. & Smith, J. B. Inhibitory properties of endogenous subunit Epsilon in the *Escherichia coli* F_1 ATPase. *Arch. Biochem. Biophys.* **197**, 83-89(1979).
306. Kato-Yamada, Y. *et al.* ε Subunit, an endogenous inhibitor of bacterial F_1-ATPase, also inhibits F_0F_1-ATPase. *J. Biol. Chem.* **274**, 33991-33994 (1999).
307. Yagi, H. *et al.* Structural and functional analysis of the intrinsic inhibitor subunit ε of F_1 -ATPase from photosynthetic organisms . *Biochem. J.* **425**, 85-94 (2009).
308. Kato-Yamada, Y. Isolated ε subunit of *Bacillus subtilis* F_1 -ATPase binds ATP. *FEBS Lett.* **579**, 6875-6878 (2005).
309. Feniouk, B. A. *et al*. The role of subunit epsilon in the catalysis and regulation of F_0F_1-ATP synthase. *Biochim. Biophys. Acta.* **1757**, 326-338 (2006).
310. Xu, T. & Forgac, M. Subunit D (Vma8p) of the yeast vacuolar H^+-ATPase plays a role in coupling of proton transport and ATP hydrolysis. *J. Biol. Chem.* **275**, 22075-22081 (2000).
311. Spöring, I. *et al.* Regulation of Flagellum Biosynthesis in Response to Cell Envelope Stress in *Salmonella enterica* Serovar Typhimurium. *MBio.* **9**, e00736-17. (2018).
312. Adams, P. *et al.* Proteomic detection of PhoPQ- and acid-mediated repression of *Salmonella* motility. *Proteomics.* **1**, 597-607 (2005).

313. Miao, E. A. & Rajan, J. V. *Salmonella* and Caspase-1: A complex interplay of detection and evasion. *Front. Microbiol.* **2**, 85 (2011).
314. Yamaguchi, S. *et al.* Genetic analysis of three additional fla genes in *Salmonella* typhimurium. *J. Gen. Microbiol.* **130**, 3339-3342 (1984).
315. Bennett, J. C. Q. *et al*. Substrate complexes and domain organization of the *Salmonella* flagellar export chaperones FlgN and FliT. *Mol. Microbiol.* **39**, 781–791 (2001).
316. Miroux, B. & Walker, J. E. Over-production of proteins in *Escherichia coli*: Mutant hosts that allow synthesis of some membrane proteins and globular proteins at high levels. *J. Mol. Biol.* **260**, 289-298 (1996).
317. Harper, S. & Speicher, D. W. Purification of proteins fused to glutathione S-transferase. *Methods Mol. Biol.* **681**, 259-280 (2011).

Appendix A

A1.1. Reagents, buffers and media

Name	Composition
Luria-Bertani (LB) broth	1% w/v tryptone, 0.5% w/v yeast extract, 1% w/v NaCl
Luria-Bertani (LB) agar	1% w/v tryptone, 0.5% w/v yeast extract, 1% w/v NaCl, 1.5% w/v agar
Terrific broth	1.2% w/v tryptone 2.4% w/v yeast extract, 0.4% w/v glycerol, 17 mM KH_2PO_4 72 mM K_2HPO_4
Motility agar	1% w/v tryptone, 0.5% w/v NaCl, 0.25% w/v agar
2x yeast tryptone (2xYT) broth	1.6% tryptone, 1% yeast extract, 0.5% w/v NaCl
Super optimal broth with catabolite repression (SOC)	2% w/v tryptone, 0.5% w/v yeast extract, 2.5 mM KCl, 10 mM NaCl 10 mM $MgCl_2$ 20 mM glucose
SDS loading dye (2x)	100 mM Tris-HCl pH. 6.8, 4% w/v SDS (sodium dodecyl sulphate), 0.2% w/v bromophenol blue, 20% w/v glycerol, 100 mM β-mercaptoethanol
SDS running buffer (1x)	25 mM Tris-HCl pH 8.0, 192 mM glycine, 0.1% w/v SDS
Transfer buffer (1x)	10 mM cyclohexyl-3-aminopropanesulfonic acid (CAPS) pH 11.0, 10% v/v methanol
Tris-Acetate-EDTA (TAE) buffer (1x)	40 mM Tris base, 20 mM Acetic acid, 1 mM EDTA

Tris/Borate/EDTA (TBE) buffer (1x)	90 mM Tris, 90 mM boric acid, 2 mM EDTA
Phosphate buffered saline (PBS) (1x)	137 mM NaCl, 2.7 mM KCl, 10 mM Na_2HPO_4, 1.8 mM KH_2PO_4,
Phosphate buffered saline containing Triton X-100 (PBST) (1x)	137 mM NaCl, 2.7 mM KCl, 10 mM Na_2HPO_4, 1.8 mM KH_2PO_4, 0.05% Triton X-100
Profiling buffer	20 mM Tris-HCL, 140 mM KCl, 5 mM $MgCl_2$, 0.5% w/v NP-40, 1% v/v Triton X-100 35% PGB 0.5 mM DTT, 1500 µg/ml chloramphenicol 100 U/ml DNase I
2x fragmentation buffer	2 mM EDTA pH 8.0, 12 mM Na_2CO_3, 90 mM $NaHCO_3$
Alkaline hydrolysis stop solution	0.3 M $NaCH_3COO$
RNA acrylamide gel extraction buffer	0.3 M $NaCH_3COO$, 1 mM EDTA, 0.25% w/v SDS, 10 mM Tris-HCl pH 7.5
DNA acrylamide gel extraction buffer	0.3 M NaCl, 1 mM EDTA, 10 mM Tris-HCl
4X hybridisation buffer	200 mM HEPES pH 7.5, 2 M NaCl
Buffer A	25 mM Tris-HCl, 500 mM NaCl, 20 mM imidazole
Buffer B	25 mM Tris-HCl, 150 mM NaCl, 500 mM imidazole
Buffer C	25 mM Tris-HCl, 150 mM NaCl
Buffer D	50 mM sodium phosphate pH 7.4, 150 mM NaCl, 20 mM imidazole, 1 mM β -mercaptoethanol

Buffer E	50 mM sodium phosphate pH 7.4, 150 mM NaCl, 1 mM β -mercaptoethanol

A1.2. Strains and recombinant plasmids

Strains	Description	Source
Salmonella enterica serovar Typhimurium		
SJW1103	wild type	[314]
recA null	Δ*recA*::Km^R	This study
flgD null	Δ*flgD*::Km^R	[141]
fliP(M210A)$_{internalHAtag}$, *flgD* null	*fliP*(M210A) 21(3xHA tag)22, Δ*flgD*::Km^R	This study
fliP$_{internalHAtag}$, *flgD* null	*fliP* 21(3xHA tag)22, Δ*flgD*::Km^R	This study
fliR(F110A)	*fliR* F110A variant	This study
fliR(F113A)	*fliR* F113A variant	This study
fliR(F110A, F113A)	*fliR* F110A, F133A variant	This study
fliR(G117D)	*fliR* G117D variant	This study
fliR(F110A), *flgD* null	*fliR* F110A variant, Δ*flgD*::Km^R	This study
fliR(F113A), *flgD* null	*fliR* F113A variant, Δ*flgD*::Km^R	This study
fliR(F110A, F113A), *flgD* null	*fliR* F110A, F133A variant, Δ*flgD*::Km^R	This study
fliR(G117D), *flgD* null	*fliR* G117D variant, Δ*flgD*::Km^R	This study
fliR(Δ110-116)	*fliR* Δ110-116 variant	This study
fliR(Δ110-116), *flgBCDEFGHIJ null*	*fliR* Δ110-116 variant, Δ*flgBCDEFGHIJ*:: Km^R	This study
flgBCDEFGHIJ null	Δ*flgBCDEFGHIJ*:: Km^R	This study
flhA(K203A)	*flhA* K203A variant	This study
flhA(K203A), *fliR*(F113A)	*flhA* K203A variant, *fliR* F113A variant	This study
flhA(K203A), *fliR*(G117D)	*flhA* K203A variant, *fliR* G117D variant	This study
flhA(K203A), *adiA* null, *speA* null	*flhA* K203A variant, Δ*adiA*::Km^R, Δ*speA*::Sm^R	This study

adiA null, *speA* null	Δ*adiA*::Km^R, Δ*speA*::Sm^R	This study
fliR(F113A), *fliHI* null, *flgM* null	*fliR* F113A variant, Δ*fliHI*, Δ*flgM*::Sm^R	This study
fliR(G117D), *fliHI* null, *flgM* null	*fliR* F113A variant, Δ*fliHI*, Δ*flgM*::Sm^R	This study
flhB(P28T), *fliHI* null, *flgM* null	*flhB* P28T variant, Δ*fliHI*, Δ*flgM*::Sm^R	This study
fliHI null, *flgM* null	Δ*fliHI*, Δ*flgM*::Sm^R	This study
flhB(P28T), *flgD* null	*fliR F113A* variant, Δ*flgD*::Km^R	This study
flhA(A113E)	*flhA* A113E variant	This study
flhA(G115C)	*flhA* G115C variant	This study
flhA(V134L)	*flhA* V134L variant	This study
flhA(A181T)	*flhA* A181T variant	This study
flhA(A113E), *flgD* null	*flhA* A113E variant, Δ*flgD*::Km^R	This study
flhA(G115C), *flgD* null	*flhA* G115C variant, Δ*flgD*::Km^R	This study
flhA(V134L), *flgD* null	*flhA* V134L variant, Δ*flgD*::Km^R	This study
flhA(A181T), *flgD* null	*flhA* A181T variant, Δ*flgD*::Km^R	This study
flgE null	Δ*flgE*::No resistance	141
flhB P238A, N269A	*flhB* P238A, N269A variant	This study
flhB P28T, *FliHI* null, *flgM* null, *fliMN* null	*flhB* P28T, Δ*fliHI*::No resistance, Δ*flgM*::Sm^R Δ*fliMN*::Km^R	This study
flgN null	Δ*flgN*::Km^R	315
flhB P28T, *FliHI* null, *flgM* null	*flhB* P28T, Δ*fliHI*::No resistance, Δ*flgM*::Sm^R	This study
(his)6-FliJ	Nt-(His)6-fliJ	This study
(his)6-FliJ, flgN null	Nt-(His)6-fliJ, Δ*flgN*::Km^R	This study

flgN(Y122A)	*flgN* Y122A variant	This study
*flgN(*Δ112-121)	*flgN* 1-111, 122-140aa	This study
flgN(Δ90-100)	*flgN* 1-89, 101-140aa	This study
flgN(Δ120-140)	*flgN* 1-119aa	This study
flhB P28T, *FliHIJ* null, *flgM* null	*flhB* P28T, Δ*fliHIJ*::No resistance, Δ*flgM*::Sm^R	This study
flgN W78A	*flgN* W78A variant	This study
flgN Δ76-78	*flgN* 1-75, 79-140aa	This study
flgN Δ90-100	*flgN* 1-89, 101-140aa	This study
fliT(L72A)	*fliT* L72A variant	This study
fliT(Y106A)	*fliT* Y106A variant	This study
fliT null	*fliT*::Cm^R	315
Escherichia coli		
C41	*F ompT gal dcm hsdS$_B$ (r_B^- m_B^-)*[32]	316
TOP10	F- *mcrA* Δ(*mrr-hsd*RMS-*mcr*BC) Φ80*lac*ZΔM15 Δ *lac*X74 *rec*A1 *ara*D139 Δ(*araleu*)7697 *gal* U *gal*K *rps*L (Str^R) *end*A1 *nup*G	Laboratory stock
Plasmids		
pTrc99a FlgD	1-232aa	This study
pTrc99a FlgDΔ2-5	1, 6-232aa	This study
pTrc99a FlgDΔ2-5, Δ36-40	1, 6-35, 41-232aa	This study
pTrc99a FlgDΔ2-5, M7I	1, 6-232aa, M7I	This study
pTrc99a FlgDΔ2-5, M7V	1, 6-232aa, M7V	This study

pTrc99a FlgDΔ2-5, N8I	1, 6-232aa, N8I	This study
pTrc99a FlgDΔ2-5, D9A	1, 6-232aa, D9A	This study
pTrc99a FlgDΔ2-5, P10L	1, 6-232aa, P10L	This study
pTrc99a FlgDΔ2-5, T11I	1, 6-232aa, T11I	This study
pTrc99a FlgDΔ2-5, 23(TTGSGS)24	1-19, Thr-Thr-Gly-Ser-Gly-Ser, 20-232aa	This study
pTrc99a FlgDΔ2-5, 23(TTGSGSTTGSGS)24	1-19, Thr-Thr-Gly-Ser-Gly-Ser- Thr-Thr-Gly-Ser-Gly-Ser, 20-232aa	This study
pTrc99a FlgDΔ2-5, 27(GSMTGS)28	1-19, Gly-Ser-Met-Thr-Gly-Ser, 20-232aa	This study
pTrc99a FlgDΔ2-5, 19(AGAGAG)20	1-19, Ala-Gly-Ala-Gly-Ala-Gly, 20-232aa	This study
pTrc99a FlgDΔ2-5, 19(STSTST)20	1-19, Ser-Thr-Ser-Thr-Ser-Thr, 20-232aa	This study
pTrc99a FlgDΔ2-5, 19(GSGSMT)20	1-19, Gly-Ser-Gly-Ser-Met-Thr, 20-232aa	This study
pTrc99a FlgDΔ2-5, 19(GSGSMT)20, V15A	1-19, Gly-Ser-Gly-Ser-Met-Thr, 20-232aa, V15A	This study
pTrc99a FlgDΔ2-5, 19(GSGSMT)20, V15A, M7I	1-19, Gly-Ser-Gly-Ser-Met-Thr, 20-232aa, V15A, M7I	This study
pTrc99a FlgDΔ2-5, 19(GSGSMT)20, V15A, D9A	1-19, Gly-Ser-Gly-Ser-Met-Thr, 20-232aa, V15A, D9A	This study
pTrc99a FlgDΔ2-5, 19(GSGSMT)20, V15A, T11I	1-19, Gly-Ser-Gly-Ser-Met-Thr, 20-232aa, V15A, T11I	This study
pTrc99a FlgDΔ2-5, 19(GSGSMT)20, V15A, G14V	1-19, Gly-Ser-Gly-Ser-Met-Thr, 20-232aa, V15A, G14V	This study
pTrc99a FlgDΔ9-32, 8(4xGSTNAS)33	1-8, 4x(Gly-Ser-Thr-Asn-Ala-Ser), 33-232aa	This study

pTrc99a FlgDΔ9-32, 8(3xGSTNAS)33	1-8, 3x(Gly-Ser-Thr-Asn-Ala-Ser), 33-232aa	This study
pTrc99a FlgDΔ9-32, 8(2xGSTNAS)33	1-8, 2x(Gly-Ser-Thr-Asn-Ala-Ser), 33-232aa	This study
pTrc99a FlgDΔ9-32, 8(1xGSTNAS)33	1-8, Gly-Ser-Thr-Asn-Ala-Ser, 33-232aa	This study
pTrc99a FlgDΔ9-32	1-8, 33-232aa	This study
pTrc99a FlgDΔ9-32, 8(G, 2xGSTNAS)33	1-8, Gly, 2x(Gly-Ser-Thr-Asn-Ala-Ser), 33-232aa	This study
pTrc99a FlgDΔ9-32, 8(GS, 2xGSTNAS)33	1-8, Gly-Ser, 2x(Gly-Ser-Thr-Asn-Ala-Ser), 33-232aa	This study
pTrc99a FlgDΔ9-32, 8(GST, 2xGSTNAS)33	1-8, Gly-Ser-Thr, 2x(Gly-Ser-Thr-Asn-Ala-Ser), 33-232aa	This study
pTrc99a FlgDΔ9-32, 8(GSTN, 2xGSTNAS)33	1-8, Gly-Ser-Thr-Asn, 2x(Gly-Ser-Thr-Asn-Ala-Ser), 33-232aa	This study
pTrc99a FlgDΔ9-32, 8(GSTNA, 2xGSTNAS)33	1-8, Gly-Ser-Thr-Asn-Ala, 2x(Gly-Ser-Thr-Asn-Ala-Ser), 33-232aa	This study
pTrc99a FlgDΔ9-32, 8(2xGSTNAS)32, 32(TNPGSTNAS)33	1-8, 2x(Gly-Ser-Thr-Asn-Ala-Ser)-(Thr-Asn-Pro-Gly-Ser-Thr-Asn-Ala-Ser), 33-232aa	This study
pTrc99a FlgDΔ9-32, 8(2xGSTNAS)32, 32(GNASGSTNAS)33	1-8, 2x(Gly-Ser-Thr-Asn-Ala-Ser)-(Gly-Asn-Ala-Ser-Gly-Ser-Thr-Asn-Ala-Ser), 33-232aa	This study
pTrc99a FlgDΔ9-32, 8(2xGSTNAS)32, 32(QSSFLTLLVAQLKNQDPTNPLQNNELTTQLA)33	1-8, 2x(Gly-Ser-Thr-Asn-Ala-Ser)-(Gln-Ser-Ser-Phe-Leu-Thr-Leu-Leu-Val-Ala-Gln-Leu-Lys-Asn-Gln-Asp-Pro-Thr-Asn-Pro-	This study

	Leu-Gln-Asn-Asn-Glu-Leu-Thr-Thr-Gln-Leu-Ala), 33-232aa	
pTrc99a FlgDΔ9-32, 8(2xGSTNAS)32, 32(TNASGSTNAS)33	1-8, 2x(Gly-Ser-Thr-Asn-Ala-Ser)-(Thr-Asn-Ala-Ser-Gly-Ser-Thr-Asn-Ala-Ser), 33-232aa	This study
pTrc99a FlgDΔ9-32, 8(2xGSTNAS)32, 32(QSSLGSTNAS)33	1-8, 2x(Gly-Ser-Thr-Asn-Ala-Ser)-(Gln-Ser-Ser-Leu-Gly-Ser-Thr-Asn-Ala-Ser), 33-232aa	This study
pTrc99a FlgDΔ9-32, 8(2xGSTNAS)32, 32(QNASGSTNAS)33	1-8, 2x(Gly-Ser-Thr-Asn-Ala-Ser)-(Gln-Asn-Ala-Ser-Gly-Ser-Thr-Asn-Ala-Ser), 33-232aa	This study
pTrc99a FlgDΔ9-32, 8(2xGSTNAS)32, 32(TNTFGTLIAS)33	1-8, 2x(Gly-Ser-Thr-Asn-Ala-Ser)-(Thr-Asn-Thr-Phe-Gly-Thr-Leu-Ise-Ala-Ser), 33-232aa	This study
pTrc99a $FlgG_{internal3xFLAG}$ Δ11-35, 10(4xGSTNAS)36	1-10, 4x(Gly-Ser-Thr-Asn-Ala-Ser), 36-144, FLAGx3, 145-260aa	This study
pTrc99a $FlgG_{internal3xFLAG}$ Δ11-35	1-10, 36-144, FLAGx3, 145-260	This study
pTrc99a $FlgG_{internal3xFLAG}$	1-144, FLAGx3, 145-260aa	This study
pTrc99a $FlgE_{internal3xFLAG}$ Δ9-32, 8(4xGSTNAS)33	1-8, 4x(Gly-Ser-Thr-Asn-Ala-Ser), 33-234, FLAGx3, 235-403aa	This study
pTrc99a $FlgE_{internal3xFLAG}$ Δ9-32	1-8, 33-234, FLAGx3, 235-403aa	This study
pTrc99a $FlgE_{internal3xFLAG}$	1-234, FLAGx3, 235-403aa	This study
pTrc99a $FlgE_{internal3xFLAG}$ Δ9-32, ΔGRM	1-8, 33-38, 44-234, FLAGx3, 235-403aa	This study
pTrc99a $FlgE_{internal3xFLAG}$ ΔGRM	1-38, 44-234, FLAGx3, 235-403aa	This study

pTrc99a FlgD Δ9-32, ΔGRM	1-8, 33-35, 41-232aa	This study
pTrc99a $FlgE_{internal3xFLAG}$ ΔCt	1-234, FLAGx3, 235-359aa	This study
pTrc99a $FlgD_{internal3xFLAG}$	1-172, FLAGx3, 173-232aa	This study
pTrc99a $FlgD_{internal3xFLAG}$ ΔCt	1-172, FLAGx3, 173-190aa	This study
pTrc99a $FlgC_{internal3xFLAG}$	1-69, FLAGx3, 70-134aa	This study
pTrc99a $FlgC_{internal3xFLAG}$ ΔCt	1-69, FLAGx3, 70-90aa	This study
pTrc99a $FlgG_{internal3xFLAG}$ ΔCt	1-144, FLAGx3, 145-217aa	This study
pTrc99a $FlgE_{internal3xFLAG}$ Δ341-350	1-234, FLAGx3, 235-340, 351-403aa	This study
pTrc99a $FlgE_{internal3xFLAG}$ Δ351-360	1-234, FLAGx3, 235-350, 361-403aa	This study
pTrc99a $FlgE_{internal3xFLAG}$ Δ361-370	1-234, FLAGx3, 235-360, 371-403aa	This study
pTrc99a $FlgE_{internal3xFLAG}$ Δ371-380	1-234, FLAGx3, 235-370, 381-403aa	This study
pTrc99a $FlgE_{internal3xFLAG}$ Δ381-390	1-234, FLAGx3, 235-380, 391-403aa	This study
pTrc99a $FlgE_{internal3xFLAG}$ Δ390-403	1-234, FLAGx3, 235-390aa	This study
pTrc99a $FlgE_{internal3xFLAG}$ E371A	1-234, FLAGx3, 235-403aa, E371A	This study
pTrc99a $FlgE_{internal3xFLAG}$ L372A	1-234, FLAGx3, 235-403aa, L372A	This study
pTrc99a $FlgE_{internal3xFLAG}$ V373A	1-234, FLAGx3, 235-403aa, V373A	This study
pTrc99a $FlgE_{internal3xFLAG}$ I376A	1-234, FLAGx3, 235-403aa, I376A	This study
pTrc99a $FlgE_{internal3xFLAG}$ V377A	1-234, FLAGx3, 235-403aa, V377A	This study
pTrc99a $FlgE_{internal3xFLAG}$ R380A	1-234, FLAGx3, 235-403aa, R380A	This study
pGEX-4T3	GST fusion	[317]
pGEX-4T3 FliJ	GST fusion, 1-147aa	[226]

pGEX-4T3 $FlhA_C$	GST fusion, 328-692aa	Laboratory strain
pGEX-4T3 FlgK	GST fusion, 1-553aa	[226]
pGEX-4T3 FlgL	GST fusion, 1-317aa	[226]
pTrc99a FlgN	1-140aa	This study
pTrc99a FlgN Y122A	1-140aa, Y122A	This study
pTrc99a FlgN Δ112-121	1-111, 122-140aa	This study
pTrc99a FlgN Δ90-100	1-89, 101-140aa	This study
pTrc99a FlgN Δ120-140	1-119aa	This study
pACT7 FlgN	1-140aa	[226]
pACT7 FlgN Y122A	1-140aa, Y122A	Sangita Ahmed
pACT7 FlgN Δ112-121	1-111, 122-140aa	Lewis Evans
pACT7 FlgN Δ90-100	1-89, 101-140aa	Sangita Ahmed
pACT7 FlgN Δ120-140	1-119aa	[176]
pACT7 FlgN W78A	W78A	This study
pACT7 FlgN Δ76-78	1-75, 79-140aa	Sangita Ahmed
pACT7 FliT94 I68A	1-94aa, Iso68Ala	This study
pACT7 FliT94 L72A	1-94aa, Leu72Ala	This study
pACT7 FliT94 N74A	1-94aa, Asn74Ala	This study
pACT7 FliT94 E75A	1-94aa, Glu75Ala	This study
pACT7 Fli94 L78A	1-94aa, Leu78Ala	This study
pACT7 FliT94 K79A	1-94aa, Lys79Ala	This study
pACT7 FliT94 L81A	1-94aa, Leu81Ala	This study
pACT7 FliT	1-122aa	[226]
pACT7 FliT L72A	1-122aa, Leu72Ala	This study

pACT7 FliT Y106A	1-122aa, Tyr106Ala	This study
pACT7 FlgN Y122A, Δ76-78	1-75, 79-140aa, Tyr122Ala	This study
pACT7 FlgN Δ70-72	1-69, 73-140aa	This study
pACT7 FlgN Δ73-75	1-72, 76-140aa	This study
pACT7 FlgN Δ76-78	1-75, 19-140aa	This study
pACT7 FlgN Δ79-81	1-78, 82-140aa	This study
pACT7 FlgN Δ82-84	1-81, 85-140aa	This study
pACT7 FlgN Δ85-87	1-84, 88-140aa	This study
pACT7 FlgN Δ88-90	1-87, 91-140aa	This study
pACT7 FlgN Δ91-93	1-90, 94-140aa	This study
pACT7 FlgN Δ94-96	1-93, 97-140aa	This study
pACT7 FlgN Δ97-99	1-96, 100-140aa	This study
pACT7 FlgN Δ100-102	1-99, 103-140aa	This study
pET15b FliJ	1-147aa, Nt-Hisx6	This study
pACT7 $FlhA_C$	328-692aa	Laboratory strain
pTrc99a FlgN Y122A, Δ76-78	1-75, 79-140aa, Tyr122Ala	This study
pWRG730	cmR. Lambda red recombinase under the P_L promoter under the control of the temperature sensitive CI857 repressor. I-SceI under the Tet promoter.	[245]
pWRG717	Km^R with I-*Sce*I recognition site	[245]